

# 博士論文

## **Studies on the carbon and energy metabolism of the thermophilic hydrogen-oxidizing bacterium *Hydrogenophilus thermoluteolus* TH-1**

(高温性水素細菌 *Hydrogenophilus thermoluteolus* TH-1  
の炭素並びにエネルギー代謝に関する研究)

東京大学大学院 農学生命科学研究科  
応用生命工学専攻 応用微生物学研究室  
平成24年度 博士課程入学  
グエン フー チー  
指導教員 石井 正治 教授

## Table of Contents

Table of Contents .....	2
Preface and Acknowledgment .....	4
Abbreviations .....	6
Motivation of this study and the general introduction .....	7
Abstract .....	9
Chapter 1. <i>Hydrogenophilus thermoluteolus</i> TH-1, a facultatively chemolithoautotrophic, hydrogen-oxidizing bacterium .....	12
1.1. Introduction .....	12
1.2. Materials and methods .....	24
1.3. Results and discussions .....	32
1.4. Conclusions .....	43
Chapter 2. The operation of glyoxylate cycle in acetate/butyrate metabolism under heterotrophic condition .....	45
2.1. Introduction .....	45
2.2. Materials and methods .....	53
2.3. Results and discussions .....	63
2.4. Conclusions .....	72
Chapter 3. Toxicity caused by photorespiration and the detoxification by function of malate synthase under mixotrophic growth in acetate/butyrate of <i>Hydrogenophilus thermoluteolus</i> TH-1 .....	73
3.1. Introduction .....	73

3.2. Materials and methods .....	76
3.3. Results and discussions.....	79
3.4. Conclusions.....	94
Chapter 4. Transcriptome and metabolome analyses of central carbon metabolism under autotrophic, heterotrophic and mixotrophic conditions in <i>Hydrogenophilus thermoluteolus</i> TH-1 .....	95
4.1. Introduction.....	95
4.2. Materials and methods .....	98
4.3. Results and discussions.....	125
4.4. Conclusions.....	170
Chapter 5. The production of poly-3-hydroxybutyrate in <i>Hydrogenophilus thermoluteolus</i> TH-1 under autotrophic and heterotrophic conditions.....	173
5.1. Introduction.....	173
5.2. Materials and methods .....	176
5.3. Results and discussions.....	180
5.4. Conclusions.....	190
Conclusions and prospects.....	193
References.....	196
Appendix.....	201

## *Preface and Acknowledgment*

This study has been carried out under the direction of Professor Masaharu Ishii in the Laboratory of Applied Microbiology, Department of Biotechnology, Graduate School of Agricultural and Life Science, The University of Tokyo during 2012-2015.

This thesis has been made possible because of the support and encouragement of various people during my PhD course in The University of Tokyo. I would like to offer my sincere gratitude to all those who have touched my life in three years in Japan.

First, I would like to express my deepest appreciation to my advisor, Professor Masaharu Ishii, for his ideas, patiences, guidances, directions and encouragements. His concerned mentorship taught me innumerable lessons, both within and beyond the boundaries of science. I still remember his speech that was read for me in the welcome party: *“I would like you to study, act, and think quite positively and deeply so that we can be the top runner in the field. I am sure you can do it. I would like every member in our laboratory to have a strong will to promote science, to make new science and to be a leader in science. Whatever you wish in your life would be, it should be best to focus on science while in laboratory. We can not change the past or make the future now. What we can do is to concentrate on the present.”* The spirit of his speech encouraged me a lot; it kept me walking step by step until I completed my PhD course. Indeed, I am indebted to him more than I expressed.

Next, I would like to appreciate Professor Yasuo Igarashi, who supported me a great opportunity to study in Japan, through the the first meeting in Ho Chi Minh City.

I would like to thank Assistant Professor Hiroyuki Arai who had been outstanding guide every time I came to him. I appreciate for his patience to explain me about microarray, genome analysis, and instructing me the molecular biology works. With his guidance, I have improved my work until today.

I would like to thank Dr. Shinichi Hirano for instructing me how to carry out microarray experiment. I still remember his advices during my microarray work, and his kindness helped me to analyze the raw data. My microarray experiment could not be successful without his directions. I do appreciate Dr. Fumiko Ishizuna for her

supports in my TEM work. I would like to appreciate Dr. Yuya Sato, a very gentle and kind person who always supported me as much as possible in my research.

Thanks are also expressed to Mr. Ato and Ms. Yamada for their assistance at the first day when I came to Japan. I am grateful for their friendship and supports.

I would also like to thank Ms. Yonezawa, the secretary of the Laboratory of Applied Microbiology for her supports, encouragements, and her assistances during my three years of study in Japan.

Sincere thanks are also to all the lab mates from the Laboratory of Applied Microbiology for their helpful advices, comments, suggestions and assistances during my course of study and research. Thanks to all my lab mates, Mr. Igarashi, Ms. Kato, Ms. Yamaguchi, Mr. Ishizaki, Mr. Sugawara, Mr. Mori, Mr. Egusa, Mr. Wakiyama, Mr. Hirai, Mr. Amano, Mr. Sakai, Mr. Kim, Mr. Inoue, Mr. Ogura, Mr. Okuda, Mr. Watanabe, Mr. Lim, and Ms. Machida for all the insightful discussions and all the fun times I had with them.

I am indebted to Ministry of Education, Culture, Sports, Science and Technology (MEXT), Japanese Government for scholarship support, providing me this golden opportunity to study in Japan.

I do appreciate to Ho Chi Minh City University of Agriculture and Forestry for all their supports during the time I studied abroad.

Most of all, my deepest appreciation to my family, your confidence in me gave me the health and strength during my study.

I would like to express my appreciations to my wife, Ms. Tran Thi Anh Tu and to my dear son, Mr. Nguyen Huu Nam for their sacrifices, loves, supports, and encouragements.

As I complete my PhD course here, I acknowledge the contribution of my father Mr. Nguyen Xuan Ke, my mother Mrs. Tran Thi Hoa, my sisters Ms. Nguyen Thi Hong Dung, Ms. Nguyen Thi Cam Chi, Ms. Nguyen Thi Cam Ly, and my younger brother Mr. Nguyen Van Sy for their supports and encouragements during my study.

Tokyo, 15<sup>th</sup> May 2015

*Nguyen Huu Tri*

## Abbreviations

ATP	adenosine triphosphate
BV	benzyl viologen
CBB cycle	Calvin-Benson-Bassham cycle
CFE	cell-free extract
CI	chloroform-isoamyl alcohol
FMN	flavin mononucleotide
GO	glycolate oxidase
Strain TH-1	<i>Hydrogenophilus thermophilus</i> TH-1
ICDH	isocitrate dehydrogenase
ICL	isocitrate lyase
KEGG	Kyoto encyclopedia of genes and genomes
MS	malate synthase
ME	malic enzyme
$\mu_{\max}$	maximum specific growth rate
MF	membrane solubilisation fraction
MBH	membrane-bound hydrogenase
NAD <sup>+</sup>	nicotinamide adenine dinucleotide
OD	optical density
PCI	phenol-chloroform-isoamyl alcohol
PHA	poly-hydroxyalkanoate
PHB	poly- $\beta$ -hydroxybutyrate
PCA	principal component analysis
PD	pyruvate dehydrogenase
POR	pyruvate: ferredoxin oxidoreductase
RH	regulatory hydrogenase
RubisCO	ribulose-1,5-bisphosphate carboxylase
SH	soluble hydrogenase
TCA	tricarboxylic acid cycle

### *Motivation of this study and the general introduction*

The world which covers our life contains so much mystery things. Once our knowledge is improved, we could improve the present world or build a better future world.

Biotechnology is a new prospect and it will improve our life and lead us to the sustainable development. The knowledge is unlimited; it is vast as the ocean. However, I believe that the more time we spend in serious study, the more knowledge we gain. My knowledge is still too humble while the world of microorganism is becoming attractive to me so much. All of them are colorful and attractive to me but sometime they make me fear. I talk to myself that I need to study more, improve myself more. By understanding about microbiology word, I will not be feared. The most favorite quote that impressed me come from Marie Curie, a French (Polish-born) chemist & physicist (1867-1934): *“I am among those who think that science has great beauty. A scientist in his laboratory is not a technician: he is also a child placed before natural phenomena which impress him like a fairy tale”*. Indeed, the world of microbiology is a fairy tale to me. It brings me a strong motivation. It makes me keep moving forward to discover and to understand the world that covers around me.

Nowadays, global warming is making the climate change worse. Global warming is the result of excess greenhouse gases (GHG) collected in the atmosphere. GHG greatly affects the increase of temperature of the Earth. How to archive the target to reduce the GHG emission is a hard question and depend on the management of many levels. We have to try to reduce industry, business, transportation, and individual households. In this process, science plays an important role for supplying the new solution, the new technology, and the new knowledge for reducing GHG emission (<http://2050.nies.go.jp/index.html>).

Carbon fixation is the dominant biochemical processes in biosphere, supplying the carbon building blocks for all living organisms [1].

*Hydrogenophilus thermoluteolus* is a gram-negative, non spore-forming, thermophilic hydrogen-oxidizing microorganism. It was isolated from a hot spring in Izu peninsula, Shizuoka Prefecture, Japan. The optimum temperature and pH for growth are 50°C

and 7.0, respectively. The maximum specific growth rate ( $\mu_{max}$ ) of strain TH-1 is determined as  $0.68\ h^{-1}$  under optimal condition. It is found to belong to the  $\beta$ -proteobacteria to grow either autotrophically on  $H_2$ ,  $O_2$  and assimilate  $CO_2$  via Calvin cycle. This bacterium shows a high potential for application in biotechnology. Hence, via using *H. thermoluteolus* in industry application, we could proceed for GHG emission reduction.

In this study, I would like to elucidate the energy metabolism and carbon metabolism of *H. thermoluteolus* TH-1. Especially, I want to clarify such metabolism in terms of trophic system of this strain. Such studies will clarify the molecular basis for autotrophy, heterotrophy or mixotrophy and lead us to some value-added product by using *H. thermoluteolus* in the future.

In order to elucidate the energy metabolism and carbon metabolism of strain TH-1, the growth profiles and the expressions of key enzymes of autotrophic metabolism during heterotrophically or mixotrophically growth is needed to be investigated.

## *Abstract*

### **Chapter 1. *Hydrogenophilus thermoluteolus* TH-1 a facultatively chemolithoautotrophic, hydrogen-oxidizing bacterium**

The facultative chemolithoautotroph has an ability to grow autotrophically by using the inorganic carbon and inorganic electron donor. Moreover, this kind of microorganism can grow heterotrophically when organic carbon is available or it can grow mixotrophically when inorganic carbon, inorganic electron donor and the organic carbon source are available at the same time.

This chapter describes the ability of strain TH-1 to grow autotrophically, heterotrophically and mixotrophically with different kinds of substrate. The specific growth rate was recorded in detail.

Specific enzymatic activities for autotrophic growth, hydrogenase and ribulose-1,5-biphosphate carboxylase/oxygenase, were measured. The utilization of each substrate was discussed in detail.

### **Chapter 2. The operation of glyoxylate cycle in acetate/butyrate metabolism**

Glyoxylate cycle is an important pathway for acetate fixation or it can play an important role as an anaplerotic pathway to replenish immediate substrates for TCA cycle. Pyruvate: ferredoxin oxidoreductase (POR) also functions as an acetate accumulation pathway by fixing CO<sub>2</sub> with acetate to generate pyruvate. The interesting thing was that genes involved in two acetate accumulation pathway (glyoxylate cycle and pyruvate: ferredoxin oxidoreductase) were found in the genome of strain TH-1. Malate synthase activity was high in cell-free extract when strain TH-1 utilized acetate or butyrate for heterotrophic growth. This result implied that in strain TH-1 glyoxylate cycle was operative in acetate or butyrate metabolism.

This chapter describes the function of glyoxylate in acetate or butyrate metabolism. The enzymatic activities of glyoxylate cycle were measured for isocitrate lyase and malate synthase. In addition, some enzymes belonging to TCA cycle and gluconeogenesis were also measured. The functions of POR and glyoxylate cycle were analyzed and discussed.

### **Chapter 3. Toxicity caused by photorespiration and the detoxification of glycolate by function of glyoxylate cycle under mixotrophic growth on acetate/butyrate of *Hydrogenophilus thermoluteolus* TH-1**

Calvin-Benson-Bassham cycle (CBB cycle) is an important pathway for carbon fixation in the biosphere. CBB cycle is popularly distributed in plants and many autotrophic microorganisms. In bacteria domain, totally six carbon fixation pathways were reported to date: CBB cycle, Acetyl CoA pathway, reductive TCA cycle, 3-hydroxypropionate bicycle, 3-hydroxypropionate/4-hydroxybutyrate cycle, 2-hydroxycarboxylate/4-hydroxybutyrate cycle. CBB cycle is the most popular among autotroph.

The main enzyme of CBB cycle and also the most abundant protein on the Earth is ribulose-1,5-biphosphate carboxylase/oxygenase (RubisCO). This enzyme catalyses the first step of carbon fixation that fixes CO<sub>2</sub> to ribulose-1,5-biphosphate when CO<sub>2</sub> is a substrate. However, RubisCO can also incorporate O<sub>2</sub> to ribulose-1,5-biphosphate by oxygenation activity via a process so-called photorespiration. Photorespiration is a waste process that decreases carbon fixation efficiency to approximately 25% by producing 2-phosphoglycolate. Furthermore, 2-phosphoglycolate was reported as an inhibitor of carbon fixation process and other by-products such as ammonia and peroxide were found to be toxic to the cells.

This chapter describes the operation of CBB cycle under autotrophic or mixotrophic conditions with different carbon sources. The toxification caused by photorespiration was investigated and the detoxification system was discussed.

### **Chapter 4. Transcriptome and metabolome analyses of central carbon metabolism under autotrophic, heterotrophic, and mixotrophic conditions in *Hydrogenophilus thermoluteolus* TH-1**

Nowadays, microarray is a new and good molecular method with highly potential application in many fields such as academia, medical science, pharmaceutical, biotechnological, agrochemical, and food industries.

Microarray is a powerful tool to research about the expression of genes because with one single experiment, we can get over 10,000 of blotting data, which makes monitoring of the genome activity possible.

This chapter describes the expression of whole genes of TH-1 under autotrophic condition, heterotrophic or mixotrophic conditions with butyrate as substrate. The expression profiles of all central carbon metabolic pathways were evaluated and discussed.

#### **Chapter 5. The production of poly-3-hydroxybutyrate in *Hydrogenophilus thermoluteolus* TH-1 under autotrophic and heterotrophic conditions.**

This chapter describes the ability of strain TH-1 to accumulate PHB under autotrophic or heterotrophic induction condition. The roles of three PHA synthase genes were analyzed; phylogenetic tree was constructed and discussed. After induction by nitrogen starvation, PHB rapidly accumulated under autotrophic and heterotrophic conditions. PHB granules accumulated in globular form with a diameter of 0.2-0.5  $\mu\text{m}$ . They located close to or in contact with the membrane under autotrophic condition, but were randomly distributed in cytosol under heterotrophic condition. The highest percentages of PHB accumulation under autotrophic and heterotrophic conditions were 38.6% after 360 minutes and 53.8% after 180 minutes, respectively.

## **Chapter 1. *Hydrogenophilus thermoluteolus* TH-1, a facultatively chemolithoautotrophic, hydrogen-oxidizing bacterium**

### **1.1. Introduction**

#### *1.1.1. Hydrogenophilus thermoluteolus* TH-1

Many aerobic hydrogen-oxidizing bacteria have been isolated as gram-negative or gram-positive organisms [2, 3]. The group of the aerobic hydrogen-oxidizing is defined on the basis of physiological capabilities to utilize hydrogen ( $H_2$ ) as the sole energy source. They are termed chemolithoautotrophs. Chemolithoautotrophs are able to grow in a medium containing the usual mineral salts and trace elements when the necessary gaseous components ( $H_2$ ,  $O_2$ , and  $CO_2$ ) are supplied. Most of these hydrogen bacteria are facultative chemolithoautotrophs [4]. The metabolism of this group bacterium was significantly affected by the habitats. Hydrogen-oxidizing bacteria obtain energy for  $CO_2$  fixation by the oxidation of  $H_2$  gas with  $O_2$  and they are isolated from the natural environment, especially soil, ocean, rivers and hot springs [5]. Natural habitat of chemolithoautotrophs is very limited in nutrition.  $H_2$  is not the only energy source and concentration is very low. For adaptation toward the shortage of nutrition they have to metabolize other alternative energy sources. These features explain the extremely versatile metabolism of facultative chemolithoautotrophs. These bacteria preferentially utilize organic acid as a carbon source for heterotrophic growth or utilize organic acid as a carbon source while utilizing  $H_2$  as an electron donor for mixotrophic growth [6, 7].

*H. thermoluteolus* strain TH-1 is rod shaped with a single polar flagellum, gram-negative, non spore-forming, thermophilic hydrogen-oxidizing microorganism [7].



Figure 1-1. Scanning electron micrograph of strain TH-1<sup>T</sup>. Bar, 1μm [3]

It was isolated from a hot spring in Izu peninsula, Shizuoka Prefecture, Japan. The optimum temperature and pH for growth are 50°C and 7.0, respectively. The maximum specific growth rate ( $\mu_{\max}$ ) of strain TH-1 is  $0.68\ h^{-1}$  under optimal condition. It belongs to the  $\beta$ -proteobacteria which is able to grow autotrophically on  $H_2$ ,  $O_2$  and assimilate  $CO_2$  via Calvin-Benson-Bassham cycle. Under heterotrophic condition, strain TH-1 uses acetate, propionate, butyrate, succinate, DL-lactate, pyruvate or  $\alpha$ -ketoglutarate as electron donors and carbon sources. Ammonium ions, nitrate ions and urea are utilized solely as nitrogen sources; however, strain TH-1 cannot utilize nitrite ions or gaseous nitrogen. Even nitrite inhibited the growth of strain TH-1 [2, 3].

At the early step of classification, TH-1 was described as rod shape, mostly single or in pair, no capsule formation. TH-1 cell appeared in width 0.5 μm to 0.6 μm, length from 2 μm to 3 μm. TH-1 cells could move with polar flagella. Because strain TH-1 possessed a single polar flagellum, it was suggested that it belong to *Pseudomonas* as a new species: *Pseudomonas hydrogenothermophila* nov. sp. Goto, Kodama and Minoda. Type strain: TH-1 [7]. However, based on 16S rDNA sequences analysis, TH-1 was re-classified as a new genus and species: *Hydrogenophilus thermoluteolus* gen. nov. sp. nov.,. The type strain is strain TH-1<sup>T</sup> (IFO 14978<sup>T</sup>). In general, strain TH-1 is classified as follows (Wikipedia):

Kingdom: *Bacteria*

Phylum: *Proteobacteria*

Class: *Betaproteobacteria*

Order: *Hydrogenophilales*

Family: *Hydrogenophilaceae*

Genera: *Hydrogenophilus*

Species: *Hydrogenophilus thermoluteolus*

*Hydrogenophilus* (Hy.dro.ge.nó.phi.lus) means hydrogen lover and *thermoluteolus* (ther.mo.lu.téo.lus) means hot and light-yellow. The name *Hydrogenophilus thermoluteolus* was proposed for strain TH-1 because it can utilize hydrogen as an energy source for growth at high temperature (50°C-52°C) and the bacterial colonies appeared in yellow color [3].

Among hydrogen-oxidizing bacteria, *Ralstonia eutropha* is the most intensively researched bacterium [8-10]. One of the important features of *R. eutropha* is that it can grow autotrophically better than the other autotrophs [5]. The maximum specific growth rate of *R. eutropha* of  $0.42\text{ h}^{-1}$  was attained at about 0.05 atm of oxygen partial pressure. *R. eutropha* could not grow at a dissolved oxygen concentration higher than 0.3 atm [11]. However, strain TH-1 showed a higher specific growth rate than that of *R. eutropha*. Strain TH-1 showed the highest  $\mu_{max}$ ,  $0.68\text{ h}^{-1}$  among all the autotrophic organisms, including plants, algae and bacteria. The reason to explain this high specific growth rate of strain TH-1 is that TH-1 can grow well under the partial pressure of oxygen, 0.33 atm in shaken cultures [2].

Table 1-1. List of methods for the autotrophic, high-density cultivation of hydrogen-oxidizing bacterium [2]

Strain	Culture method	Cell concentration (g l <sup>-1</sup> ·h <sup>-1</sup> )	Cell productivity (g l <sup>-1</sup> ·h <sup>-1</sup> )	Reference
<i>Ralstonia eutropha</i>	Batch	25.0	1.00	Repask and Meyer 1976
<i>Pseudomonas hydrogenovora</i>	Batch	24.0	0.50	Goto et al. 1977b
<i>Ralstonia eutropha</i>	Continuous	—	0.40	Morinaga et al. 1978
<i>Pseudomonas hydrogenothermophila</i>	Continuous	—	3.00	Igarashi 1986
<i>Alcaligenes hydrogenophilus</i>	Continuous	—	0.33	Miura et al. 1982

As shown in Table 1-1, *H. thermoluteolus* TH-1 (former name is *Pseudomonas hydrogenothermophila*) cell productivity is significantly higher than that of the other autotrophs [5].

Now, draft genome of strain TH-1 is available. So, research about metabolism is welcoming new field in which strain TH-1 will be used as a new platform of biotechnological application.

### 1.1.2. CO<sub>2</sub> fixation system and hydrogenase system and in *Hydrogenophilus thermoluteolus* TH-1

#### 1.1.2.1. CO<sub>2</sub> fixation system

In the cells growing autotrophically, two necessary functions are hydrogen-oxidizing system and carbon-fixation system. The latter one even plays critical role in the control of the autotrophic metabolism [12]. Today, six autotrophic carbon dioxide fixation pathways have been identified: CBB cycle, the reductive TCA cycle, the 3-hydroxypropionate bicycle, the 3-hydroxypropionate/4-hydroxybutyrate cycle, the dicarboxylate/4-hydroxybutyrate cycle, and reductive acetyl-CoA pathway. The CBB cycle is the predominant pathway by which many prokaryotes and plants fix CO<sub>2</sub> [13]. Although some chemolithoautotrophs fix CO<sub>2</sub> by reductive TCA cycle, CBB cycle is the most common pathway chemolithotrophs use to fix CO<sub>2</sub> [14]. *H. thermoluteolus* TH-1 also fixes CO<sub>2</sub> through CBB cycle. CBB cycle comprises 11 different enzymes catalyzing 13 enzymatic reactions in which ribulose-1,5-bisphosphate carboxylase (RubisCO) is the most important [15]. RubisCO is a protein of high molecular weight [16]. This enzyme contains two sub-units which are encoded by *cbbL* and *cbbS* genes organized within *cbb* operon. RubisCO are composed of eight large and small subunits (L<sub>8</sub>S<sub>8</sub>). The active site for enzymatic activity is located in large subunits [17]. The large subunit has a molecular weight of 51,000 to 58,000 while the small subunit has 12,000 to 14,000. The large subunits are catalytically active even when small subunits are lacking [16].

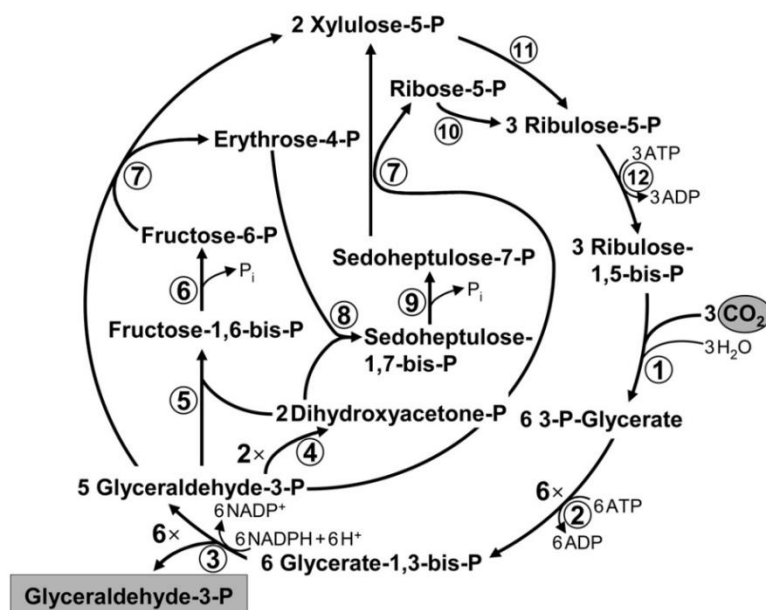


Figure 1-2. Calvin-Benson-Bassham cycle [18]. 1, Ribulose-1,5-bisphosphate carboxylase/oxygenase; 2, 3-Phosphoglycerate kinase; 3, Glyceraldehyde-3-phosphate dehydrogenase; 4, Triose-phosphate isomerase; 5, Fructose-bisphosphate aldolase; 6, Fructose-bisphosphate phosphatase; 7, Transketolase; 8, Sedoheptulose-bisphosphate aldolase; 9, Sedoheptulose-bisphosphate phosphatase; 10, Ribose-phosphate isomerase; 11, Ribulose-phosphate epimerase; and 12, Phosphoribulokinase.

All genes that encode enzymes for CBB cycle were found in TH-1 genome. RubisCO catalyzes a dual reaction: carboxylation and oxygenation. Carboxylation is the major activity of RubisCO where  $\text{CO}_2$  is fixed into ribulose-1,5-bisphosphate to form two molecules of glycerate-3-phosphate. The oxygenase activity was proposed by Ogren & Bowes in 1971 after they observed the inhibitory effect of oxygen toward  $\text{CO}_2$  fixation. By the observation, they suggested that oxygen may be competitive with carbon dioxide at the reactive centre. In oxygenase reaction, ribulose-1,5-bisphosphate is oxidized to 2-phosphoglycolate, which is converted into glycolate, a toxic compound. Increase of  $\text{O}_2$  increases the rate of phosphoglycolate production, and by this way the intermediates amount of CBB cycle reduce [19]. CBB cycle operates in some thermophiles but never in hyperthermophile. The reason is explained by the heat instability of some intermediates of the cycle and by the possible production of toxic compounds such as methylglyoxal at high temperature [18]. Then, the investigation of

the autotrophic and mixotrophic growth of strain TH-1 at high temperature (50°C) should be an interesting topic.

#### 1.1.2.2. *Hydrogenase system*

Another system required for autotrophic growth is hydrogenase. This is the key enzyme involved in the metabolism of H<sub>2</sub>. Hydrogen is a popular energy source for the microorganism that possesses hydrogenase system. For many bacteria in nature, H<sub>2</sub> is an energy source, which yields high chemical energy by the oxidation of H<sub>2</sub> by O<sub>2</sub> [20]. Hydrogenase catalyzes the oxidation of H<sub>2</sub> with the reduction of electron acceptor. Hydrogenase is classified to three groups: Ni-Fe hydrogenase, Fe-Fe hydrogenases, and Fe hydrogenase. In general, hydrogenase contains one large subunit with active site and small subunits with Fe-S cluster required for electron transfer. However, those hydrogenases are different in the function from point of view of turn over rate, or the oxygen sensitivity [20, 21]. Normally, hydrogenase is highly sensitive toward oxygen. But Ni-Fe hydrogenase, a predominant hydrogenase in aerobic or facultative aerobic hydrogen-oxidizing bacteria, is known as oxygen-tolerant hydrogenase.

The hydrogenase system in *Ralstonia eutropha* is the representative in facultative aerobic bacteria. The intensive research reported that three types of hydrogenase exist in *R. eutropha*. The first is membrane-bound hydrogenase (MBH). MBH enzymes couple to respiratory electron transport chain via cytochrome *b* to generate ATP. The second is a soluble hydrogenase (SH), which directly reduces NAD<sup>+</sup>, generating reducing equivalent NADH for biological synthesis. The third is also a soluble hydrogenase, a regulatory hydrogenase (RH). However, the function of RH is not to gain energy but it plays a role as a hydrogen sensor in the regulation of the expression of the genes related to hydrogen oxidation [21].

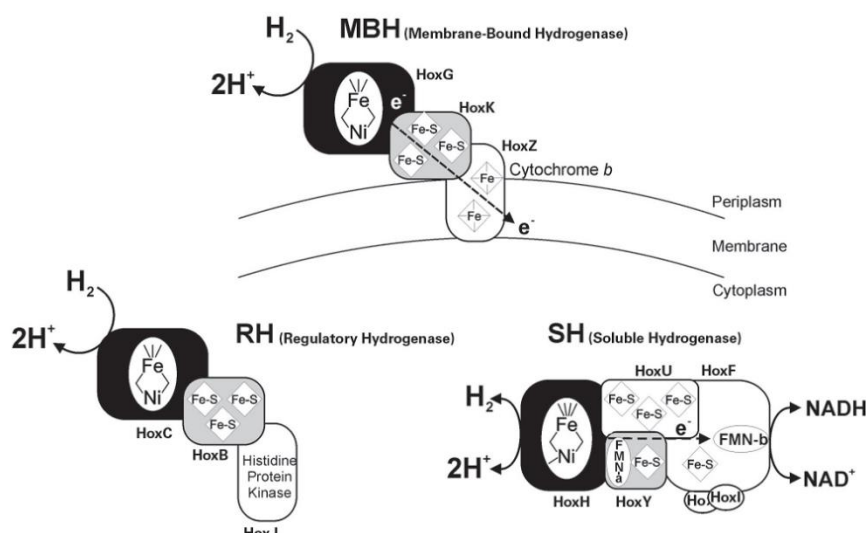


Figure 1-3. Three types [NiFe]-hydrogenases of *R. eutropha* H16 [21]

By using TH-1 genome and *R. eutropha* genome, I found that strain TH-1 has hydrogenase system similar to that of *R. eutropha*.

The experiments for the measurements of SH and MBH were required to evaluate the roles of hydrogenases under autotrophic condition.

The chemolithoautotrophic characteristic is the ability to grow autotrophically by using the inorganic carbon and inorganic electron donor. Moreover, this kind of microorganism can grow heterotrophically when organic carbon is available or it can grow mixotrophically when inorganic carbon, inorganic electron donor, and organic carbon source are available.

This chapter focuses on the investigation for the ability of strain TH-1 to grow under autotrophic, heterotrophic, or mixotrophic condition with different kinds of substrates.

The specific growth rate in each condition was recorded.

Specific enzymatic activities for autotrophic growth such as hydrogenase or ribulose-1,5-biphosphate carboxylase/oxygenase were measured.

### 1.1.3. The study of bacterial growth

When microbes are provided with nutrients and the required environmental factors, they become metabolically active and grow [22]. The growth of microorganism was researched and observed from two points of view: at first, the growth that is the

increasing size of single microbes and the second, the growth that is the increasing of the population of microbes. In this study, I analyzed it from second view.

In general, in a cycle of life, bacteria start collecting the nutrition from the ambient environment, conduct various metabolisms by catalyzing various reactions, grow and generate a new generation. The new generation is created through a process so-called replication in which one bacterium cell is divided by mitosis to make two new daughter cells. By mitosis process, the number of microorganism increases following the time of incubation. The study about microbe's growth is to study about the change in population size of microbe concerned.

Quantitative laboratory studies indicate that a population typically displays a predictable pattern, or growth curve, over time. The method traditionally used to observe the population growth pattern is a viable count technique, in which the total number of living cells is counted over a given time period. In brief, this method entails (1) placing a tiny number of cells into a sterile liquid medium; (2) incubating this culture over a period of several hours; (3) sampling the broth at regular intervals during incubation; (4) plating each sample onto solid media; and (5) counting the number of colonies present after incubation [22]

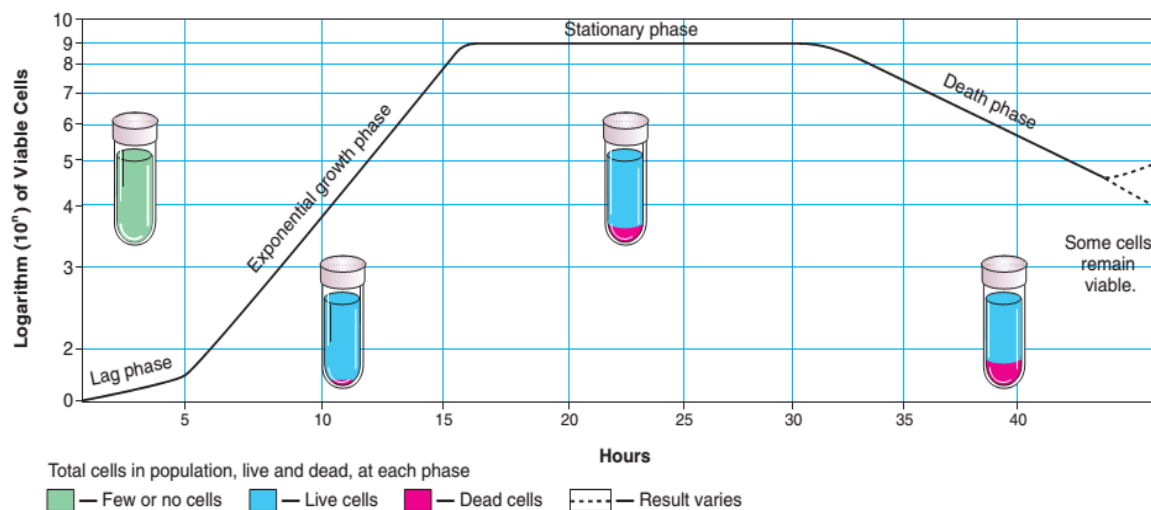


Figure 1-4. The growth curve in a bacterial culture. On this graph, the number of viable cells expressed as a logarithm (log) is plotted against time [22].

In a typical growth curve, it contains four phase as in Fig. 1-4: lag phase, exponential growth phase (or logarithmic growth phase), stationary phase, and death phase.

The lag phase is the period time in which bacteria appears not to be growing or is growing at less than the exponential rate. There are three reasons why lag phase occurred. (1) The newly inoculated cells require a period of adjustment, enlargement, and synthesis; (2) the cells are not yet multiplying at their maximum rate; and (3) the population of cells is so sparse or dilute that the sampling misses them [22]. The length of lag phase depends on the kind of bacteria and the culture conditions such as the nutrition components, pH, temperature, etc. So it varies from bacterium to bacterium, from condition to condition. The length of lag phase also reflects the ability of the microbes to adapt to a new environment. Under favourable nutrition or physical condition, microbe can take up the nutrition and start growth soon. Therefore, lag phase in this case is short. On the other hand, under unfavourable condition about nutrition or physical condition, the growth of bacteria is delayed or inhibited, so the length of lag phase is long. The growth of bacteria just starts after it adapts to new condition.

After lag phase, bacteria enter a logarithmic phase (exponential growth phase). The growth of bacteria reaches the maximum rate during the phase. The length of logarithmic phase depends on the nutrition condition as well as the density of the population of bacteria. Once bacteria reach the maximum growth rate, the robust increase of population size followed by the consumption of nutrition will make the carbon source and energy source exhausted. In the study about growth of bacteria, logarithmic phase is the most important period time. By analysis of the trend for growth we can understand the growth feature of microbe under each nutrition condition. Because of robust growth in logarithmic phase, the metabolic transformation in microbe also reaches maximum rate. Hence, for enzymatic activity measurement, the logarithmic phase is the most important. In logarithmic phase, the growth curve increases geometrically. It makes an upward slope as in figure 1-4.

Following the logarithmic phase is the stationary growth phase. At this phase, because amount of the nutrition decreases and the population increases, the growth rate of

bacteria slows down. At this phase, the growth rate and death rate of microbe are thought to be in balance. Bacteria sometimes excrete secondary metabolites when bacteria enter the stationary phase. These secondary metabolites may be organic acids, antibiotics or other toxic compounds. For biotechnological application, stationary phase is very important. Based on this natural feature, we can make the microbe excrete the secondary metabolites or materials.

In death phase, the nutrition is exhausted, and the ambient environment contains a lot of unfavourable metabolites that were excreted in stationary phase. Bacteria almost stop the growth [22].

There are many methods that can be applied to the measurement of growth as well as growth curve construction. Direct viable plate count technique, direct microscopic count of bacteria, or measurement of the turbidity can be an indicator for growth. Turbidity measurement is the simplest method for evaluation for the change of size of microbe. This technique relies on the simple observation that a tube of clear nutrient solution loses its clarity and becomes cloudy, or turbid. Together with the increase in the population of bacteria, the turbidity also increases. Based on the evaluation of the turbidity through optical density (OD), we can know the population of bacteria.

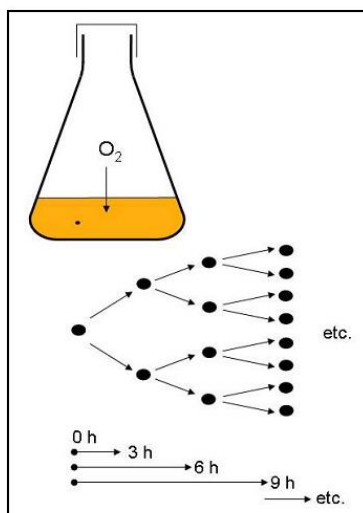


Figure 1-5. How to imagine cell growth that began with a single cell (Widdel F. Theory and Measurement of Bacterial Growth, Basic practical microbiology, 4<sup>th</sup> Semester, (ed. Widdel F.). 2007 (corrected 2010)).

Nowadays, by using the new spectrophotometry equipment, we can measure until 96 samples at the same time. So, this method is more convenient to study about the growth of population bacteria under various conditions with high confidence level.

Friedrich Widdel, a German researcher developed and proved a mathematic equation that enabled us to determine the specific growth rate ( $\mu$ ) from OD value. This is a simple development of a growth equation.

The equation was suggested to understand the growth of bacteria cells from a single cell. The equation for calculation the number of bacterial after “n” time of division from a single cell is:  $N = 2^n$  (1)

t is the time passed from the beginning and  $t_d$  is the doubling time (generation time), we have:  $n = \frac{t}{t_d}$  (2)

Now, (1) become:  $N = 2^{\frac{t}{t_d}}$  (3)

So, if the culture starts with any cell number,  $N_o$  the equation would be:

$$N = N_o \cdot 2^{\frac{t}{t_d}} \quad (4)$$

By definition of the natural logarithm, the number 2 can be written as:  $2 = e^{\ln 2}$  (5)

This converts equation (4) to:  $N = N_o \cdot (e^{\ln 2})^{\frac{t}{t_d}} = N_o \cdot (e^{\frac{\ln 2}{t_d}})^t$  (6)

For each specific bacterium, the doubling time,  $t_d$  is a kind of species-specific. The doubling time of a specific bacterial species growing optimally can thus be regarded as a fixed value. Hence, we can define a new constant,  $\mu$ .

$$\frac{\ln 2}{t_d} = \frac{0.693}{t_d} = \mu \quad (7)$$

The new constant  $\mu$  is used to represent the specific growth rate (unit:  $d^{-1}$ ,  $h^{-1}$ ,  $min^{-1}$ ).

From this, we obtain the growth equation well-know form:  $N = N_o \cdot e^{\mu t}$  (8)

By definition of the natural logarithm, the equation (8) can be written as:

$$\ln N = \ln N_o + \mu t \quad (9)$$

And become:  $\mu t = \ln N - \ln N_o = \ln \frac{N}{N_o}$  (10)

Assuming the cell density is the cell number ( $N^{\text{sample}}$ ) available in the given volume sample ( $V^{\text{sample}}$ ), so:

$$\text{Cell density at } t=0: \frac{N_o^{sample}}{V^{sample}} \quad (11)$$

$$\text{Cell density at } t: \frac{N^{sample}}{V^{sample}} \quad (12)$$

The cell density is measured optically by a photometer through optical density (OD) value, showing a representative for cell density:

$$\frac{N^{sample}}{V^{sample}} \sim \text{OD} \quad (13)$$

Substitute (11) and (12) to (8) we have:

$$\frac{N^{sample}}{V^{sample}} = \frac{N_o^{sample}}{V^{sample}} e^{\mu t} \quad (14)$$

Combine with (13), equation (14) becomes:  $\text{OD} = \text{OD}_o e^{\mu t}$  (15) with  $\text{OD}_o$  is the optical density at  $t=0$ .

$$\text{We could re-write (15) as: } e^{\mu t} = \frac{\text{OD}}{\text{OD}_o} \quad (16)$$

By definition of the natural logarithm, the equation (16) can be written as:

$$\mu t = \ln \left( \frac{\text{OD}}{\text{OD}_o} \right) = \ln \text{OD} - \ln \text{OD}_o \quad (17)$$

For two values chosen on the growth curve line,  $\text{OD}_1$  and  $\text{OD}_2$ , the corresponding time points are  $t_1$  and  $t_2$ , respectively:

$$\mu t_1 = \ln \text{OD}_1 - \ln \text{OD}_o \quad (18)$$

$$\mu t_2 = \ln \text{OD}_2 - \ln \text{OD}_o \quad (19)$$

$$\text{Take (19) - (18) yields: } \mu (t_2 - t_1) = \ln \text{OD}_2 - \ln \text{OD}_1 \quad (20)$$

$$\text{And for } \mu = \frac{(\ln \text{OD}_2 - \ln \text{OD}_1)}{(t_2 - t_1)} \quad (21)$$

Or with conversion to the decadic logarithm, lg

$$\mu = \frac{2.303 (\lg \text{OD}_2 - \lg \text{OD}_1)}{(t_2 - t_1)} \quad (22)$$

So, the application of equation (22) is convenient to determine the specific growth rate of bacteria based on optical density data. This equation was employed in determining the growth curve of strain TH-1 that grows under autotrophic, heterophic, or mixotrophic condition with different substrates.

## 1.2. Materials and methods

### 1.2.1. Bacterial strains and growth condition

#### 1.2.1.1. Bacterium strain

*H. thermoluteolus* is a gram-negative, non spore-forming, thermophilic hydrogen-oxidizing microorganism, isolated from a hot spring in Izu district, Japan.

Table 1-2. The components of basic cultivation medium

Deionized Water	1.0 L
(NH <sub>4</sub> ) <sub>2</sub> SO <sub>4</sub>	3.0 g
KH <sub>2</sub> PO <sub>4</sub>	1.0 g
K <sub>2</sub> HPO <sub>4</sub>	2.0 g
NaCl	0.25 g
FeSO <sub>4</sub> ·7H <sub>2</sub> O	0.014 g
Trace elements solution	0.5 mL
Final pH	7.0

Table 1-3. The components of trace elements solution

Deionized Water	1.0 L
MoO <sub>3</sub>	4.0 mg
ZnSO <sub>4</sub> ·7H <sub>2</sub> O	28 mg
CuSO <sub>4</sub> ·5H <sub>2</sub> O	2.0 mg
H <sub>3</sub> BO <sub>3</sub>	4.0 mg
MnSO <sub>4</sub> ·5H <sub>2</sub> O	4.0 mg
CoCl <sub>2</sub> ·6H <sub>2</sub> O	4.0 mg

#### 1.2.1.2. Growth condition

##### a. Autotrophic cultivation

The medium employed for *H. thermoluteolus* growth consisted of (NH<sub>4</sub>)<sub>2</sub>SO<sub>4</sub> 3.0 gL<sup>-1</sup>, KH<sub>2</sub>PO<sub>4</sub> 1.0 gL<sup>-1</sup>, K<sub>2</sub>HPO<sub>4</sub> 2.0 gL<sup>-1</sup>, NaCl 0.25 gL<sup>-1</sup>, FeSO<sub>4</sub>·7H<sub>2</sub>O 0.0014 gL<sup>-1</sup>, and supplement trace element solution, pH 7.0 (Table 1-2, 1-3). Vial (100 ml) containing 10 ml of the mineral salts medium was inoculated and incubated at 50°C under a H<sub>2</sub>-O<sub>2</sub>-CO<sub>2</sub> mixture (75:10:15).

##### b. Heterotrophic cultivation

A growth experiment under heterotrophic condition was performed in an air atmosphere using the medium similar to the autotrophic condition with the addition of only one organic acid as a substrate. The organic acid added was formate (C<sub>1</sub>), acetate (C<sub>2</sub>), glyoxylate (C<sub>2</sub>), glycerol (C<sub>3</sub>), pyruvate (C<sub>3</sub>), butyrate (C<sub>4</sub>), malate (C<sub>4</sub>), 2-oxoglutarate (C<sub>5</sub>), glutamate (C<sub>5</sub>), citrate (C<sub>6</sub>), glucose (C<sub>6</sub>), or fructose (C<sub>6</sub>). The equivalent carbon concentration of organic acid was 60 mM. Strain TH-1 was inoculated and shaken on a reciprocating shaker at 50°C under the air atmosphere.

#### *c. Mixotrophic cultivation*

In the field of microbiology, the term “mixotrophic” has two meanings. At first, mixotrophic is the term definition for the growth of two or more microorganisms in the same medium culture. In this case, “mix” means the mixture of two or more microorganisms. The second meaning is the capability to activate both the autotrophic and heterotrophic mode of growth [29]. Therefore, mixotrophic culture in this research focus on the capacity of utilizing two modes of growth: autotrophically with H<sub>2</sub> and CO<sub>2</sub>, and heterotrophically with organic substrate.

Growth experiments under mixotrophic conditions were performed with the medium and gas phase as under autotrophic condition with the addition of only one organic acid. The organic acid added was formate (C<sub>1</sub>), acetate (C<sub>2</sub>), glyoxylate (C<sub>2</sub>), glycerol (C<sub>3</sub>), pyruvate (C<sub>3</sub>), butyrate (C<sub>4</sub>), malate (C<sub>4</sub>), 2-oxoglutarate (C<sub>5</sub>), glutamate (C<sub>5</sub>), citrate (C<sub>6</sub>), glucose (C<sub>6</sub>), or fructose (C<sub>6</sub>).

##### *1.2.1.2. Measurement of growth*

Growth experiments for strain TH-1 under all conditions were performed by inoculating the pre-culture grown autotrophically. The initial optical density at wavelength 540 nm was 0.04-0.06. The maximum specific growth rate of strain TH-1 with various carbon sources under different culture conditions was determined within 24 hours.

##### *1.2.1.3. Cell-free extract preparation and membrane solubilisation*

###### *a. Cell-free extracts*

Cells were grown under the specific conditions, harvested by centrifugation. Cells were harvested by centrifugation at 10,000 x g/10 minutes/4°C, and washed twice by

cell suspension buffer with centrifugation at 15,000 x g/2 minutes/4°C. Cell disruption/suspension buffer: 20 mM Tris HCl pH7.5. Cell-free extract was collected by disruption of the cell through sonication on ice twice, each 10 minutes followed by centrifugation at 15,000 x g/30 minutes/4°C. After the disruption and centrifugation, suspension was designed as cell-free extract, the precipitate was designed as a membrane fraction [23]. Cell-free extract protein concentration was measured by Bradford method (Standard curve in Appendix).

#### *b. Membrane solubilisation*

For membrane-bound hydrogenase enzymatic activity measurement, membrane fraction was solubilized. For this step, two kinds of membrane solubilization buffer (MS buffer) were prepared. MS<sub>1</sub> buffer was the potassium buffer pH 7.0 which was supplemented with DTT (1 mM), MgCl<sub>2</sub> (2 mM), EDTA (10 mM), and glycerol (30%). MS<sub>2</sub> buffer had the additional component to MS<sub>1</sub> buffer (Triton X-100 (0.2% w/v)). The membrane fraction was re-suspended in MS<sub>1</sub> buffer and MS<sub>2</sub> with the ratio (40%:60%). The mixture was mixed gently for 1 hour followed by centrifugation at 15,000 x g/30 minutes/4°C. After centrifugation, the supernatant was designed as membrane solubilization fraction [24].

For hydrogenase enzymatic activity measurement, protein concentrations of cell-free extract and membrane fraction were determined by BCA method (Standard curve in Appendix).

### 1.2.2. Ribulose-1,5-bisphosphate carboxylase/oxygenase assay

*1.2.2.1. Principle:* Ribulose-1,5-bisphosphate carboxylase/oxygenase is commonly known by the abbreviation RubisCO.

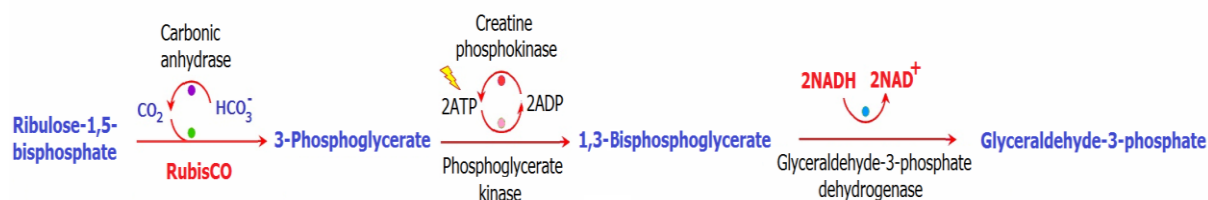


Figure 1-6. The reaction system for determining RubisCO activity

1.2.2.2. *Condition:* T = 50°C, pH = 7.0; A<sub>340</sub>, light path = 1cm

RubisCO activity was determined by measuring the rate of NADH oxidation at wavelength of 340 nm, following the method of Sharkey, T. D. et al, 1991 [25]. By following the disappearance of NADH through monitoring the A<sub>340</sub> (the extinction coefficient of NADH at this wavelength is 6.22 mM<sup>-1</sup> cm<sup>-1</sup>), the enzymatic activity was measured. The reaction mixture was prepared in a glass cuvette with the total volume of 1 mL. The reaction buffer was used as the blank; the reaction was performed at 50°C. Ten µL of cell-free extract was added to 970 µL of assay mixture (the components are shown in Table 1-2) and all mixtures were degassed and flushed with Argon gas for 2 minutes, held in the spectrophotometer for 5 minutes to allow temperature equilibration. Finally, 20 µL of ribulose-1,5-bisphosphate (100 mM) was added into the assay mixture to start the reaction and the absorbance of the mixture at 340 nm (A<sub>340</sub>) was recorded to give a background rate of NADH oxidation. The reduction of OD value was used to calculate the RubisCO activity.

1.2.2.3. *Reagents*

Table 1-4. The reaction system for determining RubisCO activity.

Reagents	Volume (mL)
Reaction buffer*	0.76
10mM NADH solution	0.02
10 mM ATP/50 mM Creatine Phosphate solution	0.10
25 U/mL Creatinephosphokinase (ORIENTAL YEAST co.,Ltd)	0.02
500 mM NaHCO <sub>3</sub> solution	0.04
10mg/mL Carbonic anhydrase (Sigma-Aldrich)	0.01
Coupling enzymes mixture**	0.02
Cell free extract	0.01
100 mM ribulose-1,5-bisphosphate	0.02
*Reaction buffer : 100 mM Bicine –NaOH pH (8.0), 20 mM MgCl <sub>2</sub> , 1 mM DTT, (set the pH before adding DTT)	
**Coupling enzymes mixture: glyceraldehyde 3-phosphate dehydrogenase (GPDH) and phosphoglycerokinase (PGK) (Sigma-Aldrich) was mixed together in the buffer (50 mM bicine, pH 7.8, 1 mM EDTA, 1 mM DTT), the final concentration for each enzyme was 25 U/mL, 20 U/mL respectively. The mixture was dialyzed overnight in the same buffer at 4°C, added glycerol to give the final concentration of 20% (v/v) glycerol. Stored this in the deep freezer -80 °C until needed.	

#### 1.2.2.4. Calculations

The following formula was used to calculate RubisCO carboxylase activity:

$$\text{Units/ml Enzyme} = \frac{(\Delta A_{340\text{nm}} / \text{min Test} - \Delta A_{340\text{nm}} / \text{min Blank})(1)(\text{df})}{2. (6.22)(0.01)}$$

1= total volume (in milliliters) of assay

2 = assuming two NADH molecules were oxidized per CO<sub>2</sub> fixed

df = dilution factor

6.22 = millimolar extinction coefficient of β-NADH at 340 nm

0.01 = Volume (in milliliters) of enzyme used

$$\text{Units/mg protein} = \frac{\text{units/ml enzyme}}{\text{mg protein/ml enzyme}}$$

#### 1.2.2.5. Unit definition

RubisCO activity was calculated by subtracting the background rate of decrease in A<sub>340</sub>. RubisCO activity was expressed as CO<sub>2</sub> fixation activity, assuming two NADH molecules were oxidized per CO<sub>2</sub> fixed. One unit of enzyme activity was defined as the amount of enzyme catalyzing the fixation of 1 μmol ribulose-1, 5-bisphosphate per minute at 50°C.

#### 1.2.3. Hydrogenase activity measurement

*1.2.3.1 Principle:* Soluble hydrogenase (SH) activity was routinely determined in a continuous spectrophotometric assay following the enzyme-, substrate-, and time-dependent reduction of NAD<sup>+</sup> at λ= 340 nm. By following the reduction of nicotinamide adenine dinucleotide (NAD<sup>+</sup>) at A<sub>340</sub> (the extinction coefficient of NADH at this wavelength is 6.22 mM<sup>-1</sup> cm<sup>-1</sup>), the enzymatic activity was measured [26].



Figure 1-7. The reaction system for determining soluble hydrogenase activity

1.2.3.2. *Condition:* T= 50°C, pH = 7.0; A<sub>340</sub>, light path = 1 cm

The reaction was prepared in a glass cuvette (5 mL) with the total volume of 2 mL. The reaction buffer was used as a blank; the reaction was performed at 50°C as follows:

Reaction buffer (1,930 µL of 50 mM HEPES buffer pH 7.0) was added into glass cuvette, capped by a rubber stop and sealed by an aluminium cap. After the H<sub>2</sub> was bubbled for 5 minutes, cuvette was incubated for over 5 minutes at 50°C. Then, 20 µL of dithionite and 100 µL of cell-free extract (soluble fraction) were added and the cuvette was held in the spectrophotometer for 3 minutes at 50°C to allow temperature equilibration. Finally, 40µL of NAD<sup>+</sup> (100 mM) was added into the assay mixture to start reaction and the absorbance of the mixture at 340 nm (A<sub>340</sub>) was recorded. The reduction of OD value was used to calculate the hydrogenase activity.

#### 1.2.3.3. *Reagents*

The reaction system for determining soluble hydrogenase (SH) activity

Table 1-5. The reaction system for determining soluble hydrogenase (SH) activity.

	Reagents	Volume (mL)
1	Reaction buffer*	1.84
2	100 mM Na - dithionite	0.02
3	Cell free extract (Soluble fraction)	0.10
4	100 mM NAD <sup>+</sup>	0.04
	Total	2.00 mL
	*Reaction buffer : 50 mM HEPES buffer pH 7.0	

#### 1.2.3.4. *Calculations*

The following formula was used to calculate Hydrogenase activity:

$$\text{Units/ml Enzyme} = \frac{(\Delta A_{340\text{nm}} / \text{min Test} - \Delta A_{340\text{nm}} / \text{min Blank})(2)(\text{df})}{(6.22)(0.1)}$$

2 = total volume (in mililiters) of assay

df = dilution factor

6.22 = millimolar extinction coefficient of β-NADH at 340 nm

0.1 = Volume (in mililiters) of enzyme used

$$\text{Units/mg protein} = \frac{\text{units/ml enzyme}}{\text{mg protein/ml enzyme}}$$

#### 1.2.3.5. Unit definition

One unit (1U) Soluble Hydrogenase (SH) was defined as the amount of enzyme that reduces 1.0  $\mu\text{mol}$  of  $\text{NAD}^+$  per minute.

#### 1.2.4. Benzyl viologen reducing activity by membrane- bound hydrogenase (MBH)

**1.2.4.1. Principle:** Membrane-bound hydrogenase (MBH) activity was routinely determined in a continuous spectrophotometric assay following the enzyme-, substrate-, and time-dependent reduction of oxidized benzyl viologen at  $\lambda = 600 \text{ nm}$ . Following the increase of reduced Benzyl Viologen (BV) by monitoring the  $A_{600}$  (the extinction coefficient at this wavelength is  $8.30 \text{ mM}^{-1} \text{ cm}^{-1}$ ), the enzymatic activity was measured [27, 28].

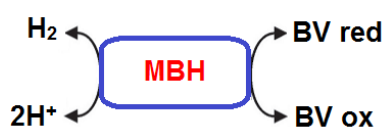


Figure 1-8. The reaction system for determining membrane-bound hydrogenase activity

#### 1.2.4.2. Condition: $T = 50^{\circ}\text{C}$ , $\text{pH} = 7.0$ ; $A_{600}$ , light path = 1cm

The reaction component was put into a glass cuvette (5 mL) with the total volume of 2 mL. The reaction buffer was used as a blank; the reaction was performed at  $50^{\circ}\text{C}$  as follows:

Reaction buffer (1,940  $\mu\text{L}$  of 50 mM K-phosphate buffer pH 7.0) was added into glass cuvette, capped by a rubber stop and sealed by an aluminium cap. After  $\text{H}_2$  was bubbled for 5 minutes, cuvette was pre-incubated for over 5 minutes at  $50^{\circ}\text{C}$ . Then, 50  $\mu\text{L}$  of cell membrane fraction (MF) was added and the cuvette was held in the spectrophotometer for 5 minutes at  $50^{\circ}\text{C}$  to allow temperature equilibration. Finally, 50  $\mu\text{L}$  of Benzyl Viologen (400 mM) was added into the assay mixture to start reaction and the absorbance of the mixture at 600 nm ( $A_{600}$ ) was recorded. The reduction of OD value was used to calculate the membrane- bound hydrogenase activity.

#### 1.2.4.3. Reagents

The reaction system for determining membrane-bound hydrogenase (MBH) activity

Table 1-6. The reaction system for determining MBH activity

	Reagents	Volume (mL)
1	Reaction buffer*	1.90
2	Membrane fraction (MF)	0.05
3	400 mM BV	0.05
	Total	2.00
	*Reaction buffer : 50 mM K-phosphate buffer pH 7.0	

#### 1.2.4.4. Calculation

The following formula was used to calculate MBH activity:

$$\text{Units/ml Enzyme} = \frac{(\Delta A_{600\text{nm}} / \text{min Test} - \Delta A_{600\text{nm}} / \text{min Blank})(2)(\text{df})}{(8.3)(0.05)}$$

2 = total volume (in mililiters) of assay

df = dilution factor

8.3 = millimolar extinction coefficient of Benzyl Viologen at 600 nm

0.05 = Volume (in mililiters) of enzyme used

$$\text{Units/mg protein} = \frac{\text{units/ml enzyme}}{\text{mg protein/ml enzyme}}$$

#### 1.2.4.5. Unit definition

One unit (1U) MBH was defined as the amount of enzyme that reduces 1.0  $\mu\text{mol}$  of Benzyl Viologen per minute.

### 1.3. Results and discussions

1.3.1. The growth of *Hydrogenophilus thermoluteolus* TH-1 under autotrophic, heterotrophic or mixotrophic condition with various organic substrates.

#### 1.3.1.1. Autotrophic growth

The growth curve was obtained when *H. thermoluteolus* TH-1 was cultured autotrophically in mineral-salts medium under gas components H<sub>2</sub>: O<sub>2</sub>: CO<sub>2</sub> (75%: 10%: 15%). Under autotrophic condition, the maximum specific growth rate was seen in logarithmic phase after 3 hours of lag phase. The maximum growth rate ( $\mu_{max}$ ) was  $0.60\ h^{-1}$ , at 50°C. This result confirmed that TH-1 can grow autotrophically favourably with gas components H<sub>2</sub>: O<sub>2</sub>: CO<sub>2</sub> (75%: 10%: 15%).

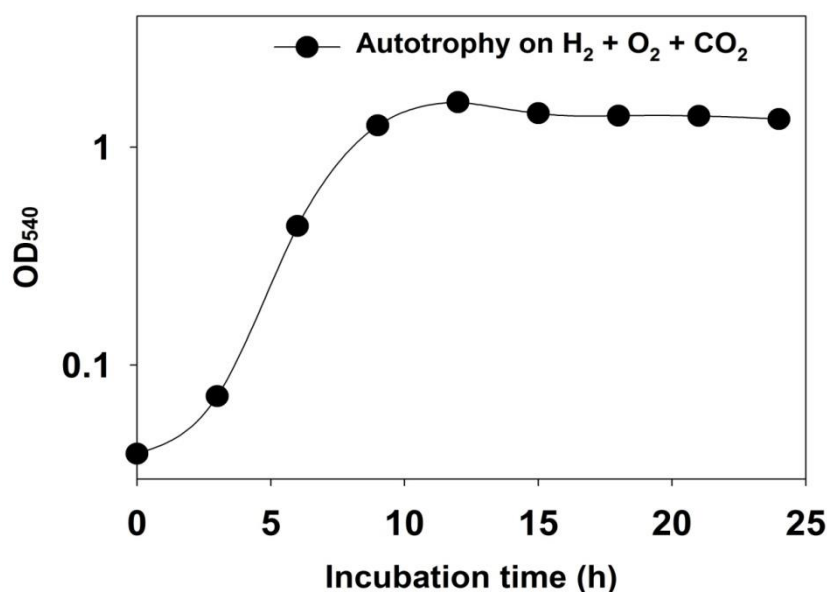


Fig.1-9. The growth curves of TH-1 under autotrophic condition with mineral-salts medium, with gas components (H<sub>2</sub>: O<sub>2</sub>: CO<sub>2</sub> (75%: 10%: 15%))

#### 1.3.1.2. Heterotrophic growth

The heterotrophic growth of cells with formate, glyoxylate, glycerol, glutamate, citrate, glucose or fructose was not seen. The reason may be because these substrates are difficult to be incorporated.

Table 1-7. Specific growth rate of TH-1 under heterotrophic condition

Substrate	$\mu_{\max}$
Malate 15 mM	0.73
Autotrophic ( $H_2 + CO_2$ )	0.60
Butyrate 15 mM	0.48
Acetate 30 mM	0.39
Pyruvate 20 mM	0.28
2-oxoglutarate 12 mM	0.19
Glycerol 20 mM	0.19
Glyoxylate 30 mM	0.10
Glucose 10 mM	0.08
Glutamate 12 mM	0.08
Formate 60 mM	0.07
Citrate 10 mM	0.06
Fructose 10 mM	0.02

The growth curves were obtained when *H. thermoluteolus* TH-1 were cultured heterotrophically with acetate, butyrate, malate, and pyruvate (Figure 1-10, 1-11). With the equivalent carbon concentration to 60 mM, the best heterotrophic growth of strain TH-1 was obtained in malate condition. The maximum growth rate under heterotrophic condition was  $0.73\ h^{-1}$ . This value was seen in logarithmic phase after 3 hours of lag phase. The maximum growth rate under heterotrophic condition with malate was significantly different from that under heterotrophic condition with acetate ( $\mu_{\max}$ :  $0.39\ h^{-1}$ ), butyrate ( $\mu_{\max}$ :  $0.48\ h^{-1}$ ), or pyruvate ( $\mu_{\max}$ :  $0.28\ h^{-1}$ ) (Table 1-7).

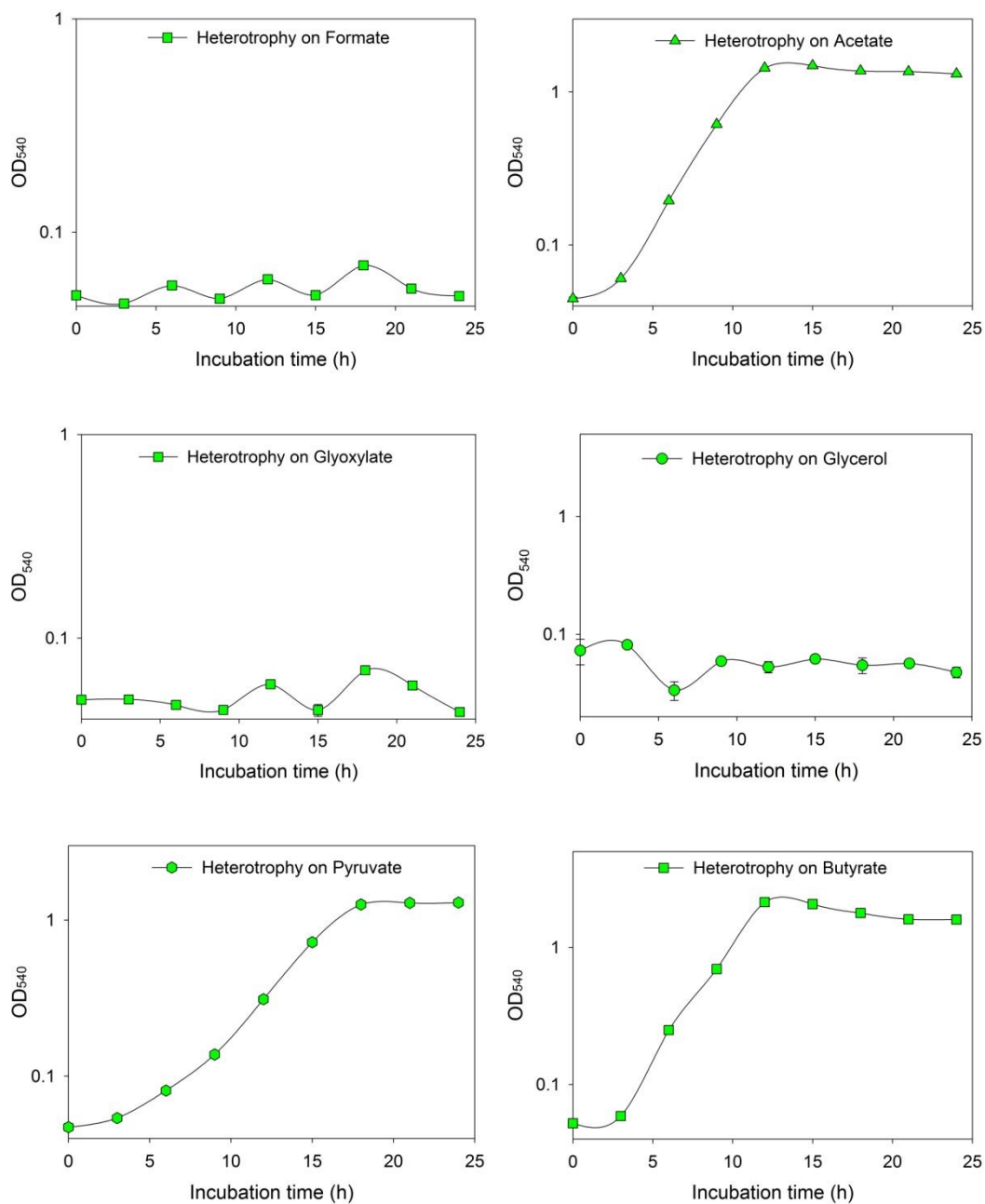


Fig.1-10. The growth curves of *H. thermoluteolus* TH-1 under heterotrophic condition with formate, acetate, glyoxylate, glycerol, pyruvate, butyrate. Ordinate is a logarithmic scale.

Especially, from results of growth curve, strain TH-1 showed a better ability in growth under autotrophic condition than one in acetate, butyrate, or pyruvate.

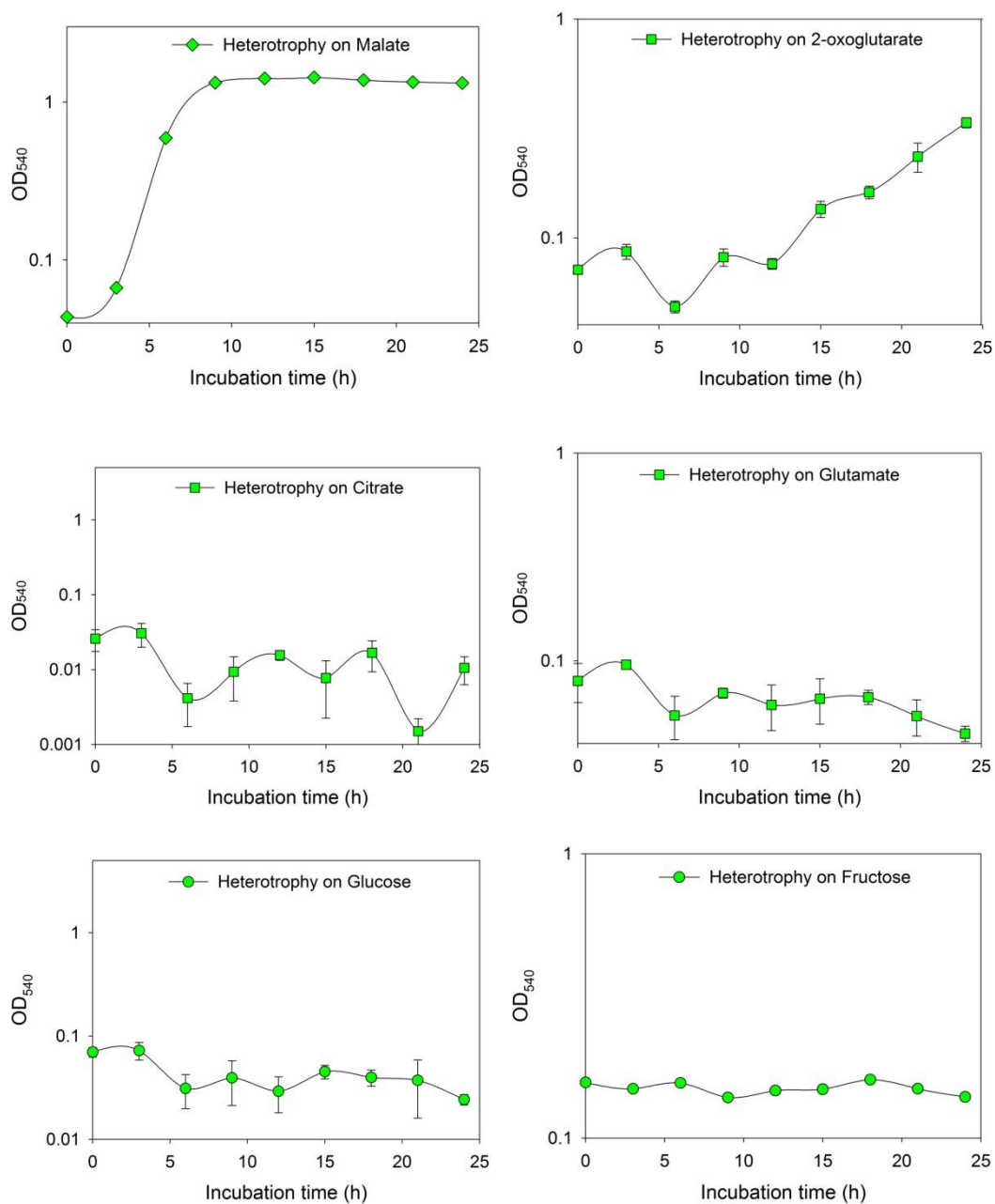


Figure 1-11. The growth curves of *H. thermoluteolus* TH-1 under heterotrophic condition with malate, 2-oxoglutarate, citrate, glutamate, glucose, fructose. Ordinate is a logarithmic scale.

### 1.3.1.3. Mixotrophic growth

Table 1-8. Specific growth rate of TH-1 under mixotrophic condition

Substrate	$\mu_{\max}$
Malate 15 mM	1.00
Pyruvate 20 mM	0.80
Autotrophic	0.60
Glutamate 12 mM	0.43
Citrate 10 mM	0.42
Glucose 10 mM	0.41
2-oxoglutarate 12 mM	0.41
Glycerol 20 mM	0.41
Butyrate 15 mM	0.16
Formate 60 mM	0.07
Fructose 10 mM	0.06
Glyoxylate 30 mM	0.05
Acetate 30 mM	0.05

Growth experiment under mixotrophic condition was performed with the medium and gas phase as under autotrophic condition with the addition of only one organic acid.

The growth curves were obtained when *H. thermoluteolus* TH-1 was cultured mixotrophically with malate, pyruvate, glutamate, citrate, 2-oxoglutarate, glucose, or glycerol (Figure 1-12, 1-13). The mixotrophic growth with malate was favorable. The maximum growth rate under mixotrophic condition with malate was  $1.0\ h^{-1}$ . This result correlated with the growth of strain TH-1 in malate under heterotrophic condition.

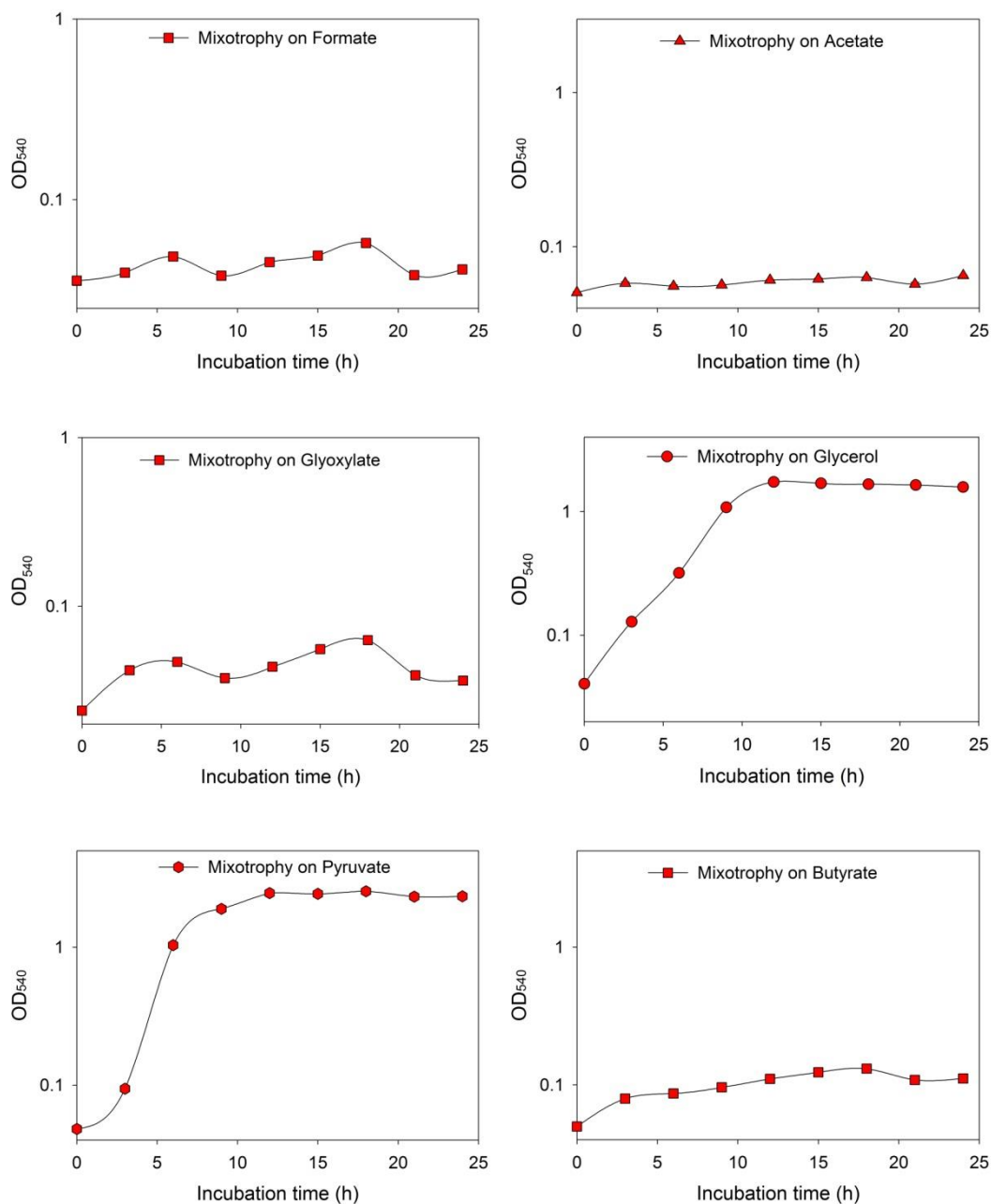


Fig.1-12. The growth curves of *H. thermoluteolus* TH-1 under mixotrophic condition with formate, acetate, glyoxylate, glycerol, pyruvate, or butyrate. Incubation was performed under 75% H<sub>2</sub>, 10% O<sub>2</sub>, 15% CO<sub>2</sub>. Ordinate is a logarithmic scale.

With formate, glyoxylate, or fructose the growth of strain TH-1 was inhibited completely not only in heterotrophic but also in mixotrophic condition (Figure 1-12, 1-13). The growth of bacteria could not be seen even gas mixture H<sub>2</sub>, O<sub>2</sub> and CO<sub>2</sub> was available.

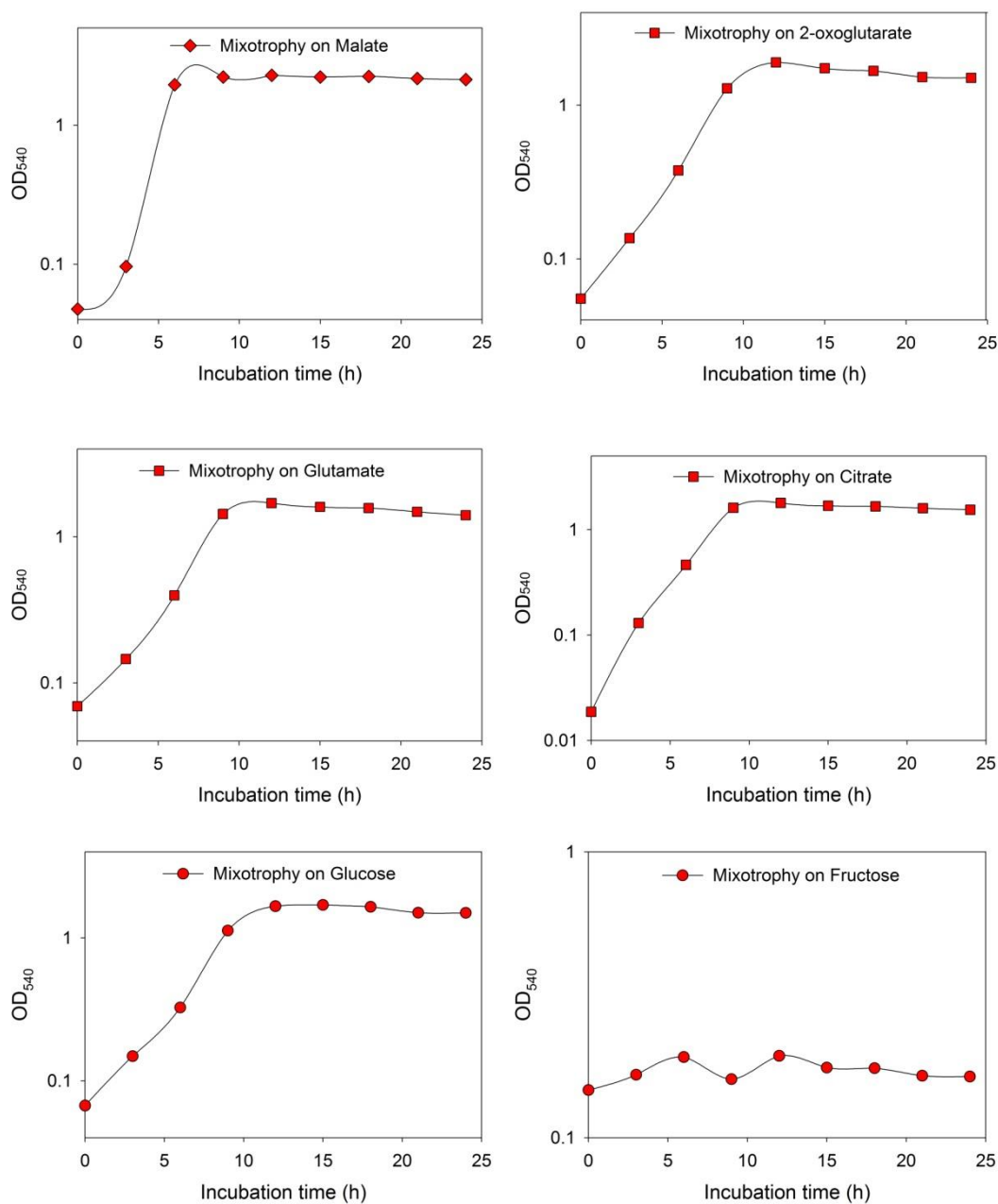


Fig.1-13. The growth curves of *H. thermoluteolus* TH-1 under mixotrophic condition with malate, 2-oxoglutarate, citrate, glutamate, glucose, fructose. Incubation was performed under 75% H<sub>2</sub>, 10% O<sub>2</sub>, 15% CO<sub>2</sub>. Ordinate is a logarithmic scale.

Under heterotrophic condition with glutamate, citrate, or glucose, the growth of strain TH-1 was not seen. However, under mixotrophic condition, the growth of strain TH-1 in these substrates was clearly observed. The bacterium could grow in the presence of

glutamate, citrate, glucose, 2-oxoglutarate or glycerol with maximum specific growth rate  $0.43\ h^{-1}$ ,  $0.42\ h^{-1}$ ,  $0.41\ h^{-1}$ ,  $0.41\ h^{-1}$ ,  $0.41\ h^{-1}$ , respectively. (Table 1-8).

Surprisingly, under mixotrophic condition, the growth under pyruvate became more favorable.  $\mu_{max}$  increased from  $0.28\ h^{-1}$  under heterotrophic condition to  $0.80\ h^{-1}$  under mixotrophic condition. On the other hand, the growth on acetate or butyrate under mixotrophic condition was inhibited. Within 24 hours,  $\mu_{max}$  drastically decreased from  $0.39\ h^{-1}$  and  $0.48\ h^{-1}$  under heterotrophic condition to  $0.05\ h^{-1}$  and  $0.16\ h^{-1}$  under mixotrophic condition.

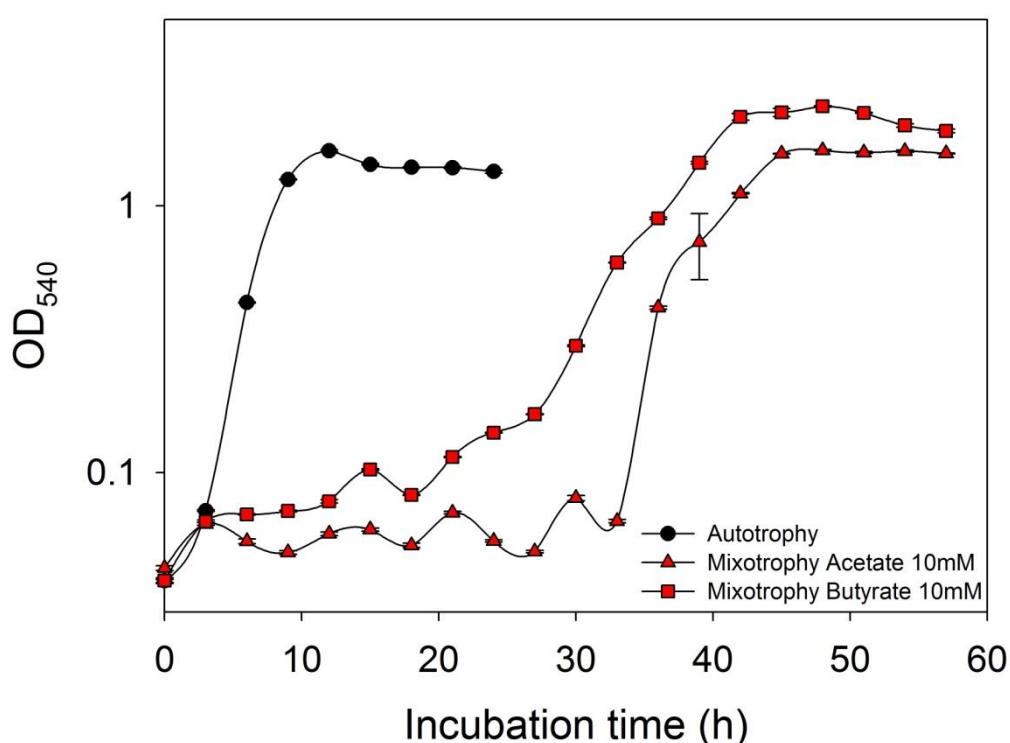


Figure 1-14. The growth curves of *H. thermoluteolus* TH-1 under autotrophic and mixotrophic conditions with acetate or butyrate. Incubation was performed under 75% H<sub>2</sub>, 10% O<sub>2</sub>, 15% CO<sub>2</sub>. Ordinate is a logarithmic scale.

Interestingly, under mixotrophic condition with butyrate (10 mM) or acetate (10 mM) was used, a long lag phase was observed before vigorous growth (Figure 1-14). In case of mixotrophic growth with butyrate, lag phase continued until 27 hours. With acetate, lag phase lasted for 33 hours.

### 1.3.2. RubisCO activity

RubisCO activity under autotrophic condition was significantly higher than that of under mixotrophic conditions but the activity was not detected under heterotrophic conditions. RubisCO enzymatic activity was highest under autotrophic condition; it was  $0.19 \pm 0.01$  unit/mg protein. This result confirmed that under autotrophic condition, the fixation of carbon dioxide was conducted at high level. RubisCO could also be measured under mixotrophic condition with acetate, butyrate, malate, or pyruvate (Appendix Table 1-9). During mixotrophic growth with acetate or butyrate, a long lag phase was seen. However, once the cells of strain TH-1 started to grow, it showed RubisCO activity higher than that of under mixotrophic growth with malate or pyruvate (Figure 1-16).

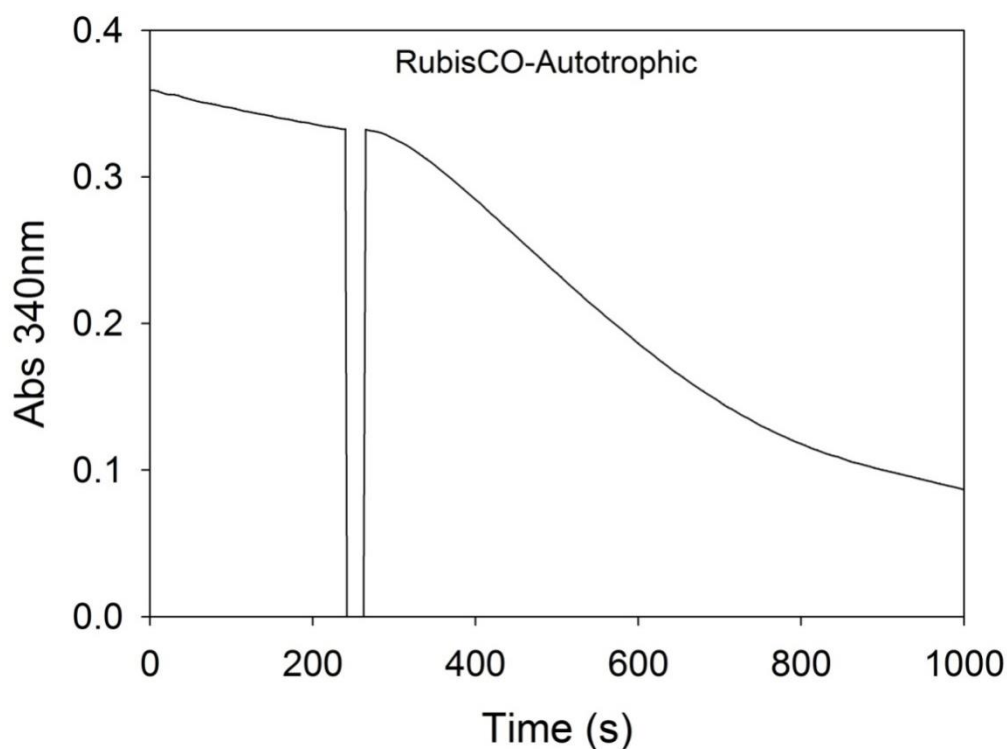


Figure 1-15. The absorbance at wavelength 340 nm of the NADH was decreased with cell-free extract of cells grown autotrophically.

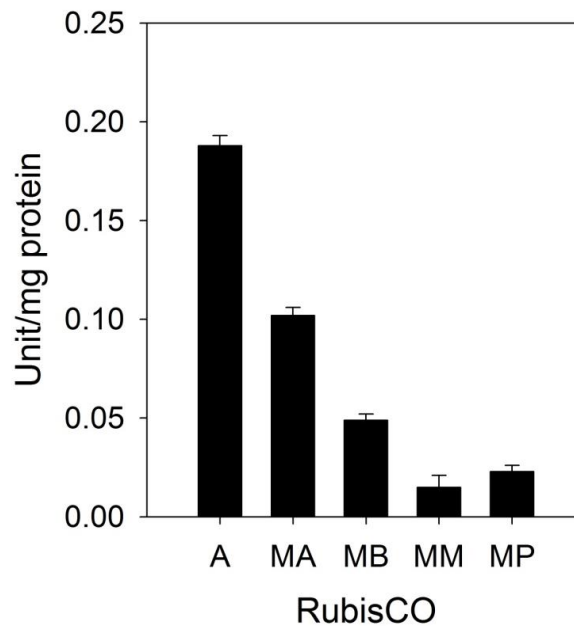


Figure 1-16. RubisCO activity in cell-free extract of cells grown under autotrophic (A) or mixotrophic condition with acetate (MA), butyrate (MB), malate (MM), or pyruvate (MP).

The result that no RubisCO activity was seen in cell-free extract of strain TH-1 cells grown heterotrophically suggests that CBB cycle was derepressed under heterotrophic condition.

### 1.3.3. Hydrogenase activity

Following the alignment of strain TH-1 genome with *Ralstonia eutropha*, it was suggested that strain TH-1 genome contains a similar hydrogenase system to that of *R. eutropha*. To demonstrate that TH-1 has a hydrogenase system with membrane-bound hydrogenase and soluble hydrogenase, the hydrogenase assay was carried-out with cell-free extract and membrane fraction.

As I expected, hydrogenase activity was obtained with both fractions. Moreover, the total activity of membrane-bound hydrogenase was  $0.40 \pm 0.01$  unit/g cell, 2.5-fold higher than that of cell-free extract fraction ( $0.16 \pm 0.01$  unit/g cell). This result implies that during autotrophic growth, ATP is highly demanded. Therefore, membrane-bound hydrogenase dominates over soluble hydrogenase in strain TH-1.

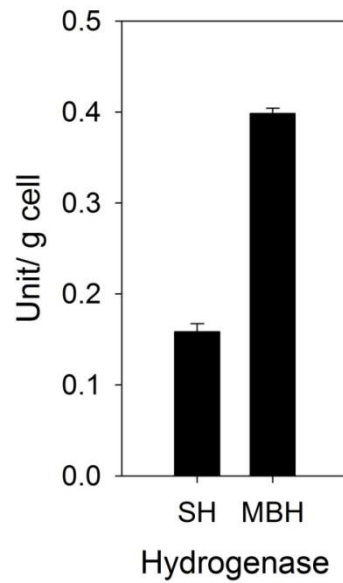


Figure 1-17. Hydrogenase activity, membrane-bound hydrogenase (MBH) and soluble hydrogenase (SH) in cells TH-1 grown under autotrophic condition.

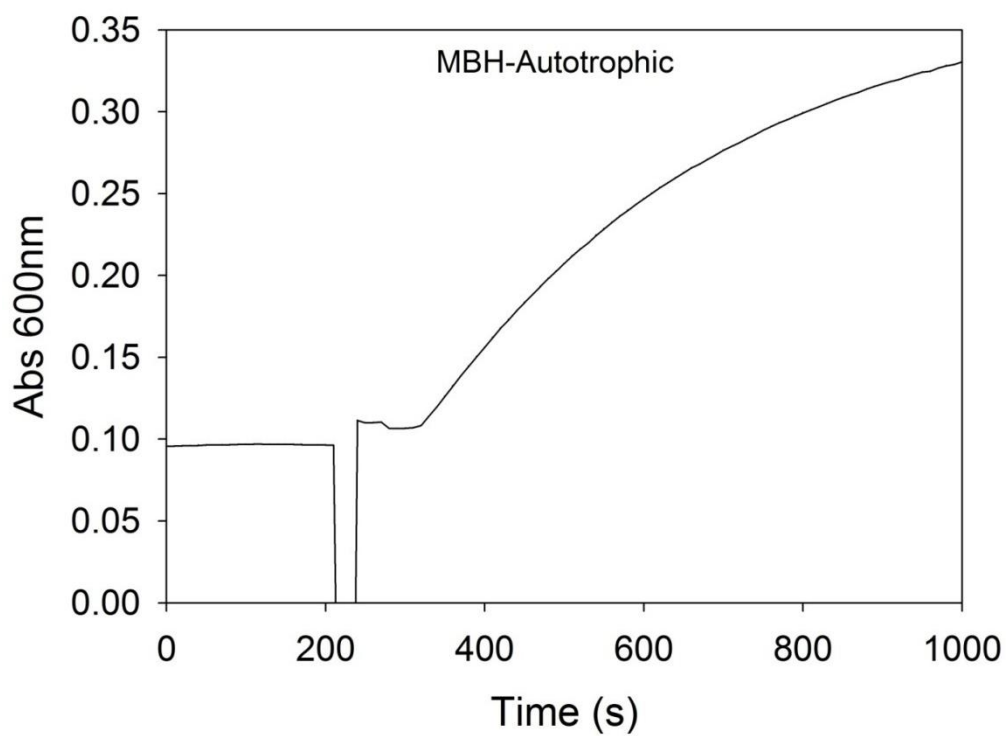


Figure 1-18. The absorbance at wavelength 600 nm of the Benzyl viologen caused by the activity of membrane-bound hydrogenase (MBH).

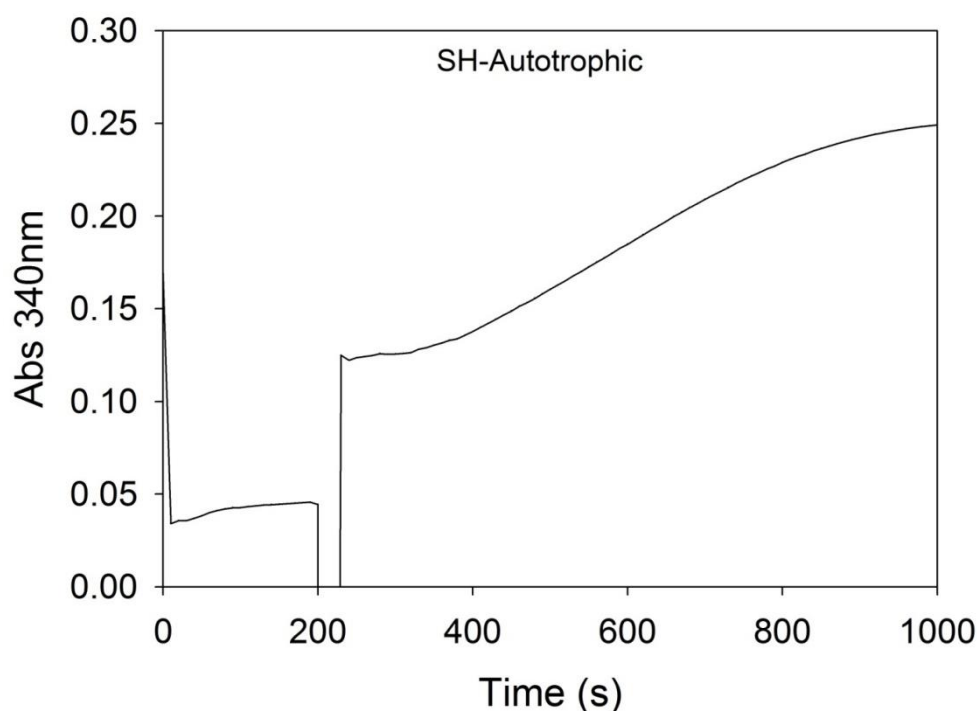


Figure 1-19. The absorbance change at wavelength 340 nm caused by the activity of soluble hydrogenase (SH).

#### 1.4. Conclusions

In this chapter, the capacity to utilize various substrates under different modes of growth was investigated under autotrophic, heterotrophic, or mixotrophic condition. The result shows that *H. thermoluteolus* TH-1 is a flexible bacterium. Most Gram-negative facultative autotrophs grow heterotrophically using organic substrates better than autotrophically [4]. However, strain TH-1 showed better growth rate under autotrophic condition compared with heterotrophic condition using various organic acids. This is the desirable feature for using in biotechnological applications. It not only grows autotrophically with  $H_2$  as energy source and  $CO_2$  as a sole carbon source, but also utilizes many kinds of organic substrates such as acetate, butyrate, malate, or pyruvate for heterotrophic or mixotrophic growth (when  $H_2$ ,  $O_2$ , and  $CO_2$  are available). The maximum specific growth rate determined under autotrophic condition was  $0.6\ h^{-1}$ . Cells of strain TH-1 showed the ability to grow favorably with malate

under heterotrophic, or mixotrophic condition with corresponding maximum growth rate  $0.73\ h^{-1}$  and  $1.0\ h^{-1}$ , respectively.

Under mixotrophic condition with acetate or butyrate, a long lag phase was seen. This phenomenon may come from some inhibitory effect when  $CO_2$  and the intermediate metabolite which are derived from acetate or butyrate metabolism appear at the same time. Long time of growth delay before the start of robust growth implies that the cells might come up with solution for the problem.

RubisCO activity was highest under autotrophic condition when compared with that of under mixotrophic condition, suggesting that CBB cycle under autotrophic condition operates at high level for carbon dioxide fixation.

The hydrogenase activity was obtained in both membrane fraction and cell-free extract, confirming the existence of membrane-bound hydrogenase and soluble hydrogenase in TH-1.

## **Chapter 2. The operation of glyoxylate cycle in acetate/butyrate metabolism under heterotrophic condition**

### **2.1. Introduction**

In chapter 1, I noticed an interesting phenomenon that strain TH-1 can grow heterotrophically with acetate/butyrate. However, under mixotrophic condition, the growth of strain TH-1 was unfavorable. A long lag phase was observed when strain TH-1 grows mixotrophically. The inhibition phenomenon similarly occurred when strain TH-1 consumed acetate or butyrate for mixotrophic growth, implying that acetate or butyrate has the same route for metabolism. Therefore, it is interesting to investigate the metabolism of acetate or butyrate in strain TH-1.

The biosynthesis of cell constituents in all living cell starts from a few so-called precursor metabolites that include the C<sub>2</sub> compound acetyl-CoA, the C<sub>3</sub> compound pyruvate (or phosphoenolpyruvate), the C<sub>4</sub> compound oxaloacetate, and the C<sub>5</sub> compound 2-oxoglutarate. In bacterial cells, most carbon is derived from pyruvate/phosphoenolpyruvate (about 50%), acetyl-CoA (about 30%), oxaloacetate (about 13%), and 2-oxoglutarate (about 7%) [30]. Pyruvate and phosphoenolpyruvate are the major carbon sources because they are the intermediate metabolites belonging to the gluconeogenesis pathway leading to cell wall components and nucleotides. The bacteria growing by utilizing the carbon sources that are not metabolized through pyruvate or PEP will face trouble. The trouble comes from the lack of necessary intermediates that are required for TCA cycle operation or substrates used to synthesize cellular building blocks [14]. Anaplerotic pathway is the alternative pathway that replenishes the intermediates in metabolic pathway such as TCA cycle through generating malate or oxaloacetate [31]. In acetate/butyrate metabolism, the operations of TCA cycle together with the operation of respiratory chain supplies the energy for microorganism to grow. However, in terms of carbon metabolism, gluconeogenesis pathway is utilized to synthesize cellular materials. The conversion of acetyl-CoA to cell carbon constituents is referred as acetyl-CoA assimilation. Many microorganisms have been reported to grow heterotrophically or mixotrophically (in

the presence of CO<sub>2</sub>) by using acetate by employing one of three acetate assimilation pathways: the glyoxylate cycle, pyruvate: ferredoxin oxidoreductase (pyruvate synthase) or ethylmalonyl-CoA pathway [31]. All three pathways also generate malate or oxaloacetate, the metabolites belonging to TCA cycle.

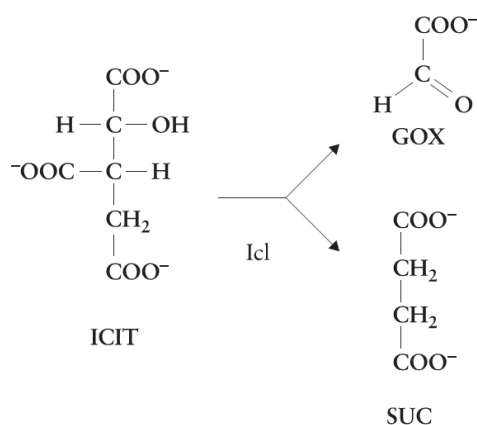
The glyoxylate cycle is more preferable than pyruvate: ferredoxin oxidoreductase or ethylmalonyl-CoA pathway. It shares many intermediate substrates with TCA cycle such as malate, oxaloacetate, citrate, isocitrate, and succinate. These intermediates replenish TCA cycle or become precursor for many synthetic pathways. Another point is that glyoxylate cycle is energetically favourable than pyruvate: ferredoxin oxidoreductase or ethylmalonyl-CoA pathway. Pyruvate: ferredoxin oxidoreductase requires ferredoxin for fixing CO<sub>2</sub> to acetyl-CoA to produce pyruvate, which is converted into oxaloacetate through pyruvate carboxylase, or into malate through malic enzyme. In case of ethylmalonyl-CoA pathway, it consumes 2 NADPH to assimilate 3 acetyl-CoA and 2 CO<sub>2</sub> to generate 1 malate, and 1 succinyl-CoA. On the other hand, glyoxylate cycle fixes 2 acetyl-CoA to generate 1 malate. When succinate or malate is converted into fumarate or oxaloacetate, respectively, it can produce reducing equivalent. Glyoxylate cycle also plays a critical role in the regulation of energy flow in bacterial cells.

Pyruvate: ferredoxin oxidoreductase (POR) is an enzyme that catalyzes the ferredoxin-dependent carboxylation of acetyl-CoA to pyruvate or the ferredoxin-dependent decarboxylation of pyruvate to acetyl-CoA [32]. In the bacteria lacking glyoxylate cycle, POR is necessary for acetate assimilation. In order to convert acetate into pyruvate, both carbon dioxide and acetate are assimilated. The POR utilizes ferredoxins with low redox potential, thus enabling it to catalyze the reaction where pyruvate is synthesized from acetyl-CoA. Energy that is supplemented for this enzymatic activity comes from ferredoxin. Therefore, this pathway is distributed mostly among anaerobic bacteria [31], or the bacteria that employ reductive TCA cycle for CO<sub>2</sub> fixation such as *Hydrogenobacter thermophilus* TK-6 [32].

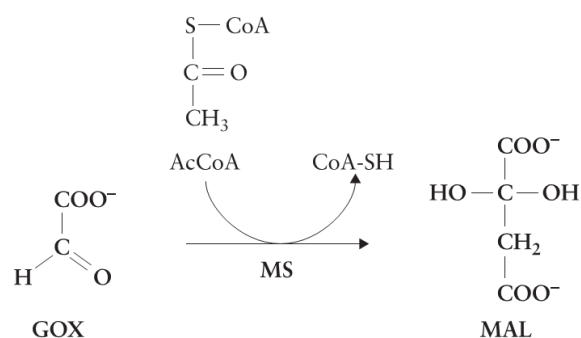
The ethylmalonyl-CoA pathway (EMC pathway) is a central carbon metabolism for many  $\alpha$ -proteobacteria, isocitrate lyase-negative bacteria like *Rhodobacter*

*sphaeroides* and *Methylobacterium extorquens* as well as actinomycetes (*Streptomyces* spp.). Its function is to convert acetyl-CoA, a central carbon intermediate, to other metabolites for cell carbon biosynthesis. So, the ethylmalonyl-CoA pathway represents an alternative to the glyoxylate cycle [33].

The glyoxylate cycle, sometime called as glyoxylate pathway or glyoxylate shunt [34], is a metabolic pathway by which organism can synthesize carbohydrates from C<sub>2</sub> compound [35]. Since the first discovery by Kornberg and Krebs in 1957, glyoxylate cycle is found to be widespread and well documented in archaea, bacteria, protists, plants, fungi and nematode until now [36]. Most microorganisms that utilize acetate or other fatty acids as sole carbon source employ glyoxylate cycle for biosynthesis of precursors of cell component [37]. This cycle plays a critical role as an anaplerotic pathway since it by-passes the CO<sub>2</sub>-generating steps of TCA cycle. Glyoxylate cycle contains five reaction steps in which it shares three steps with TCA cycle. The unique enzymes of this route are isocitrate lyase (threo-D<sub>s</sub>-isocitrate-glyoxylate-lyase, EC 4.1.3.1) and malate synthase (L -malate glyoxylate-lyase, EC 4.1.3.2) [34, 38]. In this cycle, isocitrate undergoes an aldol cleavage to succinate and glyoxylate by isocitrate lyase as:



The following step is the combination of acetyl-CoA and glyoxylate to generate L-malate by the catalysis of malate synthase as [34]:



By each turn of operation for glyoxylate cycle, 2 mol of acetyl-CoA is introduced, resulting in the synthesis of 1 mol of four-carbon compound oxaloacetate [37]. For the next turn, oxaloacetate plays a role as a substrate for citrate synthase. By this way, acetyl-CoA is incorporated to the metabolism net when the microorganism utilizes acetate, ethanol, fatty acids or poly- $\beta$ -hydroxybutyrate as a carbon source [36].

In any case, pyruvate synthase or EMC pathway was only used for acetate assimilation in the bacteria which lack glyoxylate cycle. By using pyruvate synthase or ethylmalonyl-CoA pathway for acetate assimilation, it also includes the assimilation of carbon dioxide or bicarbonate. There exists an energy barrier when the microorganisms employ those pathways for acetate assimilation. Energetically unfavorable feature may explain why ethylmalonyl-CoA pathway is rare distributed in the bacteria domain.

Currently, strain TH-1 draft genome data are available for analysis. The genome analysis shows that strain TH-1 possesses a putative pyruvate: ferredoxin oxidoreductase (contig00003\_orf00259). In addition, the analysis also shows the existence of gene coding isocitrate lyase (contig00010\_orf00035). However, no information about malate synthase was found in strain TH-1 genome. Then, the search for malate synthase in genome of strain TH-1 was conducted. I found that contig00004\_orf00057 was 75 percent homologous to malate synthase of *R. eutropha*. Therefore, contig00004\_orf00057 is a potential putative malate synthase of strain TH-1. Malate synthase is divided into two distinct classes. *AceB* encodes the A-form, and the *glcB* encodes the G-form [37]. The multiple alignments of the nucleotide sequences of putative malate synthase from *H. thermoluteolus* TH-1 followed by phylogenetic tree construction was conducted (contig00004\_orf00057) with 13

corresponding malate synthase sequences from A-form and G-form. The result shown in figure 2-1 suggested that strain TH-1 malate synthase belongs to A-form group.

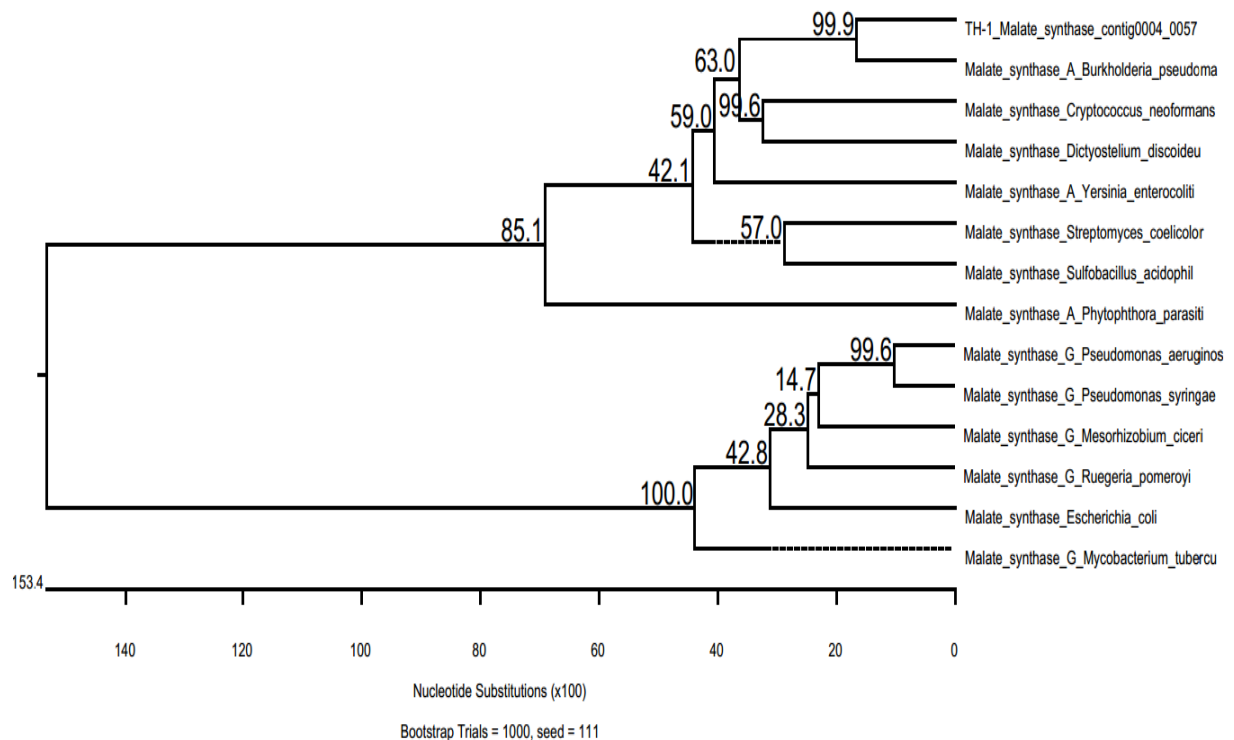


Figure 2-1. Phylogenetic tree of malate synthase from *H. thermoluteolus* and their related sequences from NCBI. Sequences are separated into two classes for tree construction: class A-form and class G-form.

The alignment of the partial deduced amino sequences of malate synthase gene from *H. thermoluteolus* TH-1 (contig00004\_orf00053) was carried-out with the nearest A-form malate synthase from *Burkholderia pseudomallei* K96243 (Genbank accession no.CAH36194.1) in the phylogenetic tree. The result showed high homology between strain TH-1 malate synthase and A-form malate synthase from *Burkholderia pseudomallei* K96243. It suggested that malate synthase of strain TH-1 belongs to A-form class of malate synthase.

```

Malate_synthase_A_Burkholderia      MTTTLKLPQGMAITGEIKPGYEAILTPEALELVAKLHRQFELRRRELLAA
TH-1_Malate_synthase_contig000      -----MHPRFDEILTPEALSFVAKLHRKFEPRRQELLRA
                                     ::* :: *****.:*****:* *:*:* *
Malate_synthase_A_Burkholderia      RVERTQRLDAGERPDFLAETKSIREGDWKIAPLPADLQCRVEITGPV-E
TH-1_Malate_synthase_contig000      RVERQARIDAGEMPNFLPETAHIREGDWKIAPVPKALECRRVEITGPASD
                                     **** *:**** *:*.* *****:* *:*****. :
Malate_synthase_A_Burkholderia      RKMIINALNSGADSYMTDFEDSNAPSWTNQIDGQINLKDAVRRRTISLEQ-
TH-1_Malate_synthase_contig000      RKMVINAFNSGADSYMTDFEDANSPNWFNQIQGQINVDYDAIRRIDFVAE
                                     ***:***:*****:*.:. * *:***: *:*** *.:
Malate_synthase_A_Burkholderia      NGKSYKLNDKIATLIVRPRGWLDEKHSVTVDGQRVSGGVDFDFFLFLFHNA
TH-1_Malate_synthase_contig000      NGKEYKLNKIAVLQIRPRGWLDEKHSVTVDGQRVSGGLDFDGLAFFHNA
                                     ***.***:***.* :***** *****:***.* :****
Malate_synthase_A_Burkholderia      QELIARGSGPYFYLPKMESHLEARLWNDIFVAAQEALGVPRGTIRATVLI
TH-1_Malate_synthase_contig000      KEQIARGAGPFYFYPKLENHLEARLWNDVFHFAEDELGLPRGTIKATVLI
                                     :* ****:***:***:*.*****:* *: :*:*****:*****
Malate_synthase_A_Burkholderia      ETILAAFEMDEILYELREHSSGLNAGRWDYIFSAIKKFKNDRDFCLADRA
TH-1_Malate_synthase_contig000      ETILAAFEMEEILYELRDHSAGLNAGRWDYIFSCIKKFKKNKDFCLADRN
                                     *****:*****:*.*****:*****:*.*****
Malate_synthase_A_Burkholderia      KITMTVPFMRAYALLLKTCHKRNAPAIIGMSALIPKNDPEANDRAMAG
TH-1_Malate_synthase_contig000      LITMEVPFMRAYALSVVKACHKRGAPAIIGMSALIPKNDPEANARALEG
                                     *** ***** :*:***.***** ***** *: *
Malate_synthase_A_Burkholderia      VRADKARDAGDGYDGGWVAHPGLVSLAMEEFVKVLGDKPNQIGKQRDDVQ
TH-1_Malate_synthase_contig000      VRKDKRRDANDGFDGGWVAHPGLVPIAMEEFVAVLGDKNQWEKQR-TET
                                     ** ** **.**:*****.***** ***** **
Malate_synthase_A_Burkholderia      IEGKNLLDFQPEAPITEAGLRNNINVGIIHYLGSWLAGNGCVPIHNLMEDA
TH-1_Malate_synthase_contig000      FTAKELLDFRPEQPIITEAGLRNNINVAIHYLGAWLNGGAVAIHNLMEDA
                                     :. *:***:*** *****:*** **.*.*****
Malate_synthase_A_Burkholderia      ATAEISRSQVQWQWIRSPKGTLDGRKVTAEVLVREYAKVELANVQVVG-
TH-1_Malate_synthase_contig000      ATAEIARSQVQWQWVYSPKGILTGRKVTAEVLVRLPIEELDKVKAVVAAQ
                                     *****:*****: **** * *****. ** :** **..
Malate_synthase_A_Burkholderia      --DTAPYDRAAAIFEQMSTSENFTFLTLPLYEEI-
TH-1_Malate_synthase_contig000      GEPLETYEQAAQIFEKIALDPEFPEFTLTLPLYEAMP
                                     .*:** ***:.. . :*.***** :

```

Figure 2-2. The alignment of the partial deduced amino sequences of malate synthase gene from *H. thermoluteolus* TH-1 (contig00004\_orf00053) with the nearest A-form malate synthase from *Burkholderia pseudomallei* K96243 (Genbank accession no.CAH36194.1)

Moreover, genes coding glyoxylate metabolism in strain TH-1 were found when blasting genome of strain TH-1 to Kyoto Encyclopedia of Genes and Genomes-GenomeNet database (KEGG). In figure 2-3, isocitrate lyase (EC. 4.1.3.1) and malate synthase (EC. 2.3.3.9) are shown.

These evidences suggest the existence of glyoxylate cycle in strain TH-1 and also suggest that it can function when strain TH-1 grows with acetate or butyrate.

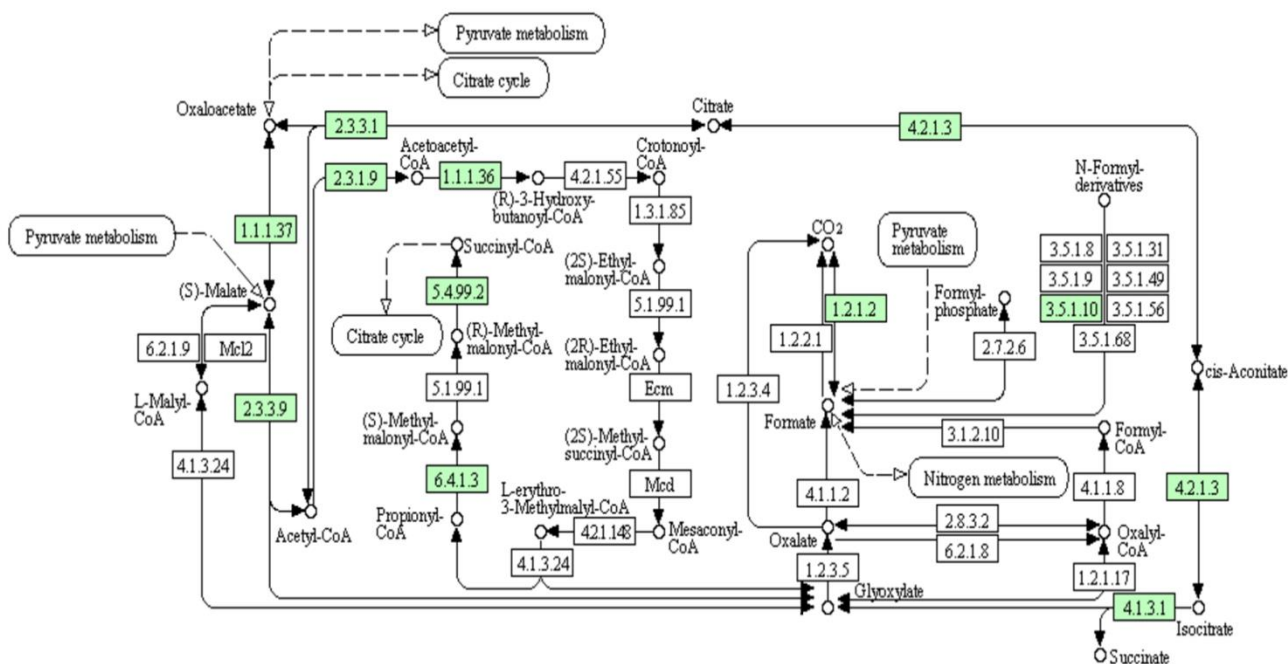


Figure 2-3. Glyoxylate and two carboxylic acid metabolism. This figure was from KEGG pathway database (<http://www.genome.jp/kegg/pathway.html>). Green boxes indicate the genes that exist in TH-1 genome.

Glyoxylate cycle is an important pathway for acetate fixation, and it plays an important role as an anaplerotic pathway to replenish immediate substrates for TCA cycle. Pyruvate: ferredoxin oxidoreductase also functions as acetate accumulation pathway by incorporation  $\text{CO}_2$  to acetate to generate pyruvate. The interesting points are that genes involving two acetate accumulation pathways (glyoxylate cycle and pyruvate: ferredoxin oxidoreductase) are present in the genome of strain TH-1.

This chapter focuses on investigation of the function of glyoxylate cycle under heterotrophic condition with acetate/butyrate. The key enzymatic activities of glyoxylate cycle were measured for isocitrate lyase and malate synthase. Furthermore, the enzymatic activities were compared with those of cells grown under heterotrophic condition with malate or pyruvate.

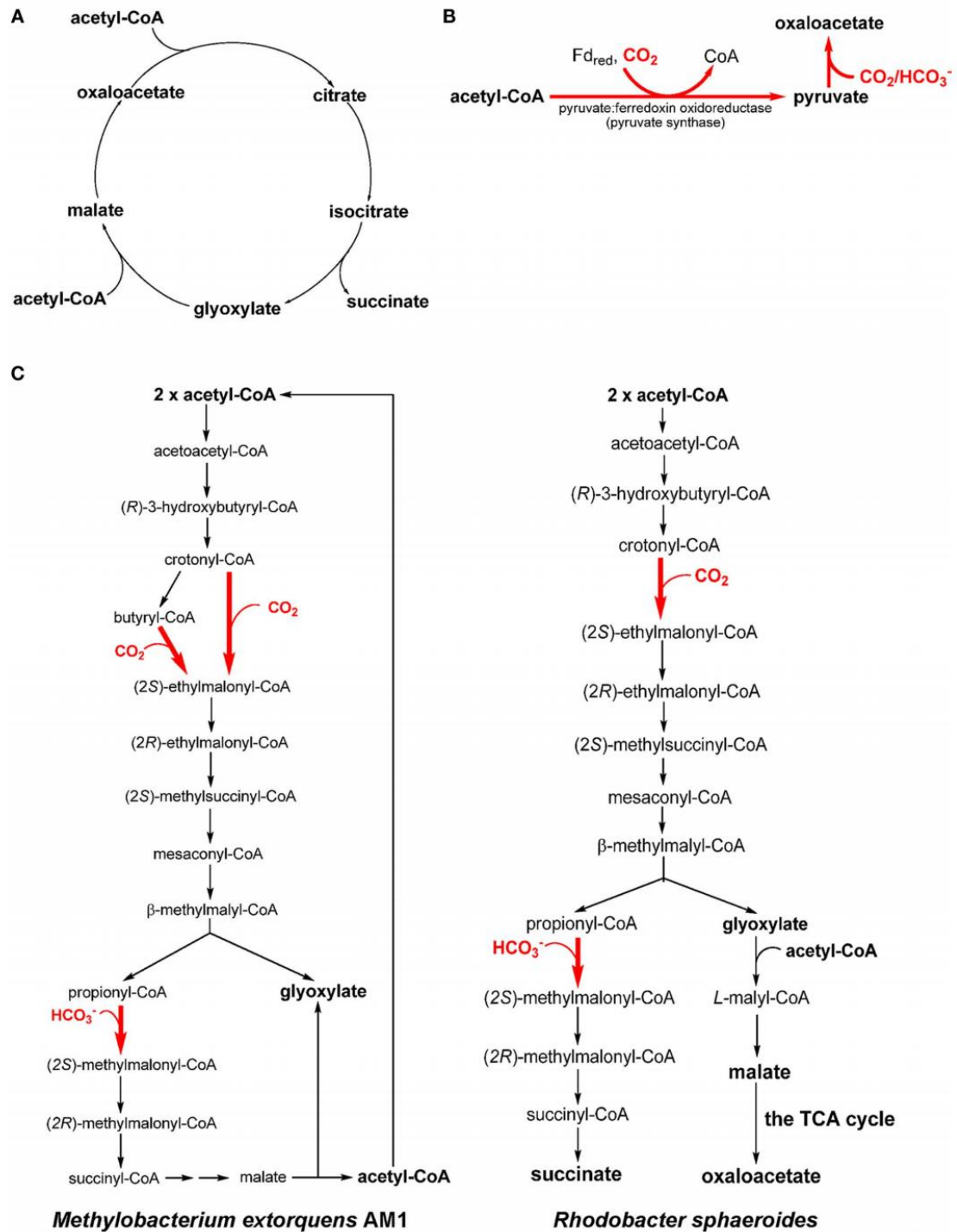


Figure 2-4. Three acetate assimilation pathways, the (oxidative) glyoxylate cycle (A), the reaction catalyzed by pyruvate synthase (B) and the ethylmalonyl-CoA pathway (C) [31].

## 2.2. Materials and methods

### 2.2.1. Bacterial strains and growth condition

Bacterial strains and growth condition is similar to part 1.2.1 in chapter 1.

Cell-free extract preparation for enzymatic activity assay is similar to part 1.2.1.3 in chapter 1.

### 2.2.2. Enzymatic assay of pyruvate dehydrogenase (PDH) [EC:1.2.4.1]

**2.2.2.1. Principle:** Pyruvate dehydrogenase activity was routinely determined in a continuous spectrophotometric assay following the enzyme-, substrate-, and time-dependent reduction of  $\beta$ -NAD<sup>+</sup> at wavelength of 340 nm. This protocol was modified from Brown, J.P., et al, 1976 protocol [39]. By following the reduction of  $\beta$ -NAD<sup>+</sup> by monitoring the  $A_{340}$  (the extinction coefficient of  $\beta$ -NADH at this wavelength is 6.22 mM<sup>-1</sup> cm<sup>-1</sup>), the enzymatic activity was measured.

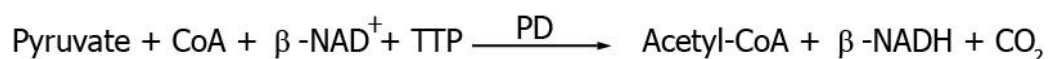


Figure 2-5. The reaction system for determining pyruvate dehydrogenase activity

#### 2.2.2.2. Condition: T = 50°C, pH = 7.4; $A_{340}$ , light path = 1cm

The reaction was prepared in a glass cuvette with the total volume of 1 mL. The reaction buffer was used as a blank; the reaction was performed at 50°C. CFE of 20  $\mu$ L was added to 930  $\mu$ L of assay mixture (the components are shown in Table 2-1) and all mixtures were degassed and flushed with Argon gas for 5 minutes. Twenty  $\mu$ L of  $\beta$ -NAD<sup>+</sup> was supplied and the cuvette was held in the spectrophotometer for 5 minutes to allow temperature equilibration. Finally, sodium pyruvate was added into the assay mixture to start the reaction and the absorbance of the mixture at 340nm ( $A_{340}$ ) was recorded to give a background rate of  $\beta$ -NAD<sup>+</sup> reduction. The reduction of OD value was used to calculate the PDH activity.

### 2.2.2.3. *Reagents*: The reaction system for determining PDH activity

Table 2-1. The reaction system for determining PDH activity.

	Reagents	Volume (mL)
1	Reaction buffer*	0.82
2	2.5 mM Coenzyme A	0.02
3	20 mM TTP	0.05
4	Cell free extract	0.04
5	250 mM $\beta$ -NAD <sup>+</sup>	0.02
6	200 mM Sodium pyruvate	0.05
	*Reaction buffer: 150 mM MOPS HCl buffer pH 7.4 at 30°C supplement MgCl <sub>2</sub> 2 mM, CaCl <sub>2</sub> 0.03 mM and L-Cystein solution 8 mM.	

### 2.2.2.4. *Calculations*

The following formula was used to calculate PDH activity:

$$\text{Units/ml Enzyme} = \frac{(\Delta A_{340\text{nm}} / \text{min Test} - \Delta A_{340\text{nm}} / \text{min Blank})(1)(\text{df})}{(6.22)(0.04)}$$

1 = total volume (in mililiters) of assay

df = dilution factor

6.22 = millimolar extinction coefficient of  $\beta$ -NADH at 340 nm

0.04 = Volume (in mililiters) of enzyme used

$$\text{Units/mg protein} = \frac{\text{units/ml enzyme}}{\text{mg protein/ml enzyme}}$$

### 2.2.2.5. *Unit definition*

One unit (1U) PDH was defined as the amount of enzyme that reduces 1.0  $\mu\text{mol}$  of  $\beta$ -NAD<sup>+</sup> per minute

## 2.2.3. Enzymatic assay of pyruvate oxidoreductase (POR) [EC:1.2.7.1]

**2.2.3.1. *Principle*:** POR activity was routinely determined in a continuous spectrophotometric assay following the enzyme-, substrate-, and time-dependent reduction of oxidized benzyl viologen at  $A_{600}$ . This protocol was from Dorner, E., et al, 2002 protocol [40]. The increase of  $A_{600}$  (the extinction coefficient at this wavelength is  $8.3 \text{ mM}^{-1} \text{ cm}^{-1}$ ) was used for measuring the enzymatic activity.



Figure 2-6. The reaction system for determining pyruvate oxidoreductase activity

2.2.3.2. *Condition:* T = 50°C, pH = 7.6; A<sub>600</sub>, light path = 1cm

The reaction was prepared in a glass cuvette with the total volume of 1 mL. The reaction buffer was used as the blank; the reaction was performed at 50°C. CFE of 20 µL was added to 930 µL of assay mixture (the components are shown in Table 2-2) and all mixtures were degassed and flushed with Argon gas for 5 minutes. Twenty µL of BV was added and the cuvette was held in the spectrophotometer for 5 minutes to allow temperature equilibration. Finally, 50 µL of sodium pyruvate was added into the assay mixture to start reaction and the absorbance of the mixture at 600 nm (A<sub>600</sub>) was recorded to give a background rate of BV reduction. The reduction of OD value was used to calculate the POR activity.

2.2.3.3. *Reagents:* The reaction system for determining POR activity

Table 2-2. The reaction system for determining POR activity.

	Reagents	Volume (mL)
1	Reaction buffer*	0.89
2	2.5 mM Coenzyme A	0.02
3	Cell free extract	0.02
4	250 mM Benzyl viologen	0.02
5	200 mM Sodium pyruvate	0.05
	*Reaction buffer : 100 mM Phosphate buffer pH 7.6 supplement MgCl <sub>2</sub> 2 mM and Dithiothreitol 1 mM	

2.2.3.4. *Calculations*

The following formula was used to calculate POR activity:

$$\text{Units/ml Enzyme} = \frac{(\Delta A_{600\text{nm}} / \text{min Test} - \Delta A_{600\text{nm}} / \text{min Blank})(1)(\text{df})}{(8.3)(0.02)}$$

1 = total volume (in milliliters) of assay

df = dilution factor

8.3 = millimolar extinction coefficient of Benzyl Viologen at 600 nm

0.02 = Volume (in milliliters) of enzyme used

$$\text{Units/mg protein} = \frac{\text{units/ml enzyme}}{\text{mg protein/ml enzyme}}$$

#### 2.2.3.5. Unit definition:

One unit (1U) POR was defined as the amount of enzyme that reduces 1.0  $\mu\text{mol}$  of Benzyl Viologen per minute.

#### 2.2.4. Enzymatic assay of isocitrate dehydrogenase ( $\text{NADP}^+$ ) [EC 1.1.1.42]

2.2.4.1. *Principle:* isocitrate dehydrogenase ( $\text{NADP}^+$ ) activity was routinely determined in a continuous spectrophotometric assay following the enzyme-, substrate-, and time-dependent reduction of  $\beta\text{-NADP}^+$  at wavelength 340 nm. This protocol was from Karr, D. B., et al, 1984 protocol [41]. By following the increase of the  $A_{340}$  (the extinction coefficient of  $\beta\text{-NADH}$  at this wavelength is  $6.22 \text{ mM}^{-1} \text{ cm}^{-1}$ ), the enzymatic activity was measured.

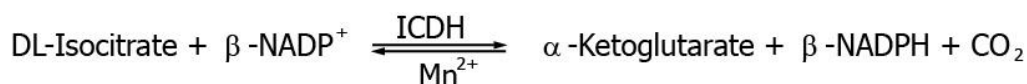


Figure 2-7. The reaction system for determining isocitrate dehydrogenase activity

#### 2.2.4.2. Conditions: $T = 50^\circ\text{C}$ , $\text{pH} = 7.4$ , $A_{340 \text{ nm}}$ , Light path = 1 cm

The reaction was prepared in a glass cuvette with the total volume of 3 mL. The reaction buffer was used as the blank; the reaction was performed at  $50^\circ\text{C}$ . CFE of 10  $\mu\text{L}$  was added to 2,640  $\mu\text{L}$  of assay mixture (the components are shown in Table 2-3) and incubated for 5 minutes at  $50^\circ\text{C}$ . Then, 150  $\mu\text{L}$  of  $\beta\text{-NADP}^+$  was added and the cuvette was held in the spectrophotometer for 5 minutes to allow temperature equilibration. Finally, 200  $\mu\text{L}$  of DL-Isocitrate acid was added into the assay mixture to start the reaction and the absorbance of the mixture at 340 nm ( $A_{340}$ ) was recorded to give a background rate of oxidized NADPH reduction. The reduction of OD value was used to calculate the isocitrate dehydrogenase activity.

#### 2.2.4.3. Reagents:

Table 2-3. The reaction system for determining isocitrate dehydrogenase activity.

	Reagents	Volume (mL)
1	Deionized Water	1.95
2	Reaction Buffer *	0.59
3	6.6 mM DL-Isocitric Acid	0.20
4	20 mM $\beta$ -NADP <sup>+</sup>	0.15
5	18 mM Manganese Chloride	0.10
6	CFE	0.01
	Total	3.0
	*Reaction buffer: 250 mM Glycylglycine Buffer, pH 7.4 at 50°C. Prepare 50 ml in deionized water using Gly-Gly, Free Base. Adjust to pH 7.4 at 37°C with 1 M NaOH.)	

#### 2.2.4.4. Calculations

$$\text{Units/ml Enzyme} = \frac{(\Delta A_{340\text{nm}} / \text{min Test} - \Delta A_{340\text{nm}} / \text{min Blank})(3)(\text{df})}{(6.22)(0.01)}$$

3 = total volume (in mililiters) of assay

df = dilution factor

6.22 = millimolar extinction coefficient of  $\beta$ -NADH at 340 nm

0.01 = Volume (in mililiters) of enzyme used

$$\text{Units/mg protein} = \frac{\text{units/ml enzyme}}{\text{mg protein/ml enzyme}}$$

#### 2.2.4.5. Unit definition:

One unit (1U) was defined as amount of enzyme that converts 1.0  $\mu$ mole of isocitrate to  $\alpha$ -ketoglutarate per minute at pH 7.4 at 50°C.

#### 2.2.5. Enzymatic assay of isocitrate lyase [EC: 4.1.3.1]

**2.2.5.1 Principle:** isocitrate lyase activity was routinely determined in a continuous spectrophotometric assay. As the result of lyase activity, isocitrate lyase cleaves isocitrate to succinate and glyoxylate. By adding phenylhydrazine in the reaction mixture, the generated glyoxylate combines with phenylhydrazine to create a colored product, Phenylhydrazone Glyoxylate. This protocol was modified from Dixon, G. H.

and Kornberg, H. L., 1959 protocol [42]. By following the increase of absorbance of performing Phenylhydrazone Glyoxylate by monitoring the  $A_{324\text{nm}}$  (the extinction of Phenylhydrazone Glyoxylate coefficient at this wavelength is  $16.8 \text{ mM}^{-1} \text{ cm}^{-1}$ ), the isocitrate lyase enzymatic activity was measured.

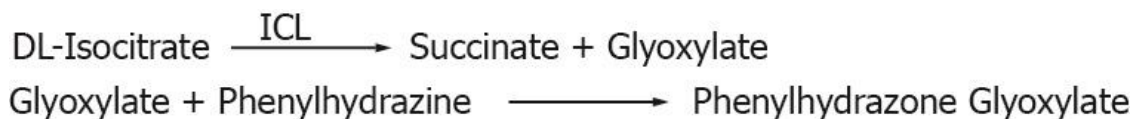


Figure 2-8. The reaction system for determining isocitrate lyase activity

#### 2.2.5.2. Conditions: T=50°C, pH=6.8, $A_{324 \text{ nm}}$ , light path=1cm

The reaction was prepared in a glass cuvette with the total volume of 1 mL. The reaction buffer was used as the blank; the reaction was performed at 50°C. CFE of 10  $\mu\text{L}$ , 790  $\mu\text{L}$  of assay mixture (the components are shown in Table 2-4), and 100  $\mu\text{L}$  of phenylhydrazine HCl (40 mM) was added and the cuvette was held in the spectrophotometer for 5 minutes to allow temperature equilibration. Finally, 100  $\mu\text{L}$  of DL-Isocitric acid was added into the assay mixture to start the reaction. Mixing by inversion was done. The absorbance of the mixture at 324 nm ( $A_{324\text{nm}}$ ) was recorded to give a background phenylhydrazone glyoxylate. The increasing of OD value was used to calculate the isocitrate lyase activity.

#### 2.2.5.3. Reagents

Table 2-4. The reaction system for determining isocitrate lyase activity.

	Reagents	Volume (mL)
1	Reaction buffer	0.59
2	50 mM $\text{MgCl}_2$	0.10
3	10 mM EDTA	0.10
4	40 mM Phenylhydrazine HCl	0.10
5	CFE	0.01
6	10mMDL-IsocitricAcidSolution	0.10
	Total	1.00
Reaction buffer: 50 mM Imidazole Buffer, pH 6.8 at 50°C. Prepared 50 mL in deionized waster using Imidazole. Adjusted to pH 6.8 at 50°C with 1 M HCl.		

#### 2.2.5.4. Calculations

$$\text{Units/ml Enzyme} = \frac{(\Delta A_{324\text{nm}} / \text{min Test} - \Delta A_{324\text{nm}} / \text{min Blank})(1)(\text{df})}{(16.8)(0.01)}$$

1 = total volume (in milliliters) of assay

df = dilution factor

16.8 = millimolar extinction coefficient of Phenylhydrazine Glyoxylate at 324 nm

0.01 = Volume (in milliliters) of enzyme used

$$\text{Units/mg protein} = \frac{\text{units/ml enzyme}}{\text{mg protein/ml enzyme}}$$

#### 2.2.5.5. Unit definition

One unit (1U) was defined as amount of enzyme that catalyzes the formation of 1  $\mu\text{mol}$  of glyoxylate per minute at pH 6.8 at 50°C.

#### 2.2.6. Enzymatic assay of malate synthase [EC: 4.1.3.2]

**2.2.6.1. Principle:** malate synthase activity was routinely determined in a continuous spectrophotometric assay. As the result of malate synthase activity, malate synthase condenses acetyl-CoA and glyoxylate to generate malate and releases CoA group. By supplying 5,5'-dithio-bis(2-nitrobenzoic acid) (DTNB) in the reaction buffer mixture, the releasing Co-A group immediately combines with 5,5'-dithio-bis(2-nitrobenzoic acid) to create a colour product as 5-thio-2-nitrobenzoic acid at wavelength 412 nm. This protocol was modified from Dixon, G. H. and Kornberg, H. L., 1959 protocol [42]. By following the increase of the  $A_{412}$  (the extinction of 5-thio-2-nitrobenzoic acid coefficient at this wavelength is  $13.6 \text{ mM}^{-1} \text{ cm}^{-1}$ ), the malate synthase enzymatic activity was measured.

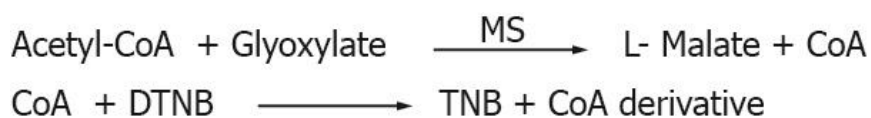


Figure 2-9. The reaction system for determining malate synthase activity. Abbreviation used: Acetyl-CoA, Acetyl-Coenzyme A; CoA, CoenzymeA; DTNB, 5, 5'-dithio-bis (2-nitrobenzoic acid); TNB, 5-thio-2-nitrobenzoic acid.

2.2.6.2. *Conditions:* T=50°C, pH8.0, A<sub>412nm</sub>, light path = 1

The reaction was prepared in a glass cuvette with the total volume of 1 mL. The reaction buffer was used as the blank; the reaction was performed at 50°C. CFE of 100 µL was added to 700 µL of assay mixture (the components are shown in Table 2-5), and was incubated for 5 minutes at 50°C, then 100 µL of DTNB (2 mM) was added and the cuvette was held in the spectrophotometer for 5 minutes to allow temperature equilibration. Finally, 100µL of Glyoxylic Acid (10 mM) was added into the assay mixture to start reaction. Mixed by inversion and equilibrated to 50°C. The absorbance of the mixture at 412 nm (A<sub>412nm</sub>) was recorded to give a background. The increase of OD value was used to calculate the malate synthase activity.

2.2.6.3. *Reagents*

Table 2-5. The reaction system for determining malate synthase activity.

	Reagents	Volume (mL)
1	Reaction buffer	0.50
2	100 mM MgCl <sub>2</sub>	0.10
3	2.5 mM Acetyl-CoA	0.10
4	10 mM Glyoxylic Acid	0.10
5	2 mM DTNB	0.10
6	CFE	0.10
	Total	1.0
Reaction buffer: 50 mM Imidazole Buffer, pH 8.0 at 50°C: Prepared 50 ml in deionized water using Imidazole. Adjusted to pH 8.0 at 50°C with 1 M HCl. 2 mM 5,5'-Dithio-bis(2-Nitrobenzoic Acid) Solution (DTNB): Prepared 10 ml in 95% (v/v) Ethanol (EtOH) using 5,5'-Dithio-bis(2- Nitrobenzoic Acid).		

2.2.6.4. *Calculations*

$$\text{Units/ml Enzyme} = \frac{(\Delta A_{412\text{nm}} / \text{min Test} - \Delta A_{412\text{nm}} / \text{min Blank})(1)(\text{df})}{(13.6)(0.1)}$$

1 = total volume (in mililiters) of assay

df = dilution factor

13.6 = millimolar extinction coefficient of TNB at 412 nm

0.1 = Volume (in mililiters) of enzyme used

$$\text{Units/mg protein} = \frac{\text{units/ml enzyme}}{\text{mg protein/ml enzyme}}$$

#### 2.2.6.5. Unit definition

One unit (1U) was defined as amount of enzyme that catalyzes the cleavage of 1.0  $\mu\text{mol}$  of acetyl-CoA per minute at pH 8.0 at 50°C, in the presence of glyoxylate.

#### 2.2.7. Enzymatic assay of malic enzyme [E.C. 1.1.1.40]

**2.2.7.1. Principle:** malic enzyme activity was routinely determined in a continuous spectrophotometric assay following the enzyme-, substrate-, and time-dependent reduction of  $\beta\text{-NADP}^+$  at wavelength 340 nm. This protocol was modified from Geer, B.W., et al, 1980 protocol [43]. Following the increase of reduced  $\beta\text{-NADP}^+$  by monitoring the  $A_{340}$  (the extinction coefficient at this wavelength is  $6.22 \text{ mM}^{-1} \text{ cm}^{-1}$ ), the malic enzyme activity was measured.



Figure 2-10. The reaction system for determining malic enzyme activity

Abbreviations used:

$\beta\text{-NADP}$  =  $\beta$ -Nicotinamide Adenine Dinucleotide Phosphate, Oxidized Form

$\beta\text{-NADPH}$  =  $\beta$ -Nicotinamide Adenine Dinucleotide Phosphate, Reduced Form

#### 2.2.7.2. Conditions: $T = 50^\circ\text{C}$ , $\text{pH} = 7.4$ , $A_{340\text{nm}}$ , light path = 1 cm

The reaction was prepared in a glass cuvette with the total volume of 3 mL. The reaction buffer was used as the blank; the reaction was performed at 50°C. CFE of 100  $\mu\text{L}$  was added to 2,750  $\mu\text{L}$  of assay mixture (the components are shown in Table 2-6), incubated in 5 minutes at 50 °C, 50  $\mu\text{L}$  of  $\beta\text{-NADP}^+$  was added and the cuvette was held in the spectrophotometer for 5 minutes to allow temperature equilibration. Finally, 100  $\mu\text{L}$  of L-Malic acid (100 mM) was added into the assay mixture to start reaction. Mixed by inversion and equilibrated to 50°C. The absorbance of the mixture at 340 nm ( $A_{340\text{nm}}$ ) was recorded to give a background rate of NADPH reduction. The reduction of OD value was used to calculate the malic enzyme activity.

### 2.2.7.3. Reagents

Table 2-6. The reaction system for determining malic enzyme activity.

	Reagents	Volume (mL)
1	Reaction buffer	2.00
2	100 mM L-Malic acid	0.10
3	20 mM $\beta$ -NADP <sup>+</sup>	0.05
4	20 mM Manganese Chloride Solution (MnCl <sub>2</sub> )	0.75
5	Cell free extract	0.10
6	Total	3.00
Reaction buffer: 100 mM Triethanolamine HCl Buffer, pH 7.4 at 50 °C. Prepared 50 ml in deionized water using Triethanolamine, Hydrochloride; adjusted to pH 7.4 at 50°C with 1 M NaOH.		

### 2.2.7.4. Calculations

$$\text{Units/ml Enzyme} = \frac{(\Delta A_{340\text{nm}} / \text{min Test} - \Delta A_{340\text{nm}} / \text{min Blank})(3)(\text{df})}{(6.22)(0.1)}$$

3 = total volume (in mililiters) of assay

df = dilution factor

6.22 = millimolar extinction coefficient of  $\beta$ -NADPH at 340 nm

0.1 = Volume (in mililiters) of enzyme used

$$\text{Units/mg protein} = \frac{\text{units/ml enzyme}}{\text{mg protein/ml enzyme}}$$

### 2.2.7.5. Unit definition

One unit (1U) was defined as amount of enzyme that converts 1.0  $\mu\text{mol}$  of L-malate and  $\beta$ -NADP to pyruvate, CO<sub>2</sub> and  $\beta$ -NADPH per minute at pH 7.4 at 50 °C.

## 2.3. Results and discussions

2.3.1. Growth profile of strain TH-1 under heterotrophic condition: This experiment has already been reported in chapter 1. I compared autotrophic growth with heterotrophic growth with different organic substrates. The growth experiments under heterotrophic conditions were performed in the air atmosphere using the medium similar to the autotrophic condition but with the addition of only one organic acid as substrate. The organic acid was acetate ( $C_2$ ), pyruvate ( $C_3$ ), butyrate ( $C_4$ ), or malate ( $C_4$ ). The equivalent carbon concentration to organic acid in culture medium was 60 mM. Under autotrophic condition, strain TH-1 gave a maximum specific growth rate of  $0.60\ h^{-1}$  at  $50^\circ C$ . Under heterotrophic conditions, growth was observed with acetate, pyruvate, butyrate, and malate (Fig. 2-11). The highest growth rate was  $0.73\ h^{-1}$  when the bacterium grew with malate.

For enzymatic activity measurement assay, bacteria were harvested at late of logarithmic phase where optical density at wavelength 540 nm was 0.8-1.0.

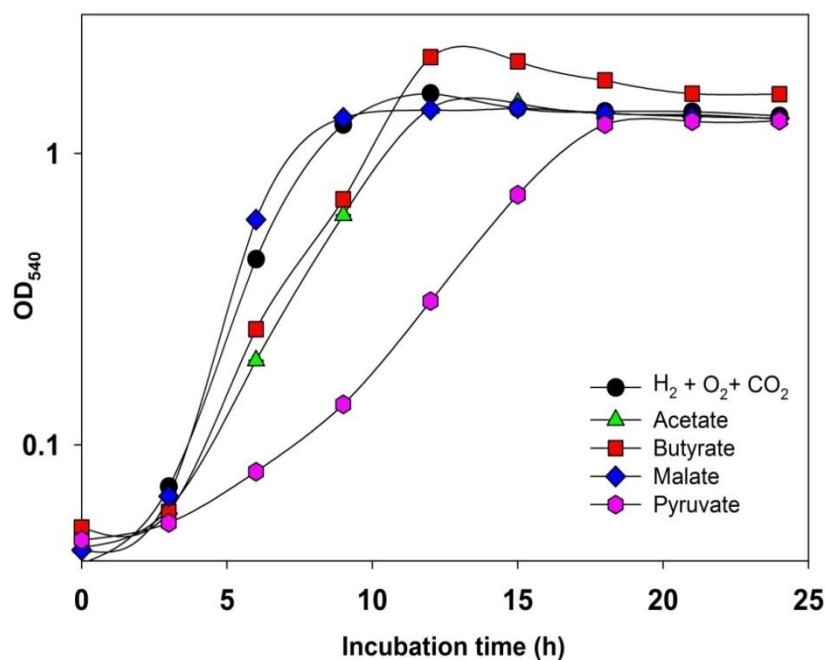


Figure 2-11. The growth curves of strain TH-1 under autotrophic or heterotrophic condition

Pyruvate is an important metabolite both in carbon metabolism and energy metabolism. For energy metabolism, pyruvate is oxidized in TCA cycle for gaining ATP and reducing equivalent. For carbon metabolism, pyruvate is an important precursor for many kinds of amino acids such as lysine, leucine, isoleucine, alanine, valine [34]. Pyruvate is the connecting point of glycolysis/gluconeogenesis pathway. There are many different pathways that use pyruvate as a starting material. In gluconeogenesis, pyruvate is converted directly to PEP, or converted into PEP via OAA by the function of pyruvate carboxylase. Pyruvate could also be converted into lactate, which is catalyzed by lactate dehydrogenase.

### 2.3.2. Pyruvate dehydrogenase and pyruvate: ferredoxin oxidoreductase activity

Table 2-7. Enzymatic activities in cell-free extracts of *H. thermoluteolus* TH-1 were grown autotrophically or heterotrophically with acetate, butyrate, malate, or pyruvate. Activities are expressed in U/mg protein: mean  $\pm$  standard deviation; The abbreviation: PD: pyruvate dehydrogenase; POR: pyruvate: ferredoxin oxidoreductase; ICDH: isocitrate dehydrogenase; ICL: isocitrate lyase; MS: malate synthase; ME: malic enzyme.

Enzyme	Cultivation condition				
	Autotrophic	Heterotrophic			
		Acetate	Butyrate	Malate	Pyruvate
Specific enzymatic activity (Unit/mg protein)					
PD	0.0180 ±0.001	0.0410 ±0.006	0.009 ±0.001	0.0520 ±0.006	0.0280 ±0.003
POR	N.D.	0.0081 ±0.0005	0.0037 ±0.0006	0.0117 ±0.003	0.0136 ±0.001
ICDH	0.1310 ±0.005	0.8780 ±0.055	0.3770 ±0.008	0.9820 ±0.005	0.6680 ±0.041
ICL	0.0110 ±0.002	0.3420 ±0.013	0.1300 ±0.013	0.0210 ±0.001	0.008 ±0.001
MS	0.1720 ±0.007	0.4790 ±0.022	0.5230 ±0.020	0.1840 ±0.013	0.2220 ±0.002
ME	0.0280 ±0.002	0.0440 ±0.003	0.0330 ±0.011	0.0600 ±0.004	0.1080 ±0.005

N.D.: not detected

However, the major fate of pyruvate is to be converted into acetyl-CoA. Pyruvate dehydrogenase (*pdh*) and pyruvate-ferredoxin/flavodoxin oxidoreductase (*por*) are enzymes responsible for conversion between pyruvate and acetyl-CoA. In strain TH-1, via genome analysis I found that both genes coding pyruvate dehydrogenase (*aceE*: contig00006\_orf00155; *aceF*: contig00006\_orf00157) and pyruvate-ferredoxin/flavodoxin oxidoreductase (*por*: contig00003\_orf00259) exist. Hence, the existence of both enzymes is the interesting information. The activity of pyruvate dehydrogenase and pyruvate-ferredoxin/flavodoxin oxidoreductase may be regulated by concentration of CoA-SH, NAD<sup>+</sup>, and pyruvate. Furthermore, pyruvate dehydrogenase is allosterically activated by F1,6P, and inhibited by acetyl-CoA and NADH [14].

Pyruvate dehydrogenase is the enzyme which irreversibly converts pyruvate to acetyl CoA and generates energy via NADH.

Pyruvate dehydrogenase activity was detected in CFE of strain TH-1 cells grown under autotrophic or heterotrophic condition. PDH activity in CFE was highest under heterotrophic condition with malate. Specific activity of PDH in CFE under heterotrophic condition with malate was 0.05±0.01 unit/ mg protein, 2.9-fold higher than that under autotrophic condition. Pyruvate dehydrogenase is the enzyme that converts pyruvate into acetyl-CoA. The reason for the highest PDH activity under heterotrophically with malate may be that acetyl-CoA was required to operate TCA cycle under heterotrophic growth with malate.

On the other hand, pyruvate-ferredoxin/flavodoxin oxidoreductase (POR) is reversible enzyme that functions for synthesis of acetyl-CoA from pyruvate by carboxylase reaction or decarboxylate pyruvate to acetyl-CoA and releasing ferredoxin.

The result that no POR activity was detected under autotrophic condition implies that this enzyme expression was repressed under autotrophic condition. Under heterotrophic growth, only very weak activity of POR was detected.

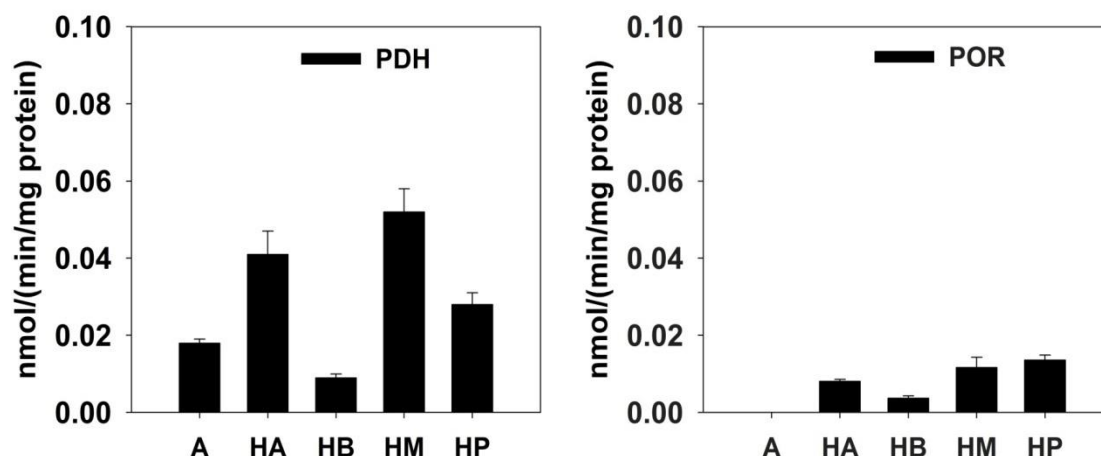


Figure 2-12. Enzymatic activities in cell-free extracts of *H. thermoluteolus* TH-1 grown autotrophically (A) or heterotrophically with acetate (HA), butyrate (HB), malate (HM), pyruvate (HP). The abbreviation: PD: pyruvate dehydrogenase; POR: pyruvate: ferredoxin oxidoreductase.

The POR activity was expected to be high under heterotrophic condition with acetate or butyrate because POR took part in process in which acetyl-CoA was converted into pyruvate. This result indicates that POR is not the enzyme which functions for the main rout of acetate or butyrate metabolism. The highest POR activity under heterotrophic condition with malate and pyruvate was  $0.012 \pm 0.003$  unit/mg protein, and  $0.014 \pm 0.001$  unit/mg protein, respectively. It means that when the cells are grown under heterotrophic condition with malate or pyruvate, POR may catalyze a little conversion of pyruvate into acetyl-CoA, the intermediate required for operating TCA cycle.

### 2.3.3. Isocitrate lyase and malate synthase activity

Glyoxylate cycle or glyoxylate shunt is the pathway including 5 steps in which 3 steps are identical to those of TCA cycle and 2 steps are unique. Two unique steps are catalyzed by 2 key enzymes of this cycle: isocitrate lyase (*aceA*) and malate synthase (*aceB*) [35, 44].

As I expected, high enzymatic activity of isocitrate lyase (ICL) and malate synthase

(MS) were obtained under heterotrophic condition with acetate or butyrate. The ICL activity under heterotrophic condition with acetate and butyrate was  $0.34 \pm 0.01$  unit/mg protein,  $0.13 \pm 0.01$  unit/mg protein, respectively. Apparently, the ICL activity in the strain TH-1 cells grown under heterotrophic condition with acetate was 31-fold higher than that under autotrophic condition. However, isocitrate lyase of glyoxylate cycle is not always high. Interestingly, the ICL activity under heterotrophic condition with malate or pyruvate was very low. The ICL activity under heterotrophic condition with malate and pyruvate was  $0.021 \pm 0.013$  unit/mg protein,  $0.008 \pm 0.001$  unit/mg protein, respectively.

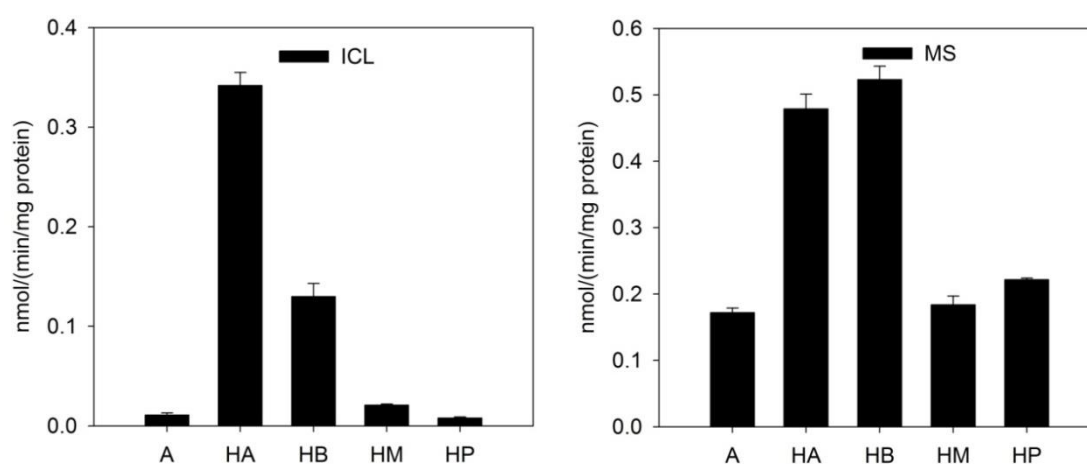


Figure 2-13. Enzymatic activities in cell-free extracts of *H. thermoluteolus* TH-1 were grown autotrophically or heterotrophically with acetate, butyrate, malate, pyruvate. The abbreviation: ICL: isocitrate lyase; MS: malate synthase; ME: malic enzyme. A refers for autotrophic; HA: heterotrophic acetate; HB: heterotrophic butyrate; HM: heterotrophic malate; HP: heterotrophic pyruvate.

The ICL activity in the strain TH-1 cells grown under heterotrophic condition with acetate was 43-fold and 16.3-fold higher than that under heterotrophic condition with pyruvate and malate, respectively. In addition, the ICL activity in the cells TH-1 grown under heterotrophic condition with butyrate was 6.2-fold and 2.6-fold higher than that under heterotrophic condition with pyruvate and malate, respectively. The ICL activity in strain TH-1 grown heterotrophically with acetate and butyrate was

31.1-fold and 11.8-fold higher than that under autotrophic condition. This result emphasizes that genes belong to glyoxylate cycle was up-regulated in the medium containing acetate or butyrate. When the cells of strain TH-1 were grown in the heterotrophic condition with malate or pyruvate, the glyoxylate cycle may be depressed.

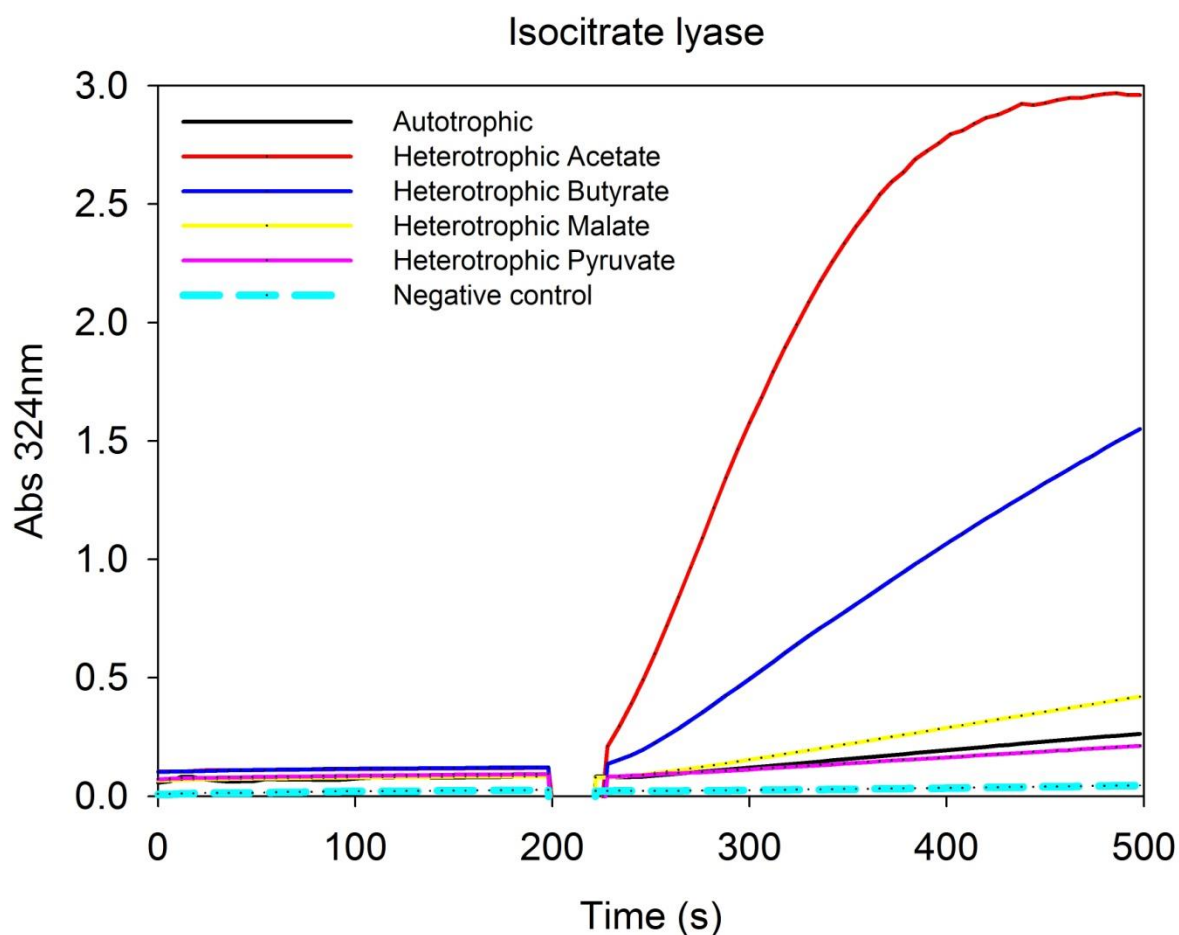


Figure 2-14. The absorbance at wavelength 324 nm of the phenylhydrazone glyoxylate was observed in isocitrate lyase assay with cell-free extract of cells grown autotrophically or heterotrophically with acetate, butyrate, malate, and pyruvate. Negative control was the assay without CFE.

In case of malate synthase, the trend was a little different. Although the highest activity was seen under heterotrophic condition with acetate or butyrate, the high activity was also observed in the CFE of cells grown heterotrophically with pyruvate,

malate or even under autotrophic condition. The same trend of enzymatic activity between malate synthase and isocitrate lyase under heterotrophic condition suggests that the strain TH-1 cells employs glyoxylate cycle for acetate or butyrate metabolism.

Glyoxylate cycle is the anaplerotic pathway that is required for bacterial growth under acetate or butyrate condition. The metabolites of TCA cycle need to be replenished [33]. By operating the glyoxylate cycle, two decarboxylation steps of TCA cycle are bypassed. As the result of two decarboxylase skips, glyoxylate is formed. In addition, bacteria have one more point where acetyl-CoA is condensed to glyoxylate to generate malate,  $C_4$  skeleton for biosynthesis.

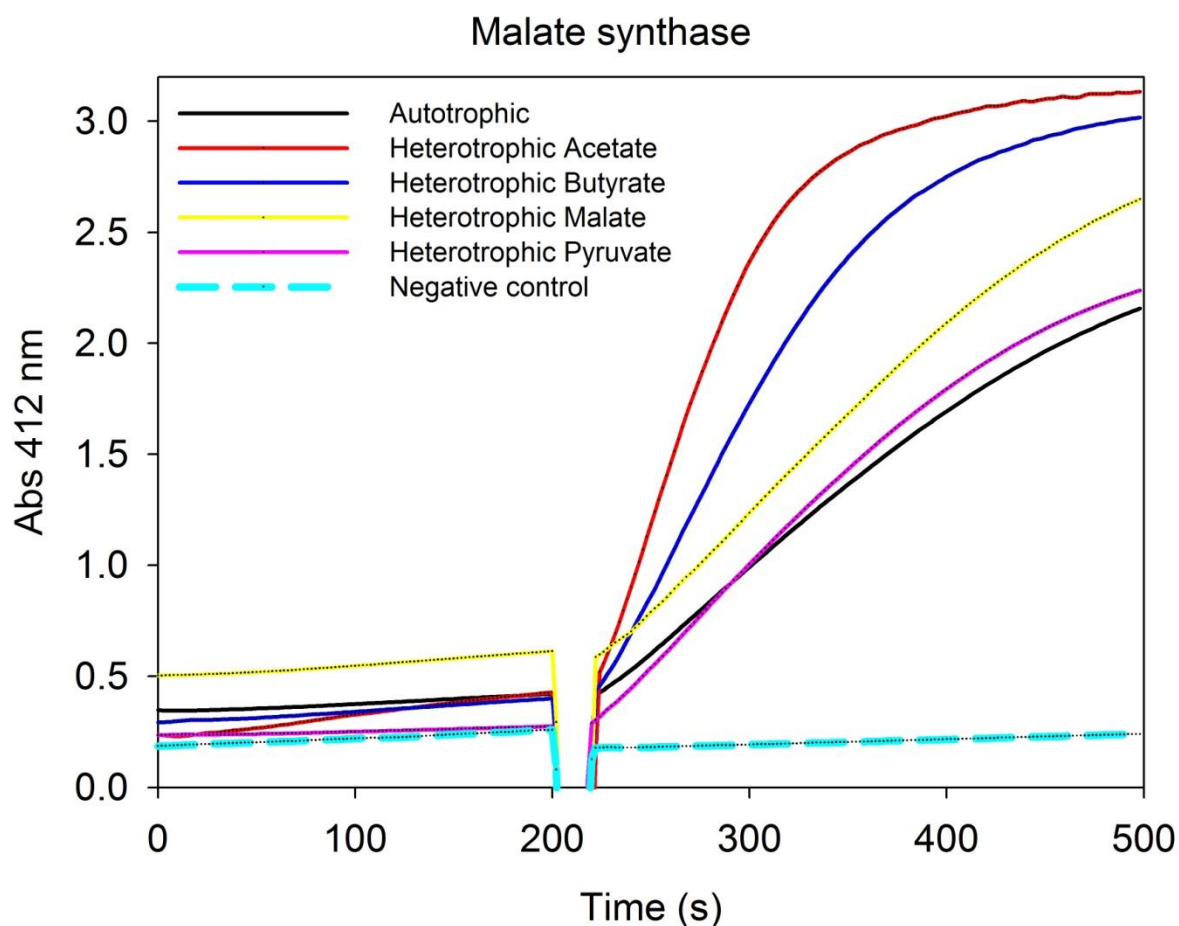
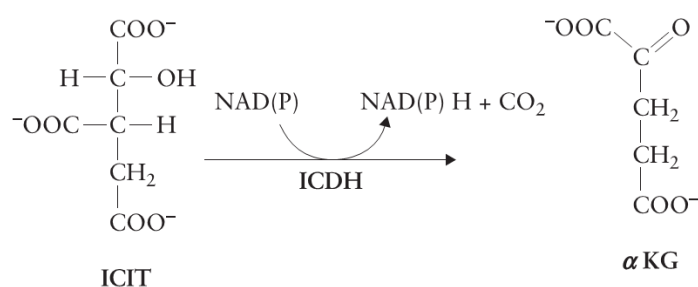


Figure 2-15. The absorbance at wavelength 412 nm of the 5-Thio-2-Nitrobenzoic Acid was observed in malate synthase assay with cell-free extract of cells grown autotrophically or heterotrophically with acetate, butyrate, malate, and pyruvate. Negative control was the assay without CFE.

The MS activity in TH-1 cells grown heterotrophically with acetate was 2.6-fold and 2.2-fold higher than that under heterotrophic condition with pyruvate and malate, respectively. In addition, the MS activity in strain TH-1 grown heterotrophically with butyrate was 2.8-fold and 2.4-fold higher than that under heterotrophic condition with pyruvate and malate, respectively. The MS activity in the cells TH-1 grown under heterotrophic with acetate and butyrate was 2.8-fold and 3.0-fold higher than that under autotrophic condition. The high activity of malate synthase under autotrophic or heterotrophic condition with malate or pyruvate indicates that malate synthase plays an important role. Glyoxylate is a highly reactive molecule, generated in the intermediary metabolism of glycine, hydroxyproline and glycolate mainly [45]. Then, malate synthase may play a critical role, in the process of removing glyoxylate which is accumulated from many steps of metabolism.

#### 2.3.4. Isocitrate dehydrogenase and malic enzyme

Isocitrate dehydrogenase (ICDH) is the enzyme that belongs to TCA cycle. It catalyzes the conversion of isocitrate into 2-oxoglutarate ( $\alpha$ -ketoglutarate). NAD(P)H and  $\text{CO}_2$  are formed through this reaction. Bacteria possess predominantly the  $\text{NADP}^+$ -specific ICDH, whereas fungi and yeasts possess the  $\text{NAD}^+$ -specific ICDH [34].



Strain TH-1 also has a  $\text{NADP}^+$ -dependent ICDH which showed high activity under heterotrophic condition. The low specific activity of ICDH was seen under autotrophic condition. The highest activity of ICDH was observed under heterotrophic condition with malate. The high activity of ICDH was observed under heterotrophic condition with acetate, butyrate, or pyruvate. The ICDH activity in the strain TH-1 cells grown under heterotrophic condition with malate was  $0.98 \pm 0.01$  unit/mg protein, 7.5-fold higher than that under autotrophic condition ( $0.13 \pm 0.01$

unit/mg protein).

The ICDH activity of strain TH-1 cells grown under heterotrophic condition with acetate and butyrate was  $0.88 \pm 0.06$  unit/mg protein and  $0.38 \pm 0.01$  unit/mg protein.

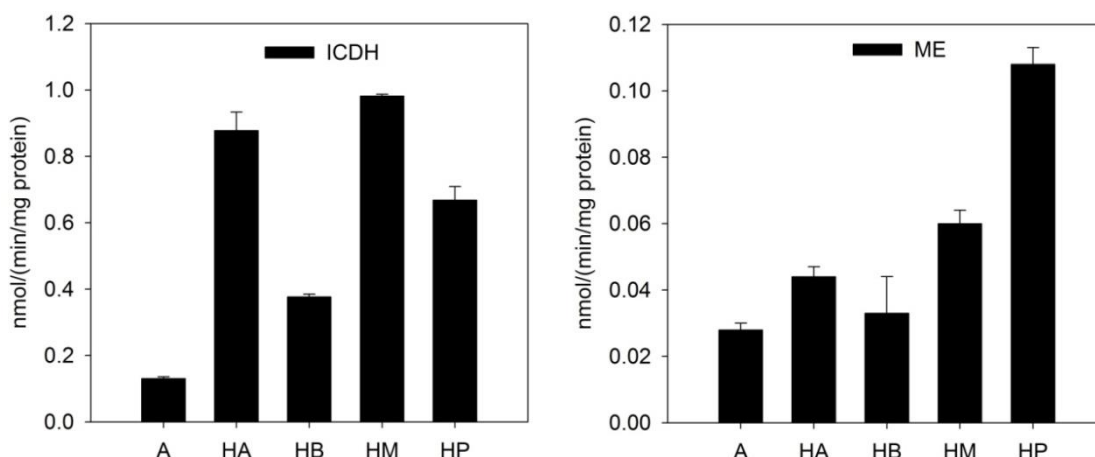
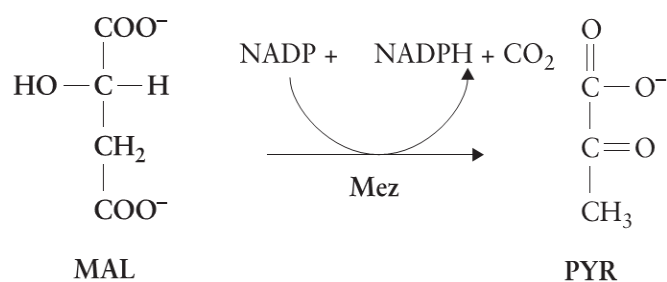


Figure 2-16. Enzymatic activities in cell-free extracts of *H. thermoluteolus* TH-1 grown autotrophically or heterotrophically with acetate, butyrate, malate, pyruvate. The abbreviation: MS: malate synthase; ME: malic enzyme. A refers for autotrophic; HA: heterotrophic acetate; HB: heterotrophic butyrate; HM: heterotrophic malate; HP: heterotrophic pyruvate.

Malate from TCA cycle or glyoxylate cycle could be converted into pyruvate by the function of malic enzyme (l-malate: NADP oxidoreductase, EC1.1.1.40) [34]



Malic enzyme (ME) catalyzes the reversible carboxylation of pyruvate to malate coupled with NADPH oxidation [46]. Highest malic enzymatic activity ( $0.11 \pm 0.01$  unit/mg protein) was obtained under heterotrophic condition with pyruvate, 3.9-fold higher than that under autotrophic condition ( $0.028 \pm 0.002$  unit/mg protein). It was suggested that under this heterotrophic condition, ME play an important role.

## 2.4. Conclusions

It is noted that under autotrophic condition, energy metabolism is conducted through the function of hydrogenase system. Hydrogenase catalyzes conversion of high potential energy hydrogen gas into proton to store energy as ATP or reducing equivalent as NADH. ATP and NADH are used for the fixation of CO<sub>2</sub> in CBB cycle. Therefore, the main role of TCA cycle under autotrophic condition is to supply the precursor metabolites for biosynthesis. On the other hand, under heterotrophic condition, energy metabolism is conducted through TCA cycle. The reducing equivalent NADH obtained from the complete oxidation of acetyl-CoA is used for ATP production via respiratory chain or used for other biosynthetic process. From this point of view, the function of TCA cycle under heterotrophic condition is very important for the growth of strain TH-1. Hence, the activity of ICDH was high under heterotrophic condition.

In the final conclusion of this chapter, it was confirmed that in strain TH-1 under heterotrophic growth on acetate or butyrate, carbon metabolism was conducted through glyoxylate cycle, whereas energy metabolism was conducted through TCA cycle. Because malate or pyruvate itself is an important intermediate metabolite that belongs to TCA cycle or gluconeogenesis pathway, then it is easy for them to be metabolized. It was suggested under heterotrophic condition with malate or pyruvate; the glyoxylate cycle was depressed; however exception was malate synthase, which may take part in the glyoxylate detoxification process in the cells.

# Chapter 3. Toxicity caused by photorespiration and the detoxification by function of malate synthase under mixotrophic growth in acetate/butyrate of *Hydrogenophilus thermoluteolus* TH-1

## 3.1. Introduction

Calvin-Benson-Bassham cycle (CBB cycle) is an important pathway for carbon fixation in the biosphere. CBB cycle is distributed in plants and many autotrophic microorganisms. In bacteria domain, totally six carbon fixation pathways were reported to date: CBB cycle, Acetyl CoA pathway, reductive TCA cycle, 3-hydroxypropionate bicycle, 3-hydroxypropionate/4-hydroxybutyrate cycle, 2-hydroxycarboxylate/4-hydroxybutyrate cycle.

In facultative chemolithoautotroph *H. thermoluteolus* TH-1, CBB cycle is employed for CO<sub>2</sub> fixation. CBB cycle is the most significant CO<sub>2</sub> fixation pathway on Earth and this is the only one carbon fixation in plants [13].

*H. thermoluteolus* TH-1 fixes CO<sub>2</sub> through CBB cycle. CBB cycle comprises 11 different enzymes catalyzing 13 enzymatic reactions, including ribulose-1,5-bisphosphate carboxylase (RubisCO) that is the most important in the cycle [15].

In strain TH-1, all the genes that code for CBB cycle enzymes were found in the genome and annotated as in Figure 3-1.

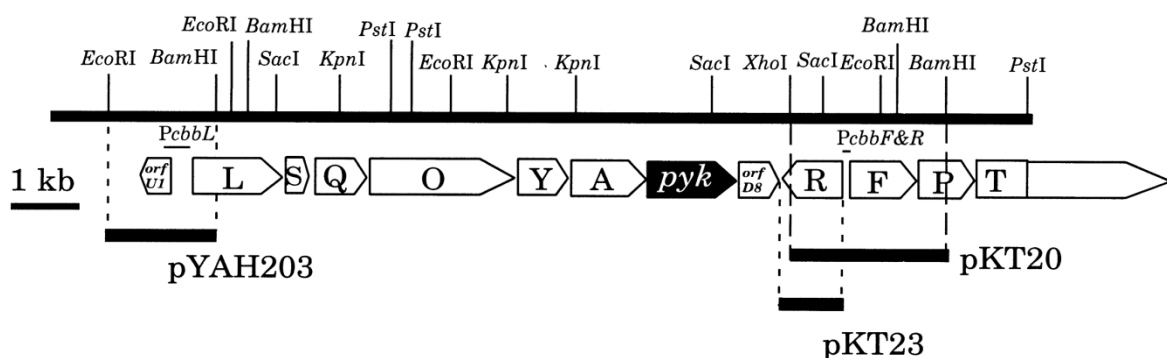


Figure 3-1. Physical map of the *cbb* genes of *H. thermoluteolus*. White pentagons are *cbb* genes, and the black pentagon is the gene for the glycolytic pathway. L and S encode large and small subunits of RubisCO, respectively. Q, O, and Y encode CbbQ, CbbO, and CbbY, respectively. A encodes fructose 1, 6-bisphosphate aldolase, and

*pyk* encodes pyruvate kinase. R, F, P, and T encode the LysR-type transcriptional regulator, fructose 1, 6-bisphosphatase (FBP), phosphoribulokinase (PRK), and transketolase (TKT), respectively [17].

All the genes for CBB cycle enzymes were identified and annotated: ribulose-bisphosphate carboxylase large chain [EC:4.1.1.39] (*rbcL*: contig00002\_orf00214); ribulose-bisphosphate carboxylase small chain [EC:4.1.1.39] (*rbcS*: contig00002\_orf00216); phosphoribulokinase [EC:2.7.1.19] (*prkB*: contig00002\_orf00231); phosphoglycerate kinase [EC:2.7.2.3] (*pgk*: contig00002\_orf00236); glyceraldehyde 3-phosphate dehydrogenase [EC:1.2.1.12] (*gapA*: contig00002\_orf00235); transaldolase [EC:2.2.1.2] (*talA*: contig00012\_orf00079); sedoheptulose-1,7-bisphosphatase [EC:3.1.3.11,3.1.3.37] (*fbp-SEBP*: contig00002\_orf00229); transketolase [EC:2.2.1.1] (*tktA*: contig00002\_orf00233); fructose-bisphosphate aldolase, class I [EC:4.1.2.13] (*fba*: contig00002\_orf00238); fructose-1,6-bisphosphatase I [EC:3.1.3.11] (*fbp*: contig00002\_orf00229, contig00010\_orf00079); ribose 5-phosphate isomerase A [EC:5.3.1.6] (*rpiA*: contig00004\_orf00011); ribulose-phosphate 3-epimerase [EC:5.1.3.1] (*rpe*: contig00005\_orf00146); transcription regulator LysR (*cbbR*: contig00002\_orf00228).

The main enzyme of CBB cycle and also the most abundant protein on Earth is ribulose-1,5-bisphosphate carboxylase/oxygenase (RubisCO). This enzyme catalyses the first step of carbon fixation that fix CO<sub>2</sub> to ribulose-1,5-bisphosphate when CO<sub>2</sub> is a substrate.

However, RubisCO can also incorporate O<sub>2</sub> to ribulose-1,5-bisphosphate by oxygenation activity via a process so-called photorespiration. Photorespiration is a waste-process that affects carbon fixation up to approximately 25% by producing 2-phosphoglycolate. Furthermore, 2-phosphoglycolate was reported as an inhibitor of carbon fixation process and other by-products as ammonia and peroxide are known to be toxic to the cells.

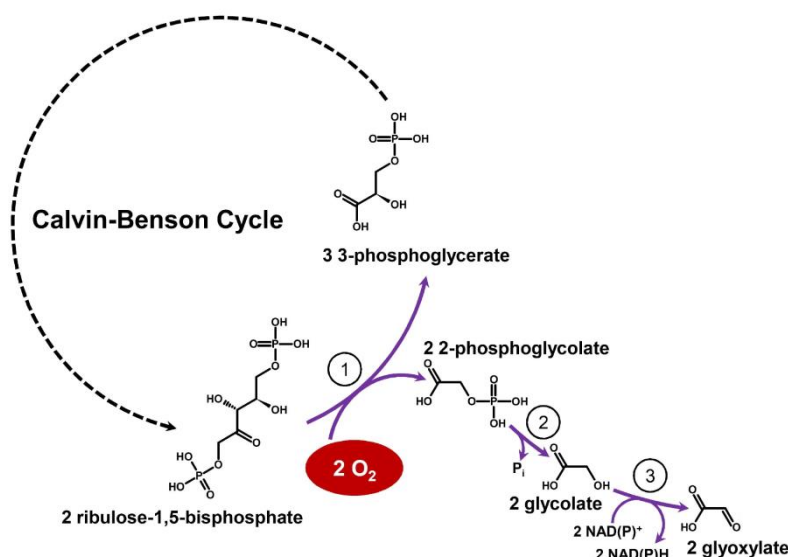


Figure 3-2. Conventional photorespiratory in cyanobacteria, modified from Patrick M. Shih et al. [47]. Ribulose-1,5-bisphosphate carboxylase/oxygenase (1), phosphoglycolate phosphatase (2), glycolate dehydrogenase (3).

The active site of RubisCO cannot distinguish the two similar substrates  $\text{O}=\text{C}=\text{O}$  and  $\text{O}=\text{O}$ . Hence, if the concentration of  $\text{O}_2$  is high in the environment, the chance increases for photorespiration to occur. Temperature also influences the relative rates of photorespiration and CBB cycle. Because the increase of the temperature will proceed to remove  $\text{CO}_2$  faster than it does  $\text{O}_2$ , high temperature favours photorespiration. (Koning, Ross E. 1994. Photorespiration. Plant Physiology Information Website). This explains why CBB cycle is normally distributed in mesophilic microorganism but rare in thermophile microorganism.

Strain TH-1 is an aerobic thermophilic bacterium that requires oxygen (10-15%) for growth, and the temperature optimum for growth is 50-52°C. These features show that photorespiration occur in strain TH-1 when the bacterium grows under autotrophic or mixotrophic conditions. Therefore, the cells are at high risk of encountering toxic phenomenon. In order to grow or survive in such toxic enviroment, the bacterium has to possess a detoxification system to solve this problem.

This chapter focuses on investigation of CBB cycle operation under autotrophic or mixotrophic conditions with different kind of carbon sources. Malate synthase plays a

critical role as a detoxification system during photorespiration in strain TH-1. The toxic compounds caused by photorespiration were analyzed and the detoxification system was discussed.

## **3.2. Materials and methods**

### **3.2.1 Bacterial strains and growth condition**

Bacterial strains and growth condition is similar to part 1.2.1 in chapter 1.

Cell-free extract preparation for enzymatic activity assay is similarly to part 1.2.1.3 in chapter 1.

3.2.2. Enzymatic assay of isocitric dehydrogenase ( $\text{NADP}^+$ ) [EC 1.1.1.42], the protocol is similar to part 2.2.4, chapter 2

3.2.3. Enzymatic assay of isocitric lyase [EC: 4.1.3.1], protocol is similar to part 2.2.5, chapter 2

3.2.4. Enzymatic assay of malate synthase [EC: 4.1.3.2] protocol is similar to part 2.2.6, chapter 2

3.2.5. Enzymatic assay of malic enzyme [E.C. 1.1.1.40], the protocol is similar to part 2.2.7, chapter 2

3.2.6. Enzymatic assay of glycolate oxidase [EC 1.1.3.15]

3.2.6.1. *Principle:* Glycolate oxidase activity was routinely determined in a continuous spectrophotometric assay. Through the function of glycolate oxidase activity, glycolate oxidase oxidizes glycolate to glyoxylate. By supplying phenylhydrazine in the reaction buffer mixture, the generated glyoxylate immediately combines with phenylhydrazine to create a colored product as phenylhydrazone glyoxylate at wavelength 324 nm. This protocol was modified from Dixon, G. H. and Kornberg, H. L., 1959 protocol [42]. Following the increasing of the  $A_{324}$  (the extinction of phenylhydrazone glyoxylate coefficient at this wavelength is  $16.8 \text{ mM}^{-1} \text{ cm}^{-1}$ ), the glycolate oxidase activity was measured.

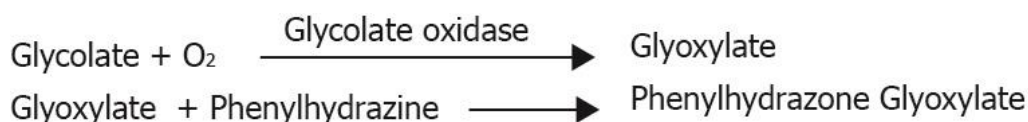


Figure 3-3. The reaction system for determining glycolate oxidase activity

3.2.6.2. *Conditions*: T=50°C, pH=6.8, A<sub>324nm</sub>, light path=1 cm

3.2.6.3. *Reagents*

Table 3-1. The reaction cocktail for oxygenation

Reagent	Volume (ml)
Buffer	22.00
40 mM Glycolate	5.00
100 mM L-Cysteine	1.00
100 mM Phenylhydrazine HCl	1.00
Buffer 100 mM Phosphate Buffer, pH 7.8 at 50°C. Prepared 100 ml in deionized water using Potassium Phosphate, Monobasic, and Anhydrous. Adjusted to pH 7.8 at 50°C with 1 M KOH.	

Mixed and adjusted to pH 7.8 at 50°C with 1 M KOH, if necessary. Oxygenate by bubbling 99.9% pure O<sub>2</sub> through the solution for 5 to 7 minutes (this must be done prior to each assay).

The reaction was prepared in a glass cuvette with the total volume of 3 mL. The reaction cocktail (the components are shown in Table 3-1) was used as a blank; the reaction was performed at 50°C. One hundred µL of flavin mononucleotide solution (10 mM) was added to 2,800 µL of reaction cocktail (the components are shown in Table 3-2), and the cuvette was held in the spectrophotometer for 5 minutes to allow temperature equilibration. Finally, 100 µL of CFE was added into the assay mixture to start reaction. Mixed by inversion and equilibrated to 50°C. The absorbance of the mixture at 324 nm (A<sub>324</sub>) was recorded to give a background phenylhydrazone glyoxylate performing. The increase of OD value was used to calculate the glycolate oxidase activity.

Table 3-2. The reaction system for determining glycolate oxidase activity.

	Reagents	Volume (mL)
1	Oxygenated Reaction Cocktail	2.80
2	10 mM Flavin Mononucleotide Solution (FMN)	0.10
3	CFE	0.10
4	Total	3.00

#### 3.2.6.4. Calculations

$$\text{Units/ml Enzyme} = \frac{(\Delta A_{324\text{nm}} / \text{min Test} - \Delta A_{324\text{nm}} / \text{min Blank})(3)(\text{df})}{(16.8)(0.1)}$$

3 = total volume (in milliliters) of assay

df = dilution factor

16.8 = millimolar extinction coefficient of Phenylhydrazine Glyoxylate at 324 nm

0.1 = Volume (in milliliters) of enzyme used

$$\text{Units/mg protein} = \frac{\text{units/ml enzyme}}{\text{mg protein/ml enzyme}}$$

#### 3.2.6.5. Unit definition

One unit (1U) was defined as amount of enzyme that produces 1.0  $\mu\text{mol}$  of glyoxylate from glycolate per minute at pH 7.8 at 50°C, in the presence of phenylhydrazine.

### 3.3. Results and discussions

#### 3.3.1. Growth profile of strain TH-1 under mixotrophic condition

This experiment has already been reported in chapter 1. Strain TH-1 showed the autotrophic growth and heterotrophic growth with different organic substrates. Growth experiments under mixotrophic conditions were performed with the medium and gas phase as under autotrophic condition (75% $H_2$ , 10% $O_2$ , 15% $CO_2$ ) with the addition of only one organic acid.

Malate was favorable for mixotrophic growth of strain TH-1. The maximum growth rate under mixotrophic condition with malate was  $1.0\ h^{-1}$ . This result is correlated with the growth of strain TH-1 in malate under heterotrophic condition, supporting that malate is a favourable substrate for strain TH-1.

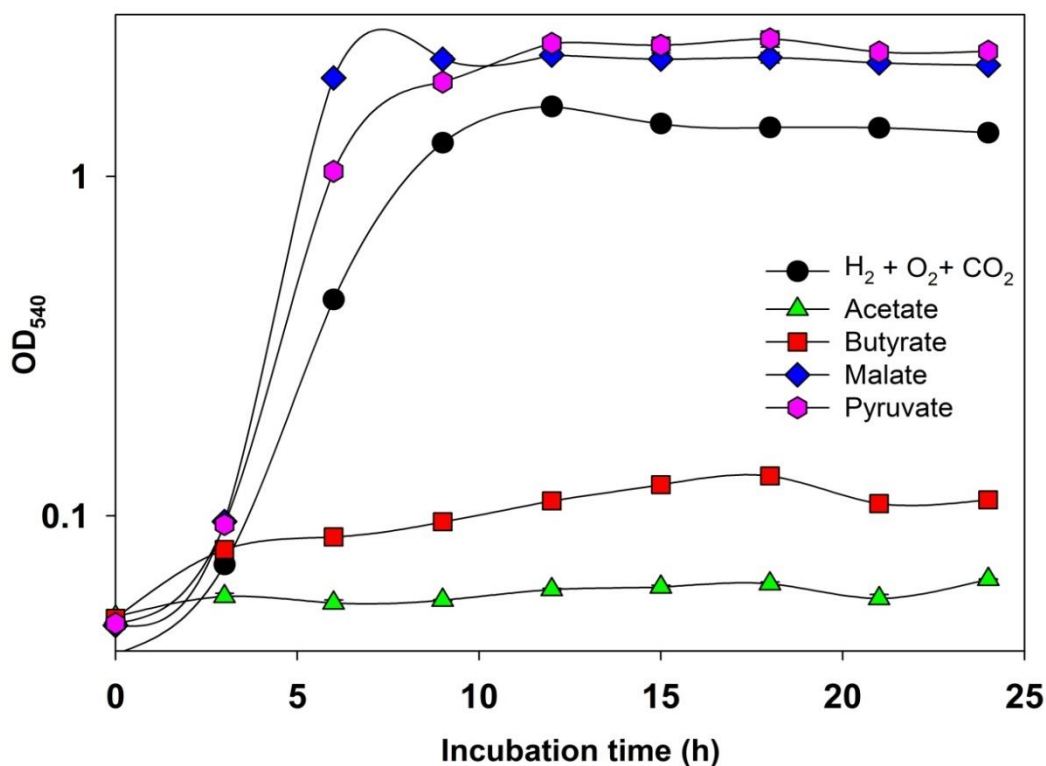


Figure 3-4. The growth curves of strain TH-1 under autotrophic and mixotrophic condition. Ordinate is a logarithmic scale.

Surprisingly, under mixotrophic condition with acetate (20 mM) or butyrate (15 mM), no growth was seen within 24 hours. As we discussed in chapter 2, glyoxylate cycle was employed when strain TH-1 cells were grown heterotrophically with acetate or butyrate. It is noted that the pre-culture was performed under autotrophic condition; it means that the cells in pre-culture grow using CBB cycle. Therefore just after the bacteria were inoculated to mixotrophic condition with CO<sub>2</sub>, the CBB cycle must be operating (gas phase 75% H<sub>2</sub>, 10% O<sub>2</sub>, 15% CO<sub>2</sub>). As I mentioned in the introduction of chapter 3, when CBB cycle was in operation, photorespiration also occurs. The product of photorespiration is 2-phosphoglycolate which is converted into glycolate. Glycolate was converted into glyoxylate by the function of glycolate oxidase. At the same time, when acetate or butyrate was present in the medium, it was converted into acetyl-CoA. Acetyl-CoA was condensed with oxaloacetate to citrate. Citrate was converted into isocitrate in TCA cycle, which is cleaved to glyoxylate and succinate through the catalysis of isocitrate lyase in glyoxylate cycle. The operation of CBB cycle under mixotrophic condition led to accumulation of glycolate. Because high concentration of glyoxylate came from the function of isocitrate lyase, glycolate could not be converted into glyoxylate. Both glyoxylate and glycolate are highly reactive molecule and toxic to the cell. In vitro, glyoxylic acid may be degraded to formic acid and CO<sub>2</sub> by non-enzymatic oxidation by the H<sub>2</sub>O<sub>2</sub> formed in the prior oxidation of glycolic acid. Enzymatic oxidation of glyoxylic acid to oxalic acid has been reported [48-51]. Under high temperature, glycolate or glyoxylate could be converted into oxalate by the function of glycolate oxidase [51], and oxalate is oxidized to formic acid and all steps of this oxidizing process also release another toxic compound, H<sub>2</sub>O<sub>2</sub>. These toxic compounds may inhibit the growth of strain TH-1 cells under mixotrophic condition with acetate or butyrate. The increases of oxygen concentration, or the increase of acetate/butyrate concentration in the presence CO<sub>2</sub>, will negatively affect the growth of strain TH-1 cells.

### 3.3.2. Growth profiles of strain TH-1 under autotrophic condition with different oxygen concentration

To demonstrate the negative effect of oxygen to CBB cycle, the autotrophic culture experiment of strain TH-1 was carried-out under different oxygen gas concentration. The experiment was designed with the same hydrogen concentration (55%), carbon dioxide (15%), and oxygen varied in the range of 10% to 30%.

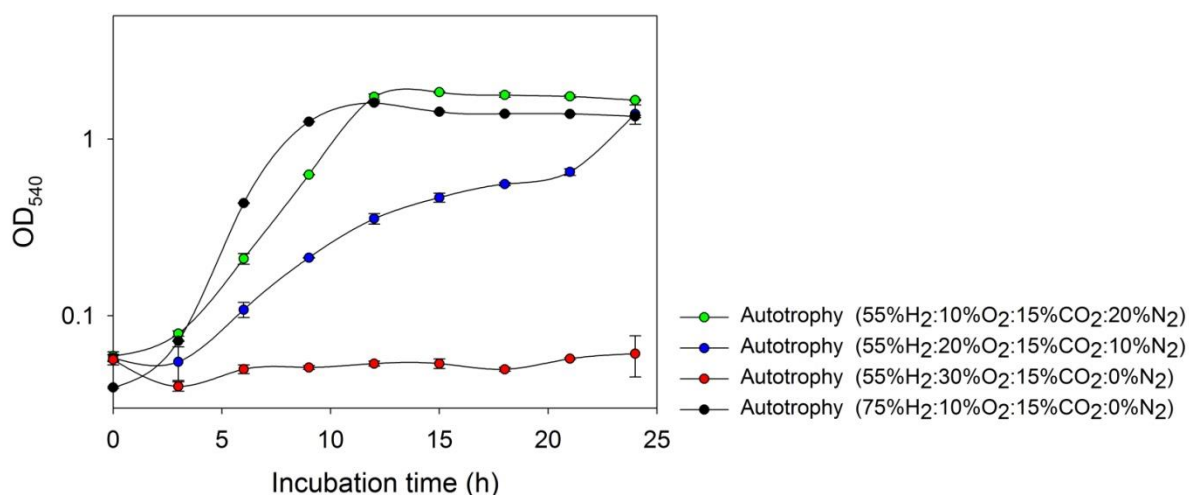


Figure 3-5. The growth curves of strain TH-1 under autotrophic condition with different gas components were supplied. Ordinate is a logarithmic scale.

As I expected, when the concentration of hydrogen and carbon dioxide gas were kept constant, the more oxygen concentration, the less bacteria grew. In the figure 3-5, no growth was seen when the ratio of oxygen in culture medium was 30%. The maximum growth rate of strain TH-1 under autotrophic condition corresponding to the concentration of oxygen at 30%, 20%, and 10% was  $0.07\ h^{-1}$ ,  $0.23\ h^{-1}$ , and  $0.37\ h^{-1}$ , respectively. The maximum growth rate of strain TH-1 under normal condition of gas components (gas phase 75% H<sub>2</sub>, 10% O<sub>2</sub>, 15% CO<sub>2</sub>) was  $0.60\ h^{-1}$ . This result supports my hypothesis that the high concentration of oxygen will enhance photorespiration activity. The toxic compounds produced by photorespiration such as 2-

phosphoglycolate, glycolate, and  $\text{H}_2\text{O}_2$ , have negative effect on the growth of strain TH-1.

### 3.3.3. Growth profiles of strain TH-1 under mixotrophic condition with acetate or butyrate

This experiment was designed to check the growth of strain TH-1 under mixotrophic condition with the same concentration of acetate (20 mM) or butyrate (15 mM). My question was what will happen if one of the gas components was changed. To see the effect, gas was replaced by nitrogen gas.

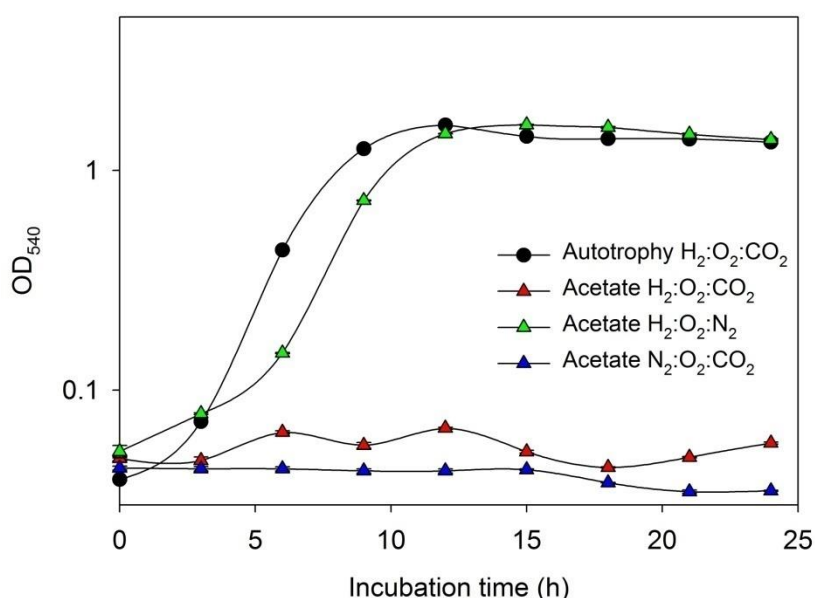


Figure 3-6. The growth curves of strain TH-1 under autotrophic or mixotrophic condition under acetate with different gas components. Ordinate is a logarithmic scale.

As shown in figure 3-6, when acetate, oxygen, and carbon dioxide co-existed, no growth of the cells was seen in 24 hours. However, when carbon dioxide was replaced with nitrogen gas, the strain TH-1 started to grow vigorously, almost without lag phase.

The similar phenomenon was seen under mixotrophic condition with butyrate in figure 3-7, when butyrate, oxygen, and carbon dioxide co-existed, no growth was seen in 24 hours.

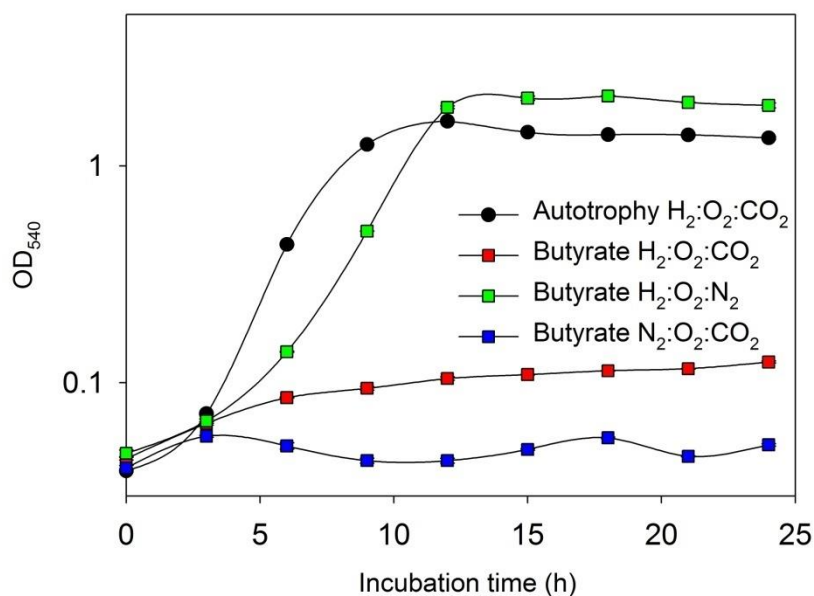


Figure 3-7. The growth curves of strain TH-1 under autotrophic or mixotrophic condition in butyrate with different gas components. Ordinate is a logarithmic scale.

The experiment was designed to observe strain TH-1 growth of heterotrophically or mixotrophically with different concentration of acetate or butyrate.

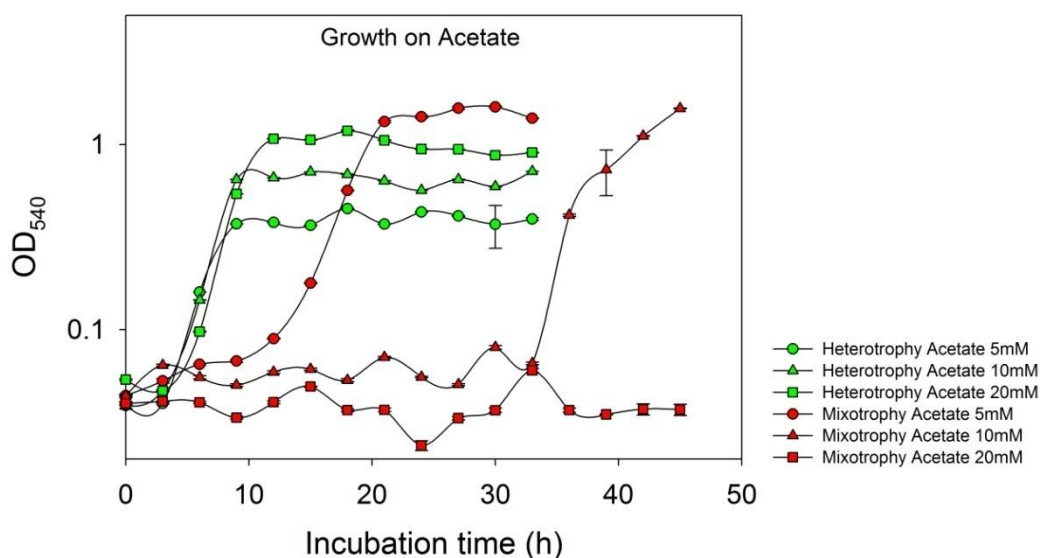


Figure 3-8. The growth curves of strain TH-1 under heterotrophic or mixotrophic condition with different acetate concentrations. Ordinate is a logarithmic scale.

As we see in figure 3-8 and 3-9, under heterotrophic condition, when the concentration of acetate or butyrate increased, the growth of strain TH-1 cells was enhanced. On the contrary, under mixotrophic condition with gas ratio of 75% $H_2$ , 10% $O_2$ , 15% $CO_2$ , the growth of strain TH-1 cells decreases when the concentration of acetate or butyrate increases.

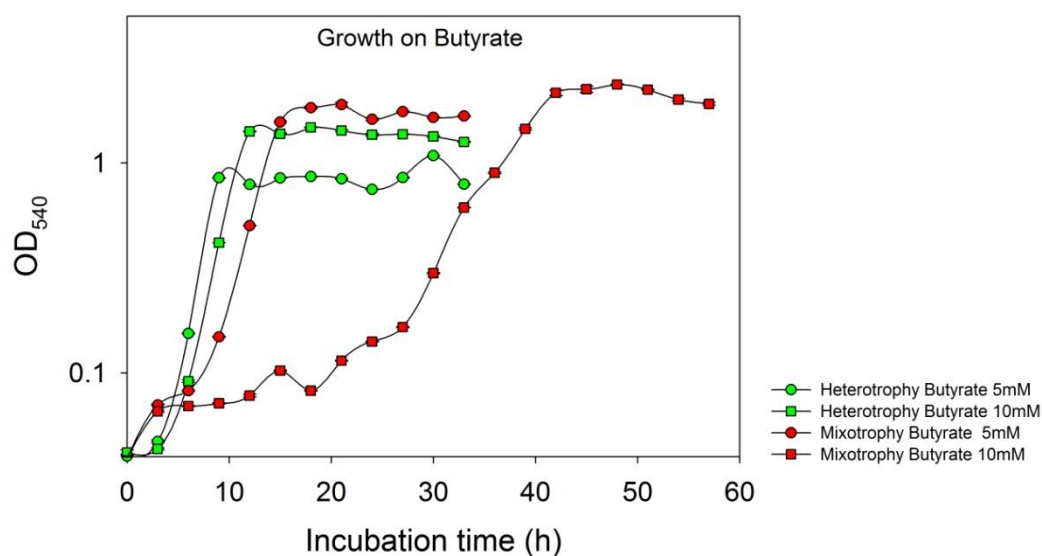


Figure 3-9. The growth curves of strain TH-1 under heterotrophic or mixotrophic condition with different butyrate concentrations. Ordinate is a logarithmic scale.

To support the hypothesis, the experiment was designed as follows: bacteria grown autotrophically in pre-culture were inoculated to the medium which allows mixotrophic growth with butyrate (10 mM) and the gas components of 75% $H_2$ :10% $O_2$ :15% $CO_2$ . After 9 hours from the first inoculation as a pre-culture, the gas components of mixotrophic (75% $H_2$ , 10% $O_2$ , 15% $CO_2$ ) were replaced by air atmosphere. It means that the strain TH-1 cells were changed from mixotrophic growth to heterotrophic growth at this point. After 6 hours from the point gas was changed to air atmosphere (15 hours from start culture), the strain TH-1 cells started to grow. The detailed analysis by HPLC confirmed that the strain TH-1 cells started to consume butyrate with the increase of growth curve. In case of mixotrophic condition,

after incubating 27 hours, TH-1 cells started growth with butyrate consumption (Figure 3-11).

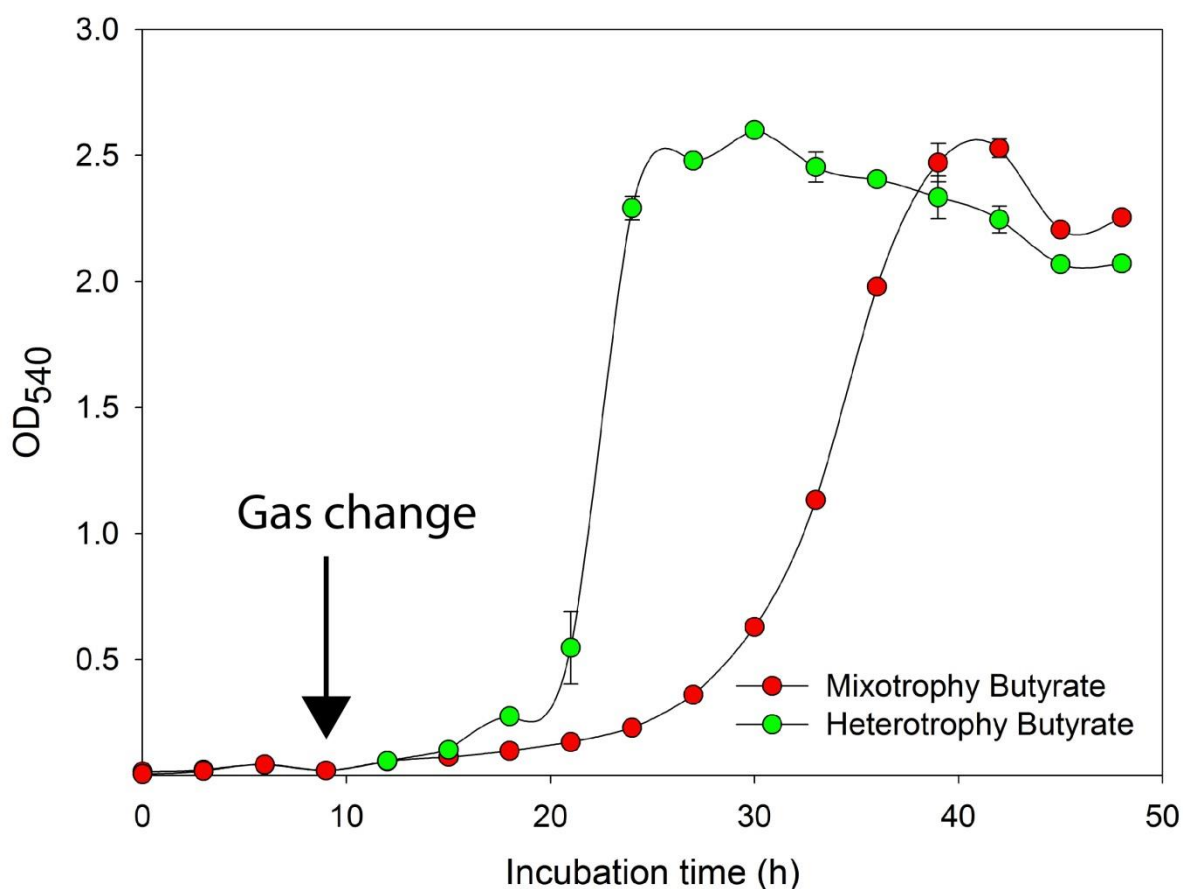


Figure 3-10. The growth curves of strain TH-1 heterotrophic or mixotrophic condition.

All these evidences confirmed the hypothesis about the inhibition of the growth of strain TH-1 cells under mixotrophic condition when  $O_2$ ,  $CO_2$  and acetate or butyrate co-existed.

Under mixotrophic condition with acetate (10 mM) or mixotrophic condition with butyrate (10 mM), a long lag phase was observed before vigorous growth (Figure 3-8, 3-9). In case of mixotrophic condition with in butyrate, lag phase lasted for 27 hours, which correlates with the value under mixotrophic condition with acetate (10 mM) of 33 hours. This means that when toxic compounds were removed, the cells started to

grow mixotrophically. As I mentioned in chapter 2, malate synthase may be the factor that is involved in detoxification. Therefore, enzymatic measurement of malate synthase is required.

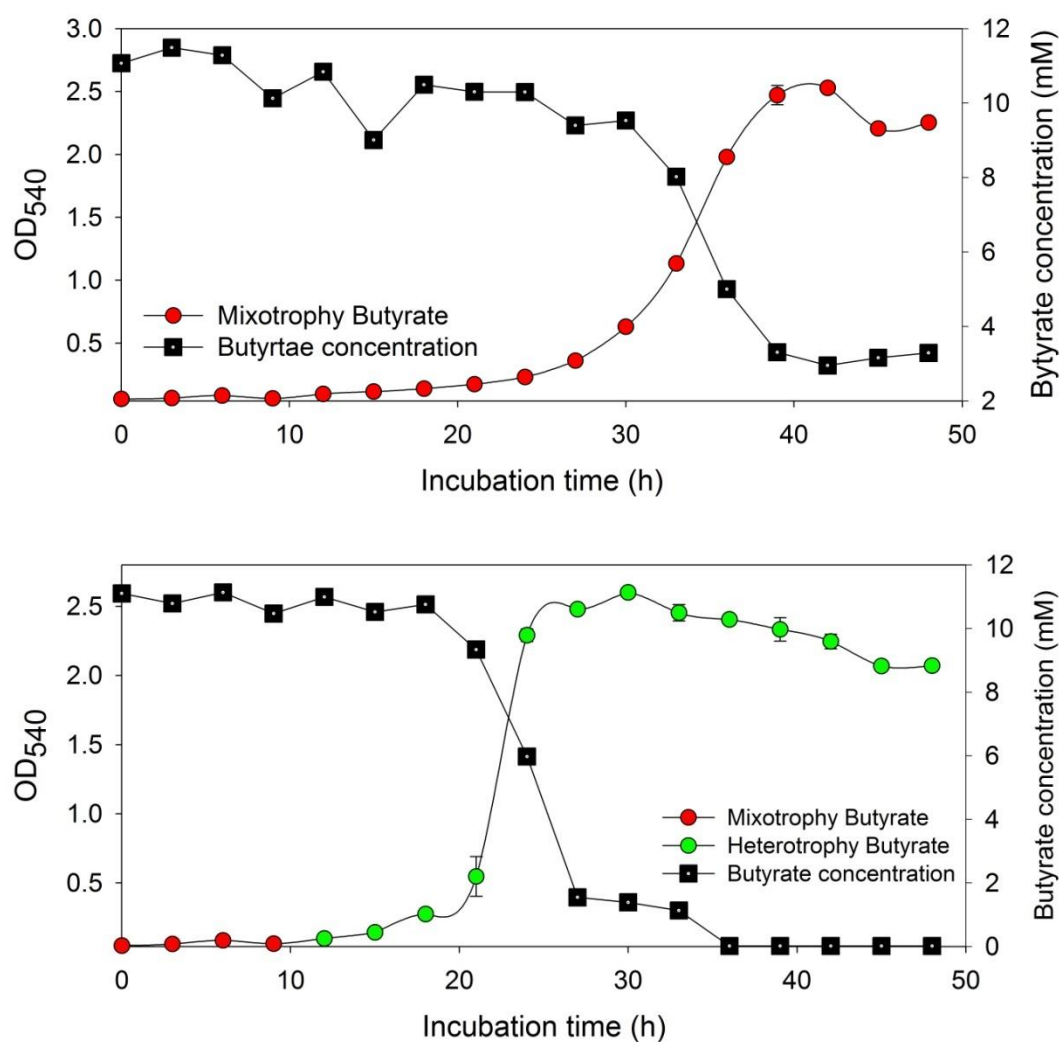


Figure 3-11. The growth curves of strain TH-1 under heterotrophic or mixotrophic condition with butyrate (10 mM) corresponding with the butyrate consumption.

Table 3-3. Enzymatic activities in cell-free extracts of *H. thermoluteolus* TH-1 were grown autotrophically or heterotrophically with acetate, butyrate, malate, pyruvate. Activities are expressed in U/ mg protein: mean  $\pm$  standard deviation; The abbreviation: ICDH: isocitrate dehydrogenase; ICL: isocitrate lyase; MS: malate synthase; ME: malic enzyme. GO: glycolate oxidase

Enzyme	Cultivation condition				
	Autotrophic	Mixotrophic			
		Acetate	Butyrate	Malate	Pyruvate
Specific enzymatic activity (Unit/mg protein)					
ICDH	0.131±0.005	0.24±0.005	0.12±0.005	0.349±0.004	0.355±0.005
ICL	0.011±0.002	0.108±0.006	0.062±0.005	0.04±0.001	0.018±0.001
MS	0.172±0.007	1.478±0.122	1.992±0.096	1.277±0.057	0.845±0.015
ME	0.028±0.002	0.198±0.013	0.295±0.007	0.16±0.007	0.27±0.016
GO	0.014±0.001	0.026±0.004	0.042±0.005	0.01±0.0001	0.025±0.002
	Heterotrophic				
GO	0.014±0.001	0.014±0.001	0.011±0.002	0.006±0.001	0.005±0.0001

### 3.3.4. Isocitrate lyase and malate synthase activity

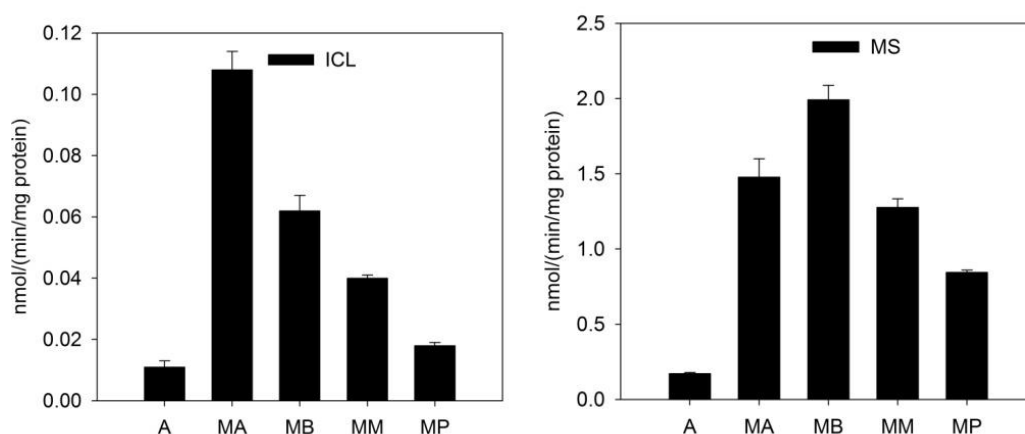


Figure 3-12. Activity in cell-free extracts of *H. thermoluteolus* TH-1 grown autotrophically or mixotrophically with acetate, butyrate, malate, pyruvate. The abbreviation: ICL: isocitrate lyase; MS: malate synthase. A refers for autotrophic; MA: mixotrophic acetate; MB: mixotrophic butyrate; MM: mixotrophic malate; MP: mixotrophic pyruvate.

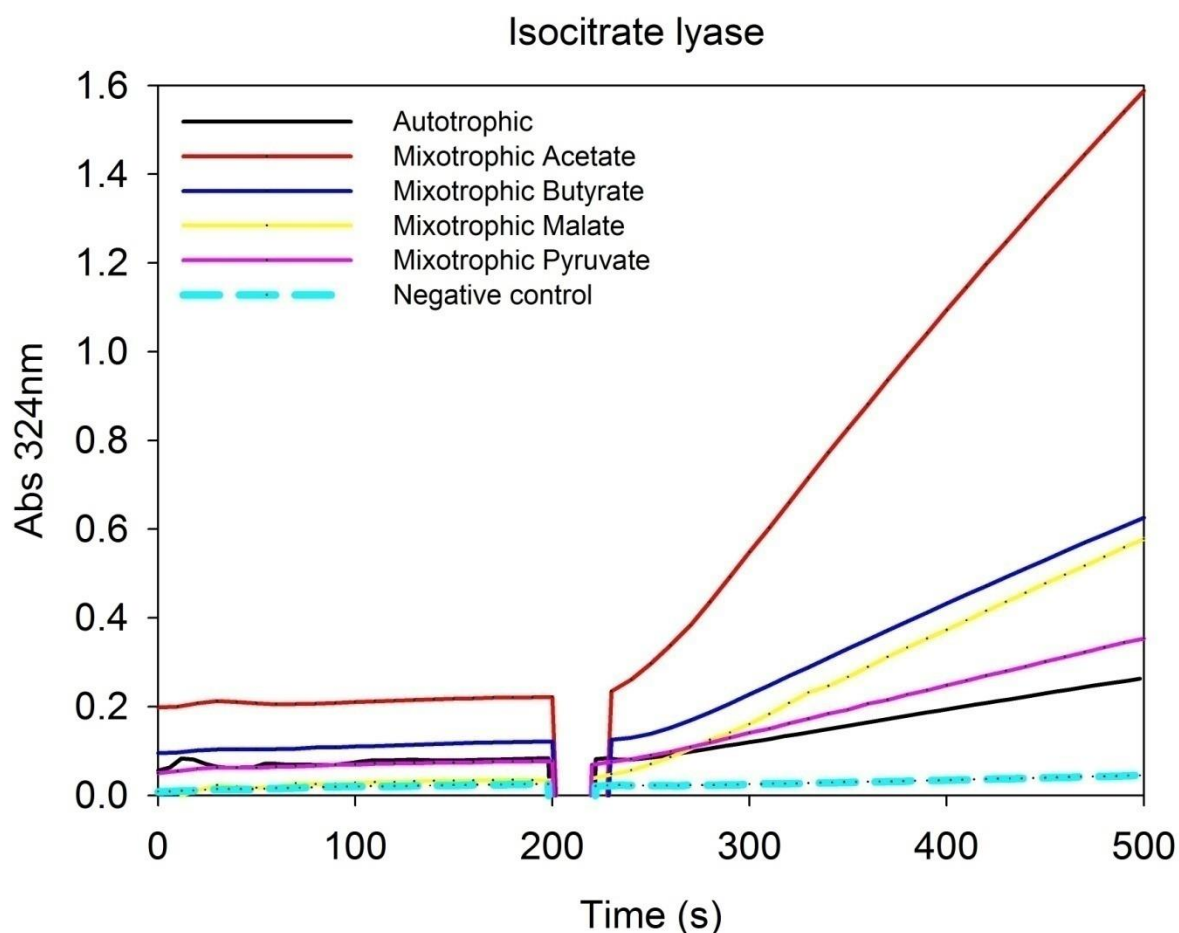


Figure 3-13. The absorbance at wavelength 324 nm of the phenylhydrazone glyoxylate was performed in isocitrate lyase assay with cell-free extract of cells grown autotrophically or mixotrophically with acetate, butyrate, malate, pyruvate. Negative control was the assay without CFE.

The high enzymatic activity of isocitrate lyase (ICL) and malate synthase (MS) were detected under mixotrophic growth with acetate or butyrate. The ICL activity under mixotrophic condition with acetate and butyrate was  $0.108 \pm 0.006$  unit/mg protein,  $0.062 \pm 0.005$  unit/mg protein, respectively. Apparently, the ICL activity in the strain TH-1 cells grown mixotrophically with acetate and butyrate was 9.8-fold and 5.6-fold higher than that under autotrophic condition. Interestingly, the ICL activity under mixotrophic condition with malate and butyrate slightly increased compared with that under heterotrophic condition. The ICL activity under mixotrophic condition with

malate and pyruvate was  $0.04 \pm 0.001$  unit/mg protein,  $0.018 \pm 0.001$  unit/mg protein, respectively.

Moreover, when I compared the ICL activity under mixotrophic condition with malate and pyruvate to those under heterotrophic condition, ICL activity under mixotrophic condition with malate and pyruvate was slightly enhanced 1.9-fold and 2.3-fold, respectively, indicating that glyoxylate cycle functions under mixotrophic condition with malate or pyruvate.

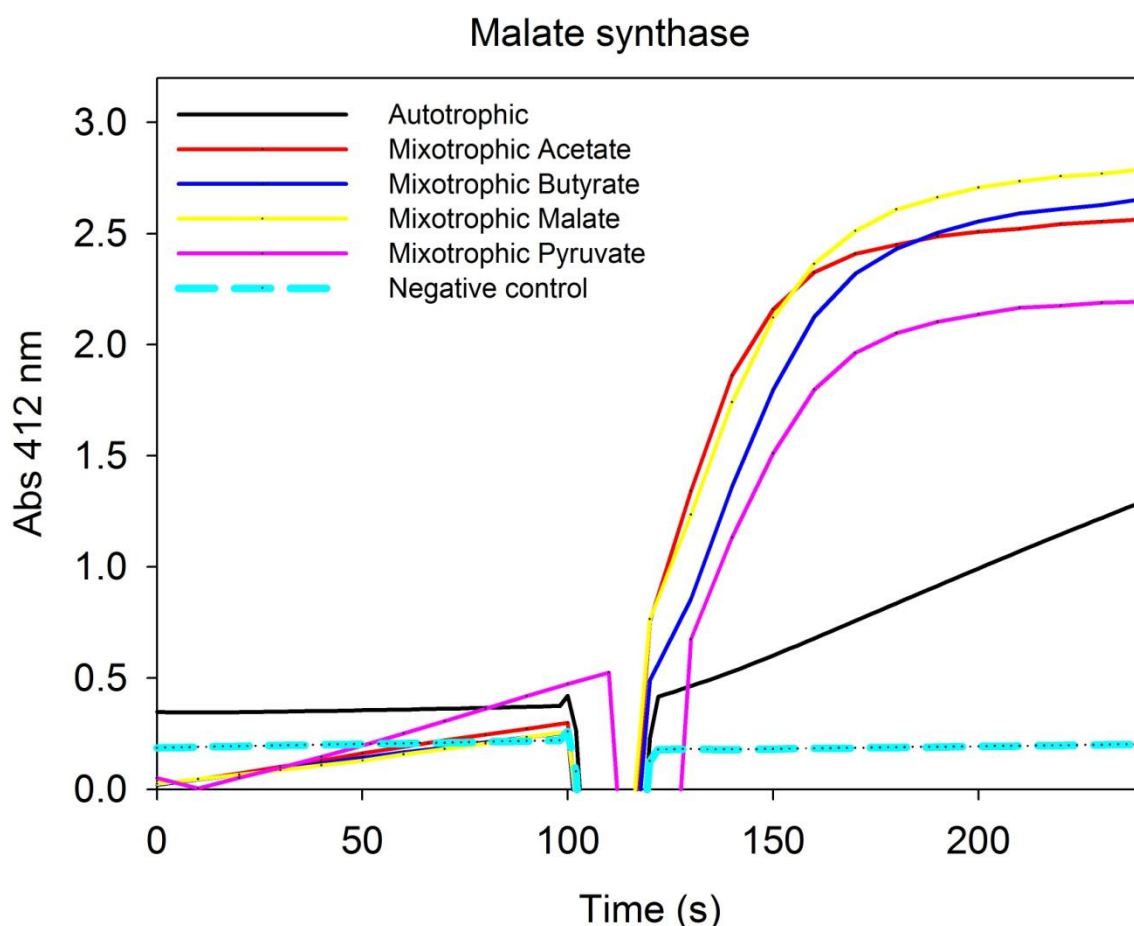


Figure 3-14. The absorbance at wavelength 412 nm of the 5-thio-2-nitrobenzoic acid was performed in malate synthase assay with cell-free extract of cells grown autotrophically or mixotrophically with acetate, butyrate, malate, pyruvate. Negative control was the assay without CFE.

The MS activity under mixotrophic condition with acetate and butyrate was

1.48±0.12 unit/mg protein, 1.99±0.10 unit/mg protein, respectively. Apparently, the MS activity in TH-1 cells grown mixotrophically with acetate and butyrate was 8.6-fold and 11.6-fold higher than that under autotrophic condition. The ICL activity under mixotrophic condition with malate and pyruvate was 1.28±0.06 unit/mg protein, 0.85±0.02 unit/mg protein, respectively.

ICL activity was slightly enhanced under mixotrophic condition, compared with that under heterotrophic condition with malate or pyruvate. In contrast, when I compared the MS activity under mixotrophic condition with malate or pyruvate, MS activity was significantly enhanced 6.9-fold and 3.8-fold respectively, indicating that glyoxylate cycle functions under mixotrophic condition with malate or pyruvate.

Until now, the evidence strongly supports the operation of glyoxylate cycle under mixotrophic condition not only with acetate or butyrate but also with malate or pyruvate.

Since glyoxylate cycle is not necessary for malate or pyruvate metabolism, the function of glyoxylate cycle in this case was suggested to detoxify the toxic compounds caused by photorespiration. Hence, glyoxylate cycle plays a role in acetate or butyrate metabolism and detoxification under autotrophic or mixotrophic condition.

### 3.3.5. Isocitrate dehydrogenase and malic enzyme activity

Strain TH-1 also has a NADP<sup>+</sup>-dependent ICDH. It showed high activity under mixotrophic condition. Surprisingly, the low specific activity of ICDH was seen under mixotrophic condition. The highest activity of ICDH was observed under mixotrophic condition with pyruvate. The ICDH activity in strain TH-1 grown under mixotrophic with pyruvate was 0.355±0.005 unit/mg protein. All ICDH specific enzymatic activities under mixotrophic condition were lower than those under heterotrophic condition. The major role of TCA cycle might be directing ATP production under mixotrophic condition.

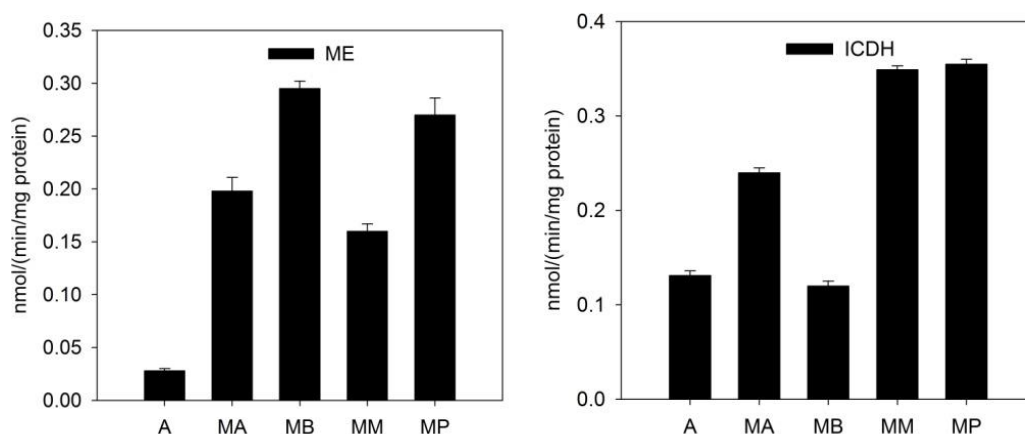


Figure 3-15. Enzymatic activities in cell-free extracts of *H. thermoluteolus* TH-1 were grown autotrophically or heterotrophically with acetate, butyrate, malate, pyruvate. The abbreviation: MS: malate synthase; ME: malic enzyme. A refers for autotrophic; MA: mixotrophic acetate; MB: mixotrophic butyrate; MM: mixotrophic malate; MP: mixotrophic pyruvate.

On the other hand, the activity of malic enzyme (ME) under mixotrophic condition was higher than those under heterotrophic condition. In case of butyrate and acetate, fold change was 8.9 times and 4.5 times. This bias reflected the enhancement of glyoxylate cycle under mixotrophic condition. The high activity of MS correlating with the high activity of ME might be detoxification machinery for solving glyoxylate coming from acetate or butyrate metabolism as well as glycolate coming from photorespiration.

### 3.3.6. Glycolate oxidase activity

Photorespiration process is a wasteful step because it reduces the efficiency of CO<sub>2</sub> fixation. In addition, glycolate is a toxic compound to the cell and inhibits CO<sub>2</sub> fixation. For recovery of carbon and detoxification the harmful compounds, cells have to convert glycolate into glyoxylate by glycolate dehydrogenase [EC: 1.1.99.14] and glycolate oxidase [EC:1.1.3.15].

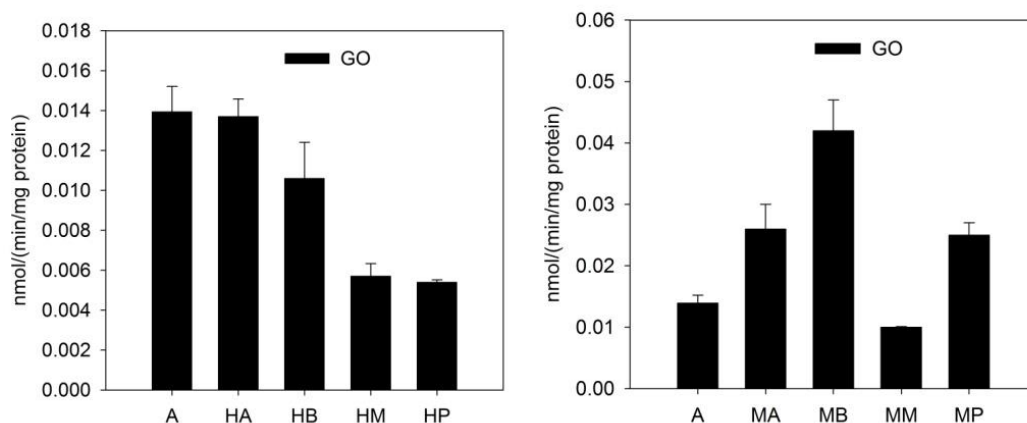


Figure 3-16. Enzymatic activities in cell-free extract of *H. thermoluteolus* TH-1 grown autotrophically or mixotrophically with acetate, butyrate, malate, pyruvate. The abbreviation: GO: glycolate oxidase. A: autotrophic; HA: heterotrophic acetate; HB: heterotrophic butyrate; HM: heterotrophic malate; HP: heterotrophic pyruvate; MA: mixotrophic acetate; MB: mixotrophic butyrate; MM: mixotrophic malate; MP: mixotrophic pyruvate.

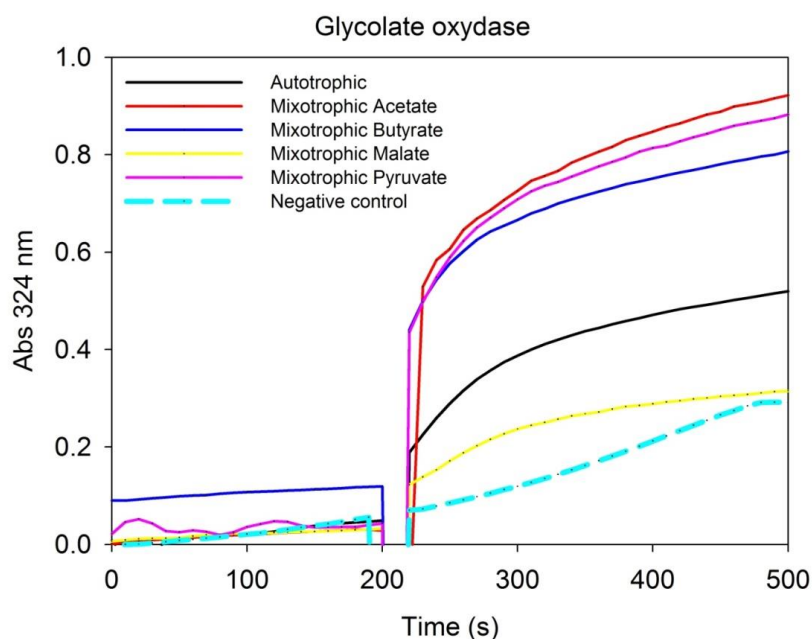


Figure 3-17. The absorbance at wavelength 324 nm of the phenylhydrazone glyoxylate was monitored in glycolate oxidase assay with cell-free extract of cells grown autotrophically, or mixotrophically with acetate, butyrate, malate, and pyruvate. Negative control was the assay without CFE.

The glycolate oxidase (GO) activity under autotrophic condition was slightly higher than that under heterotrophic condition. This could be explained by the operation of CBB cycle. The activity of GO under mixotrophic condition was significantly higher than those under heterotrophic condition with the same organic substrate. The highest activity of GO was observed under mixotrophic condition with butyrate. The GO activity in the strain TH-1 cells grown mixotrophically with butyrate was  $0.04 \pm 0.01$  unit/mg protein, 4-fold higher than under heterotrophic condition ( $0.011 \pm 0.002$  unit/mg protein).

The similar tendency in increasing activity of MS and GO was observed under mixotrophic condition when compared to that under heterotrophic condition, indicating that MS and GO are metabolically connected. Glyoxylate is consumed by many biochemical pathways. Malate synthase from glyoxylate cycle incorporate acetyl-CoA and glyoxylate to yield malate. However, under heterotrophic and mixotrophic condition, a pool of glyoxylate exists from the metabolism of butyrate or acetate. When glyoxylate concentration is high, glycolate oxidase can not convert glycolate into glyoxylate. The accumulation of high concentration of glycolate will lead to the toxic situation. This may be the reason for the growth inhibition of strain TH-1 with a long lag phase under mixotrophic condition. Once the detoxification occurs, strain TH-1 under mixotrophic condition with butyrate starts to grow. This result suggests that malate synthase in glyoxylate cycle functions as a detoxification system when bacterium cells counter with toxic compounds coming from glyoxylate cycle and glycolate derived from photorespiration.

### **3.4. Conclusions**

From all above evidence and discussions, the hypothesis about growth inhibition of strain TH-1 cells under mixotrophic condition when CO<sub>2</sub> and acetate or butyrate co-existed is becoming reality. The result of this chapter also suggests the combination in function of enzymes, glycolate oxidase and malate synthase, for the detoxification system for photorespiration under mixotrophic condition.

## **Chapter 4. Transcriptome and metabolome analyses of central carbon metabolism under autotrophic, heterotrophic and mixotrophic condition in *Hydrogenophilus thermoluteolus* TH-1**

### **4.1. Introduction**

*H. thermoluteolus* TH-1 is a thermophilic, facultatively chemolithoautotrophic, hydrogen-oxidizing bacterium. It shows ability to grow autotrophically, heterotrophically, or mixotrophically. For autotrophic growth with H<sub>2</sub> and CO<sub>2</sub> as energy source and carbon source, strain TH-1 operates CBB cycle for CO<sub>2</sub> fixation [7]. However heterotrophic or mixotrophic growth on various carbon source, the carbon and energy metabolism of strain TH-1 are still unclear. Under optimum condition, the autotrophic growth is favourable and the maximum specific growth rate of strain TH-1 is 0.68 h<sup>-1</sup> [2, 3]. Autotrophic growth rate of strain TH-1 is the highest among autotrophs indicating that strain TH-1 has high potential for industrial application. For doing that, the knowledge about the carbon metabolism and energy metabolism is required. The draft genome sequence of strain TH-1 was determined by whole genome shotgun sequencing. Availability of strain TH-1 draft genome is an advantage for metabolic research. The genes coding for all enzymes that relate to the central carbon metabolisms such as CBB cycle, TCA cycle and glycolysis/gluconeogenesis were identified. Moreover, strain TH-1 can even grow well under heterotrophy with acetate or butyrate. But mixotrophic growth is unfavourable because a long lag phase was observed. In strain TH-1, the evidence about the operation of glyoxylate cycle under heterotrophic and mixotrophic condition with acetate/butyrate had already been reported in Chapter 2.

In addition to the operation of glyoxylate cycle, the function of RubisCO in strain TH-1 under autotrophic or mixotrophic condition causes the inhibition of the growth of strain TH-1, as reported in chapter 3. Although biochemical data has been accumulating and draft genome information of *H. thermoluteolus* TH-1 is available, the expression patterns of the responsible genes have not been analyzed systematically. Because strain TH-1 showed ability for autotrophic, heterotrophic, or mixotrophic

growth, it is interesting to carry-out the microarray and metabolome analyses in strain TH-1.

Nowadays, microarray is a new and good molecular method with high potential application for many fields such as academia, medicine, pharmaceutical, biotechnology, agro-chemical, and food industries [52]. Based on the central dogma theory of life, the expression of the genes contains three main steps: DNA replication, RNA transcription and protein translation. If one gene was expressed to give functional protein, the first step must be transcription. By transcription, messenger RNAs (mRNAs) were synthesized. Messenger RNAs will work as a template on which ribosome translates the genetic code to amino acid, a monomer of protein chain. Therefore, mRNA represents gene function. When we measure the level of a mRNA, we are monitoring the activity of a gene transcription. Thus, if we can understand all the level of mRNAs, we can study the expression of whole genes under different conditions. Microarray is a powerful tool to research about the expression of genes because with one single experiment, we can get over 10,000 blotting data which make monitoring the genome activity possible [52]. Microarray analysis is powerful but microarray workflow is a complicated system. The final result of microarray was affected by each step of manipulation. We have to manipulate a huge genome containing many genes. Another point is that mRNA contains genetic information in a single chain of ribonucleotides. Also, mRNA is unstable and easy to be damaged by RNase or physical factor such as temperature or light rays. Hence, microarray analysis should be carried out very carefully and controlled in each step.

In experimental design for microarray, there are two methods: single-sample hybridization and competitive hybridization. The single-sample hybridization is the method in which target molecules from each biological sample are labeled with fluorescent dye and hybridized to the surface of single array. By this way, the signal is measured absolutely. On the other hand, the competitive hybridization designs measure the relative concentration of each probed species in two or more samples. The samples are then mixed and hybridized on the surface of an array. Both of these hybridization strategies have been used in the microarray field to produce accurate and

reproducible data. However, the disadvantage of competitive hybridization designs is that, with two samples used per array, costs are double. A second consideration is that no two dyes will perform identically in an array experiment [53]. From this point of view, single-sample hybridization for research in strain TH-1 is used.

Another approach to study about metabolism of bacteria that increases the attention at recent time is metabolomics research. Metabolome analysis is a comprehensive identification and quantification of intracellular metabolites to evaluate the metabolic process of carbon substrate of bacteria. Such information allows us to study about cellular metabolic status. Many researchers have expressed their opinion that metabolomics describe the function within the cell better than genomics, transcriptomics or proteomics. The metabolomics are also useful to evaluate impact of genetic modifications and change of culture conditions. However, metabolome analysis is also a challenge because we have to work with a huge data of various different metabolites. Until now, there is no single method for detecting all the metabolites of the cells. Metabolome analysis is performed by two directions: using nuclear magnetic resonance (NMR) or using mass spectrometry. NMR is applied by basing on the information about proton spectrum,  $C^{13}$  spectrum, etc, for determination the structure of metabolites. This method is time consuming and could not be applied for whole cells metabolomics analysis since an enormous spectrum data and information are required [54]. Mass spectrometry is more applicable. Recently, a new device CE-TOFMS was developed by combination of capillary electrophoresis (CE) and time-of-flight mass spectrometry (TOFMS), which is capable to analyze ionic metabolic intermediates quantitatively and comprehensively even in a very small amount. Therefore, I applied CE-TOFMS to analyze metabolomics of strain TH-1 under autotrophic, heterotrophic and mixotrophic condition with butyrate.

Here, in this chapter, I focused on the investigation for the expression of genes from whole genome of strain TH-1, and metabolomic analysis under autotrophic condition, heterotrophic or mixotrophic conditions with butyrate as substrate. The expression profile of the genes and intermediate metabolites that belong to central carbon

metabolic pathways including the biochemistry as well as their ecological relevance were evaluated and discussed.

## 4.2. Materials and methods

### 4.2.1. Microarray construction

A custom gene expression microarray for *H. thermoluteolus* TH-1 was designed according to the draft genome sequence and this draft genome sequence was used to determine the expression level of genes under autotrophic condition, heterotrophic condition, or mixotrophic condition with butyrate. This work should be completed before RNA extraction step because it takes time for designing probes and also for ordering the microarray slide.

Custom array design work includes 4 steps: 1. Login to Agilent eArray site (<https://earray.chem.agilent.com/earray/>), 2. Probe design; 3. Array format design; 4. Order .

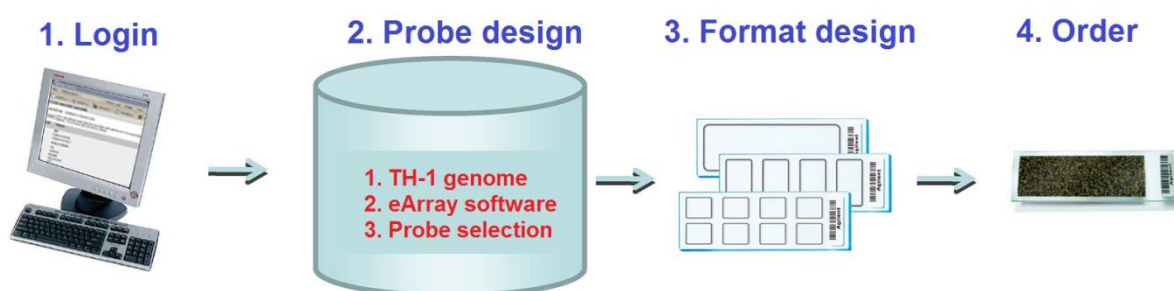


Figure 4-1. The workflow of custom array design (Agilent Technologies, Inc)

*H. thermoluteolus* TH-1 draft genome is available, and the size of genome is about 2,253,820 bp. The annotated genes are 2,152 genes which are distributed in 38 contigs. All of genes were annotated by using NCBI blast tool (<http://blast.ncbi.nlm.nih.gov/Blast.cgi>), Brenda protein database (<http://www.brenda-enzymes.org/>), and KEGG pathway database (<http://www.genome.jp/kegg/pathway.html>).

For microarray analysis, all the available open frame readings (ORFs) were used for probe design after deleting the shorth length ORFs (size of ORFs were smaller than 200 bp).

Microarray experiments were performed for two biological replicates for each growth condition.

#### 4.2.1.1 Probe design

Each ORF was used to produce 7 specific probes by using one file in FASTA format that contains the gene sequence. The probes were designed by submitting ORF sequence to the e-Array tool that integrates in the website of Agilent (<https://earray.chem.agilent.com/earray/>). Each probe contains 60 unique oligonucleotides for specific target gene. In strain TH-1, totally 14,175 probes were created from 2,025 ORFs.

#### 4.2.1.2. Probe group

If there were not any problem about designed probes, probes were grouped by probe group function in e-Array tool. From now, we could download the probe group files to the computer and join all groups to the array file.

Additionally, in order to validate the transcriptome experiment, the reference probes are required. However, because this was the first time when microarray analysis was applied for the research in strain TH-1, I did not have information about house keeping genes for reference.

Table 4-1: List of house keeping genes for making reference probes set

	Contig	Gene	Enzyme/Protein
1	contig00001_orf00376	<i>nuoG</i>	NADH dehydrogenase I, chain G
2	contig00002_orf00184	<i>lysC</i>	aspartate kinase
3	contig00003_orf00055	<i>atpA</i>	ATP synthase alpha chain
4	contig00003_orf00190	<i>gyrB</i>	DNA gyrase subunit B
5	contig00005_orf00053	<i>ccoN</i>	cytochrome c oxidase, cbb3-type, subunit I
6	contig00005_orf00130	<i>sucA</i>	2-oxoglutarate dehydrogenase
7	contig00005_orf00132	<i>gltA</i>	citrate synthase
8	contig00005_orf00137	<i>sdhA</i>	succinate dehydrogenase, flavoprotein subunit
9	contig00009_orf00075	<i>recA</i>	RecA protein
10	contig00010_orf00075	<i>groEL</i>	chaperonin GroEL
11	contig00010_orf00086	<i>qcrB</i>	cytochrome b
12	contig00014_orf00007	<i>rpoA</i>	DNA-directed RNA polymerase alpha subunit
13	contig00015_orf00028	<i>infC</i>	translation initiation factor IF-3
14	contig00015_orf00033	<i>acoA</i>	aconitate hydratase
15	contig00016_orf00044	<i>rpoD</i>	DNA-dependent RNA polymerase sigma subunit

Thus, I selected 15 genes described below from all genes. These genes have important function in metabolism in TH-1 strain. Then till this step, I have 2 probe groups (for all genes, and reference genes).

#### 4.2.1.3 Array design

The format of array was chosen as 8x15K because it is validated prokaryote gene expression microarray protocol. The number of available features on 8 X 15K format is 15,208 features ([Total 15,744 features]-[Agilent control spot 536 features]).

From 2 probe group files (for all genes, and reference genes), the array was designed by using e-Array tool. The summary of microarray information is as follows:

- Reference genes (105 probes, replicate 9 times): 945 features.
- All genes (14,175 probes, replicate 1 time): 14,175 features.
- Then, total features without Agilent control is 15,120 features.
- Final features of the array with Agilent control (536 spot) is 15,656 features.

The details of microarray are listed as below:

- Microarray design name: *Hydrogenophilus thermoluteolus* TH-1
- Design ID: 070160
- Slide format: 8 X 15K
- Application: Expression
- Type: single color Cyanine 3-CTP (Cy3)
- Platform: surface by glass
- Probe: oligonucleotide DNA

#### 4.2.2. Total RNA extraction

##### 4.2.2.1. Bacterial culture for RNA extraction

The growth curves of *H. thermoluteolus* TH-1 under autotrophic, heterotrophic, or mixotrophic condition were constructed. Growth characteristics were determined by monitoring the optical density (OD<sub>540</sub>) with culture volume of 10 mL in 100 mL vials. Autotrophic growth was performed using mineral salts medium with the trace elements (final gas phase consisting of H<sub>2</sub>:O<sub>2</sub>:CO<sub>2</sub> (75:10:15)).

Growth experiments under heterotrophic conditions were performed in air atmosphere using the medium for autotrophic condition with addition of butyrate as sole carbon source.

Growth experiments under mixotrophic conditions were performed with the medium and gas phase as under autotrophic condition with addition of butyrate.

*H. thermoluteolus* TH-1 was grown in 10 mL medium culture for three conditions in a 100 mL vial. For all conditions, 10 mL of the culture was mixed with 1 volume of RNA protect (Quiagen, Hilden, Germany) when the optical density (OD) at 540 nm reached approximately 0.4-0.6 to stabilize total RNA.

Cells of strain TH-1 were collected by centrifugation for 10 minutes at 3,000 x g. RNA was extracted from the cell pellet by a hot-phenol method.

#### *4.2.2.2. Preparation of Lysis sol*

The Lysis sol is required for total RNA extraction. At first, in a clean bench in RNA zone, 10 ml of RNA Protect was put in 50 ml centrifuge tubes, then 10 ml culture solution was added in the centrifuge tube, and the tubes were vortexed. The tubes were centrifuged at 4,000 x g for 10 minutes. After centrifugation, supernatant was removed by decantation. The tubes were inverted and dried for 30 minutes. When the sample was dried, next step was extraction of total RNA.

For cell lysis, 1000 µl of 1.0 mg /ml lysozyme (TE pH 8.0) was added into the tube that contains the sample, and the tube was vortexed. The bacteria were dissolved until the solution became clear. Then, 80 µl of the 10% SDS was put into the tube and heat treatment was done for 1 minute at 65°C. The tube was shaken to eliminate the precipitation of bacteria until solution became clear. This solution is called as Lysis sol.

#### *4.2.2.3. RNA extraction*

For RNA extraction: prepare 2 mL tube, and add 88 µl of 1M Na- acetate (pH 5.2) and 1 mL of Water Saturated Phenol (pH 7.0) and keep at 65°C. Then, the total amount of the Lysis sol was put into the prepared tube and inverted. The tubes were incubated at

65°C for 7 minutes. After incubation, the tubes were centrifuged at 13,000 x g for 10 minutes at 4°C.

During centrifugation, 1,000 µl of PCI (Phenol-Chloroform-Isoamyl Alcohol) was added in a new 2 ml tube. After centrifugation, 800 µL of the upper transparent layer was taken, and put it into a PCI tube and invert. After several times of the inversion of the tube, centrifugation at 13,000 x g for 10 minutes at 4°C was performed.

During centrifugation, 1000 µl the CI (Chloroform-Isoamyl Alcohol) was added to a new 2 ml tube. After centrifugation, 300 µL of the upper layer was taken and added to a tube CI, and mixed by inverting (10 times). After centrifugation at 13,000 x g for 5 minutes at 4°C, 300 µl of the upper layer was transferred to 1.5 ml tube.

Per each sample, two tubes were made. In each tube: 3M Na - acetate (pH 5.2) (40 µl), 1 mM EDTA (40 µl), and cold ethanol (800 µl) were added, and inverted (10 times). The samples were incubated at -80°C overnight. After overnight incubation, the sample was centrifuged at 14,000 x g for 25 minutes at 4°C.

After the centrifugation, the supernatant was removed. The white precipitation was made. The precipitate was washed by adding 1 ml of 80% cold ethanol and centrifugated at 14,000 x g for 5 minutes at 4°C. After centrifugation, the supernatant was discarded. After successive centrifugation at 15,000 x g for 1 ~ 2 minutes, the supernatant was removed.

The pellete was dried, and dissolved in the water (40 µl) by firm vortexing. Finally, the sample in two tubes was collected into a single tube.

#### *4.2.2.4. DNase treatment*

Ten µl of 10× DNase buffer was added into the tube that contains 80 µl of the sample, and mixed by pipetting. DNase of 10 µl was added, vortexed instantly and flashed. Sample was incubated at 37°C for 1 hour.

#### *4.2.2.5. RNA Cleanup*

RLT buffer (350 µl) was added to the sample and inverted. Then, 250µl of 96-100% ethanol was added into each tube and inverted.

The entire amount (700  $\mu$ l) of sample was transferred to RNeasy Mini Spin Column (below, I call it column). Then, the sample was centrifuged at 9,100 x g for 15 seconds at 25°C. After centrifugation, the flow-through was discarded and 500  $\mu$ l of RPE buffer was put into the column. Sample was centrifuged at 10,000 x g for 15 seconds at 25°C. After centrifugation, the flow-through was discarded. Then, 500  $\mu$ l of RPE buffer was added into the column and centrifuged at 9,100 x g for 2 minutes at 25°C. Column was put in a new 2 ml tube. After the sample was centrifuged at 9,100 x g for 1 minute at 25°C, the column was put in 1.5 ml tubes and 40  $\mu$ l of RNase - free water was added to the column. The tube was centrifuged at 9,100 x g for 1 minute at 25°C. Then, 40  $\mu$ l of RNase-free water was added into the column. The tube was centrifuged at 9,100 x g for 1 minute at 25°C. Finally, the elution ended at 80  $\mu$ l.

After the treatment, the sample was treated second round of RNA cleanup.

In second round of RNA Cleanup:

RNase-free water (30  $\mu$ l) was added into the column and centrifuged at 9,100 x g for 1 minute at 25°C. Re-elution was done by adding the eluate into the column, the tube was centrifuged at 9,100 x g for 1 minute at 25°C. Elution ended at 30  $\mu$ l of total RNA, the sample was stored at -80°C.

#### *4.2.2.6. RNA quantification*

Prepare 50  $\mu$ L PCR tube (contains 18  $\mu$ L RNase-free water) and 1.5 mL tube (contains 72  $\mu$ L RNase-free water) for each sample.

Total RNA (2  $\mu$ L) was added to 50  $\mu$ L PCR tube (contains 18  $\mu$ L of RNase-free water, 10 times of dilution from original RNA). After the sample was mixed by vortex, 18  $\mu$ L of sample was transferred to 1.5 mL tube (contains 72  $\mu$ L RNase-free water, in totally 50 times of dilution from original RNA).

In the last step, PCR tube containing 2  $\mu$ L of total RNA was used as template for PCR check; 1.5 mL tube containing 90  $\mu$ L of RNA was used for Nano Drop quantification.

#### *a. PCR for DNA contamination investigate*

In order to perform microarray analysis, the total purified RNA must not be contaminated DNA. DNA contamination affects the level of gene expression in some

ways. Therefore, the DNA contamination check is required. After total RNA was isolated, DNA genome was teared into tiny fragments. So, for PCR reaction check, the length of the target gene should be the short sequence (100-300 bp). In this experiment, the target gene was a transcriptional regulator, CopG family gene (contig00023\_orf00014). The length of this gene was 219 bp. The length of PCR product was 180 bp.

Table 4-2: Components of PCR for DNA contamination check

Components	Volume (μl)
Distilled water	39.25
10×buffer	5.00
dNTP	4.00
primer F (100 pmol /μl)	0.50
primer R (100 pmol /μl)	0.50
Template	0.50
Ex taq	0.25
Total	50.0

Table 4-3: The primer profile of PCR for DNA contamination check

Primer	Start	Length	Tm	GC %	Sequence
F_contig23_orf14	23.0	20	61.57	55.0	GTCTCGACGAAACCCTCGAT
R_contig23_orf14	202.0	20	60.26	55.0	AGATGTCTTCGTTTCGGTGAGG

Negative control ..... water 0.50 μl

Positive control .....chromosome DNA of strain TH-1 (100-fold dilution) 0.50 μl

Table 4-4: PCR program for DNA contamination check

Temperature (°C)	Time	Cycle
96	2 minutes	30
98	20 seconds	
56	30 seconds	
72	30 seconds	
72	10 minutes	
4	∞	

Electrophoresis: this step is required for DNA contamination check. Because the length of PCR product is very small (180 bp), the gel concentration should be high.

Therefore, in this case, 3% agarose gel was used. After the sample was electrophoresed, ethidium bromide staining was conducted.

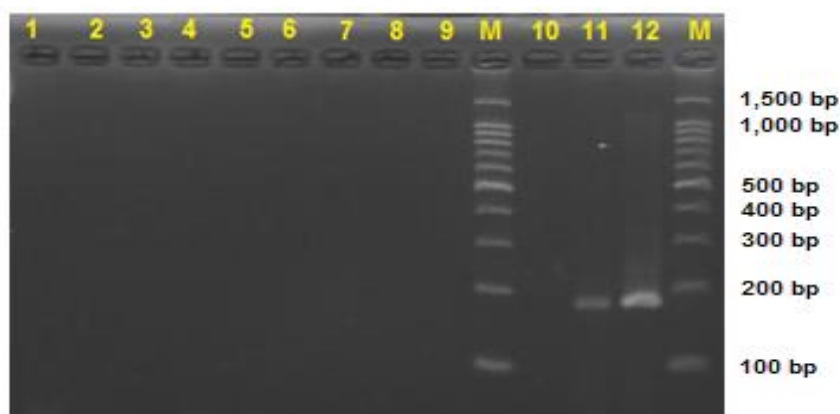


Figure 4-2. Quality of total RNA samples was good, no DNA contamination was detected. Autotrophy lane 1-3, heterotrophy lane 4-6, mixotrophy lane 7-9. Negative control lane 10. Positive control lane 11-12. Marker 100 bp: lane M

As I expected, one band corresponding with the length approximately 180 bp was seen in positive control with strain TH-1 genome (lane 11, 12), and no band appeared in negative control (lane 10). No band was seen from lane 1 to lane 9 showing that no DNA contamination in total purified RNA. Quality of total RNA samples was good, no DNA contamination was detected.

#### *b. RNA concentration*

Table 4-5: Total RNA samples were extracted from TH-1 under different conditions.

Sample ID	abs <sub>260</sub>	abs <sub>280</sub>	260/280	280/260	Protein (ug/ml)	Nucleic Acid (ug/ml)
Autotrophic 1	1.13	0.62	1.85	0.54	89.83	48.34
Autotrophic 2	0.97	0.54	1.80	0.56	100.91	41.53
Autotrophic 3	0.81	0.45	1.80	0.56	87.39	35.20
Heterotrophic 1	1.60	0.86	1.86	0.54	124.84	69.81
Heterotrophic 2	0.79	0.44	1.78	0.56	91.81	33.80
Heterotrophic 3	1.50	0.81	1.85	0.54	119.34	64.69
Mixotrophic 1	0.33	0.18	1.76	0.57	40.90	14.15
Mixotrophic 2	0.34	0.19	1.75	0.57	47.25	15.16
Mixotrophic 3	0.20	0.11	1.79	0.56	20.89	8.27

The Nano Drop equipment was used for RNA concentration measurement. The ratio of  $A_{260}/A_{280}$  from 1.8 -2.1 assumes the good quality.  $A_{260} = 1 = 0.04 \mu\text{g}/\mu\text{L}$ . So, the concentration of RNA =  $0.04 \times 50 \times A_{260} (\mu\text{g}/\mu\text{L}) = 40 \times 50 \times A_{260} (\text{ng}/\mu\text{L})$ .

*c. RNA integrity number*

After DNA contamination of sample was checked, the quality of total RNA was checked before proceeding to the next step. RNA quality is evaluated by RNA integrity number (RIN) score since RIN influence the labelling efficiency. RIN score was measured by using 2100 Bioanalyzer equipment (Agilent Technologies, Inc.).



Figure 4-3. 2100 Bioanalyzer equipment (Agilent Technologies, Inc.)

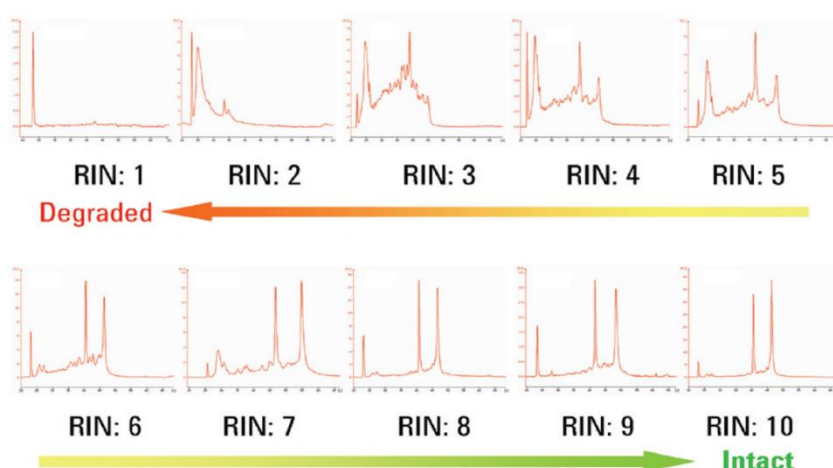
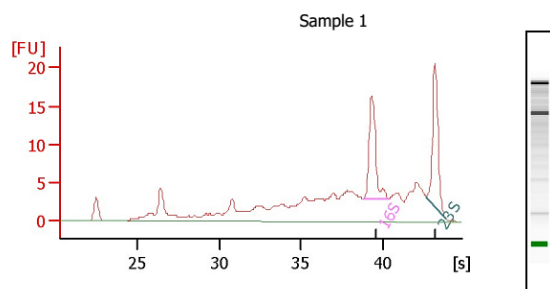


Figure 4-4. The RNA integrity number (RIN) is evaluated according to SCORE from 1 to 10 corresponding to the integrity of RNA from degraded to intact. RIN < 3 (Severe degradation), RIN < 6 (Partial degradation), RIN > 9 (Intact) (Agilent Technologies, Inc.).

For proceeding microarray analysis, as Agilent company recommendation, RIN score should be higher than 6.0.

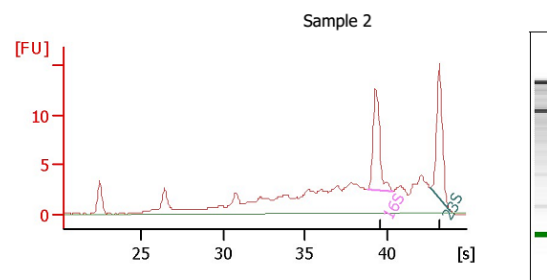


**Overall Results for sample 1 :** Sample 1

RNA Area: 150.4  
RNA Concentration: 278 ng/μl  
rRNA Ratio [23s / 16s]: 1.0  
RNA Integrity Number (RIN): 6.6 (B.02.02)

**Fragment table for sample 1 :** Sample 1

Name	Start Time [s]	End Time [s]	Area	% of total Area
16S	38.76	40.37	16.1	10.7
23S	42.68	43.87	16.3	10.9

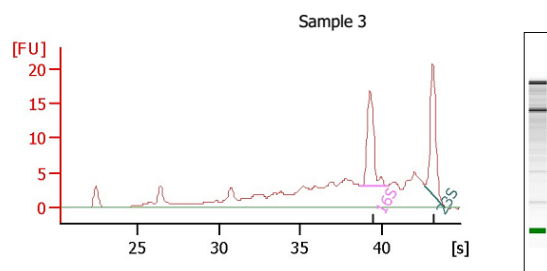


**Overall Results for sample 2 :** Sample 2

RNA Area: 114.1  
RNA Concentration: 211 ng/μl  
rRNA Ratio [23s / 16s]: 1.0  
RNA Integrity Number (RIN): 6.5 (B.02.02)

**Fragment table for sample 2 :** Sample 2

Name	Start Time [s]	End Time [s]	Area	% of total Area
16S	38.81	40.36	12.2	10.7
23S	42.61	43.83	12.3	10.8

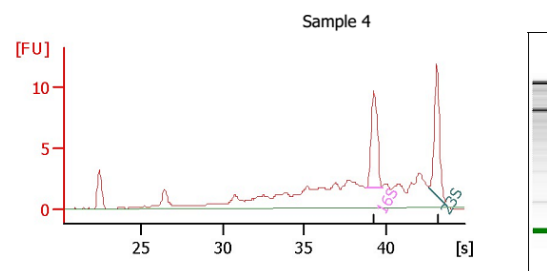


**Overall Results for sample 3 :** Sample 3

RNA Area: 148.6  
RNA Concentration: 275 ng/μl  
rRNA Ratio [23s / 16s]: 1.0  
RNA Integrity Number (RIN): 6.6 (B.02.02)

**Fragment table for sample 3 :** Sample 3

Name	Start Time [s]	End Time [s]	Area	% of total Area
16S	38.72	40.30	16.9	11.4
23S	42.63	43.88	16.7	11.2

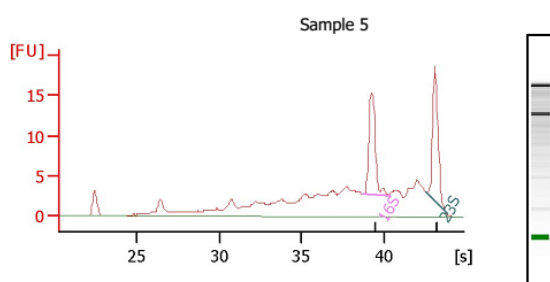


**Overall Results for sample 4 :** Sample 4

RNA Area: 76.2  
RNA Concentration: 141 ng/μl  
rRNA Ratio [23s / 16s]: 1.1  
RNA Integrity Number (RIN): 6.6 (B.02.02)

**Fragment table for sample 4 :** Sample 4

Name	Start Time [s]	End Time [s]	Area	% of total Area
16S	38.78	39.74	8.4	11.0
23S	42.60	43.71	9.2	12.0

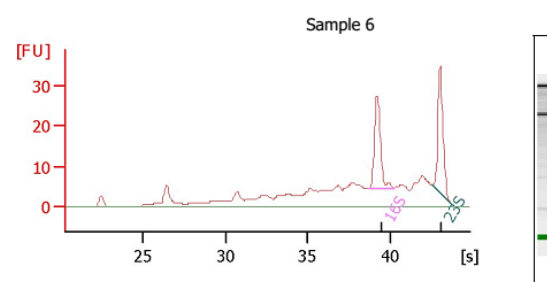


**Overall Results for sample 5 :** Sample 5

RNA Area: 131.8  
RNA Concentration: 244 ng/μl  
rRNA Ratio [23s / 16s]: 1.0  
RNA Integrity Number (RIN): 6.6 (B.02.02)

**Fragment table for sample 5 :** Sample 5

Name	Start Time [s]	End Time [s]	Area	% of total Area
16S	38.72	40.28	14.4	10.9
23S	42.57	43.81	14.9	11.3

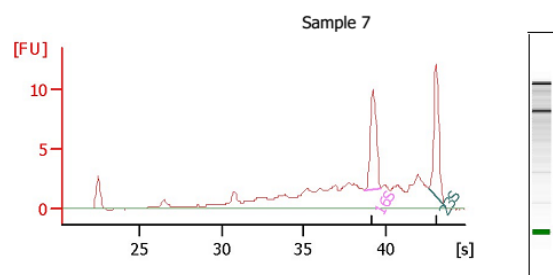


**Overall Results for sample 6 :** Sample 6

RNA Area: 228.1  
RNA Concentration: 422 ng/μl  
rRNA Ratio [23s / 16s]: 1.1  
RNA Integrity Number (RIN): 6.8 (B.02.02)

**Fragment table for sample 6 :** Sample 6

Name	Start Time [s]	End Time [s]	Area	% of total Area
16S	38.66	40.22	25.7	11.3
23S	42.52	43.71	27.2	11.9

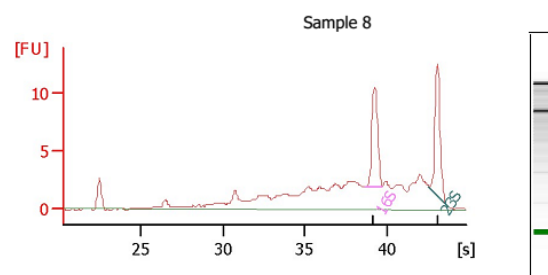


**Overall Results for sample 7 :** Sample 7

RNA Area: 74.0  
 RNA Concentration: 137 ng/μl  
 rRNA Ratio [23s / 16s]: 1.0  
 RNA Integrity Number (RIN): 6.6 (B.02.02)

**Fragment table for sample 7 :** Sample 7

Name	Start Time [s]	End Time [s]	Area	% of total Area
16S	38.68	39.70	8.7	11.7
23S	42.58	43.65	9.1	12.2

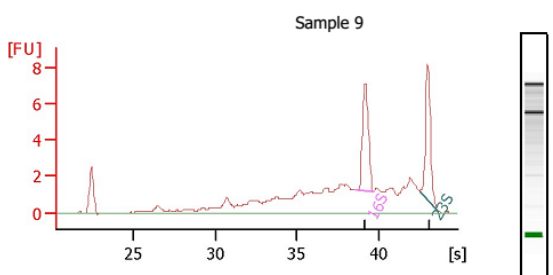


**Overall Results for sample 8 :** Sample 8

RNA Area: 86.1  
 RNA Concentration: 159 ng/μl  
 rRNA Ratio [23s / 16s]: 1.1  
 RNA Integrity Number (RIN): 6.5 (B.02.02)

**Fragment table for sample 8 :** Sample 8

Name	Start Time [s]	End Time [s]	Area	% of total Area
16S	38.70	39.68	8.8	10.3
23S	42.53	43.69	9.4	10.9

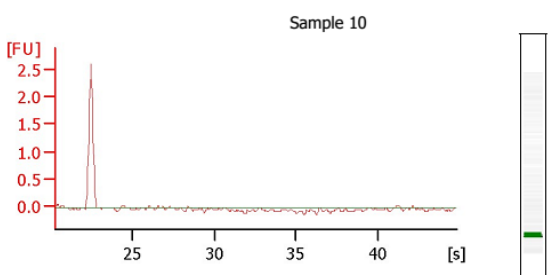


**Overall Results for sample 9 :** Sample 9

RNA Area: 52.0  
 RNA Concentration: 96 ng/μl  
 rRNA Ratio [23s / 16s]: 1.0  
 RNA Integrity Number (RIN): 6.6 (B.02.02)

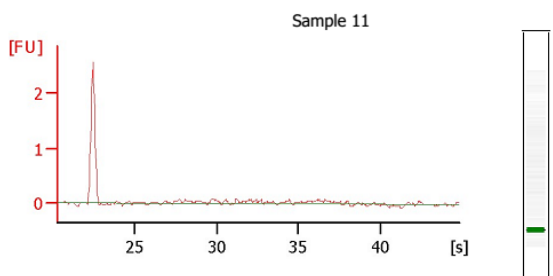
**Fragment table for sample 9 :** Sample 9

Name	Start Time [s]	End Time [s]	Area	% of total Area
16S	38.58	39.66	6.2	11.9
23S	42.52	43.59	6.1	11.6



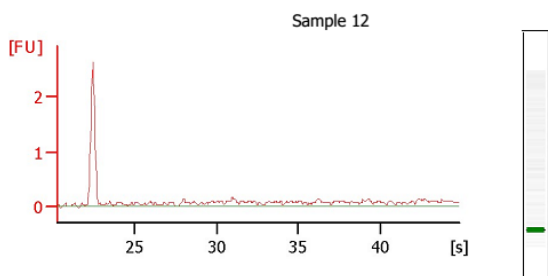
**Overall Results for sample 10 :** Sample 10

RNA Area: 0.3  
 RNA Concentration: 1 ng/μl  
 rRNA Ratio [23s / 16s]: 0.0  
 RNA Integrity Number (RIN): N/A (B.02.02)



**Overall Results for sample 11 :** Sample 11

RNA Area: 1.5  
 RNA Concentration: 3 ng/μl  
 rRNA Ratio [23s / 16s]: 0.0  
 RNA Integrity Number (RIN): N/A (B.02.02)



**Overall Results for sample 12 :** Sample 12

RNA Area: 4.8  
 RNA Concentration: 9 ng/μl  
 rRNA Ratio [23s / 16s]: 0.0  
 RNA Integrity Number (RIN): N/A (B.02.02)

Figure 4-5. RNA integrity from total RNA of strain TH-1 (sample 1-9) Sample No.1-3: autotrophic condition; Sample No.4-6: heterotrophic condition; Sample No.7-9: mixotrophic condition; Sample No.10-12: negative control.

RIN scores of all the samples were over 6.5 showing that all total RNA samples quality was sufficient to proceed for microarray analysis.

Based on the results for RNA concentration (Table 4-5), DNA contamination check and RNA integrity check, I decided the samples for each group proceeding for each growth mode as follows:

- Autotrophy: sample 1, 2
- Heterotrophy: sample 1, 3
- Mixotrophy: sample 1, 2

#### 4.2.3. Microarray analysis protocol

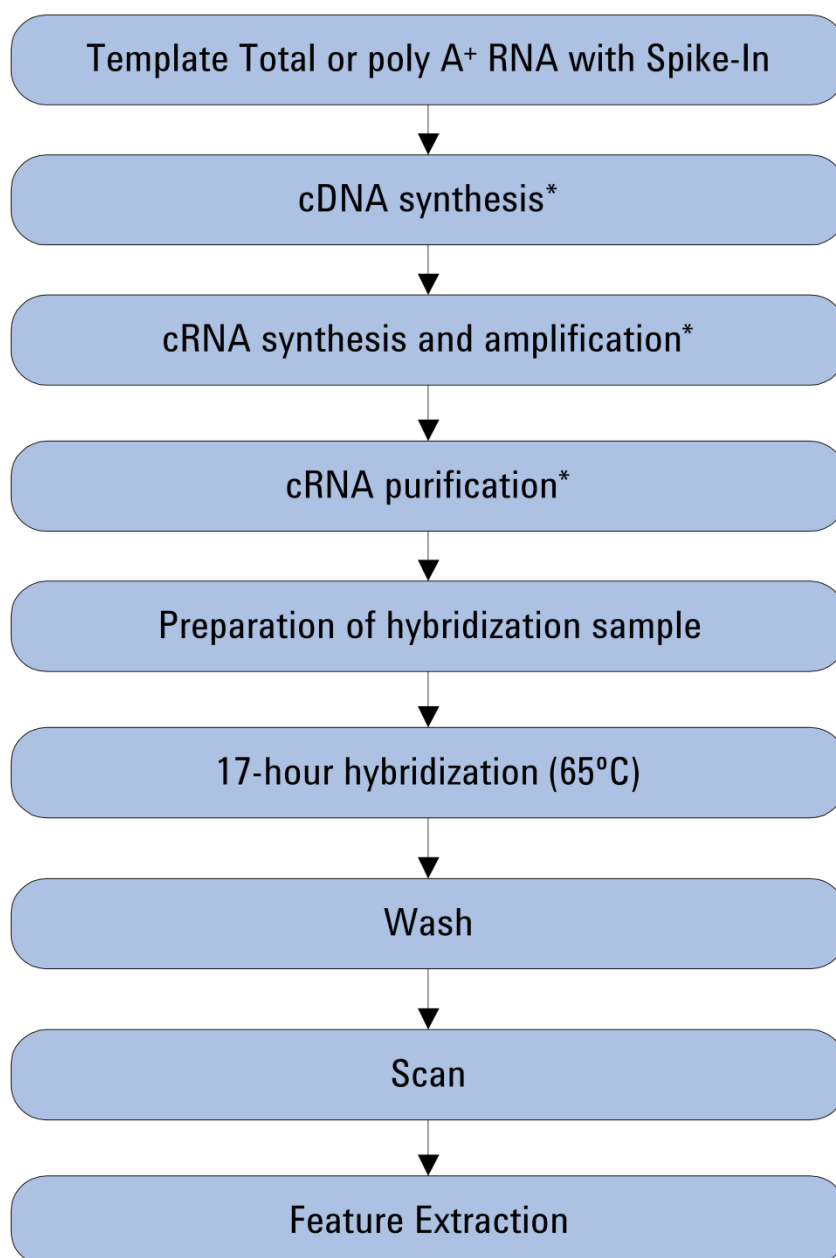
Microarray analysis experiment was conducted by following the manufacture protocol instruction. The protocol version 6.6, September 2012 for One-Color Microarray-Based Gene Expression Analysis (Quick Amp Labelling-Microarrays manufactured with Agilent SurePrint Technology) from Agilent Technologies, Inc was employed.

##### 4.2.3.1. Sample preparation

###### *a. Preparing Spike mix*

In prokaryote, the start total RNA concentration is recommended as 100 ng for optimum hybridization reaction.

For validating the microarray hybridization efficiency, the internal positive control is required. The Spike Mix reagent from Agilent Technologies, Inc contains the internal positive control stock. It needs to be diluted to proper concentration with bacteria RNA concentration. The first dilution of Spike Mix was created by diluting the Spike Mix by following ratio 1:20. The Second Dilution was created by dilution First Dilution by following ratio 1:25. The Third Dilution was created by diluting Second Dilution by following ratio 1:20. Third Dilution of 2 µL was added to 100 ng of total RNA sample and continued with Cyanine 3-CTP labeling using Agilent Low Input Quick Amp WT Kit.



\* Samples can be stored frozen at -80°C after these steps, if needed.

Figure 4-6. Workflow for sample preparation and array processing (Agilent Technologies, Inc)

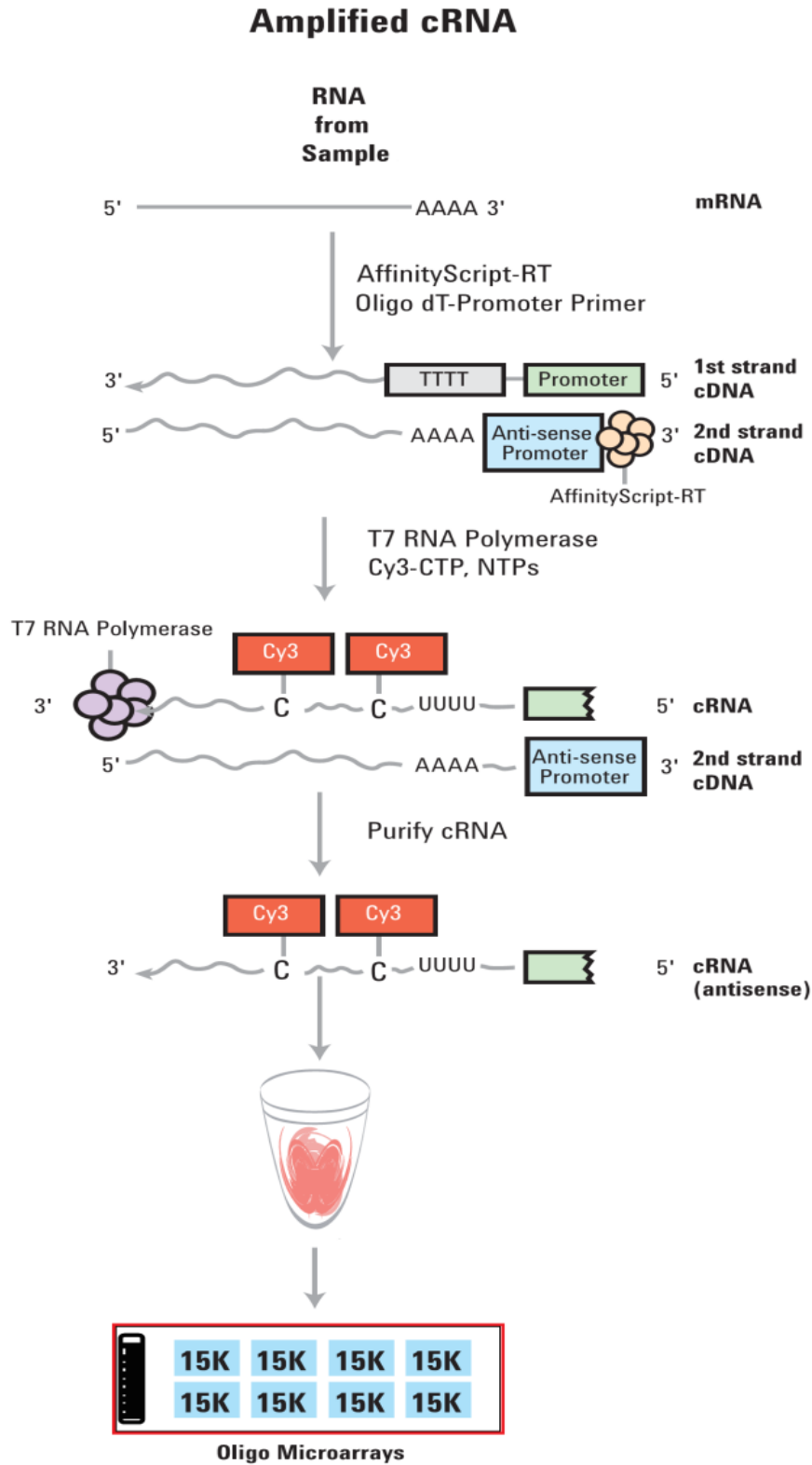


Figure 4-7. Schematic of amplified cRNA procedure. Generation of cRNA for a one-color microarray experiment, the Cy3-labeled sample is produced and hybridized (Agilent Technologies, Inc).

### *b. Preparing labelling reaction*

Total RNA (100 ng) was added into a 1.5 mL microcentrifuge tube in a final volume of 2.3  $\mu$ L. The WT Primer Master Mix was prepared and added to sample.

Volume ( $\mu$ L) of WT Primer Master Mix for 10 reactions (30  $\mu$ L): WT Primer Mix (10  $\mu$ L), Spike Mix third dilution (20  $\mu$ L).

Then, 3  $\mu$ L of WT Primer Master Mix was added into the tube that contained 2.3  $\mu$ L of total RNA and diluted RNA spike-in controls. Each tube contained a total volume of 5.3  $\mu$ L. The primer and the template were denatured by incubating the reaction at 65°C in a circulation water bath for 10 minutes. The reactions were placed on ice and incubated for 5 minutes.

The preparation of cDNA Master Mix:

The components of cDNA Master Mix for 10 reactions (47  $\mu$ L) were added into a 1.5 mL microcentrifuge tube: 5x First Strand Buffer (20  $\mu$ L), 0.1 M DTT (10  $\mu$ L), 10 mM dNTP Mix (5  $\mu$ L), Affinity Script RNase Block Mix (12  $\mu$ L).

Each tube was spun briefly in a microcentrifuge to drive down the contents from the tube walls and the lid.

The cDNA Master Mix of 4.7  $\mu$ L was added to each sample tube and mixed by pipetting up and down. Each tube contained a total volume of 10  $\mu$ L. Then, the sample was incubated at 40°C in a circulating water bath for 2 hours. The sample was put on a 70°C circulating water bath and incubated for 15 minutes.

Sample was put on ice and incubated for 5 minutes. Then, sample was spun briefly in a microcentrifuge to drive down tube contents from the tube wall and lid.

### *c. The preparation of Transcription Master Mix*

The components of Transcription Master Mix were added for 10 reactions (total volume 60  $\mu$ L): Nuclease-free water (7.5  $\mu$ L), 5x Transcription Buffer (32  $\mu$ L), 0.1 M DTT (6  $\mu$ L), NTP Mix (10  $\mu$ L), T7 RNA polymerase Blend (2.1  $\mu$ L), Cyanine 3-CTP (2.4  $\mu$ L).

Transcription Master Mix of 6  $\mu$ L was added into each sample tube and gently mixed by pipetting. Each tube contained a total volume of 16  $\mu$ L. Sample was incubated in a circulating water bath at 40°C for 2 hours.

*d. Purify the labelled/amplified RNA*

The RNeasy Mini Kit was used to purify the amplified cRNA samples.

At first, 84 µL of nuclease-free water was added to cRNA sample, for a total volume of 100 µL. Then, 350 µL of RLT buffer was added and mixed well by pipetting. Ethanol (96% to 100% purity) of 250 µL was added and mixed thoroughly by pipetting. The cRNA sample of 700 µL was transferred to an RNeasy Mini Spin Column in a Collection Tube (2 mL). The sample was spun in a centrifuge at 4°C for 30 second at 13,000 xg. The flow-through was discarded and collected. The RNeasy column was transferred to a new Collection Tube (2mL) and 500 µL of Buffer RPE (containing ethanol) was added to the column. The sample was spun at 4°C for 30 second at 13, 000 x g. Flow-through was discarded. The collection tube was re-used. Another 500 µL of RPE buffer was added to the column. The sample was centrifuged in a centrifuge at 4°C for 60 seconds at 13,000 x g. The flow-through was discarded and the tube was collected. The RNeasy column was transferred to a new Collection Tube (1.5 mL) and the sample was spun in a centrifuge at 4°C for 30 second at 13, 000 x g. This collection tube was discarded. Collection Tube (1.5 mL) was refreshed to elute the cleaned cRNA sample.

The purified cRNA sample was eluted by transferring the RNeasy column to a new Collection Tube (1.5 mL). RNase-Free Water of 30 µL was added directly onto the RNeasy filter membrane. After 60 seconds, the sample was centrifuged at 4°C for 30 seconds at 13, 000 x g. The cRNA sample-containing flow-through was maintained on ice. The RNeasy column was discarded.

*e. Quantify the cRNA*

The NanoDrop ND-1000 UV-VIS Spectrophotometer was used to quantify the cRNA.

The yield and specific activity of each reaction were determined as follows:

The concentration of cRNA (ng/ µL) was used to determine the weight of cRNA yield as follows:

$(\text{Concentration of cRNA}) \times 30 \text{ } \mu\text{L (elute volume)} / 1000 = \text{weight of cRNA (}\mu\text{g)}$

Table 4-6. Concentration of cRNA after amplification

No.	Array barcode	Sample	Dye	start total RNA amount (ng)	conc (ng/ul)	total cRNA amount (ug)	Amp.efficiency (mRNA = 2% in total RNA)
1	70160	Autotrophic 1	Cy3	100	90.6	2.72	1359
2	70160	Autotrophic 2	Cy3	100	125.2	3.76	1878
3	70160	Heterotrophic 1	Cy3	100	191.6	5.75	2874
4	70160	Heterotrophic 3	Cy3	100	217.8	6.53	3267
5	70160	Mixotrophic 1	Cy3	100	167.9	5.04	2519
6	70160	Mixotrophic 2	Cy3	100	154.1	4.62	2312

#### 4.2.3.2. Hybridization

##### a. Preparation of 10X Blocking Agent

Nuclease-free water (500  $\mu$ L) was added to the vial containing lyophilized 10X Gene Expression Blocking Agent supplied with the Gene Expression Hybridization Kit. The tube was gently mixed on a vortex mixer.

##### b. Preparation of hybridization samples

For each microarray, each of the components was added in total volume (25  $\mu$ L) as follows: Cyanine 3-labelled, linearly amplified cRNA (600 ng), 10x Gene Expression Blocking Agent (5  $\mu$ L), nuclease-free water (bring to 24  $\mu$ L) 25 X Fragmentation Buffer (1  $\mu$ L) into a 1.5 mL nuclease-free centrifuge tube.

The tube was mixed well but gently on a vortex mixer and incubated at 60°C for exactly 30 minutes to fragment RNA.

Table 4-7. Components for 8-Pack array format

No.	Array barcode	Sample	Dye	conc (ng/ul)	600ng cRNA (uL)	Blocking Agent (uL)	s.D.W. (uL)	Total (uL)
1	70160	Autotrophic 1	Cy3	90.6	6.62	5	12.38	25
2	70160	Autotrophic 2	Cy3	125.2	4.79	5	14.21	25
3	70160	Heterotrophic 1	Cy3	191.6	3.13	5	15.87	25
4	70160	Heterotrophic 3	Cy3	217.8	2.75	5	16.25	25
5	70160	Mixotrophic 1	Cy3	167.9	3.57	5	15.43	25
6	70160	Mixotrophic 2	Cy3	154.1	3.89	5	15.11	25

The sample was cooled on ice and the 2x Hi-RPM Hybridization Buffer was added to stop the fragmentation reaction. Sample was immediately cooled on ice for one minute.

2x Hi-RPM Hybridization Buffer of 25  $\mu\text{L}$  was added to stop the fragmentation reaction. So the volume became 50  $\mu\text{L}$  (25  $\mu\text{L}$ + 25  $\mu\text{L}$ ).

Table 4-8. Hybridization mix

Volumes per hybridization	
Components	8 - pack format
cRNA from Fragmentation Mix	25 $\mu\text{L}$
2x Hi-RPM Hybridization Buffer	25 $\mu\text{L}$

The tube was mixed well carefully by pipetting up and down.

The sample was spun for 1 minute at room temperature at 13,000 x g in a microcentrifuge to drive the sample off the walls and lid, and to aid bubbles reduction.

*c. Preparation of the hybridization assembly*

A clean gasket slide was loaded into the Agilent SureHyb chamber base with the label facing up and aligned with the rectangular section of chamber base.



Figure 4-8. Agilent SureHyb chamber (Agilent Technologies, Inc)

The volume of sample hybridization was slowly dispensed (prepared 50  $\mu\text{L}$ , load 40  $\mu\text{L}$ ) onto the gasket well in a “drag and dispense” manner.

Table 4-9. Hybridization Sample

Volumes per hybridization	
Components	8 - pack format
Volume prepared	50 $\mu$ L
Volume to hybridize	40 $\mu$ L

The SureHyb chamber cover was placed on the sandwiched slid and slide the clamp assembly onto both pieces. The clamp was hand-tighten firmly onto the chamber.

The assembled chamber was vertical rotated to wet gasket and assessed the mobility of the bubbles.

Assembled slide chamber was placed in a rotisserie in a hybridization oven (65°C). Hybridization rotator was set to rotate at 10 x g when uses 2x Hi-RPM Hybridization Buffer. The chamber was hybridized at 65°C for 17 hours.

#### 4.2.3.3. Microarray wash

At first, Triton X-102 (10%) was added to Gene Expression wash buffers to reduce the possibility of array artifacts. The Gene Expression Wash buffer 2 was pre-warmed at 37°C overnight. Then, the microarray slide was washed as in Table 4-10.

Table 4-10. Wash condition

	Dish	Wash Buffer	Temperature	Time
Disassembly	1	Gene Expression Wash Buffer 1	RT	
1 <sup>st</sup> Wash	2	Gene Expression Wash Buffer 1	RT	1 minutes
2 <sup>nd</sup> Wash	3	Gene Expression Wash Buffer 2	37°C	1 minutes

#### 4.2.3.4. Scanning and featuring extraction

##### a. Scanning the sildes by SureScan Microarray Scanner Bundle

After the microarray slide was washed, it was dried at room temperature for 5 minutes. The following step was to scan the microarray slide by a fluorescence scanner which was designed to read microarray with high resolution.



Figure 4-9. Agilent SureScan Microarray Scanner and microarray slide (Agilent Technologies, Inc)

*b. Extracting the data using Agilent Feature Extraction Software*

The data from scanned microarray slide was extracted by using Agilent Feature Extraction Software 10.7 ([www.agilent.com/chem/feprotocols](http://www.agilent.com/chem/feprotocols)). The raw data was processed by using software Microsoft Excel 2007 and GeneSpring GX version 13.0 (<http://www.genomics.agilent.com/>).

The raw data was analyzed as follows: Raw data from the Feature Extraction software was obtained in .txt format and normalized by using GeneSpring GX version 13.0 (Agilent Technologies, Inc).

*c. Normalizing Agilent One-Color Microarray Data by using GeneSpring GX version 13.0*

Normalization is a term that is used to describe the process of eliminating variations and allow appropriate comparison of data obtained from two or more samples. The variation is caused by various reasons, for example, by different labelling efficiency by the different amounts of starting mRNA material in two samples. Thus, in the case of microarray experiments, as for any large-scaled experiments, there are many sources of systematic variation that affect measurements of gene expression levels [55]. Many normalization strategies also include adjustments for technical bias to improve comparison between probes on the same array. For example: global mean (median) normalization, normalizing to spike-in controls (housekeeping genes), adjusting for intensity bias, or adjusting for spartial (print-tip bias) [53].

Global mean normalization is the simplest form of ratio normalization. A global adjustment is appropriate if we could assume the total amount of input material from the experimentals should be equivalent [53]. In strain TH-1 microarray experiment, because all samples contained the same total amount of 100 ng RNA (optimized for prokaryote), the global mean normalization was appropriate method for normalization of the data.

When comparing data across a set of one-color microarrays, a simple linear scaling of the data was usually sufficient for most experimental applications. Agilent has determined that the signal value of the 75th percentile of all of non-controlled probes on the microarray was a more robust and representative value of the overall microarray signal as compared to the median or 50th percentile signal. Therefore, the 75th percentile signal value was used to normalize Agilent one-color microarray signals for inter-array comparisons.

All data were normalized by Persentile Shift 75%. A baseline correction was applied to the median of all samples. Quality control on samples was shown by PCA plot. Probe sets (normalized average data) were filtered by expression [Delete spots (genes) with low level expression], and filtered on expression (-6.072 - 8.185) in the Normalized Data. Probe sets were filtered by Flags [Delete spots (genes) with bad flags] Not-detected, Comprised (Saturation, Non-uniform). Probe sets were filtered by Error: [Delete spots (genes) with low reproducibility]. Selected spots have Coefficient of variation <50%.

Table 4-11. Quality control of all samples after normalized data

Identifier	Auto 1	Auto2	Hetero 1	Hetero 3	Mixo 1	Mixo 2
Autotrophic 1	1.00	0.95	0.73	0.75	0.92	0.83
Autotrophic 2	0.95	1.00	0.70	0.72	0.92	0.84
Heterotrophic 1	0.73	0.70	1.00	0.99	0.73	0.62
Heterotrophic 3	0.75	0.72	0.99	1.00	0.73	0.61
Mixotrophic 1	0.92	0.92	0.73	0.73	1.00	0.93
Mixotrophic 2	0.83	0.84	0.62	0.61	0.93	1.00

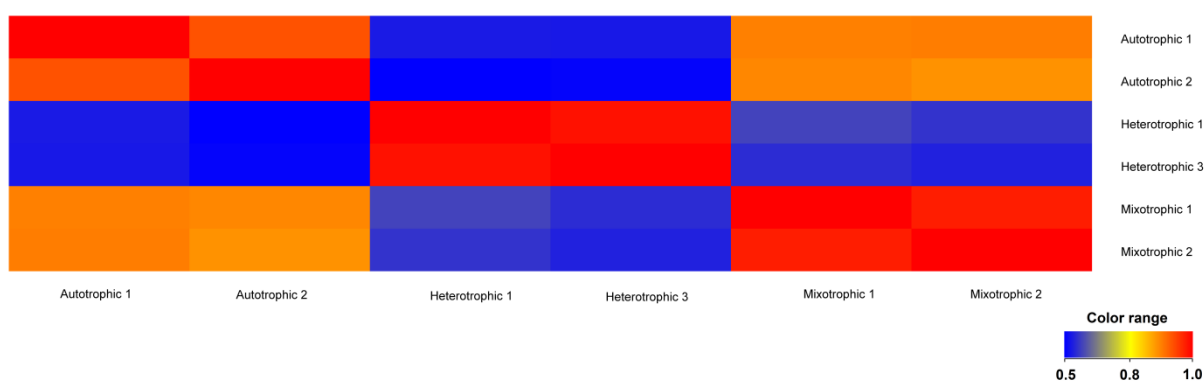


Figure 4-10. Quality control of all samples after normalized data

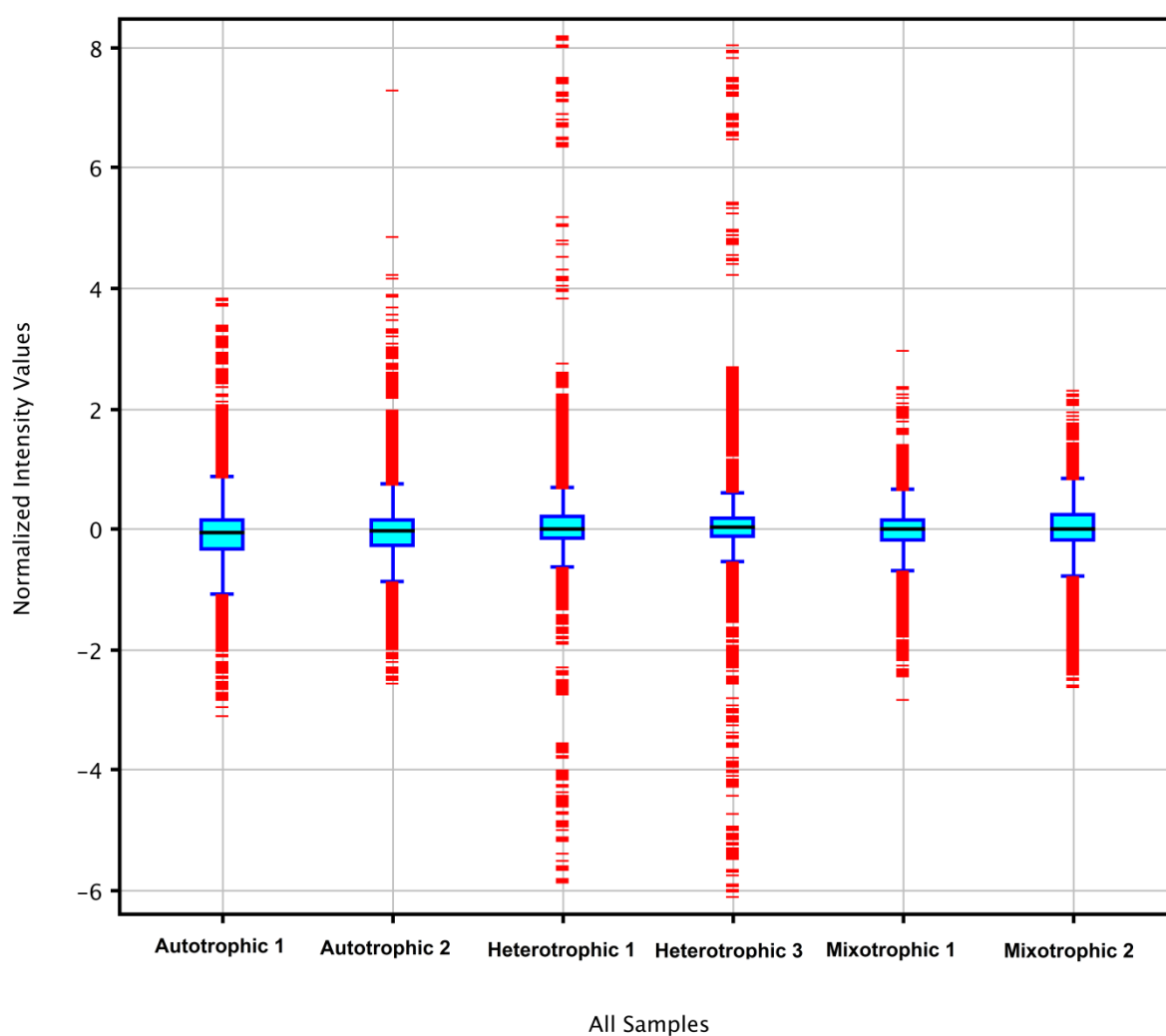


Figure 4-11. All data were normalized by Percentile Shift 75%. A baseline correction was applied to the median of all samples.

A new parameter namely growth mode was applied for 6 microarrays as follow:

- Autotrophy: Autotrophic 1 and Autotrophic 2
- Heterotrophy: Heterotrophic 1 and Heterotrophic 3
- Mixotrophy: Mixotrophic 1 and Mixotrophic 2

The representative data for the new parameter growth mode was calculated as the average data of each component.

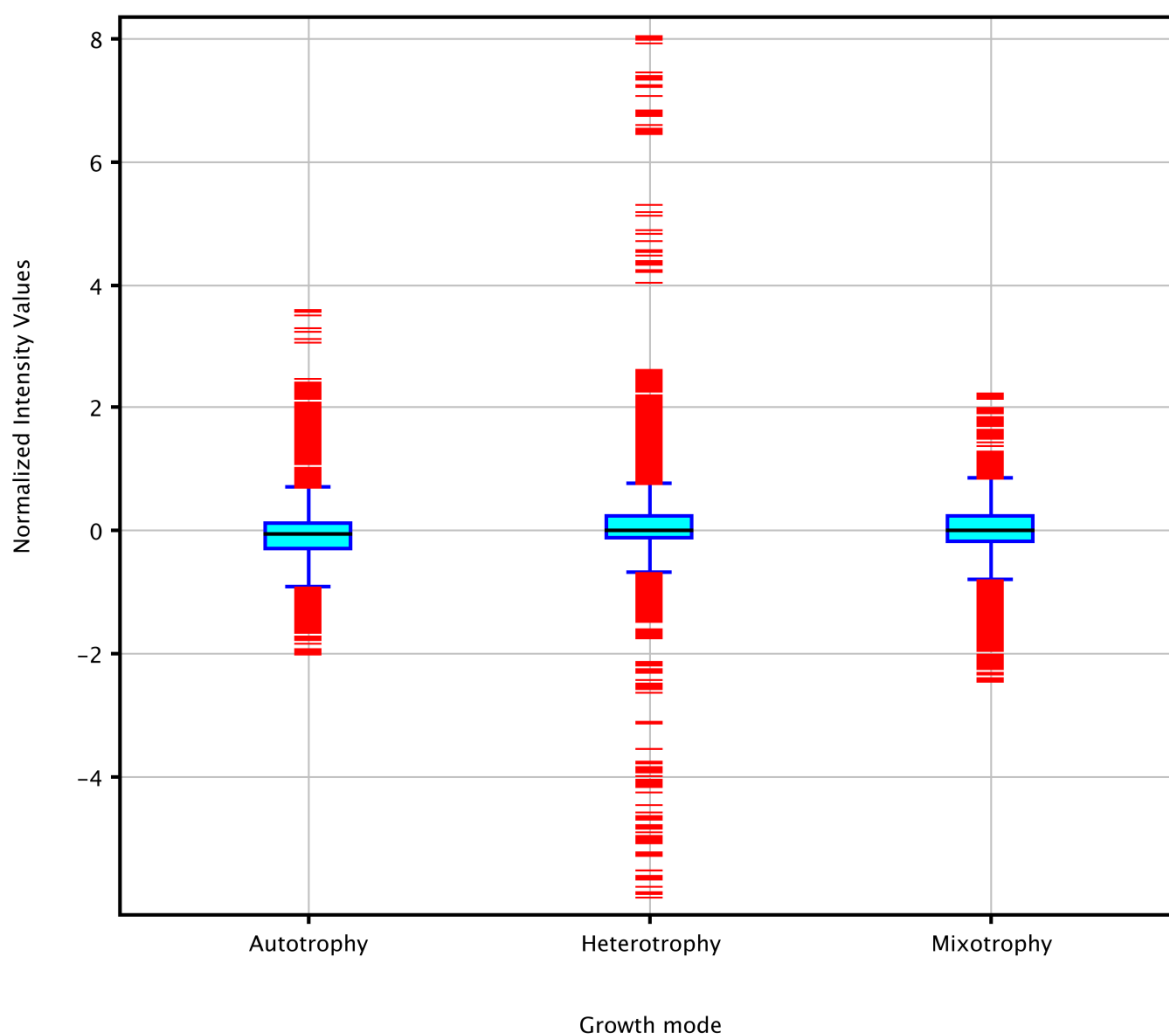


Figure 4-12. All data were normalized after setting growth mode as the new parameter in which Autotrophy representative sample Autotrophic 1 and Autotrophic 2; Heterotrophy representative sample Heterotrophic 1 and Heterotrophic 3; Mixotrophy representative sample Mixotrophic 1 and Mixotrophic 2. The value of new parameter was calculated from average value of the components.

Statistical analysis: After normalizing data, data was processed with statistic analysis. For dye Cy3 I performed one-way ANOVA on the six microarrays to identify genes that were differentially expressed between the three growth modes. Genes that showed a 2-fold or greater difference in expression level with 95% confidence were considered significant. The significance level was set at  $P \leq 0.05$ . After the Normalized data was treated with one-way ANOVA, the data was clustered for comparison.



Figure 4-13. All data were clustered after setting growth mode and statistic analysis by one way ANOVA, cut off 0.05.

For comparison of fold changes in gene expressions under two different growth modes, the moderated T-Test was applied as follows: Selected Test: Moderated T-Test, corrected p-value cut-off: 0.05. Fold change cut-off: 2.0. P-value computation: Asymptotic. Multiple Testing Corrections: Benjamini-Hochberg.

All data were expressed as the mean  $\pm$  standard deviation (SD). The mean signal value of each probe set of duplicates and their relative fold changes between the growth conditions were calculated by using software GeneSpring GX version 13.0.

#### 4.2.4. Metabolome analysis

The sample was cultured in Laboratory of Applied Microbiology, and analysis and data processing were conducted in Human Technologies Company.

#### 4.2.4.1. Samples preparation

*H. thermoluteolus* TH-1 was cultured and harvested in The University of Tokyo; used 6 samples shown in Table 4-12. The sample was packed with dry ice and sent to Human Metabolome Technologies Company (HMT).

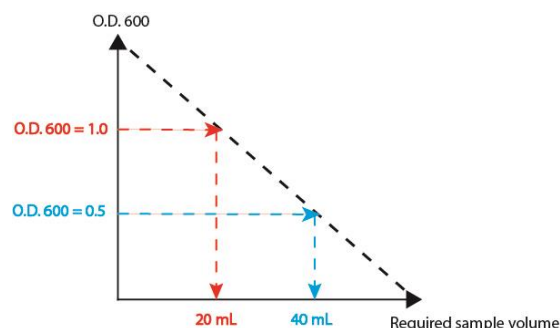


Figure 4-14. Calculate the required sample volume

$$\text{Volume sample (mL)} = 20 / \text{O.D. 600}$$

O.D. 600: Optical density is measured at wavelength 600 nm.

Table 4-12. Information of samples prepare for metabolome analysis

No	Volume (OD.mL)	Condition
1	16	Autotrophy, logarithmic phase
2	10	Autotrophy, stationary phase
3	23	Heterotrophy, logarithmic phase
4	28	Heterotrophy, stationary phase
5	31	Mixotrophy, logarithmic phase
6	10	Mixotrophy, stationary phase

#### 4.2.4.2. Pretreatments

*H. thermoluteolus* TH-1 was grown in 10 mL of medium culture for three conditions autotrophic, heterotrophic, or mixotrophic condition with butyrate in a 100 mL vial. Sample was washed and collected according to the instruction protocol of HMT.

At HMT, 1,600  $\mu\text{L}$  of chloroform and 640  $\mu\text{L}$  of Milli-Q were added to the sample, stirred, and centrifuged at  $2,300 \times g$  at  $4^\circ\text{C}$  for 5 minutes. After centrifugation, the aqueous layer was transferred into an ultracentrifugation tube, 400  $\mu\text{L} \times 4$  tubes. Each tube was centrifuged  $9,100 \times g$  at  $4^\circ\text{C}$  for 120 minutes and then ultrafiltrated. The

filtrate was dried, and then was dissolved in 50  $\mu$ L Milli-Q water again. The sample was analyzed by cationic and anionic mode of CE-TOFMS.

#### Running option of Cation mode

- Agilent CE-TOFMS system (Agilent Technologies Company)
- Capillary: fused silica capillary i.d. 50  $\mu$ m x 80 cm
- Run buffer: Cation Buffer Solution
- Rinse buffer: Cation Buffer Solution
- Sample injection: Pressure injection 50 mbar, 10 sec
- CE voltage: Positive, 27 kV
- MS ionization: ESI Positive
- MS capillary voltage: 4,000 V
- MS scan range:  $m/z$  50-1,000
- Sheath liquid: HMT Sheath Liquid

#### Running option of Anion mode

- Agilent CE-TOFMS system (Agilent Technologies Company)
- Capillary: fused silica capillary i.d. 50  $\mu$ m x 80 cm
- Run buffer: Anion Buffer Solution
- Rinse buffer: Anion Buffer Solution
- Sample injection: Pressure injection 50 mbar, 10 sec
- CE voltage: Positive, 30 kV
- MS ionization: ESI Negative
- MS capillary voltage: 3,500 V
- MS scan range:  $m/z$  50-1,000
- Sheath liquid: HMT Sheath Liquid

#### 4.2.4.3. Data processing and analysis

The raw data was aligned with HMT metabolite library and Know-Unknown peak library. The detected peak in CE-TOFMS was extracted automatically using MasterHands ver.2.1.0.8.h (Keio University development), which was the automatic integral calculus software, and the mass electric charge ratio ( $m/z$ ), the migration time

(MT) and a peak area level as peak information was obtained. The area of the provided peak level was converted into a relative area level using the following formula.

$$\text{Relative area} = \frac{\text{Area of the peak}}{\text{Area of internal control} \times \text{number of bacterial cells}}$$

Because these data included molecular weight related ions such as adduct ion and dehydration or deammonium fragment ions, those molecular ions were deleted. However, it was not possible to investigate all ions thoroughly because material-specific adduction and the fragment existed. About the peak that was investigated thoroughly, the alignment of the peak between each sample based on the  $m/z$  and value are performed.

#### *4.3.4.4. Candidate metabolite reference*

The peak information was used to search with all metabolites registered in MHT library and Known-Unknown library based on a value of  $m/z$  and the MT for peak annotation.

#### *4.3.4.5. Statistical analysis (PCA, HCA)*

The data was processed by SampleStat ver.3.14 (HTM development) for principal component analysis (PCA). PeakStat ver.3.18 (HTM development) was used for the hierarchical clustering analysis (HCA) and Heatmap notation.

#### *4.3.4.6. Drawing metabolic pathway*

The metabolic pathway was drawn by VANTED 2.2.1 (Visualization and Analysis of Networks containing Experimental Data). Because HMT drew the metabolic pathways based on enzyme system and metabolic net confirmed in human, I designed again the metabolic route for metabolic pathways that were available in strain TH-1 by using Adobe Illustrator CS5.

### 4.3. Results and discussions

#### 4.3.1. Culturing bacteria for RNA extraction

*H. thermoluteolus* TH-1 was grown in 10 mL of medium culture for three conditions in a 100 mL vial until the mid-logarithmic phase, optical density (OD) at 540 nm reached 0.4-0.6. Cells were collected by centrifugation for 10 minutes at 3,000 x g. Total RNA was extracted from the cell pellet by a hot-phenol method. The quality of total RNA was checked for microarray analysis.

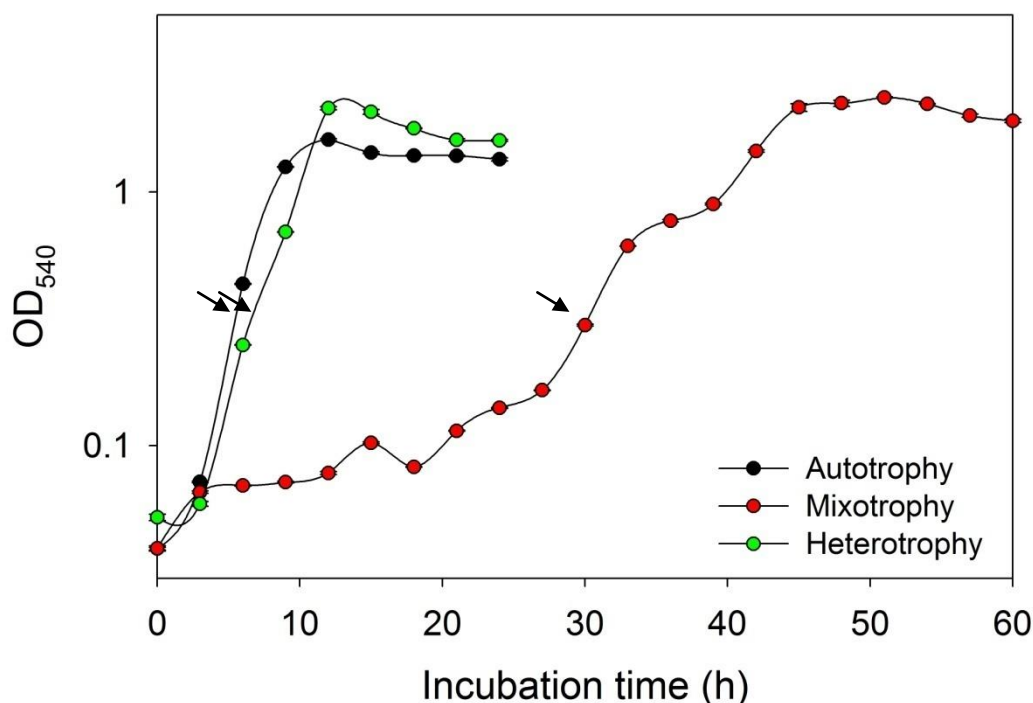


Figure 4-15. Growth profiles of strain TH-1 grown under autotrophic, mixotrophic and heterotrophic conditions with butyrate. Black circles represent autotrophic condition, green circles represent heterotrophic, and red circles represent mixotrophic condition. The head of arrows indicated the time of samples collected.

Under autotrophic condition, strain TH-1 grew favourably with a specific growth rate of  $0.60\ h^{-1}$ , at  $50^{\circ}\text{C}$ . The growth under heterotrophic condition was delayed a short time before growth. Interestingly, under mixotrophic condition with butyrate as a substrate, long lag phase before robust growth was found.

### 4.3.2. Microarray analysis

#### 4.3.2.1. General profile

In general, the expression of genes under three condition: autotrophic, heterotrophic, and mixotrophic conditions with butyrate showed significant difference when analyzed by software GeneSpring GX version 13.0 and Microsoft Excel 2007. The detailed information is as follows:

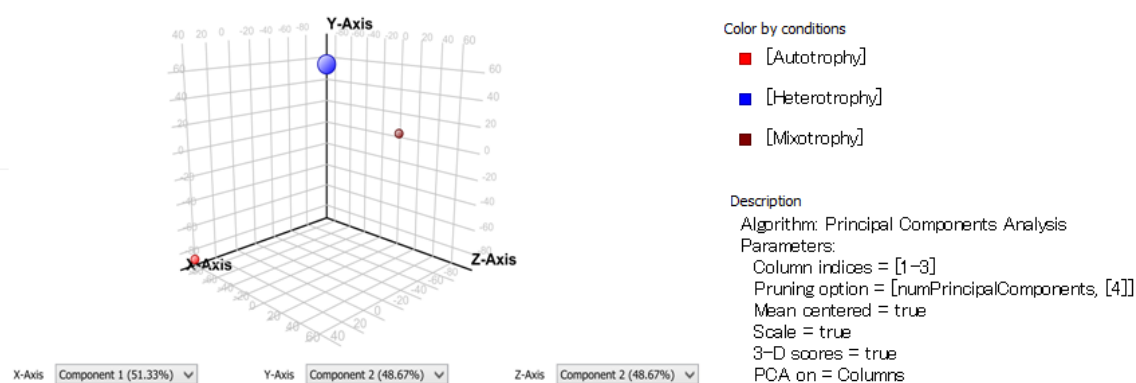


Figure 4-16. Quality control on samples was shown by principle component analysis (PCA) plot.

#### *a. Mixotrophy versus Autotrophy*

In general, the fluorescent intensity of Agilent internal positive control under autotrophic and mixotrophic conditions were quite similar. In figure 4-17, the fluorescent intensity of all genes of strain TH-1 under autotrophic versus those under mixotrophic is shown. The result that most spots located up-side of identity line indicates the levels expression of genes under mixotrophic condition were up-regulated compared to those under autotrophic condition. Under autotrophic condition several spots gave higher expression than those under mixotrophic condition. Detailed investigation revealed that such spots represented for genes coding for enzymes of CBB cycle.

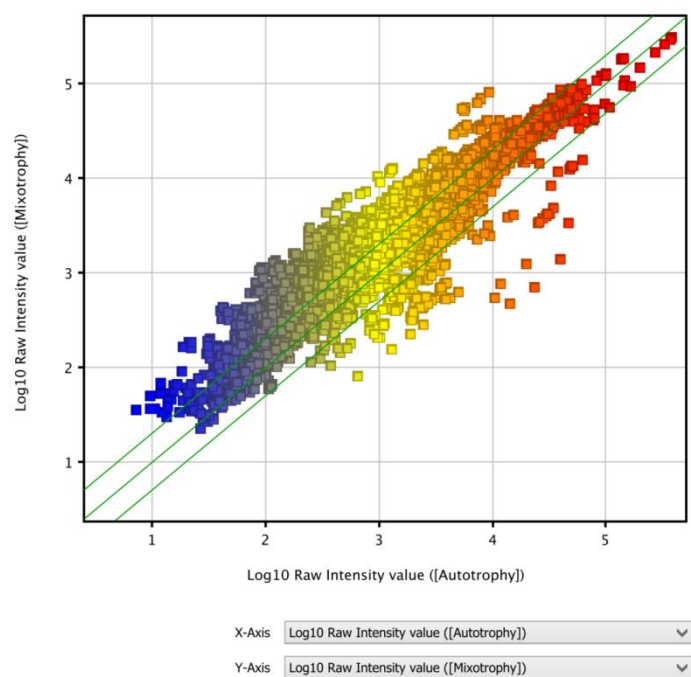


Figure 4-17. Intensity scatter plots of raw data of an autotrophically grown culture ( $\text{H}_2\text{-O}_2\text{-CO}_2$ ) versus a mixotrophically grown culture (butyrate- $\text{H}_2\text{-O}_2\text{-CO}_2$ ). The middle solid line is the identity line that indicates the same transcription level.

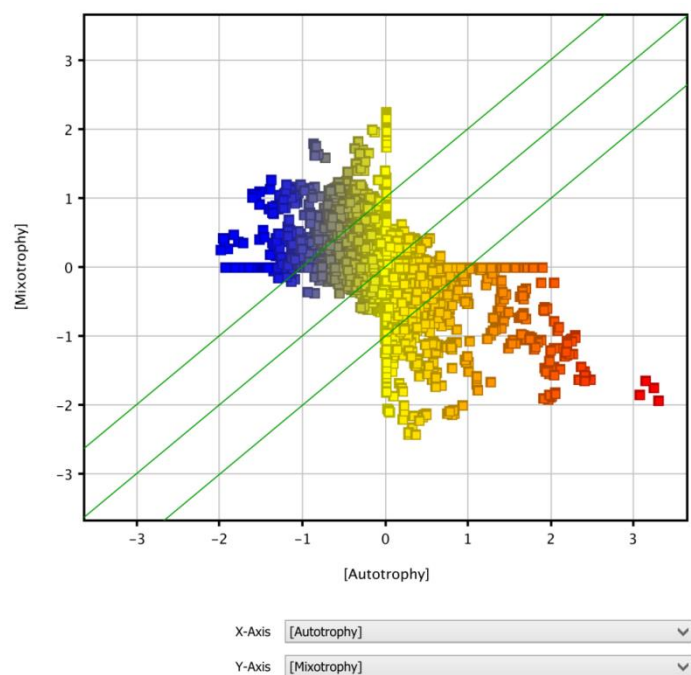


Figure 4-18. Intensity scatter plots of normalized data an autotrophically grown culture ( $\text{H}_2\text{-O}_2\text{-CO}_2$ ) versus a mixotrophically grown culture (butyrate-  $\text{H}_2\text{-O}_2\text{-CO}_2$ ).

Table 4-13. Fold change of levels expression of genes under mixotrophic and autotrophic condition

Test Description	Moderated T-test					
P-value computation	Asymptotic					
Multiple Testing Correction	Benjamini-Hochberg					
Result Summary						
	P all	P<0.05	P<0.02	P<0.01	P<0.005	P<0.001
Fold change all	9236	1177	216	116	25	0
Fold change >1.1	7774	1177	216	116	25	0
Fold change >1.5	3498	1177	216	116	25	0
Fold change >2.0	1251	974	216	116	25	0
Fold change >3.0	380	344	189	116	25	0

The moderated T-test analysis displaying 974 entities out of 9,236 satisfying p-value cut-off 0.05 and fold change cut off 2.0.

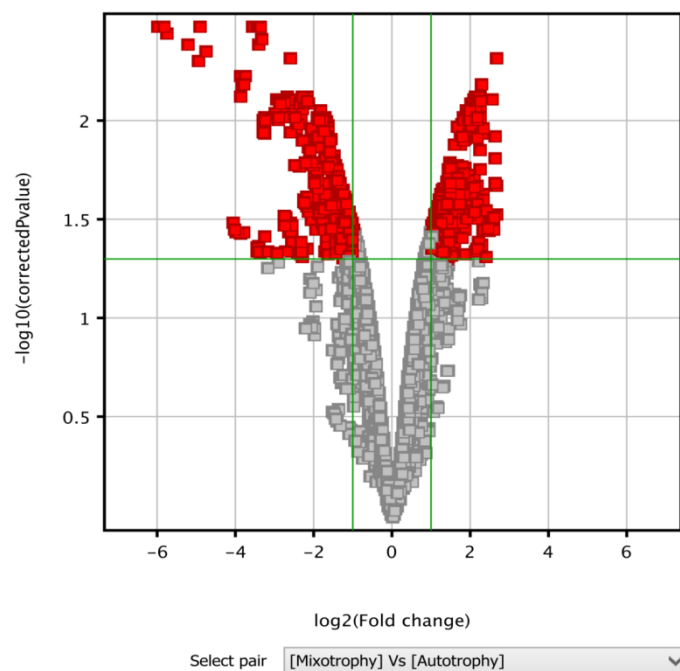


Figure 4-19. Volcanic filter the fold change of level expression of genes under mixotrophy (butyrate - H<sub>2</sub>-O<sub>2</sub>-CO<sub>2</sub>) versus autotrophy condition (H<sub>2</sub>-O<sub>2</sub>-CO<sub>2</sub>).

*b. Heterotrophy versus Autotrophy*

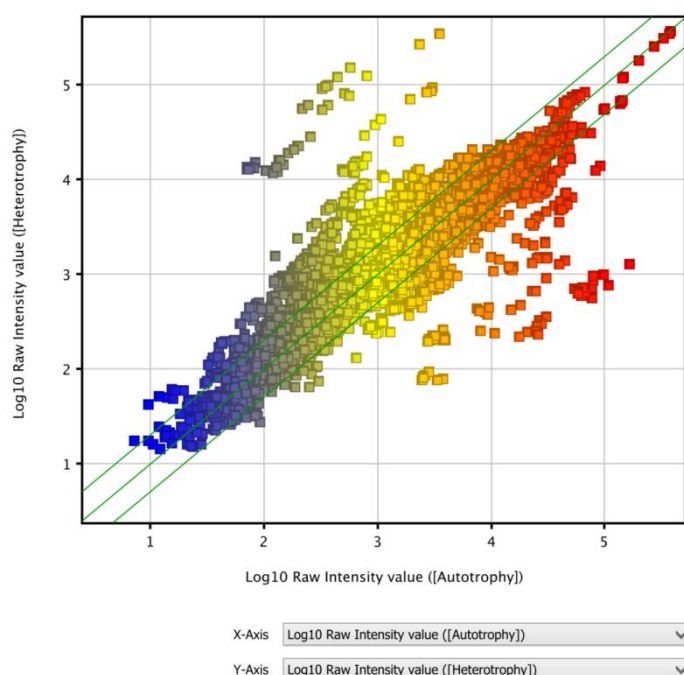


Figure 4-20. Intensity scatter plots of raw data of a heterotrophically grown culture (butyrate) versus autotrophically grown culture ( $\text{H}_2\text{-O}_2\text{-CO}_2$ ). The middle solid line is the identity line that indicates the same transcription level.

In general, the fluorescent intensity of Agilent internal positive control under autotrophic and heterotrophic conditions was quite similar. Figure 4-20 showed the fluorescent intensity of all genes of strain TH-1 under autotrophic versus those under heterotrophic condition. The result that most spots located on or near the identity line, indicates that such genes play an important role for the growth of bacteria cells TH-1. They may function as house keeping genes which are necessary for the growth of bacteria. Under autotrophic condition several spots were more highly expressed than those under heterotrophic condition. Such spots corresponded to genes coding for enzymes of CBB cycle. This result suggested the important function of CBB cycle under autotrophic condition in carbon fixation.

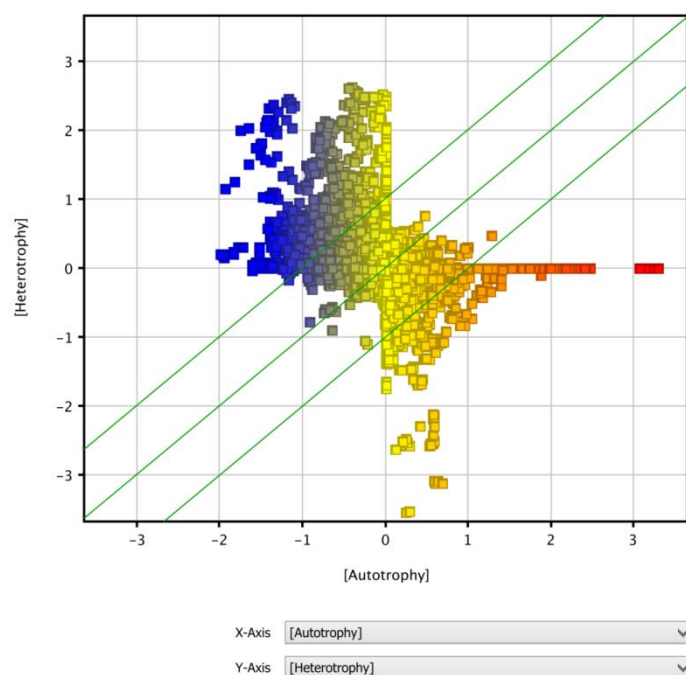


Figure 4-21. Intensity scatter plots of nomalized data of heterotrophically grown culture (butyrate) versus autotrophically grown culture (H<sub>2</sub>-O<sub>2</sub>-CO<sub>2</sub>)

Table 4-14. Fold change of levels expression of genes under heterotrophic and autotrophic condition

Test Description	Moderated T-test					
P-value computation	Asymptotic					
Multiple Testing Correction	Benjamini-Hochberg					
Result Summary						
	P all	P<0.05	P<0.02	P<0.01	P<0.005	P<0.001
Fold change all	9236	1472	638	438	279	149
Fold change >1.1	7863	1472	638	438	279	149
Fold change >1.5	3215	1472	638	438	279	149
Fold change >2.0	1357	1077	638	438	279	149
Fold change >3.0	626	561	478	401	279	149

The moderated T-test analysis displaying 1,077 entities out of 9,236 satisfying p-value cut-off 0.05 and fold change cut off 2.0

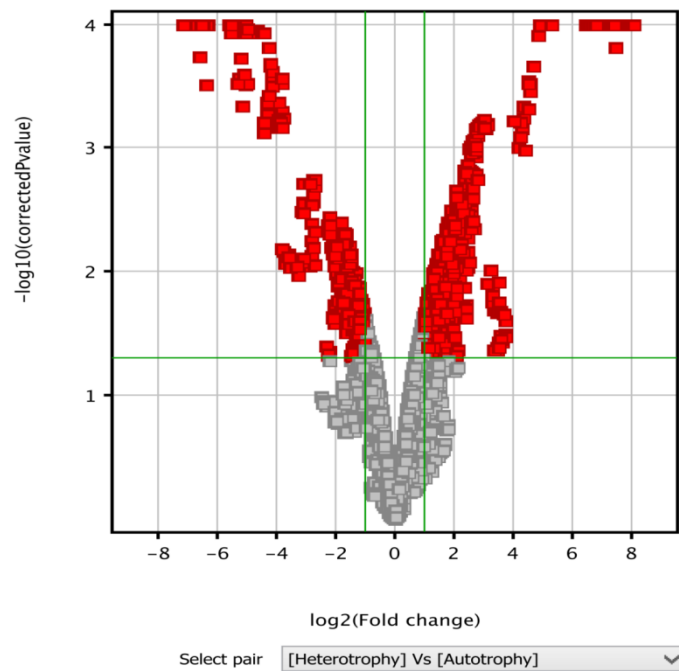


Figure 4-22. Volcanic filter the fold change of level expression of genes under heterotrophy (butyrate) versus autotrophy ( $\text{H}_2\text{-O}_2\text{-CO}_2$ ) condition.

*c. Mixotrophy versus Heterotrophy*

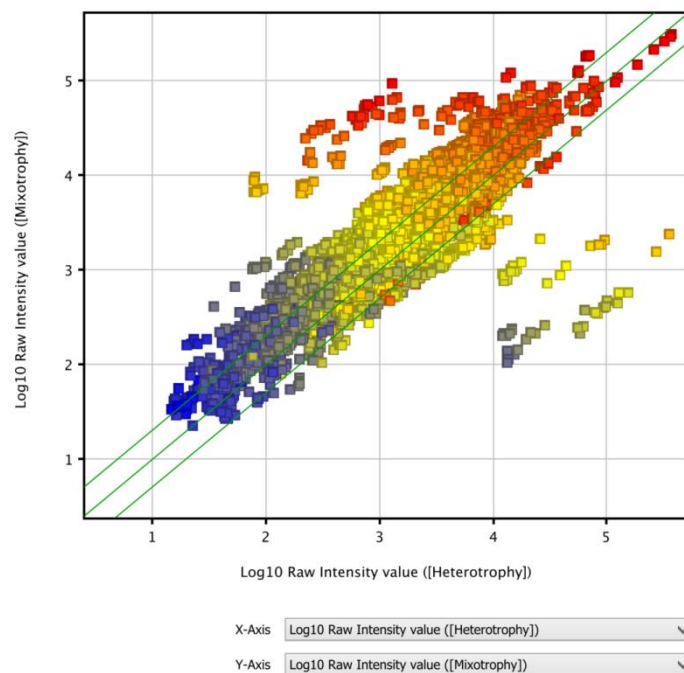


Figure 4-23. Intensity scatter plots of raw data of a heterotrophically grown culture (butyrate) versus a mixotrophically grown culture (butyrate- $\text{H}_2\text{-O}_2\text{-CO}_2$ ). The middle solid line is the identity line that indicates the same transcription level.

From the obtained results, the fluorescent intensity of Agilent internal positive control under heterotrophic and mixotrophic condition were quite similar. Figure 4-23 shows the fluorescent intensity of all genes of strain TH-1 under heterotrophic condition versus those under mixotrophic condition.

Most spots located up-side of identity line, which indicates the expression levels of genes under mixotrophic condition were up-regulated compared with those under heterotrophic condition.

This result suggested that the metabolism of cells of strain TH-1 grown under mixotrophic condition with butyrate and gas mixture  $H_2$ ,  $CO_2$ ,  $O_2$ , was significantly stronger than that under heterotrophic condition.

Table 4-15. Fold change of levels expression of genes under mixotrophic and heterotrophic condition

Test Description		Moderated T-test					
P-value computation		Asymptotic					
Multiple Testing		Benjamini-Hochberg					
Correction							
Result Summary							
		P all	P<0.05	P<0.02	P<0.01	P<0.005	P<0.001
Fold change all		9236	3965	2898	2165	1569	644
Fold change >1.1		7935	3965	2898	2165	1569	644
Fold change >1.5		3545	3402	2898	2165	1569	644
Fold change >2.0		1559	1545	1525	1489	1365	644
Fold change >3.0		534	534	532	529	525	508

The moderated T-test analysis displaying 1,545 entities out of 9,236 satisfying p-value cut-off 0.05 and fold change cut off 2.0.

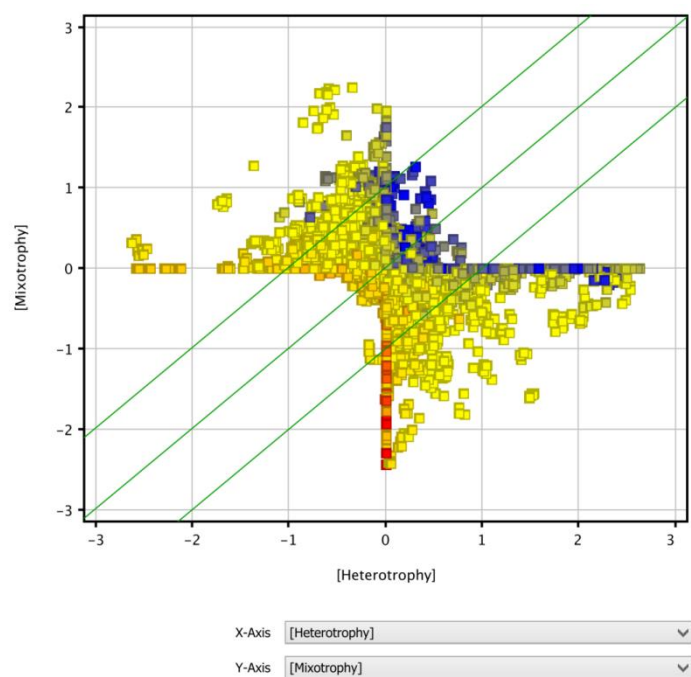


Figure 4-24. Intensity scatter plots of nomalized data of a heterotrophically grown culture (butyrate) versus a mixotrophically grown culture (butyrate- $\text{H}_2\text{-O}_2\text{-CO}_2$ ).

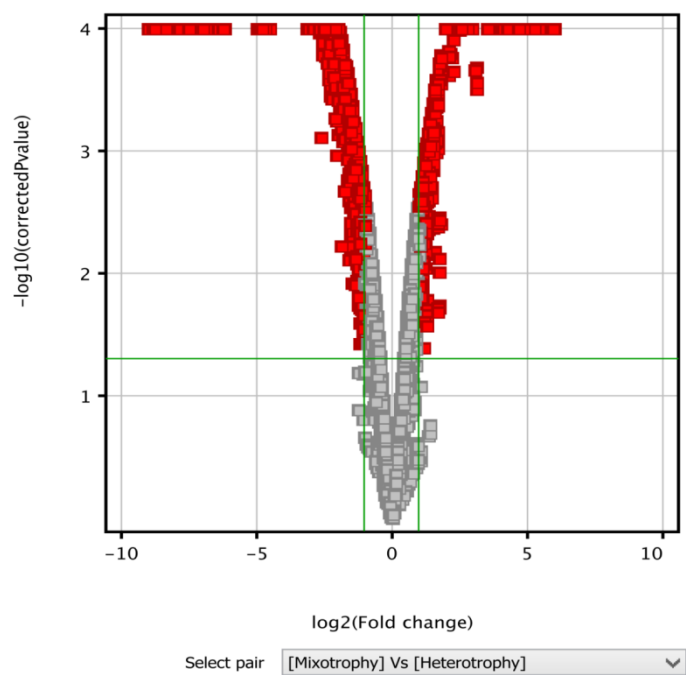


Figure 4-25. Volcanic filter the fold change of level expression of genes under mixotrophy (butyrate  $\text{H}_2\text{-O}_2\text{-CO}_2$ ) versus heterotrophy (butyrate) condition.

#### 4.3.2.2. Central carbon metabolic pathway

##### a. Hydrogenase system in strain TH-1

Hydrogenase functions reversibly as hydrogen oxidation or hydrogen evolution. In hydrogenase-oxidizing bacteria, hydrogenase system is an important system that generates energy [21, 56]. To obtain energy, hydrogenase oxidizes hydrogen molecule from ambient environment, transfer electrons, and protons to reduce  $\text{NAD}^+$ , or generates ATP in both facultative and obligate chemolithoautotrophs [6].

As I mentioned in part 1.1.2.2 chapter 1, strain TH-1 possesses the hydrogenase system similar to *Ralstonia eutropha*. It means that strain TH-1 have three kinds of hydrogenases: MBH, SH and RH. All these genes were identified and annotated. In detail, the MBH genes cluster located in contig 1.

Table 4-16. Fold change in expression of genes of hydrogenase system under heterotrophy or mixotrophy versus autotrophy condition. The mean fold change is the mean change in level expression of given gene obtained from duplicate experiments (each gene was investigated by 7 independent probes in each experiment).

Protein/Enzyme	contig	Gene	Heterotrophy vs Autotrophy	Mixotrophy vs Autotrophy
			Fluorescence intensity fold change $\pm$ SD (mean intensity ratio [ $\log_2$ ])	
Ni-Fe hydrogenase, Uptake hydrogenase small subunit [EC:1.12.99.6]	contig00001 _orf00005	<i>hoxK</i>	-2.9 $\pm$ 0.2 (-1.6)	1.1 $\pm$ 0.1 (0.1)
Ni-Fe hydrogenase, Uptake hydrogenase large subunit [EC:1.12.99.6]	contig00001 _orf00007	<i>hoxG</i>	-3.2 $\pm$ 0.2 (-1.7)	1.3 $\pm$ 0.1 (0.4)
Ni/Fe-hydrogenase B-type cytochrome subunit	contig00001 _orf00008	<i>hoxZ</i>	-3.1 $\pm$ 0.2 (-1.6)	1.6 $\pm$ 0.1 (0.7)
Regulatory [NiFe] hydrogenase large subunit	contig00024 _orf00003	<i>hoxC</i>	1.1 $\pm$ 0.02 (0.2)	2.0 $\pm$ 0.1 (1.0)
Regulatory [NiFe] hydrogenase small subunit	contig00024 _orf00004	<i>hoxB</i>	1.1 $\pm$ 0.1 (0.2)	1.9 $\pm$ 0.3 (0.9)
transcriptional regulator	contig00024 _orf00005	<i>hoxA</i>	1.1 $\pm$ 0.1 (0.1)	2 $\pm$ 0.2 (1.0)

[NiFe] hydrogenase diaphorase moiety large subunit [EC:1.12.1.2]	contig00024_orf00008	<i>hoxF</i>	1.4±0.03 (0.4)	2.1±0.1 (1.1)
[NiFe] hydrogenase diaphorase moiety small subunit [EC:1.12.1.2]	contig00024_orf00009	<i>hoxU</i>	1.1±0.04 (0.2)	1.7±0.1 (0.7)
NAD-reducing hydrogenase small subunit [EC:1.12.1.2]	contig00024_orf00011	<i>hoxY</i>	1.0±0.04 (0.0)	1.9±0.1 (0.9)
NAD-reducing hydrogenase large subunit [EC:1.12.1.2]	contig00024_orf00012	<i>hoxH</i>	-1.1±0.02 (-0.1)	1.8±0.1 (0.9)

The main components of MBH hydrogenase type Ni-Fe hydrogenase [EC:1.12.99.6] are the gene of the large subunit *hoxG* (contig00001\_orf00007), the gene of small subunits *hoxK* (contig00001\_orf00005), and *hoxZ* (contig00001\_orf00008). The genes of SH and RH hydrogenase were organized as cluster in contig 24. RH genes involve genes: large subunit *hoxC* (contig00024\_orf00003), small subunit Fe-S cluster gene *hoxB* (contig00024\_orf00004), transcriptional subunit gene *hoxA* (contig00024\_orf00005). SH genes involve genes: large subunit with active site gene *hoxH* (contig00024\_orf00012), small subunits Fe-S cluster gene *hoxF* (contig00024\_orf00008), *hoxU* (contig00024\_orf00009), and *hoxY* (contig00024\_orf00011).

From the raw intensity data, the genes for MBH (*hoxK*, *hoxG*, *hoxZ*) are significantly up-regulated compared with genes for SH (*hoxH*, *hoxF*, *hoxU*, *hoxY*) and the genes for RH (*hoxA*, *hoxB*, *hoxC*) in the cells grown under autotrophic, heterotrophic, or mixotrophic condition. *Hox G* is the large subunit of membrane-bound hydrogenase. The expression level of *hoxG* under heterotrophic and mixotrophic condition were -3.2-fold and 1.3-fold lower than that under autotrophic condition, respectively. This result suggests that in strain TH-1, under autotrophic condition, the activity of hydrogenase is important for the growth of strain TH-1.

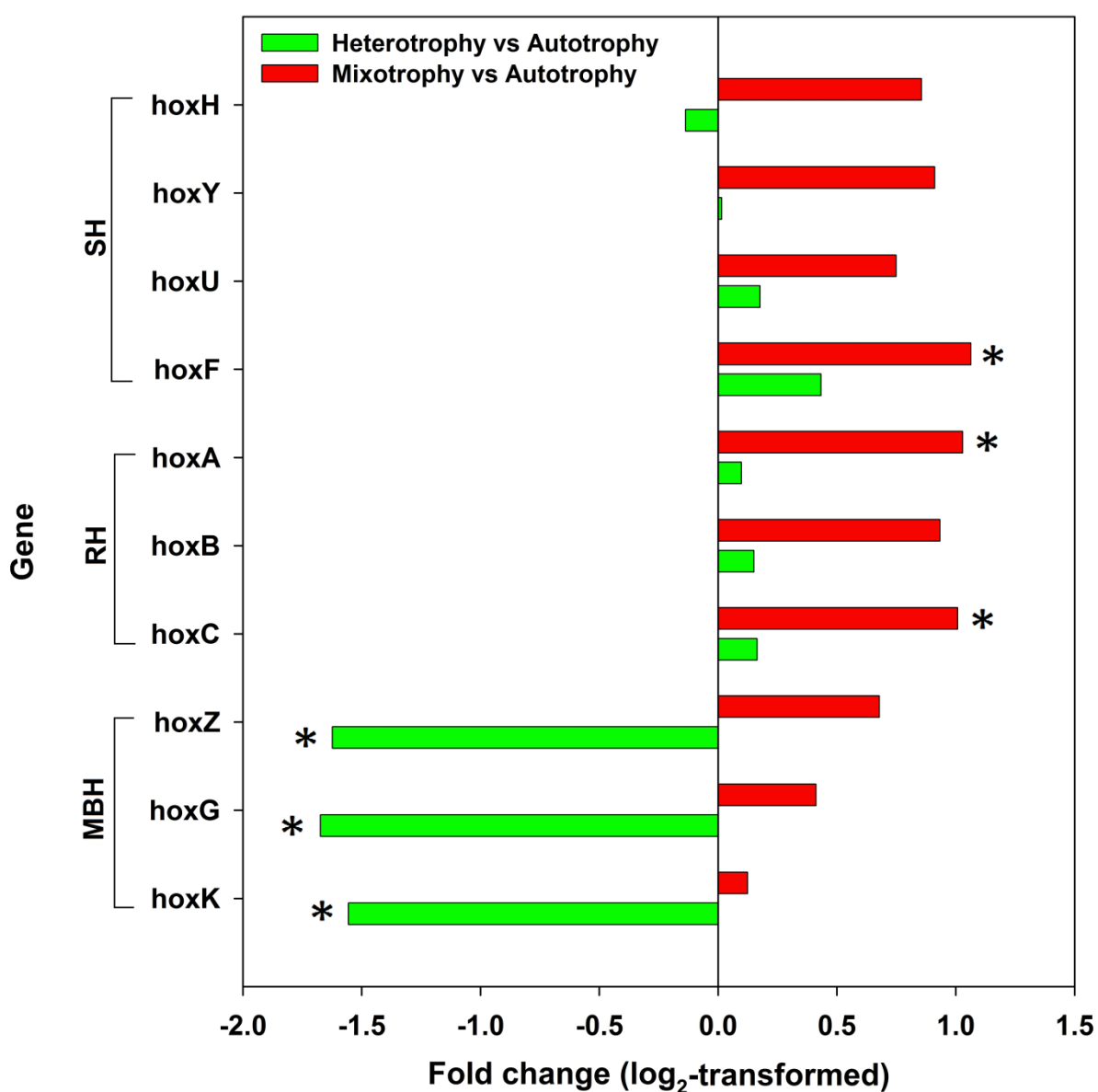


Figure 4-26. Fold change (log<sub>2</sub>-transformed) of average expression level of genes encoding hydrogenase enzymes in strain TH-1 under heterotrophy or mixotrophy versus autotrophy condition. The mean fold change is the mean change in level expression of given gene obtained from duplicate experiments. Asterisks indicate the significant difference at P value < 0.05. MBH, membrane-bound hydrogenase; SH, soluble hydrogenase, RH, regulatory hydrogenase.

### *b. Glycolysis pathway*

Glycolysis pathway or Embden-Mayerhoff-Parnas pathway is the metabolic process in which glucose is broken down to pyruvate through 10 reactions. Most of the reaction are reversible except glucokinase (*gck*) and phosphofructose kinase (*pfk*). Phosphofructose kinase is the most important enzyme for glycolysis pathway because it regulates glycolysis pathway [57]. In glucose-consuming bacteria, glycolysis pathway not only functions for glucose oxidation for ATP synthesis, but also supplies many important intermediate metabolites such as F6P, G3P, PEP, or pyruvate that are required for cellular biosynthesis [34]. Glycolysis plays an important role in the chemolithoautotroph as same way.

All the genes for glycolysis pathway enzymes were identified and annotated: glucokinase [EC:2.7.1.2] (*gck*: contig00007\_orf00005); glucose-6-phosphate isomerase [EC:5.3.1.9] (*gpi*: contig00015\_orf00043); 6-phosphofructokinase 1 [EC:2.7.1.11] (*pfk*: contig00001\_orf00392 ); fructose-bisphosphate aldolase, class I [EC:4.1.2.13] (*fba*: contig00002\_orf00238); triosephosphate isomerase (TIM) [EC:5.3.1.1] (*tpiA*: contig00001\_orf00364); glyceraldehyde 3-phosphate dehydrogenase [EC:1.2.1.12] (*gapA*: contig00002\_orf00235); phosphoglycerate kinase [EC:2.7.2.3] (*pgk*: contig00002\_orf00236); phosphoglycerate mutase [EC:5.4.2.1] (*pgam*: contig00013\_orf00078); enolase [EC:4.2.1.11] (*eno*: contig00016\_orf00055); pyruvate kinase [EC:2.7.1.40] (*pyk*: contig00002\_orf00224).

All glycolysis genes under autotrophic and mixotrophic condition were at higher level of expression than those under heterotrophic condition.

As I mentioned in chapter 1, strain TH-1 cannot consume glucose. Hence, glycolysis pathway in strain TH-1 does not function for glucose break-down but for 3PG break-down. So, gene *gck* (contig00007\_orf00005) was low in expression level under all conditions.

Table 4-17. Fold change in expression of genes encoding glycolysis enzymes in strain TH-1 under heterotrophy or mixotrophy versus autotrophy condition. The mean fold change is the mean change in level expression of given gene obtained from duplicate experiments (each gene was investigated by 7 independent probes in each experiment).

Protein/Enzyme	contig - KEGG ID	Gene	Heterotrophy vs Autotrophy	Mixotrophy vs Autotrophy
			Fluorescence intensity fold change $\pm$ SD (mean intensity ratio [ $\log_2$ ])	
glucokinase [EC:2.7.1.2]	contig00007 _orf00005 K00845	<i>gck</i>	1.6 $\pm$ 0.1 (0.7)	1.5 $\pm$ 0.1 (0.6)
glucose-6-phosphate isomerase [EC:5.3.1.9]	contig00015 _orf00043 K01810	<i>gpi</i>	1.2 $\pm$ 0.03 (0.2)	2.5 $\pm$ 0.1 (1.3)
6-phosphofructokinase 1 [EC:2.7.1.11]	contig00001 _orf00392 K00850	<i>pfk</i>	-1.3 $\pm$ 0.1 (-0.3)	2.2 $\pm$ 0.2 (1.1)
fructose-bisphosphate aldolase, class I [EC:4.1.2.13]	contig00002 _orf00238 K01624	<i>fba</i>	-8.3 $\pm$ 0.2 (-3)	1.3 $\pm$ 0.02 (0.4)
triosephosphate isomerase (TIM) [EC:5.3.1.1]	contig00001 _orf00364 K01803	<i>tpiA</i>	-1.3 $\pm$ 0.03 (-0.4)	1.8 $\pm$ 0.1 (0.9)
glyceraldehyde 3-phosphate dehydrogenase [EC:1.2.1.12]	contig00002 _orf00235 K00134	<i>gapA</i>	-6.5 $\pm$ 0.3 (-2.7)	1.4 $\pm$ 0.1 (0.5)
phosphoglycerate kinase [EC:2.7.2.3]	contig00002 _orf00236 K00927	<i>pgk</i>	-6.7 $\pm$ 0.3 (-2.8)	2.0 $\pm$ 0.1 (1)
Phosphoglycerate mutase [Thauera sp. MZ1T]	contig00013 _orf00078 K02226	<i>pgam</i>	2.1 $\pm$ 0.1 (1.1)	2.3 $\pm$ 0.1 (1.2)
enolase [EC:4.2.1.11]	contig00016 _orf00055 K01689	<i>eno</i>	-1.1 $\pm$ 0.02 (-0.1)	1.8 $\pm$ 0.03 (0.8)
pyruvate kinase [EC:2.7.1.40]	contig00002 _orf00224 K00873	<i>pyk</i>	-14.7 $\pm$ 0.5 (-3.9)	2.1 $\pm$ 0.04 (1.1)

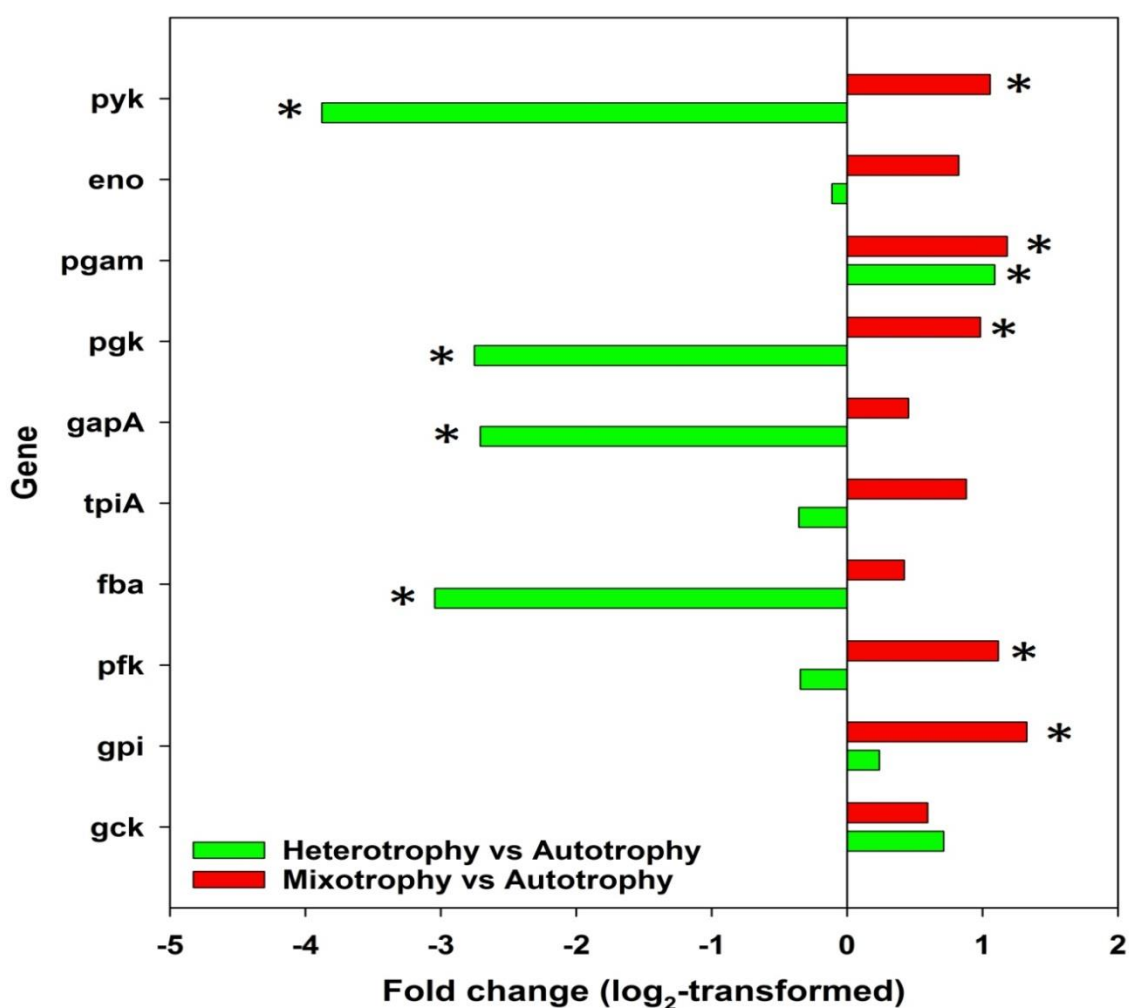


Figure 4-27. Fold change ( $\log_2$ -transformed) of average expression level of genes encoding glycolysis enzymes in strain TH-1 under heterotrophy or mixotrophy versus autotrophy condition. The mean fold change is the mean change in level expression of given gene obtained from duplicate experiment. Asterisks indicate the significant difference at P value < 0.05.

The *pgk*, *gapA*, *fba* genes of glycolysis pathway were also significantly down-regulated under heterotrophic condition, compared to that under autotrophic condition. Because these genes belong to CBB cycle, the expression levels of these genes were significantly decreased under heterotrophic condition. Fructose-bisphosphate aldolase, class I [EC:4.1.2.13] (*fba*) cleave F1,6P to G3P and DAHP. The expression level of *fba* gene under heterotrophic condition was -8.3-fold lower than that under autotrophic

condition. Glyceraldehyde 3-phosphate dehydrogenase [EC:1.2.1.12] (*gapA*) oxidizes G3P to BPG, an high energy compound. The expression level of *gapA* gene under heterotrophic condition was -6.5-fold lower than that under autotrophic condition, respectively. Similarly, the expression level of *pgk* under heterotrophic condition was -6.7-fold compared with that under autotrophic condition.

Pyruvate kinase [EC:2.7.1.40] (*pyk*) is the enzyme that catalyzes PEP into pyruvate, the final step of glycolysis pathway. The gene *pyk* was significantly down-regulated under heterotrophic condition. The expression level of *pyk* under heterotrophic condition was lower than that under autotrophic condition (-14.7-fold). This result emphasize that under heterotrophic growth, the conversion from PEP to pyruvate was depressed. Because butyrate was substrate under heterotrophic condition, it was metabolized through TCA cycle and glyoxylate cycle. Then, pyruvate was generated from malate via the function of malic enzyme.

In general, glycolysis pathway under heterotrophic condition with butyrate was down-regulated, compared with autotrophic.

### *c. Gluconeogenesis pathway*

When bacteria utilize other carbon source than glucose such as acetate, butyrate, glycerol, lactate, malate, or pyruvate, the function of gluconeogenesis is required. Gluconeogenesis is the de novo-synthesis of glucose. Many steps of gluconeogenesis pathway are catalyzed by the same enzymes with glycolysis pathway but in reverse direction [14]. When bacteria lack glucose or glucose-derivative, gluconeogenesis is employed. Similar to glycolysis pathway, gluconeogenesis pathway is used for supplying glucose-derivatives for biosynthesis process.

All the genes for gluconeogenesis pathway enzymes were identified and annotated: glucose-6-phosphate isomerase [EC:5.3.1.9] (*pgi*: contig00015\_orf00043); fructose-1,6-bisphosphatase I [EC:3.1.3.11] (*fbp*: contig00002\_orf00229); fructose-bisphosphate aldolase, class I [EC:4.1.2.13] (*fba*: contig00002\_orf00238); triosephosphate isomerase (TIM) [EC:5.3.1.1] (*tpiA*: contig00001\_orf00364); glyceraldehyde 3-phosphate dehydrogenase [EC:1.2.1.12] (*gapA*: contig00002\_orf00235); phosphoglycerate kinase [EC:2.7.2.3] (*pgk*:

contig00002\_orf00236); phosphoglycerate mutase [EC 5.4.2.1] (*pgm*: contig00013\_orf00078); enolase [EC:4.2.1.11] (*eno*: contig00016\_orf00055); phosphoenolpyruvate synthase [EC:2.7.9.2] (*ppsA*: contig00001\_orf00057); phosphoenolpyruvate carboxylase [EC:4.1.1.31] (*ppc*: contig00010\_orf00102); and malate dehydrogenase (oxaloacetate-decarboxylating) [EC:1.1.1.38] (*me*: contig00005\_orf00027, contig00018\_orf00045).

Table 4-18. Fold change in expression of genes encoding gluconeogenesis enzymes in strain TH-1 under heterotrophy or mixotrophy versus autotrophy condition. The mean fold change is the mean change in level expression of given gene obtained from duplicate experiments (each gene was investigated by 7 independent probes in each experiment).

Protein/Enzyme	Contig - KEGG ID	Gene	Heterotrophy vs Autotrophy	Mixotrophy vs Autotrophy
			Fluorescence intensity fold change $\pm$ SD (mean intensity ratio [ $\log_2$ ])	
glucose-6-phosphate isomerase [EC:5.3.1.9]	contig00015_orf00043 K01810	<i>pgi</i>	1.2 $\pm$ 0.03 (0.2)	2.5 $\pm$ 0.1 (1.3)
fructose-1,6-bisphosphatase I [EC:3.1.3.11]	contig00002_orf00229 K01086	<i>fbp</i>	-13.7 $\pm$ 3.5 (-3.8)	1.3 $\pm$ 0.1 (0.4)
fructose-bisphosphate aldolase, class I [EC:4.1.2.13]	contig00002_orf00238 K01624	<i>fba</i>	-8.3 $\pm$ 0.2 (-3)	1.3 $\pm$ 0.02 (0.4)
triosephosphate isomerase (TIM) [EC:5.3.1.1]	contig00001_orf00364 K01803	<i>tpiA</i>	-1.3 $\pm$ 0.03 (-0.4)	1.8 $\pm$ 0.1 (0.9)
glyceraldehyde 3-phosphate dehydrogenase [EC:1.2.1.12]	contig00002_orf00235 K00134	<i>gapA</i>	-6.5 $\pm$ 0.3 (-2.7)	1.4 $\pm$ 0.1 (0.5)
phosphoglycerate kinase [EC:2.7.2.3]	contig00002_orf00236 K00927	<i>pgk</i>	-6.7 $\pm$ 0.3 (-2.8)	2.0 $\pm$ 0.1 (1)
Phosphoglycerate mutase [EC 5.4.2.1T]	contig00013_orf00078 K02226	<i>pgm</i>	-2.1 $\pm$ 0.1 (-1.1)	2.3 $\pm$ 0.1 (1.2)
enolase [EC:4.2.1.11]	contig00016_orf00055 K01689	<i>eno</i>	1.1 $\pm$ 0.02 (0.1)	1.8 $\pm$ 0.03 (0.8)

pyruvate, water dikinase [EC:2.7.9.2]	contig00001 _orf00057 K01007	<i>ppsA</i>	-1.1±0.1 (-0.1)	2.3±0.3 (1.2)
--	------------------------------------	-------------	-----------------	---------------

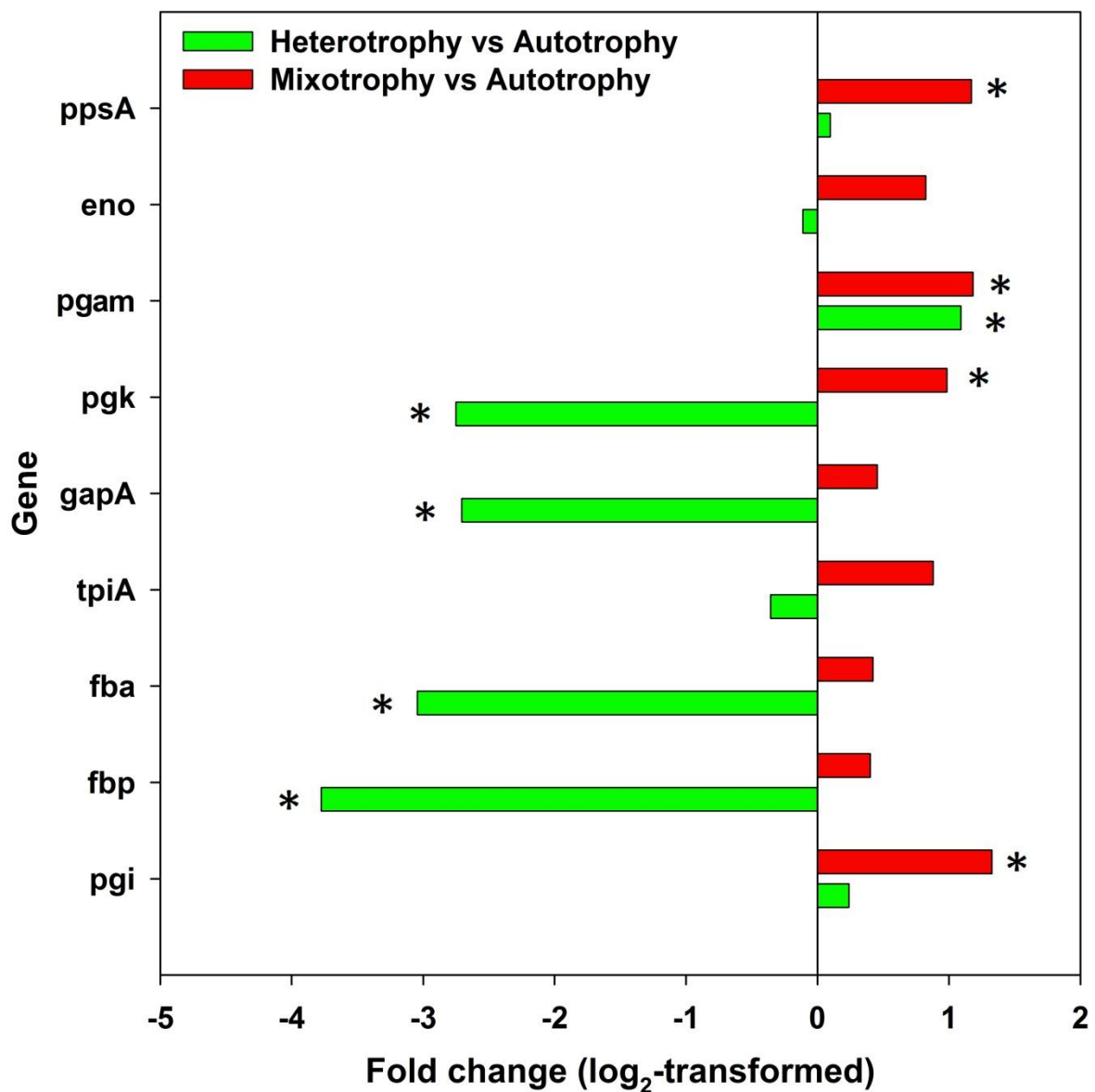


Figure 4-28. Fold change (log<sub>2</sub>-transformed) of average expression level of genes encoding gluconeogenesis enzymes in strain TH-1 under heterotrophy or mixotrophy versus autotrophy condition. The mean fold change is the mean change in level expression of given gene obtained from duplicate experiment. Asterisks indicate the significant difference at P value < 0.05.

It is important to emphasize that most enzymes of gluconeogenesis are identical to those of glycolysis pathway except for fructose-1,6-bisphosphatase I (*fbp*), pyruvate, water dikinase (*ppsA*). Thus, the level of expression of three CBB related genes, *pgk*, *gapA*, and *fba* were down-regulated under heterotrophic condition. Fructose-1,6-bisphosphatase I (*fbp*) replace 6-phosphofructokinase (*pfk*) and phosphoenolpyruvate synthase (*ppsA*) replaces pyruvate kinase (*pyk*) in gluconeogenesis of TH-1 cells [34]. Fructose-1,6-bisphosphatase I catalyzes the conversion of F1, 6P into F6P. This step is irreversible and has regulation function onto the gluconeogenesis pathway. In fact, fructose-1,6-bisphosphatase is the enzyme that belongs to both of central metabolic pathways: gluconeogenesis and CBB cycle. The expression level of the gene coding for this enzyme was significantly enhanced under autotrophic condition when CBB cycle operates. Therefore, the level of expression of *fbp* gene under heterotrophic condition was -13.7-fold lower than that under autotrophic condition.

#### *d. Calvin-Benson-Bassham cycle*

Most genes related to CBB cycle were organized in contig 2 and up-regulated under autotrophic and mixotrophic condition. The expression levels of genes belonging to CBB were lower under heterotrophic condition compared with those under autotrophic and mixotrophic conditions, which indicate that CBB cycle, might not function under heterotrophic condition. CBB cycle genes are expected to be up-regulated under autotrophic condition. However, the high expression levels of CBB cycle genes under mixotrophic condition suggest that CBB operates under mixotrophic condition.

Fold change of the level of expression of *rbcL*, *rbcS*, *prkB* under heterotrophic condition were -99.2-fold, -83.4-fold, and -29.7-fold compared to those under autotrophic condition, at p-value smaller than 0.05, respectively. The expression level of key genes coding for RubisCO (*rbsL*, *rbcL*,) under mixotrophic condition was slightly lower than those under autotrophic condition. Other CBB cycle genes under mixotrophic condition are slightly up-regulated than those under autotrophic condition. This result confirmed the operation of CBB cycle under mixotrophic condition.

Table 4-19. Fold change in expression of genes of CBB cycle under heterotrophy or mixotrophy versus autotrophy condition. The mean fold change is the mean change in level expression of given gene obtained from duplicate experiments (each gene was investigated by 7 independent probes in each experiment).

Protein/Enzyme	contig - KEGG ID	Gene	Heterotrophy vs Autotrophy	Mixotrophy vs Autotrophy
			Fluorescence intensity fold change $\pm$ SD (mean intensity ratio [ $\log_2$ ])	
ribulose-bisphosphate carboxylase large chain [EC:4.1.1.39]	contig00002_orf00214 K01601	<i>rbcL</i>	-99.2 $\pm$ 22.4 (-6.6)	-1.8 $\pm$ 0.03 (-0.8)
ribulose-bisphosphate carboxylase small chain [EC:4.1.1.39]	contig00002_orf00216 K01602	<i>rbcS</i>	-83.4 $\pm$ 8.8 (-6.4)	-1.4 $\pm$ 0.2 (-0.5)
phosphoribulokinase [EC:2.7.1.19]	contig00002_orf00231	<i>prkB</i>	-29.7 $\pm$ 1.7 (-4.9)	1.6 $\pm$ 0.2 (0.7)
phosphoglycerate kinase [EC:2.7.2.3]	contig00002_orf00236 K00927	<i>pgk</i>	-6.7 $\pm$ 0.3 (-2.8)	2.0 $\pm$ 0.1 (1.0)
glyceraldehyde 3-phosphate dehydrogenase [EC:1.2.1.12]	contig00002_orf00235 K00134	<i>gapA</i>	-6.5 $\pm$ 0.3 (-2.7)	1.4 $\pm$ 0.1 (0.5)
fructose-bisphosphate aldolase, class I [EC:4.1.2.13]	contig00002_orf00238 K01624	<i>fba</i>	-8.3 $\pm$ 0.2 (-3)	1.3 $\pm$ 0.02 (0.4)
fructose-1,6-bisphosphatase I [EC:3.1.3.11 3.1.3.37]	contig00002_orf00229 K01086	<i>fbp</i>	-13.7 $\pm$ 3.5 (-3.8)	1.3 $\pm$ 0.1 (0.4)
transketolase [EC:2.2.1.1]	contig00002_orf00233 K00615	<i>tktA</i>	-11.7 $\pm$ 6.2 (-3.6)	1.8 $\pm$ 0.1 (0.8)
CbbQ protein	contig00002_orf00217 K03841	<i>CbbQ</i>	-70.7 $\pm$ 5.6 (-6.1)	1.3 $\pm$ 0.1 (0.3)
CbbY	contig00002_orf00221 K01807	<i>CbbY</i>	-21.3 $\pm$ 4.3 (-4.4)	2.7 $\pm$ 0.1 (1.5)
CbbO	contig00002_orf00220 K01783	<i>CbbO</i>	-21.1 $\pm$ 7.1 (-4.4)	1.8 $\pm$ 0.04 (0.8)
transcription regulator LysR	contig00002_orf00228	<i>cbbR</i>	-2.5 $\pm$ 0.1 (-1.4)	1.4 $\pm$ 0.03 (0.5)

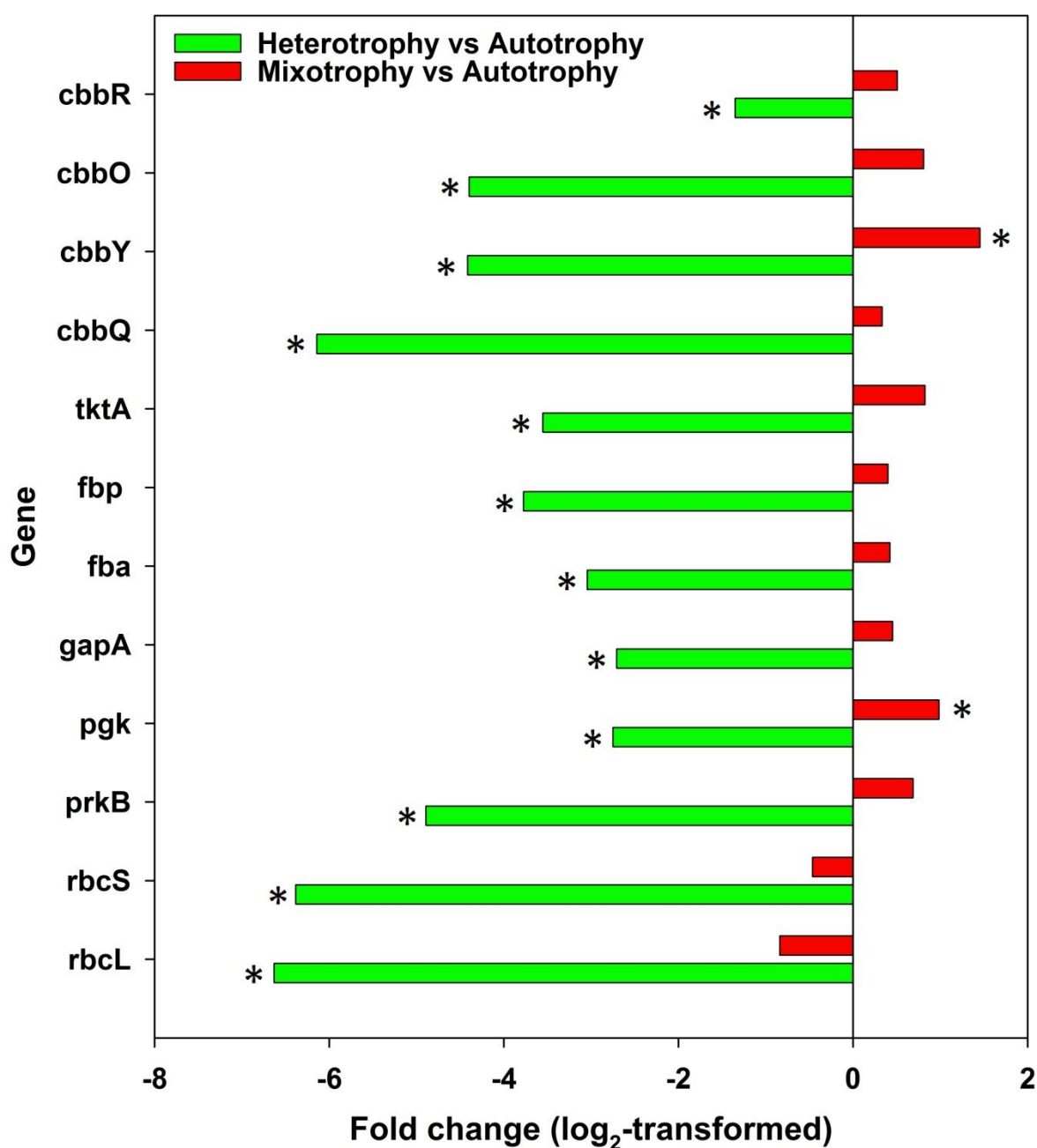


Figure 4-29. Fold change ( $\log_2$ -transformed) of average expression level of genes of CBB cycle under heterotrophy or mixotrophy versus autotrophy condition. The mean fold change is the mean change in level expression of given gene obtained from duplicate experiments. Asterisks indicate the significant difference at P value < 0.05.

The *cbbR* encodes a LysR-type transcriptional regulator from *H. thermoluteolus* which function as a regulator for CBB cycle expression. Two promoter regions with

LysR-binding site are located in the *cbbL* upstream region and *cbbR*-*cbbF* intergenic region. The previous literature reported that CbbR binds to both regions for activation CBB cycle. CbbR was also regulated by the intracellular concentration of NADPH [17]. Fold change in the level of expression under heterotrophic condition of *cbbR* was -2.5-fold, compared to that under autotrophic condition.

*e. Pyruvate dehydrogenase and pyruvate-ferredoxin/flavodoxin oxidoreductase*

The microarray results showed that the level of expression of *pdh* and *por* is high under autotrophic and low under heterotrophic and mixotrophic condition. The fold change of the level expression of *aceE* under heterotrophic and mixotrophic conditions was -5.2-fold and -7.2-fold compared to that under autotrophic condition, at p-value 0.05, respectively.

Table 4-20. Fold change in expression of genes encoding pyruvate dehydrogenase (*aceE*, *aceF*) and pyruvate-ferredoxin/flavodoxin oxidoreductase (*por*) enzymes in strain TH-1 under heterotrophy or mixotrophy versus autotrophy condition. The mean fold change is the mean change in level expression of given gene obtained from duplicate experiments (each gene was investigated by 7 independent probes in each experiment).

Protein/Enzyme	contig - KEGG ID	Gene	Heterotrophy vs Autotrophy	Mixotrophy vs Autotrophy
			Fluorescence intensity fold change $\pm$ SD (mean intensity ratio [ $\log_2$ ])	
pyruvate dehydrogenase E1 component [EC:1.2.4.1]	contig00006 _orf00155 K00163	<i>aceE</i>	-5.2 $\pm$ 0.2 (-2.4)	-7.2 $\pm$ 0.3 (-2.8)
pyruvate dehydrogenase E2 component (dihydrolipoamide acetyltransferase) [EC:2.	contig00006 _orf00157 K00627	<i>aceF</i>	-6.8 $\pm$ 0.6 (-2.8)	-9.9 $\pm$ 1.1 (-3.3)
pyruvate- ferredoxin/flavodoxin oxidoreductase [EC:1.2.7.1]	contig00003 _orf00259K03737	<i>por</i>	-3.1 $\pm$ 0.1 (-1.6)	-3.4 $\pm$ 0.4 (-1.7)

Additionally, the fold change of the expression level of gene *por* under heterotrophic and mixotrophic condition was -3.1-fold and -3.4-fold compared to that under autotrophic condition, respectively. These results indicate that under autotrophic condition, the function of pyruvate dehydrogenase and pyruvate-ferredoxin/flavodoxin oxidoreductases is the flow from pyruvate to acetyl-CoA. The reducing equivalent obtained from pyruvate oxidation may be employed for operating CBB cycle.

PDH and POR are two enzymes that catalyze the conversion between pyruvate and acetyl-CoA. The down-regulation of these genes under heterotrophic and mixotrophic conditions, compared to those under autotrophic condition, confirmed that acetyl-CoA was mainly metabolized through TCA cycle and glyoxylate cycle.

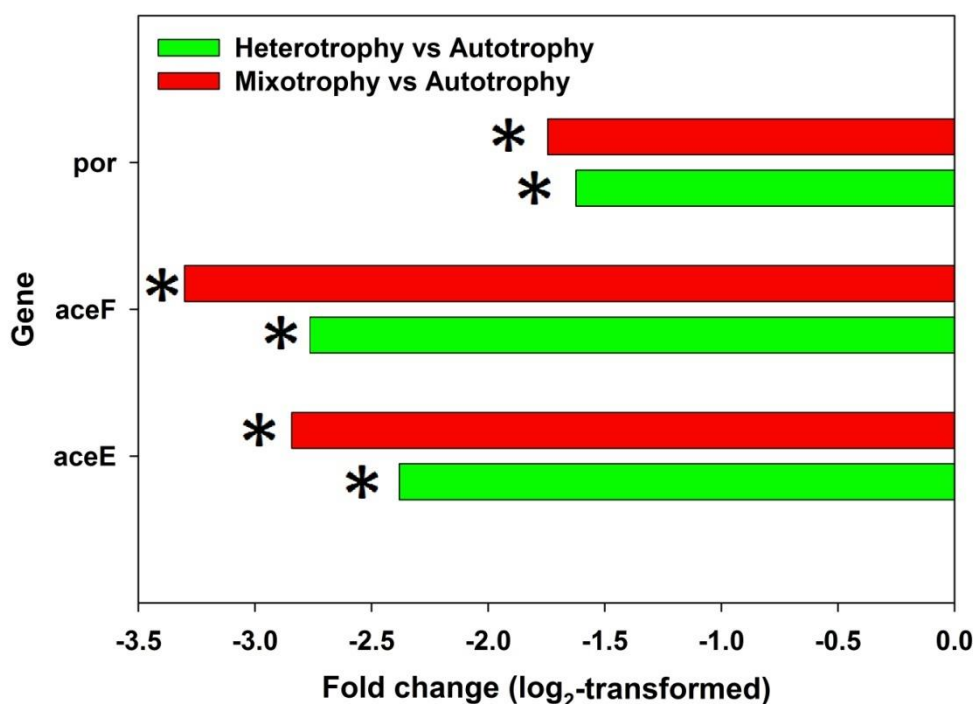


Figure 4-30. Fold change (log<sub>2</sub>-transformed) of average expression level of genes encoding pyruvate dehydrogenase (*aceE*, *aceF*) and pyruvate-ferredoxin/flavodoxin oxidoreductase (*por*) enzymes in strain TH-1 under heterotrophy or mixotrophy versus autotrophy condition. The mean fold change is the mean change in level expression of given gene obtained from duplicate experiments. Asterisks indicate the significant difference at P value < 0.05.

### *f. TCA cycle*

In energy metabolism, tricarboxylic acid cycle (TCA) is important to generate reducing equivalent that is oxidized in respiratory chain for ATP production. ATP is known as energy currency for many metabolism processes in the cell. In glucose oxidation process, glycolysis pathway break-down the glucose or other intermediate metabolites to pyruvate [58]. However, this process is incomplete in strain TH-1. Therefore, pyruvate is converted into acetyl-CoA, a central metabolite. Acetyl-CoA enters to TCA cycle where it is completely oxidized to gain 1GTP, 3NADH, and 1 FADH<sub>2</sub>. In addition, the TCA cycle can also be used for providing some important precursors for biosynthesis such as 2-oxoglutarate and oxaloacetate.

So, the operation and the regulation of TCA cycle are important to physiology of cell and the growth of the cell.

All the genes for TCA cycle enzymes were identified and annotated: citrate synthase [EC:2.3.3.1] (*cs*: contig00005\_orf00132); aconitate hydratase [EC:4.2.1.3] (*acnA1*: contig00015\_orf00033, *acnA2* contig00004\_ orf00070); isocitrate dehydrogenase [EC:1.1.1.42] ( *icdh*: contig00004\_orf00065), isocitrate dehydrogenase kinase/phosphatase [EC:2.7.11.5] (*aceK*: contig00004\_orf00066); 2-oxoglutarate dehydrogenase E1 component [EC:1.2.4.2] (*ogdh*: contig00005\_orf00130); succinyl-CoA synthetase beta subunit [EC:6.2.1.5] (*scsC*: contig00020\_orf00030; *scsD*: contig00020\_orf00033); succinate dehydrogenase/ fumarate reductase [EC:1.3.5.1 1.3.5.4] (*sdhB*: contig00005\_orf00136; *sdhA*: contig00005\_orf00137; *sdhD*: contig00005\_orf00139; *sdhC*: contig00005\_orf00140); fumarate hydratase, class I [EC:4.2.1.2] (*fumA*: contig00011\_orf00039); and malate dehydrogenase [EC:1.1.1.37] (*mdh*: contig00005\_orf00142).

In microarray expression profile, the expression levels of all genes that belong to TCA cycle were highly expressed under three conditions, autotrophic, mixotrophic and heterotrophic condition. This result indicates that they constitutively function in *H. thermoluteolus* TH-1 cells.

Table 4-21. Fold change in expression of genes encoding TCA enzymes in strain TH-1 under heterotrophy or mixotrophy versus autotrophy condition. The mean fold change is the mean change in level expression of given gene obtained from duplicate experiments (each gene was investigated by 7 independent probes in each experiment).

Protein/Enzyme	contig - KEGG ID	Gene	Heterotrophy vs Autotrophy	Mixotrophy vs Autotrophy
			Fluorescence intensity fold change $\pm$ SD (mean intensity ratio [log <sub>2</sub> ])	
citrate synthase [EC:2.3.3.1]	contig00005 _orf00132 K01647	<i>cs</i>	2.8 $\pm$ 0.1 (1.5)	2.7 $\pm$ 0.4 (1.4)
aconitate hydratase [EC:4.2.1.3]	contig00004 _orf00070 K01682	<i>acnA</i>	1.4 $\pm$ 0.1 (0.5)	2.0 $\pm$ 0.2 (1.0)
isocitrate dehydrogenase [EC:1.1.1.42]	contig00004 _orf00065 K00031	<i>icdh</i>	3.2 $\pm$ 0.1 (1.7)	1.9 $\pm$ 0.2 (0.9)
isocitrate dehydrogenase kinase/phosphatase [EC:2.7.11.5 3.1.3.-]	contig00004 _orf00066 K00906	<i>aceK</i>	1.2 $\pm$ 0.1 (0.3)	2.0 $\pm$ 0.2 (1.0)
2-oxoglutarate dehydrogenase E1 component [EC:1.2.4.2]	contig00005 _orf00130 K00164	<i>ogdh</i>	2.8 $\pm$ 0.2 (1.5)	3.3 $\pm$ 0.2 (1.7)
succinyl-CoA synthetase beta subunit [EC:6.2.1.5]	contig00020 _orf00030 K01903	<i>scsC</i>	2.7 $\pm$ 0.1 (1.4)	2.0 $\pm$ 0.1 (1.0)
succinyl-CoA synthetase alpha subunit [EC:6.2.1.5]	contig00020 _orf00033 K01902	<i>scsD</i>	1.7 $\pm$ 0.2 (0.7)	1.6 $\pm$ 0.1 (0.7)
succinate dehydrogenase/ fumarate reductase [EC:1.3.5.1 1.3.5.4]	contig00005 _orf00136 K00240	<i>sdhB</i>	1.3 $\pm$ 0.3 (0.4)	2.8 $\pm$ 0.2 (1.5)
succinate dehydrogenase/ fumarate reductase [EC:1.3.5.1 1.3.5.4]	contig00005 _orf00137 K00239	<i>sdhA</i>	1.3 $\pm$ 0.1 (0.4)	2.4 $\pm$ 0.1 (1.3)
succinate dehydrogenase/ fumarate reductase [EC:1.3.5.1 1.3.5.4]	contig00005 _orf00139 K00242	<i>sdhD</i>	1.6 $\pm$ 0.02 (0.7)	2.3 $\pm$ 0.1 (1.2)
succinate dehydrogenase/ fumarate reductase, cytochrome b subunit [EC:1.3.5.1, 1.3.5.4]	contig00005 _orf00140 K00241	<i>sdhC</i>	1.9 $\pm$ 0.1 (0.9)	3 $\pm$ 0.1 (1.6)
fumarate hydratase, class I [EC:4.2.1.2]	contig00011 _orf00039 K01676	<i>fumA</i>	-1.1 $\pm$ 0.1 (-0.1)	1.8 $\pm$ 0.2 (0.9)
malate dehydrogenase [EC:1.1.1.37]	contig00005 _orf00142 K00025	<i>mdh</i>	-1.1 $\pm$ 0.02 (-0.1)	1.2 $\pm$ 0.1 (0.3)

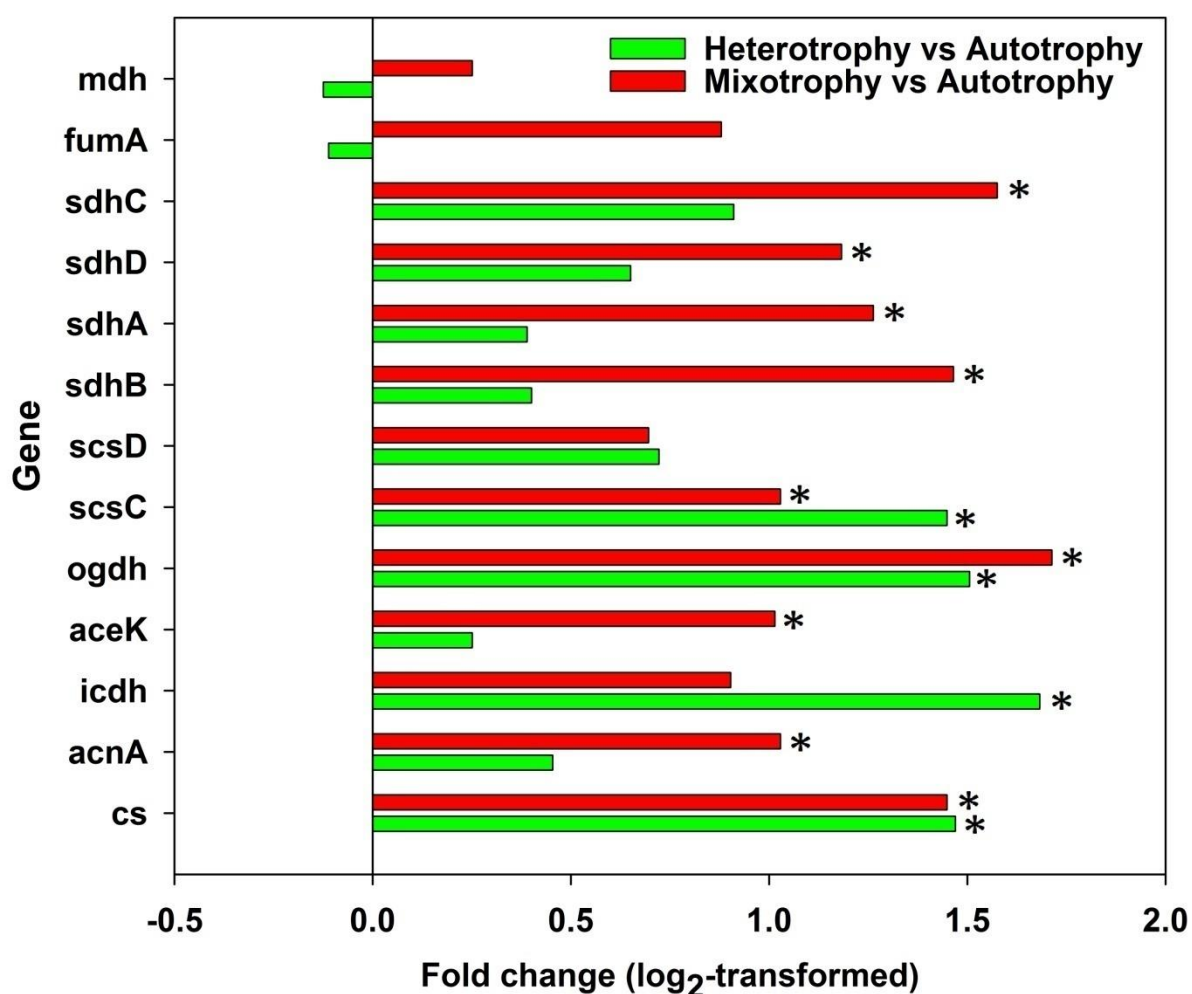


Figure 4-31. Fold change ( $\log_2$ -transformed) of average expression level of genes encoding TCA cycle enzymes strain TH-1 under heterotrophy or mixotrophy versus autotrophy condition. The mean fold change is the mean change in level expression of given gene obtained from duplicate experiments. Asterisks indicate the significant difference at P value < 0.05.

Most genes belong to TCA cycle did not change in level of expression. Apparently, the high expression of TCA cycle-related genes under all investigated condition also suggests that TCA cycle is the important metabolic pathway in strain TH-1 under all condition tested. The expression levels of all genes belonging to TCA cycle were up-regulated under heterotrophic condition, compared to those under autotrophic condition.

Fold change of the expression levels of *cs*, *icdh*, *ogdh*, and *scsC* in strain TH-1 under heterotrophic condition were 2.8-fold, 3.2-fold, 2.8-fold, and 2.7-fold up-regulated, compared to those under autotrophic condition, respectively.

The expression levels of all genes belonging to TCA cycle under mixotrophic condition were significantly higher than those under autotrophic condition as in Table 4-21.

*g. Glyoxylate cycle*

All the genes for glycolysis pathway enzymes were identified and annotated: citrate synthase [EC:2.3.3.1] (*cs*: contig00005\_orf00132); aconitate hydratase [EC:4.2.1.3] (*acnA*: contig00004\_orf00070); isocitrate lyase [EC:4.1.3.1] (*aceA*: contig00010\_orf00035); malate synthase [EC:2.3.3.9] (*aceB*: contig00004\_orf00057); and malate dehydrogenase [EC:1.1.1.37] (*mdh*: contig00005\_orf00142).

Table 4-22. Fold change in expression of genes encoding glyoxylate cycle enzymes in strain TH-1 under heterotrophy or mixotrophy versus autotrophy condition. The mean fold change is the mean change in level expression of given gene obtained from duplicate experiments (each gene was investigated by 7 independent probes in each experiment).

Protein/Enzyme	contig - KEGG ID	Gene	Heterotrophy vs Autotrophy	Mixotrophy vs Autotrophy
			Fluorescence intensity fold change $\pm$ SD (mean intensity ratio [ $\log_2$ ])	
citrate synthase [EC:2.3.3.1]	contig00005_orf00132 K01647	<i>cs</i>	2.8 $\pm$ 0.1 (1.5)	2.7 $\pm$ 0.4 (1.4)
aconitate hydratase [EC:4.2.1.3]	contig00004_orf00070 K01682	<i>acnA</i>	1.4 $\pm$ 0.1 (0.5)	2.0 $\pm$ 0.2 (1.0)
isocitrate lyase [EC:4.1.3.1]	contig00010_orf00035 K01637	<i>aceA</i>	4.4 $\pm$ 0.7 (2.1)	4.4 $\pm$ 0.4 (2.1)
malate synthase [EC:2.3.3.9]	contig00004_orf00057 K01638	<i>aceB</i>	2 $\pm$ 0.1 (1.0)	1.7 $\pm$ 0.1 (0.8)
malate dehydrogenase [EC:1.1.1.37]	contig00005_orf00142 K00025	<i>mdh</i>	-1.1 $\pm$ 0.02 (-0.1)	1.2 $\pm$ 0.1 (0.3)

The expression levels of *aceA* and *aceB* were significantly high under heterotrophic condition and mixotrophic condition compared with those under autotrophic condition.

This result confirms the operation of glyoxylate cycle under heterotrophic and mixotrophic when butyrate is available.

The high expression levels of genes coding for two key enzyme of glyoxylate cycle, isocitrate lyase (*aceA*), and malate synthase (*aceB*) emphasize the important role of glyoxylate pathway in butyrate metabolism under heterotrophic or mixotrophic condition. The expression levels of *aceA* and *aceB* under heterotrophic condition were 4.4-fold and 2.0-fold higher than those under autotrophic condition, respectively. Expression levels of *aceA* and *aceB* genes under mixotrophic condition were 4.4-fold and 1.7-fold higher than that under autotrophic condition. This observation could be explained based on carbon metabolism feature. When butyrate is the substrate for the cells, strain TH-1 grows under heterotrophic condition; butyrate should be converted into intermediate acetyl-CoA via  $\beta$ -oxidation pathway. By the function of citrate synthase (*cs*) acetyl-CoA was condensed with four carbon substrate, oxaloacetate to produce a six carbon substrate, citrate. Citrate is converted into isocitrate which is cleaved to glyoxylate and succinate by the function of isocitrate lyase.

Through the steps catalyzed by isocitrate lyase, the strain TH-1 cells under heterotrophic condition skip two complete decarboxylation of acetyl-CoA to CO<sub>2</sub> [58]. However, the rising pool of glyoxylate can cause another problem to the cells. Because glyoxylate is a toxic compound to the cell, glyoxylate itself become an inhibitory factor to the growth of the cell under heterotrophic and mixotrophic conditions. The high flux of carbon conversion at the upstream causes the accumulation of the product at the downstream of carbon flux. This result may be correlative with the growth curve with long lag phase of strain TH-1 under heterotrophic condition with butyrate.

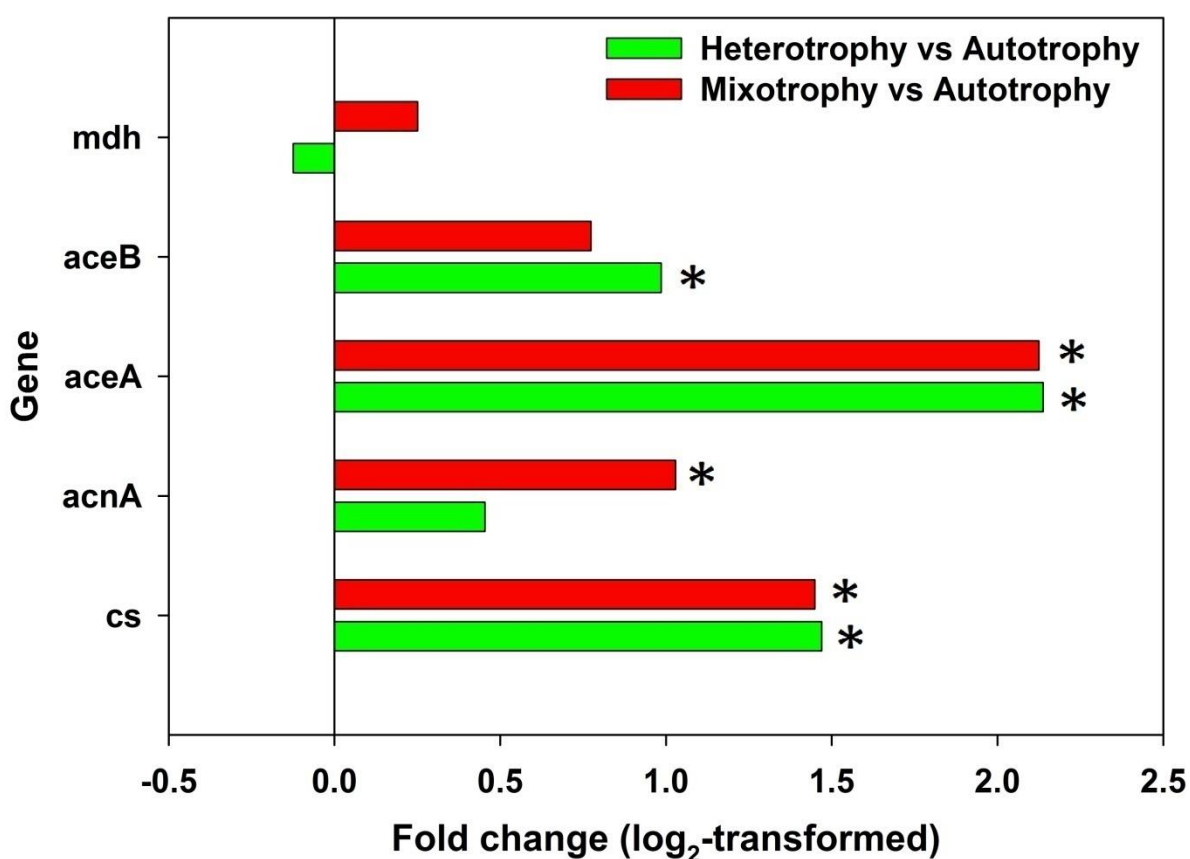


Figure 4-32. Fold change ( $\log_2$ -transformed) of average expression level of genes encoding glyoxylate cycle cycle enzymes strain TH-1 under heterotrophy or mixotrophy versus autotrophy condition. The mean fold change is the mean change in level expression of given gene obtained from duplicate experiments. Asterisks indicate the significant difference at P value < 0.05.

The microarray result suggested the important role of glyoxylate cycle in metabolism butyrate and other carbon sources that are metabolized through acetyl-CoA, like acetate. This result also confirmed the operation of glyoxylate cycle under heterotrophic and mixotrophic conditions with butyrate.

#### *h. Photorespiration related genes*

All the genes for photorespiration enzymes were identified and annotated: phosphoglycolate phosphatase [EC:3.1.3.18] (*pgp*: contig00020\_orf00038); glycolate oxidase iron-sulfur subunit [EC:1.1.3.14] (*GlcF*: contig00008\_orf00125); FAD linked

oxidase domain protein [EC 1.1.99.14] (*GlcE*:contig00008\_orf00127 K11517); glycolate oxidase subunit GlcD [EC 1.1.99.14] (*GlcD*:contig00008\_orf00128); catalase/oxidase [EC 1.11.1.6] (*catB*: contig00002\_orf00198); cytochrome-c peroxidase [EC 1.11.1.5] (*cpx*: contig00001\_orf00071).

Glyoxylate is an active compound and it is also toxic to the cells. Then, the pool of glyoxylate under heterotrophic condition causes negative effect on the growth of the cell. The cells of strain TH-1 showed slight inhibition on growth under heterotrophic condition. The question is why growth was inhibited under mixotrophic condition. From expression profile of CBB cycle, it was assumed that CBB operates under mixotrophic condition.

Table 4-23. Fold change in expression of genes encoding photorespiration related enzymes in strain TH-1 under heterotrophy or mixotrophy versus autotrophy condition. The mean fold change is the mean change in level expression of given gene obtained from duplicate experiment (each gene was investigated by 7 independent probes in each experiment).

Protein/Enzyme	contig - KEGG ID	Gene	Heterotrophy vs Autotrophy	Mixotrophy vs Autotrophy
			Fluorescence intensity fold change $\pm$ SD (mean intensity ratio [ $\log_2$ ])	
phosphoglycolate phosphatase EC:3.1.3.18]	contig00020 _orf00038 K01091	<i>pgp</i>	-2.9 $\pm$ 0.1 (-1.5)	3.6 $\pm$ 0.1 (1.9)
glycolate oxidase iron- sulfur subunit [EC:1.1.3.14]	contig00008 _orf00125 K11517	<i>GlcF</i>	1.0 $\pm$ 0.02 (0.0)	2.1 $\pm$ 0.04 (1.1)
FAD linked oxidase domain protein [EC 1.1.99.14]	contig00008 _orf00127 K11517	<i>GlcE</i>	1.1 $\pm$ 0.1 (0.2)	1.7 $\pm$ 0.3 (0.7)
glycolate oxidase subunit GlcD [EC 1.1.99.14]	contig00008 _orf00128 T00007	<i>GlcD</i>	-1.1 $\pm$ 0.1 (-0.1)	1.7 $\pm$ 0.1 (0.7)
catalase/oxidase [EC 1.11.1.6]	contig00002 _orf00198 K03781	<i>catB</i>	1.1 $\pm$ 0.03 (0.1)	1.5 $\pm$ 0.1 (0.6)
cytochrome-c peroxidase [EC 1.11.1.5]	contig00001 _orf00071	<i>cpx</i>	4.5 $\pm$ 0.1 (2.2)	7.5 $\pm$ 0.3 (2.9)

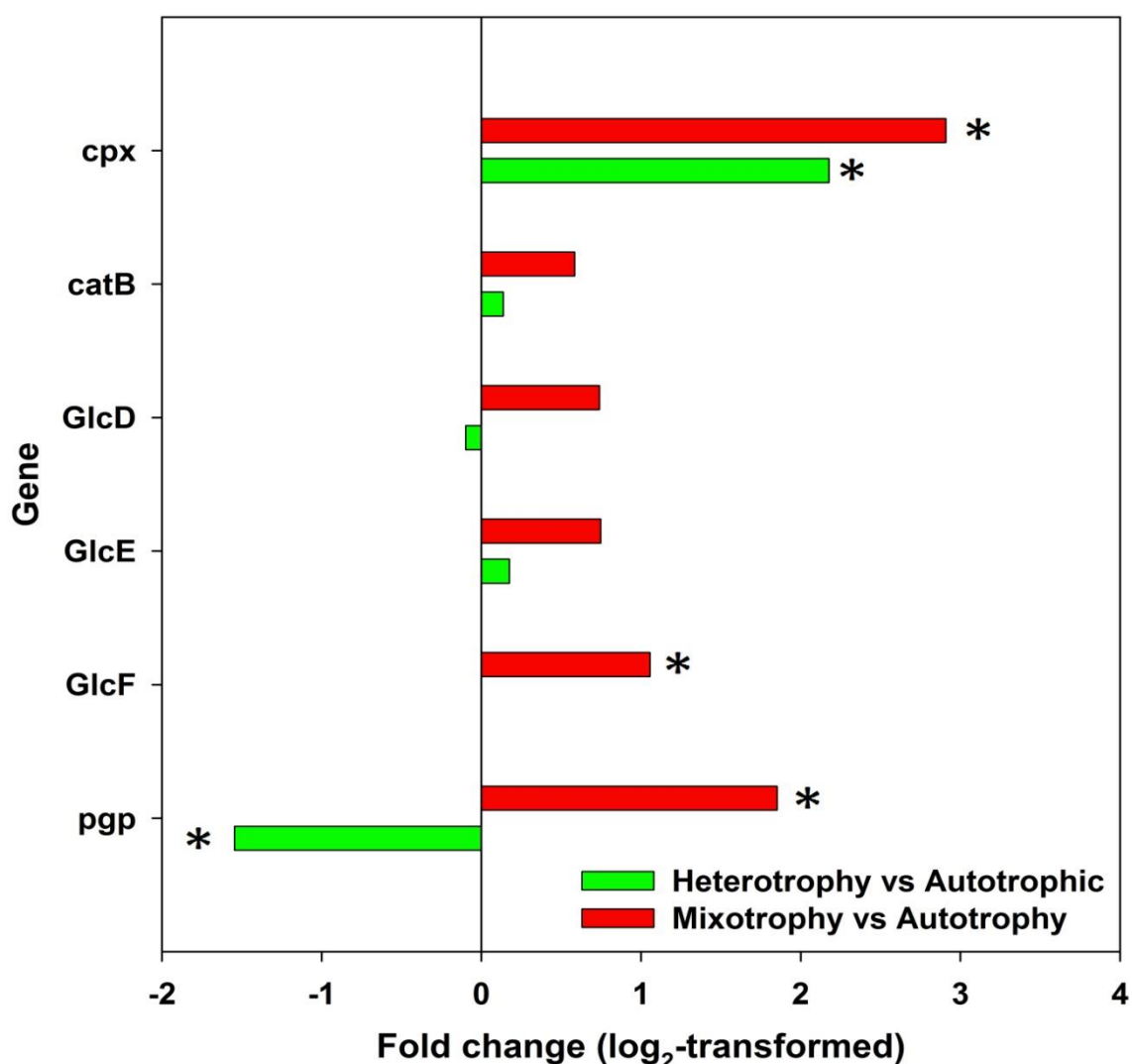


Figure 4-33. Fold change (log<sub>2</sub>-transformed) of average expression level of genes encoding photorespiration enzymes strain TH-1 under heterotrophy or mixotrophy versus autotrophy condition. The mean fold change is the mean change in level expression of given gene obtained from duplicate experiment. Asterisks indicate the significant difference at P value < 0.05.

The key enzyme of CBB cycle is RubisCO. RubisCO is the enzyme which catalyzes the fixation of CO<sub>2</sub> to a five carbon metabolite, ribulose-1,5-biphosphate and produces 2 three carbon metabolites, 3-phosphoglycerate. This is the major step of CBB cycle. Furthurmore, at the same time, RubisCO also incorporate O<sub>2</sub> into ribulose-1,5-biphosphate to produce a by-product, 2-phosphoglycolate in a process so-called

photorespiration. 2-Phosphoglycolate will be converted into glycolate by enzyme phosphoglycolate phosphatase [EC: 3.1.3.18] (*gph*) [59, 60]. Under heterotrophic condition, *gph* gene was -2.9-fold down-regulated compared to that under autotrophic condition. However, under mixotrophic condition this gene was 3.6-fold up-regulated, compared with that under autotrophic condition. This fact suggested that the photorespiration occurred during mixotrophic growth.

Interestingly, the level expression of gene *cpx* coding cytochrom *c* peroxidase was significantly enhanced under mixotrophic condition. The expression level of *cpx* under mixotrophic condition was 7.5-fold higher than that under autotrophic, suggested that cytochrom *c* peroxidase was assumed to be a detoxification system for  $\text{H}_2\text{O}_2$ .

#### *i. Oxidative phosphorylation machinery*

Respiratory machinery is one of the important parts in energy metabolism. It catalyzes the step by which electron is transported from electron carrier like NADH,  $\text{FADH}_2$  or hydrogen to a final electron acceptor. The oxidation of NADH,  $\text{FADH}_2$  or hydrogen is strongly exergonic. The energy release from this process is used for ATP production.

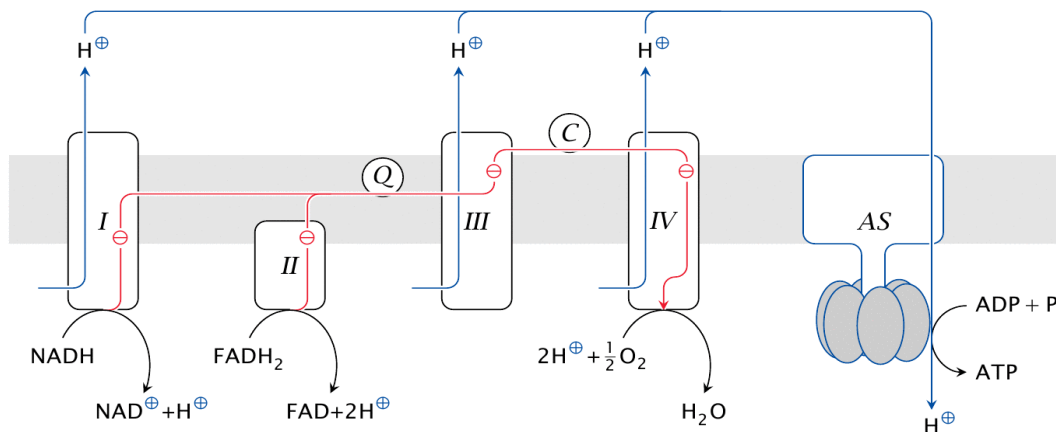


Figure 4-34. The respiratory chain involves four large protein complexes (I–IV) as well as ATP synthase (AS). All of these are embedded in the inner mitochondrial membrane. Coenzyme Q (Q) and cytochrome C (C) are diffusible electron carriers (Human metabolism lecture notes, Michael Palmer, 2014)

Respiratory machinery is a system that performs electron transport chain (ETC) with 5 complexes [34, 61]. When electron is transported from an electron donor like NADH, FADH<sub>2</sub>, or H<sub>2</sub>, to a final electron acceptor, simultaneous transmembrane gradient of proton is established. Proton will come back to cytosol via ATP synthase channel to synthesis ATP. ATP production in this case is termed as oxidative phosphorylation.

Complex I is a multicomplex enzyme that oxidizes NADH, and electron is passed to ubiquinone. The major component of complex I is NADH dehydrogenase which catalyzes NADH oxidation and feeding electron to ETC. All the genes of complex I were identified and annotated: NADH dehydrogenase [EC:1.6.5.3] (*nad*: contig00005\_orf00132); NADH-quinone oxidoreductase subunit A-N [EC:1.6.5.3]; (*nuoA*: contig00015\_orf00033; *nuoB*: contig00004\_orf00070; *nuoC*: contig00004\_orf00065; *nuoD*: contig00004\_orf00066; *nuoE*: contig00005\_orf00130; *nuoF*: contig00020\_orf00030; *nuoG*: contig00009\_orf00088; *nuoH*: contig00001\_orf00366; *nuoI*: contig00001\_orf00367; *nuoJ*: contig00001\_orf00369; *nuoK*: contig00001\_orf00371; *nuoL*: contig00001\_orf00373; *nuoM*: contig00001\_orf00374 ; and *nuoN*: contig00001\_orf00376).

The expression levels of all genes belong to complex I under mixotrophic condition were higher than those under autotrophic and heterotrophic condition

Complex II is succinate dehydrogenase, a component of TCA cycle. All the genes of complex II were identified and annotated: succinate dehydrogenase / fumarate reductase, flavoprotein subunit A-D [EC:1.3.5.1;01.3.5.4] (*sdhA*: contig00005\_orf00137; *sdhB*: contig00005\_orf00136; *sdhC*: contig00005\_orf00140; *sdhD*: contig00005\_orf00139). Complex II is the place where oxidate FADH<sub>2</sub> and pass electron to reduce ubiquinone.

Table 4-24. Fold change in expression of genes encoding complex I in strain TH-1 under heterotrophy or mixotrophy versus autotrophy condition. The mean fold change is the mean change in level expression of given gene obtained from duplicate experiments (each gene was investigated by 7 independent probes in each experiment).

Protein/Enzyme	contig - KEGG ID	Gene	Heterotrophy vs Autotrophy	Mixotrophy vs Autotrophy
			Fluorescence intensity fold change $\pm$ SD (mean intensity ratio [ $\log_2$ ])	
NADH dehydrogenase [EC:1.6.5.3]	contig00009 _orf00088 K00329	<i>nad</i>	-1.4 $\pm$ 0.02 (-0.4)	2.5 $\pm$ 0.03 (1.3)
NADH-quinone oxidoreductase subunit A [EC:1.6.5.3]	contig00001 _orf00366 K00330	<i>nuoA</i>	-1.8 $\pm$ 0.1 (-0.8)	1.9 $\pm$ 0.04 (0.9)
NADH-quinone oxidoreductase subunit B [EC:1.6.5.3]	contig00001 _orf00367 K00331	<i>nuoB</i>	-2.5 $\pm$ 0.1 (-1.3)	1.5 $\pm$ 0.1 (0.5)
NADH-quinone oxidoreductase subunit C [EC:1.6.5.3]	contig00001 _orf00369 K00332	<i>nuoC</i>	-1.7 $\pm$ 0.2 (-0.7)	1.3 $\pm$ 0.1 (0.4)
NADH-quinone oxidoreductase subunit D [EC:1.6.5.3]	contig00001 _orf00371 K00333	<i>nuoD</i>	-1.7 $\pm$ 0.2 (-0.8)	2.0 $\pm$ 0.2 (1.0)
NADH-quinone oxidoreductase subunit E [EC:1.6.5.3]	contig00001 _orf00373 K00334	<i>nuoE</i>	-1.2 $\pm$ 0.1 (-0.3)	2.7 $\pm$ 0.2 (1.4)
NADH-quinone oxidoreductase subunit F [EC:1.6.5.3]	contig00001 _orf00374 K00335	<i>nuoF</i>	-1.1 $\pm$ 0.02 (-0.1)	2.0 $\pm$ 0.1 (1.0)
NADH-quinone oxidoreductase subunit G [EC:1.6.5.3]	contig00001 _orf00376 K00336	<i>nuoG</i>	-1.4 $\pm$ 0.04 (-0.5)	2.4 $\pm$ 0.1 (1.2)
NADH-quinone oxidoreductase subunit H [EC:1.6.5.3]	contig00001 _orf00378 K00337	<i>nuoH</i>	-1.4 $\pm$ 0.1 (-0.5)	3.2 $\pm$ 0.5 (1.7)
NADH-quinone oxidoreductase subunit I [EC:1.6.5.3]	contig00001 _orf00380 K00338	<i>nuoI</i>	-1.5 $\pm$ 0.03 (-0.5)	2.8 $\pm$ 0.04 (1.5)
NADH-quinone oxidoreductase subunit J [EC:1.6.5.3]	contig00001 _orf00381 K00339	<i>nuoJ</i>	-1.1 $\pm$ 0.03 (-0.2)	3.0 $\pm$ 0.1 (1.6)
NADH-quinone oxidoreductase subunit K [EC:1.6.5.3]	contig00001 _orf00383 K00340	<i>nuoK</i>	-1.1 $\pm$ 0.02 (-0.1)	3.2 $\pm$ 0.1 (1.7)

NADH-quinone oxidoreductase subunit L [EC:1.6.5.3]		contig00001_orf00384 K00341	<i>nuoL</i>	-1.3±0.1 (-0.4)	2.6±0.1 (1.4)
NADH-quinone oxidoreductase subunit M [EC:1.6.5.3]	M	contig00001_orf00385 K00342	<i>nuoM</i>	-1.3±0.04 (-0.3)	2.6±0.1 (1.4)
NADH-quinone oxidoreductase subunit N [EC:1.6.5.3]		contig00001_orf00388 K00343	<i>nuoN</i>	-1.2±0.1 (-0.2)	2.2±0.2 (1.2)

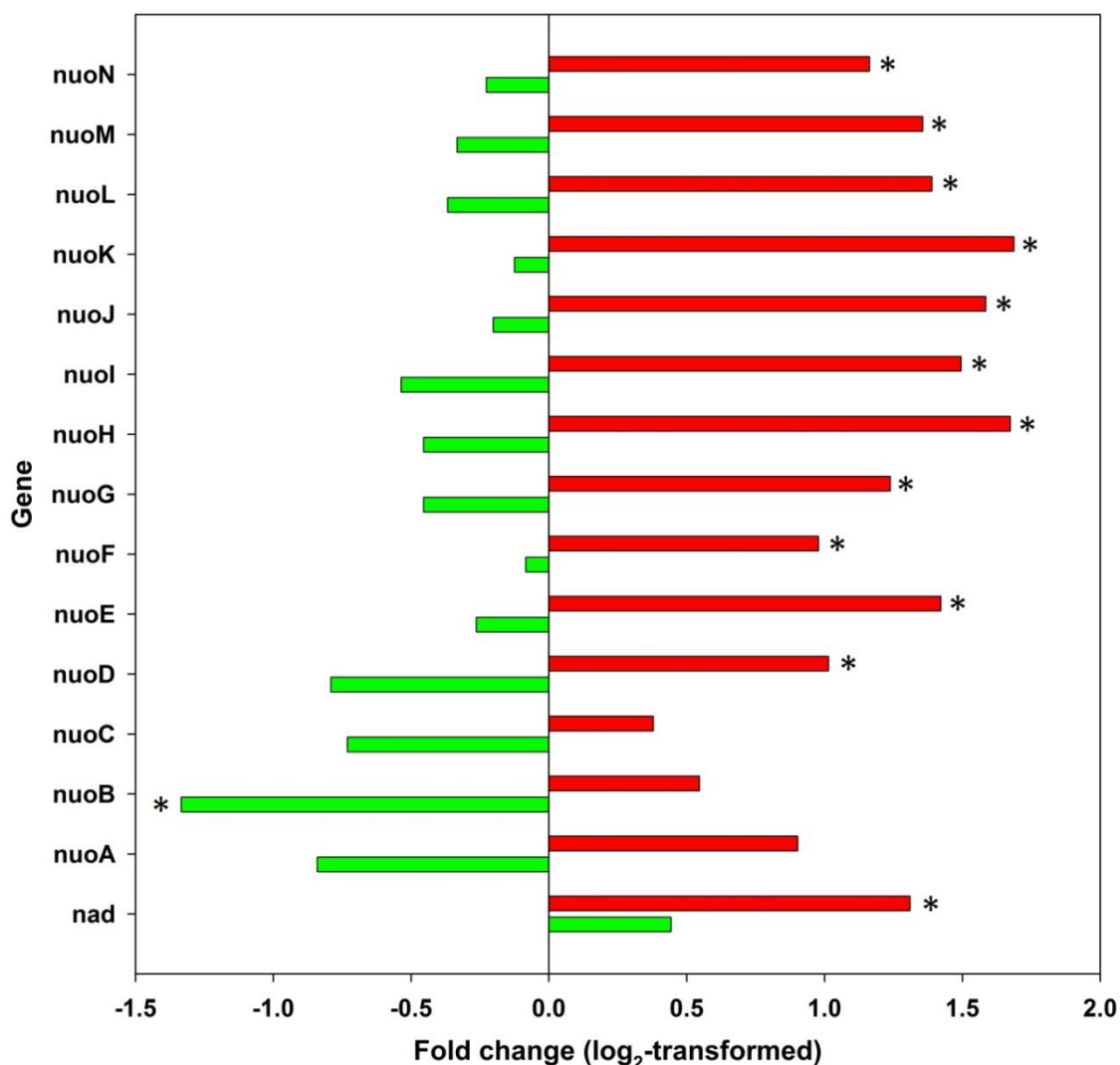


Figure 4-35. Fold change (log<sub>2</sub>-transformed) of average expression level of genes encoding complex I strain TH-1 under heterotrophy or mixotrophy versus autotrophy condition. The mean fold change is the mean change in level expression of given gene obtained from duplicate experiments. Asterisks indicate the significant difference at P value < 0.05.

Reduced ubiquinone passes electron to complex III. Complex III transfers electron to complex IV via cytochrome *c*. All the genes of complex III were identified and annotated: ubiquinol-cytochrome *c* reductase iron-sulfur subunit [EC:1.10.2.2] (*petA*: contig00010\_orf00088); ubiquinol-cytochrome *c* reductase cytochrome *b/c1* subunit (*fbcH*: contig00010\_orf00085). Complex IV is a cytochrome *c* oxidase where final electron acceptor O<sub>2</sub> is reduced to H<sub>2</sub>O. Co-current with electron transfer, I, III and IV pump proton (H<sup>+</sup>) from cytosol to inner layer of peripheral and establish proton gradient through cell membrane. All the genes of complex VI were identified and annotated: cytochrome *c* oxidase *cbb3*-type subunit I [EC:1.9.3.1] (*ccoN*: contig00005\_orf00053); cytochrome *c* oxidase *cbb3*-type subunit II (*ccoO*: contig00005\_orf00051); cytochrome *c* oxidase *cbb3*-type subunit III (*ccoP*: contig00005\_orf00049). Complex V is the ATP synthase. It is not involved in ETC, but ATP synthase is an important structure where ATP is produced.

Table 4-25. Fold change in expression of genes encoding complex II in strain TH-1 under heterotrophy or mixotrophy versus autotrophy condition. The mean fold change is the mean change in level expression of given gene obtained from duplicate experiment (each gene was investigated by 7 independent probes in each experiment).

Protein/Enzyme	contig - KEGG ID	Gene	Heterotrophy vs Autotrophy	Mixotrophy vs Autotrophy
			Fluorescence intensity fold change $\pm$ SD (mean intensity ratio [log <sub>2</sub> ])	
succinate dehydrogenase / fumarate reductase, flavoprotein subunit [EC:1.3.5.1]	contig00005 _orf00137 K00239	<i>sdhA</i>	1.3 $\pm$ 0.1 (0.4)	2.4 $\pm$ 0.1 (1.3)
succinate dehydrogenase / fumarate reductase, iron-sulfur subunit [EC:1.3.5.1]	contig00005 _orf00136 K00240	<i>sdhB</i>	1.3 $\pm$ 0.3 (0.4)	2.8 $\pm$ 0.2 (1.5)
succinate dehydrogenase / fumarate reductase, cytochrome b subunit [EC 1.3.5.1]	contig00005 _orf00140 K00241	<i>sdhC</i>	1.9 $\pm$ 0.1 (0.9)	3.0 $\pm$ 0.1 (1.6)
succinate dehydrogenase / fumarate reductase, membrane anchor subunit	contig00005 _orf00139 K00242	<i>sdhD</i>	1.6 $\pm$ 0.02 (0.7)	2.3 $\pm$ 0.1 (1.2)

All the genes of complex V were identified and annotated: polyphosphate kinase [EC:2.7.4.1] (*ppk*: contig00006\_orf00131); inorganic pyrophosphatase [EC:3.6.1.1] (*ppa*: contig00005\_orf00036); F-type H<sup>+</sup>-transporting ATPase [EC:3.6.3.14] (*atpA*: contig00003\_orf00055; *atpB*: contig00003\_orf00063; *atpC*: contig00003\_orf00050; *atpD*: contig00003\_orf00051; *atpE*: contig00003\_orf00061; *atpF*: contig00003\_orf00059; *atpG*: contig00003\_orf00053; *atpH*: contig00003\_orf00057).

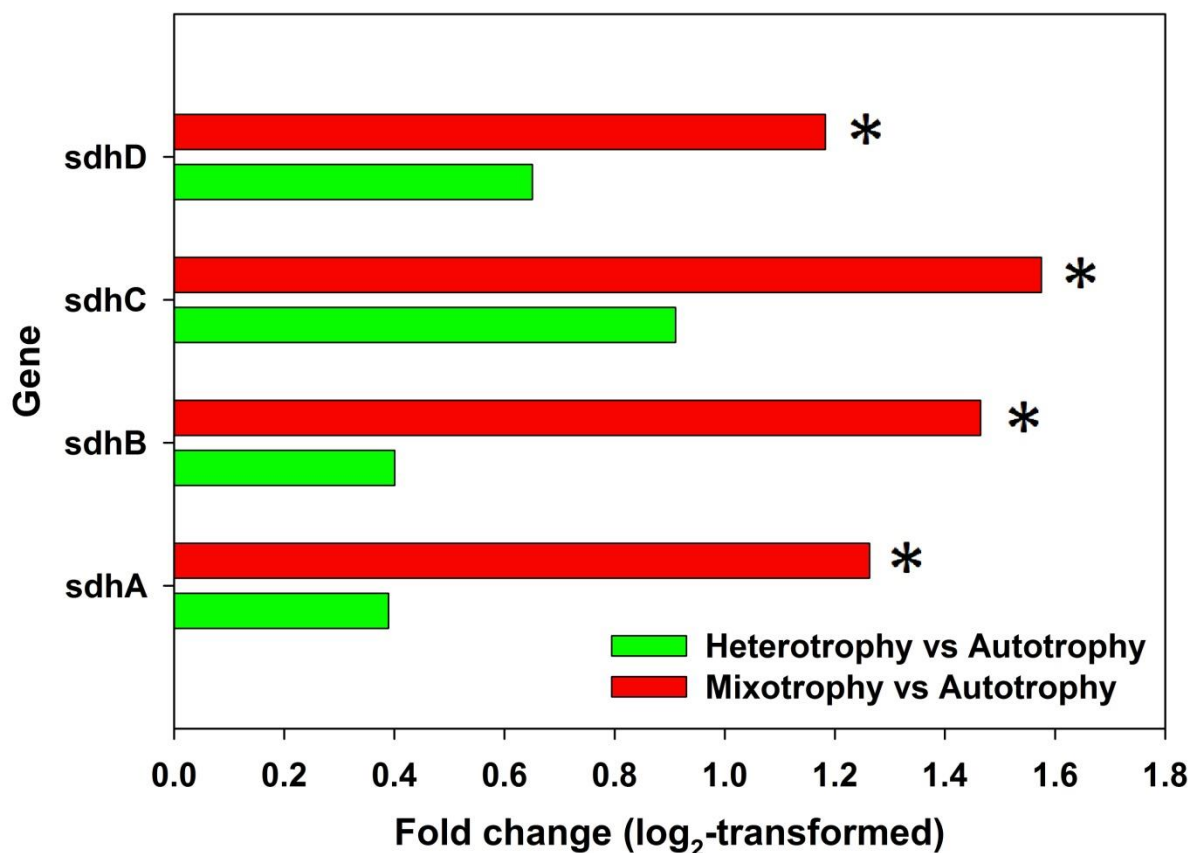


Figure 4-36. Fold change ( $\log_2$ -transformed) of average expression level of genes encoding complex II strain TH-1 under heterotrophy or mixotrophy versus autotrophy condition. The mean fold change is the mean change in level expression of given gene obtained from duplicate experiments. Asterisks indicate the significant difference at P value < 0.05.

Table 4-26. Fold change ( $\log_2$ -transformed) in expression of genes encoding complex III in strain TH-1 under heterotrophy or mixotrophy versus autotrophy condition. The mean fold change is the mean change in level expression of given gene obtained from duplicate experiment (each gene was investigated by 7 independent probes in each experiment).

Protein/Enzyme	contig - KEGG ID	Gene	Heterotrophy vs Autotrophy	Mixotrophy vs Autotrophy
			Fluorescence intensity fold change $\pm$ SD (mean intensity ratio [ $\log_2$ ])	
ubiquinol-cytochrome c reductase iron-sulfur subunit [EC:1.10.2.2]	contig00010 _orf00088 K00411	<i>petA</i>	-1.8 $\pm$ 0.03 (-0.9)	1.8 $\pm$ 0.1 (0.8)
ubiquinol-cytochrome c reductase cytochrome b/c1 subunit	contig00010 _orf00085 K00410	<i>fbcH</i>	-1.6 $\pm$ 0.4 (-0.6)	2.1 $\pm$ 0.4 (1.1)

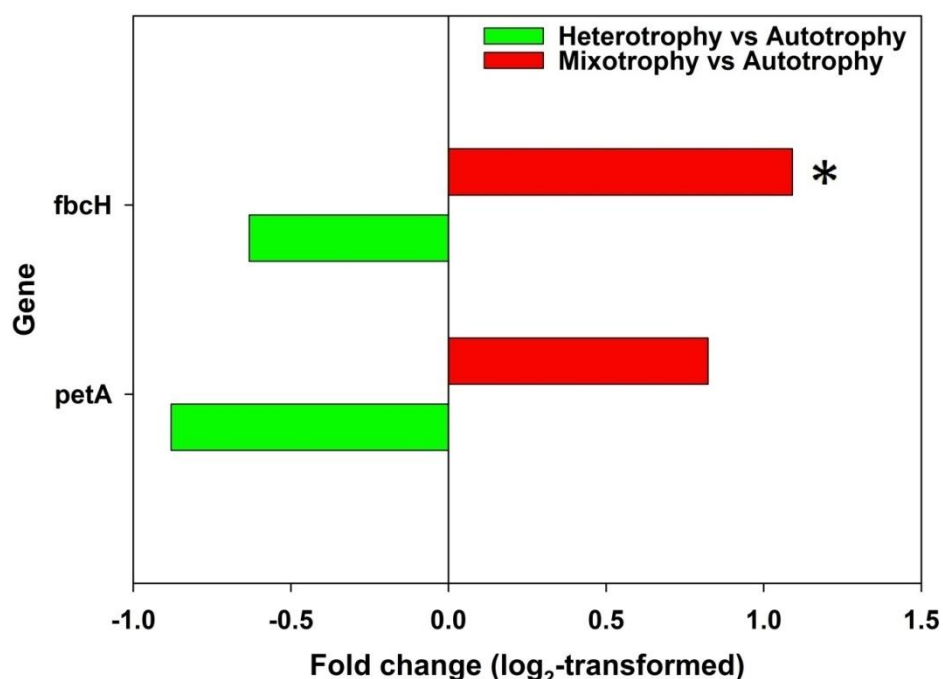


Figure 4-37. Fold change ( $\log_2$ -transformed) of average expression level of genes encoding complex III strain TH-1 under heterotrophy or mixotrophy versus autotrophy condition. The mean fold change is the mean change in level expression of given gene obtained from duplicate experiments. Asterisks indicate the significant difference at  $P$  value  $< 0.05$ .

Table 4-27. Fold change ( $\log_2$ -transformed) in expression of genes encoding complex IV in strain TH-1 under heterotrophy or mixotrophy versus autotrophy condition. The mean fold change is the mean change in level expression of given gene obtained from duplicate experiments (each gene was investigated by 7 independent probes in each experiment).

Protein/Enzyme	contig - KEGG ID	Gene	Heterotrophy vs Autotrophy	Mixotrophy vs Autotrophy
			Fluorescence intensity fold change $\pm$ SD (mean intensity ratio [ $\log_2$ ])	
cytochrome c oxidase cbb3- type subunit I [EC:1.9.3.1]	contig00005 _orf00053 K00404	<i>ccoN</i>	-2.4 $\pm$ 0.3 (-1.2)	1.8 $\pm$ 0.1 (0.8)
cytochrome c oxidase cbb3- type subunit II	contig00005 _orf00051 K00405	<i>ccoO</i>	-1.7 $\pm$ 0.04 (-0.8)	1.8 $\pm$ 0.04 (0.8)
cytochrome c oxidase cbb3- type subunit III	contig00005 _orf00049 K00406	<i>ccoP</i>	-1.4 $\pm$ 0.1 (-0.4)	2.1 $\pm$ 0.1 (1)

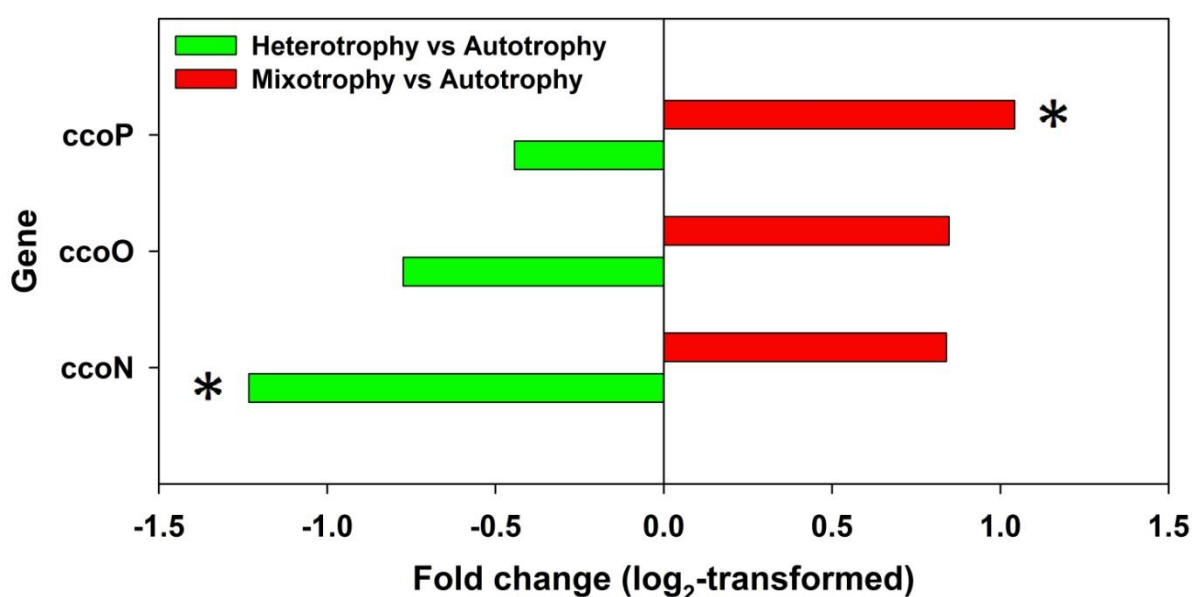


Figure 4-38. Fold change ( $\log_2$ -transformed) of average expression level of genes encoding complex VI strain TH-1 under heterotrophy or mixotrophy versus autotrophy condition. The mean fold change is the mean change in level expression of given gene obtained from duplicate experiments. Asterisks indicate the significant difference at P value < 0.05.

Table 4-28. Fold change ( $\log_2$ -transformed) in expression of genes encoding complex V in strain TH-1 under heterotrophy or mixotrophy versus autotrophy condition. The mean fold change is the mean change in level expression of given gene obtained from duplicate experiments (each gene was investigated by 7 independent probes in each experiment).

Protein/Enzyme	contig - KEGG ID	Gene	Heterotrophy vs Autotrophy	Mixotrophy vs Autotrophy
			Fluorescence intensity fold change $\pm$ SD (mean intensity ratio [ $\log_2$ ])	
polyphosphate kinase [EC:2.7.4.1]	contig00006 _orf00131 K00937	<i>ppk</i>	-1.2 $\pm$ 0.1 (-0.3)	2.3 $\pm$ 0.3 (1.2)
inorganic pyrophosphatase [EC:3.6.1.1]	contig00005 _orf00036 K01507	<i>ppa</i>	1.4 $\pm$ 0.03 (0.5)	1.4 $\pm$ 0.1 (0.4)
F-type H <sup>+</sup> -transporting ATPase subunit alpha [EC:3.6.3.14]	contig00003 _orf00055 K02111	<i>atpA</i>	-1.4 $\pm$ 0.02 (-0.5)	1.7 $\pm$ 0.03 (0.8)
F-type H <sup>+</sup> -transporting ATPase subunit a	contig00003 _orf00063 K02108	<i>atpB</i>	-1.3 $\pm$ 0.02 (-0.4)	2.1 $\pm$ 0.1 (1.1)
F-type H <sup>+</sup> -transporting ATPase subunit epsilon	contig00003 _orf00050 K02114	<i>atpC</i>	1.1 $\pm$ 0.02 (0.1)	1.5 $\pm$ 0.03 (0.6)
F-type H <sup>+</sup> -transporting ATPase subunit beta [EC:3.6.3.14]	contig00003 _orf00051 K02112	<i>atpD</i>	1.1 $\pm$ 0.1 (0.1)	2.0 $\pm$ 0.1 (1.0)
F-type H <sup>+</sup> -transporting ATPase subunit c	contig00003 _orf00061 K02110	<i>atpE</i>	-1.9 $\pm$ 0.1 (-0.9)	1.6 $\pm$ 0.02 (0.7)
F-type H <sup>+</sup> -transporting ATPase subunit b	contig00003 _orf00059 K02109	<i>atpF</i>	-1.6 $\pm$ 0.03 (-0.7)	1.9 $\pm$ 0.1 (0.9)
F-type H <sup>+</sup> -transporting ATPase subunit gamma	contig00003 _orf00053 K02115	<i>atpG</i>	1.1 $\pm$ 0.1 (0.1)	2.6 $\pm$ 0.3 (1.4)
F-type H <sup>+</sup> -transporting ATPase subunit delta	contig00003 _orf00057 K02113	<i>atpH</i>	-1.4 $\pm$ 0.02 (-0.4)	2.0 $\pm$ 0.1 (1.0)

In general, all complex of oxidative phosphorylation machinery were down-regulated under heterotrophic condition, compared to those under autotrophic condition, except for complex II, which is a component of TCA cycle. In contrast, under mixotrophic condition, all complex of oxidative phosphorylation machinery were significantly up-regulated, compared to those under autotrophic condition. This fact implies that mixotrophically growth is the combination of autotrophic growth and heterotrophic growth.

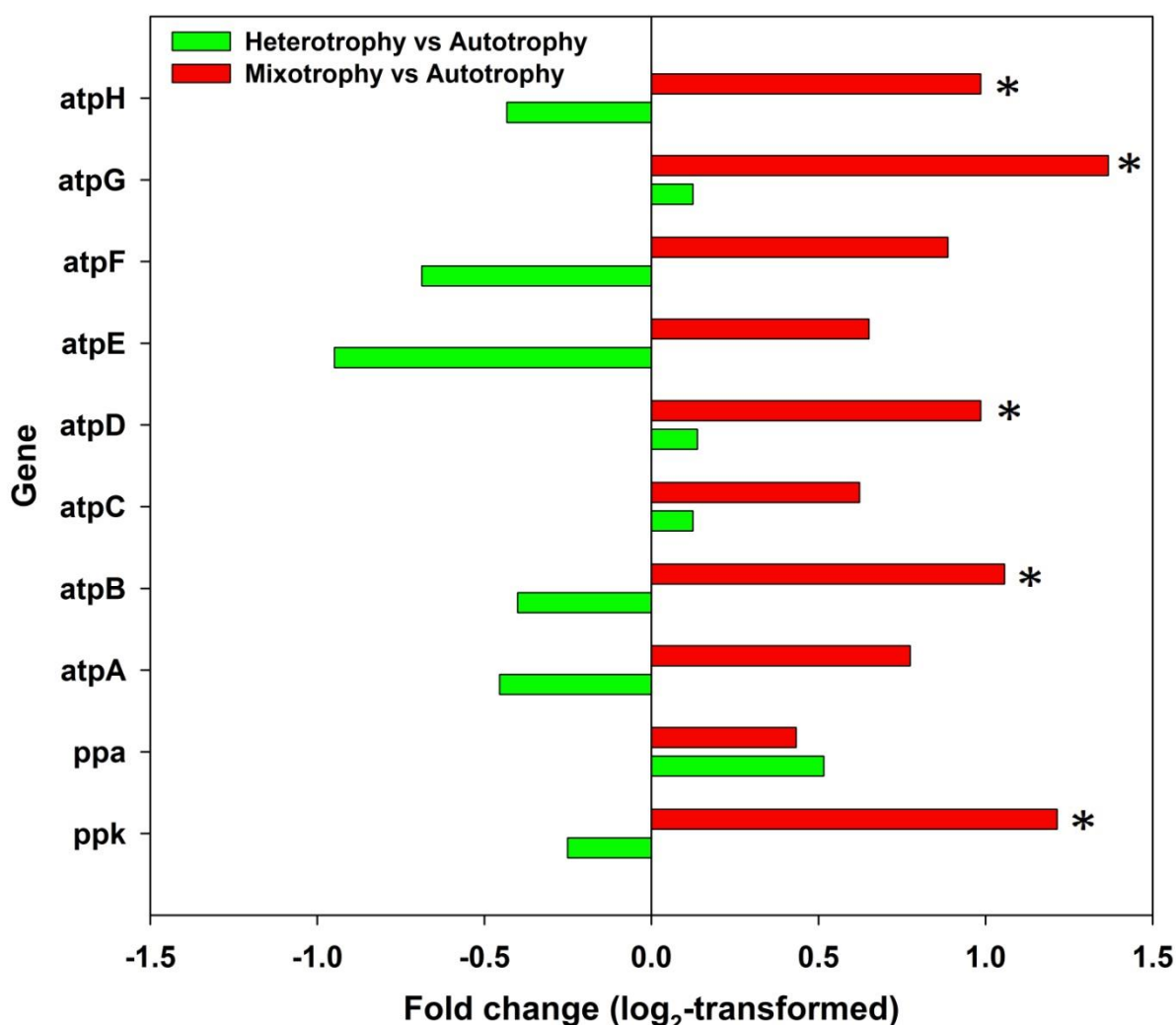


Figure 4-39. Fold change ( $\log_2$ -transformed) of average expression level of genes encoding complex V in strain TH-1 under heterotrophy or mixotrophy versus autotrophy condition. The mean fold change is the mean change in level expression of given gene obtained from duplicate experiments. Asterisks indicate the significant difference at  $P$  value  $< 0.05$ .

#### 4.3.3. Metabolome analysis

The metabolome analysis by CE-TOFMS was performed for 6 samples. From value of  $m/z$  of metabolite alignment with HMT metabolite library and Known-unknown library and the MT, 178 peaks were annotated: 89 cation peaks, 89 anion peaks (Appendix. Table 4-29). The result of the principle component analysis of 6 samples is shown in figure 4-40. In addition, a hierarchical clustering Heatmap is shown in figure 4-41.

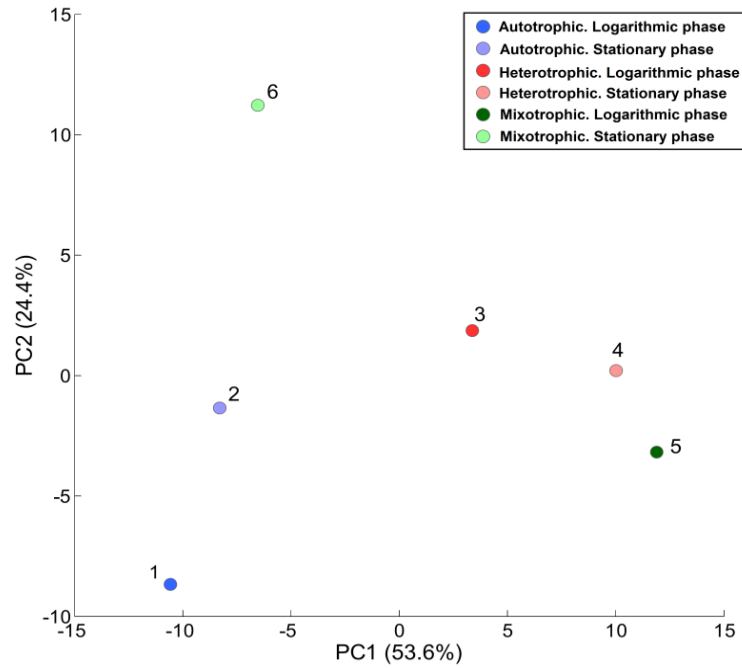


Figure 4-40. The principle component analysis map of 6 samples: Color represent for the sample; blue: autotrophic. logarithmic phase; light blue: autotrophic. stationary phase; red: heterotrophic. logarithmic phase; light red: heterotrophic. stationary phase; green: mixotrophic. logarithmic phase; light green: mixotrophic. stationary phase

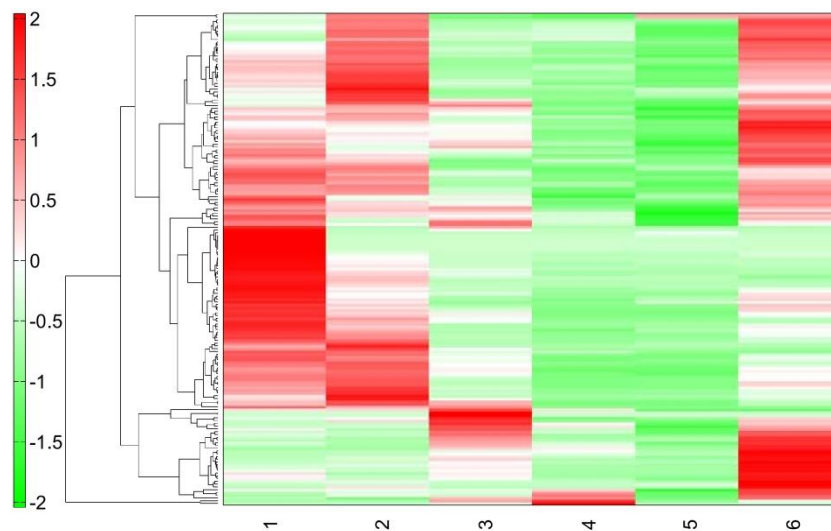


Figure 4-41. Hierarchical clustering and heatmap of 6 samples: 1: autotrophic. logarithmic phase; 2: autotrophic. stationary phase; 3: heterotrophic. logarithmic phase; 4: heterotrophic. stationary phase; 5: mixotrophic. logarithmic phase; 6: mixotrophic. stationary phase

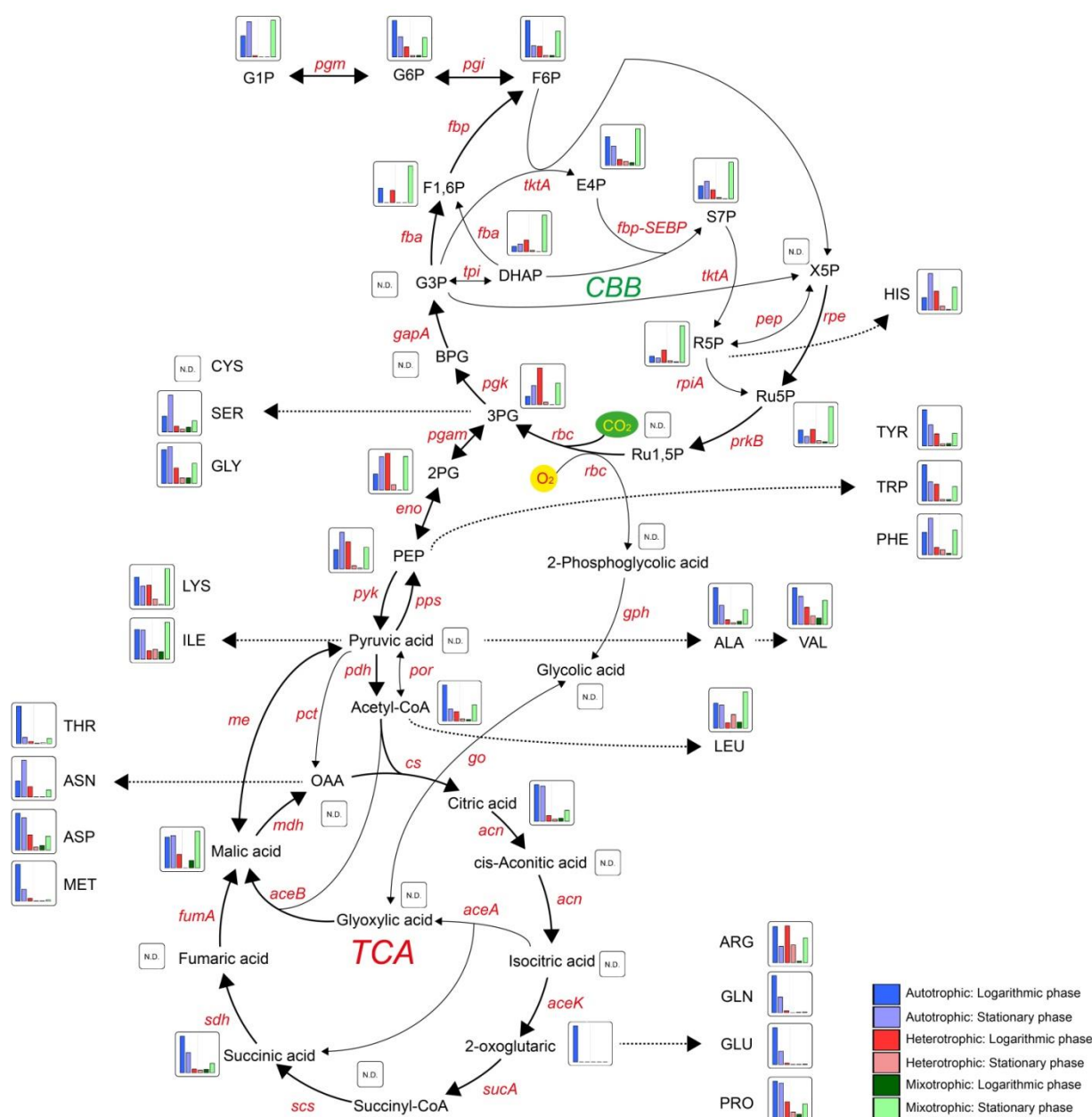


Figure 4-42. Central metabolic material pathway in strain TH-1: Glycolysis/Gluconeogenesis, CBB, TCA cycle. The metabolic map was drawn based on the alignment of detected peak with HTM material library. Blue: autotrophic, logarithmic phase; light blue: autotrophic, stationary phase; red: heterotrophic, logarithmic phase; light red: heterotrophic, stationary phase; green: mixotrophic, logarithmic phase; light green: mixotrophic, stationary phase. N.D: Not Detected.

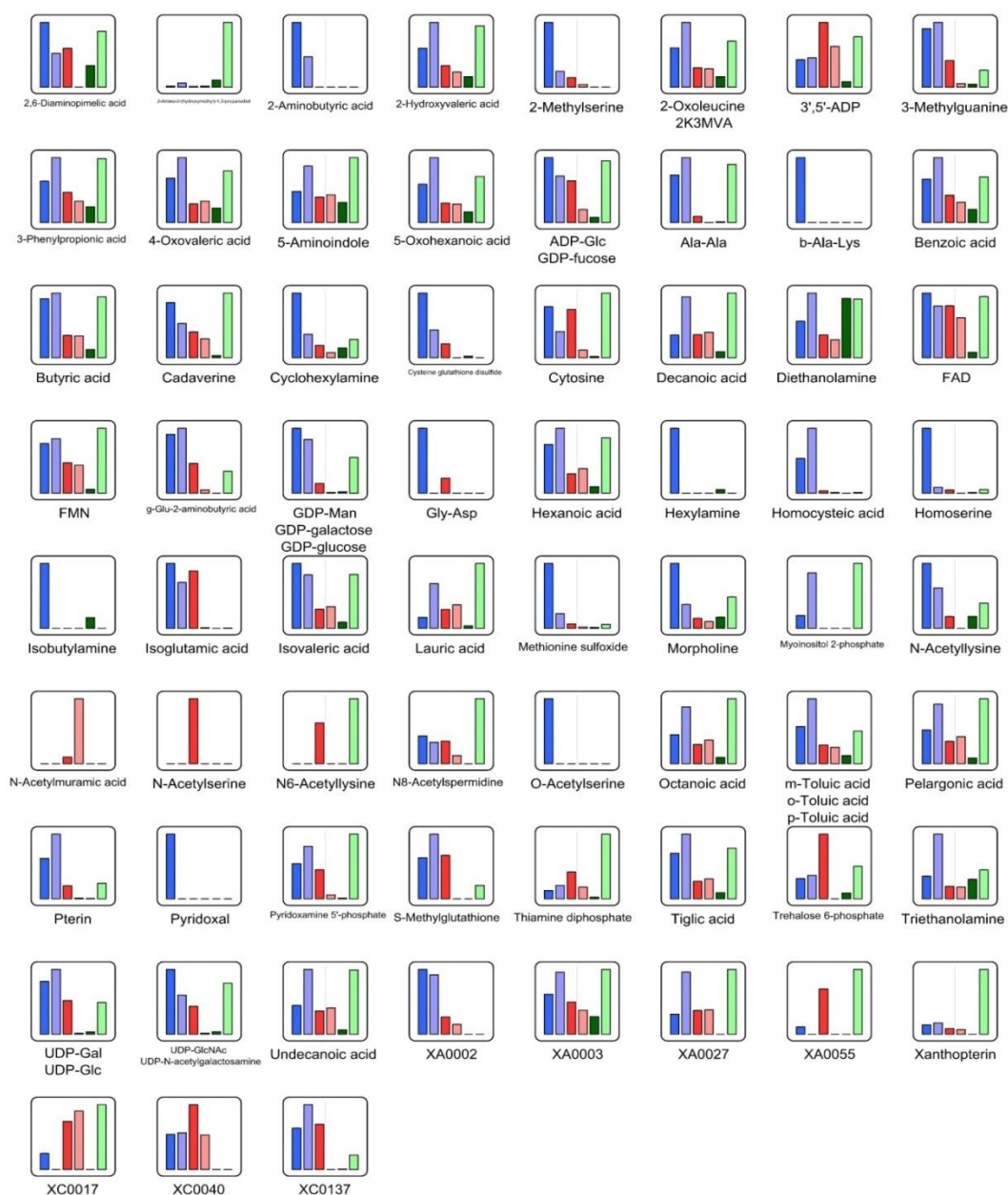


Figure 4-43. Concentration of other metabolites from samples collected at different phases of growth with different kind of substrates. Blue: autotrophic. logarithmic phase; light blue: autotrophic. stationary phase; red: heterotrophic. logarithmic phase; light red: heterotrophic. stationary phase; green: mixotrophic. logarithmic phase; light green: mixotrophic. stationary phase.

In addition, many metabolites were detected from samples of cells TH-1 under autotrophic, mixotrophic and heterotrophic conditions (Figure 4-43).

These compound candidates were drawn in glycolysis pathway/gluconeogenesis pathway, CBB cycle, TCA cycle and various amino acid concentrations in figure 4-42. The concentration and name of abbreviation can be seen in Appendix.

Metabolome analysis under autotrophic condition or mixotrophic condition showed that, the fold change of most metabolites that are involved in glycolysis/gluconeogenesis pathway, TCA cycle, CBB cycle, are significantly higher than those under heterotrophic condition, for example G1P (14-fold), G6P (3.6-fold), F6P (3.4-fold), F1,6BP (1.2-fold), E4P (4.9-fold) , S7P (1.4-fold), succinic acid (10-fold), citric acid (6.4-fold), malic acid (2.3-fold).

The most significant differences, was seen for middle segment of glycolysis/gluconeogenesis pathway, as the relative concentration of metabolites, triose phosphates, drastically increased under heterotrophic condition in logarithmic phase with butyrate compared to those under autotrophic condition in logarithmic phase: DHAP (2.2-fold), 3PGA (4.4-fold), 2PGA (2.3-fold), PEP (1.4-fold). This implies that the gluconeogenesis was up-regulated under heterotrophic condition to produce the precursors for biosynthesis.

#### 4.4. Conclusions

In this chapter, based on the analysis of the microarray profile for central carbon metabolic pathway of facultative chemolithoautotrophic hydrogen-oxidizing bacterium *H. thermoluteolus* TH-1 under autotrophic, heterotrophic and mixotrophic conditions, I revealed the central metabolic pathway of strain TH-1 as shown in figure 4-42. It also showed the role of each metabolic pathway via analysis of the expression levels of genes that belong to them. I revealed the important function of CBB cycle in carbon fixation under autotrophic and mixotrophic condition. Via observation of the constitutive expression of all genes belong to respiratory machinery; I revealed the important role of TCA cycle and respiratory chain responsible for ATP production. The evidence from the expression levels of genes belonging to glycolysis/gluconeogenesis pathway as well as the evidences from metabolome profile suggested the role of glycolysis/gluconeogenesis.

By this research, knowledge about the roles of photorespiration pathway and glyoxylate cycle is expanded. In bacteria, photorespiration does not reduce the efficiency of the carbon fixation process, but it produces glycolate, glyoxylate, and hydrogen peroxide that could become inhibitory factors to the growth of bacteria. Glyoxylate pathway is not a simple anaplerotic pathway that is required for acetate and butyrate consumption, but it participates in a detoxification system to reduce the toxicity caused by photorespiration. Moreover, the high expression level of *cpx* gene coding for cytochrom *c* peroxidase under mixotrophic condition, suggested that cytochrom *c* peroxidase was assumed to be a detoxification system for  $H_2O_2$ .

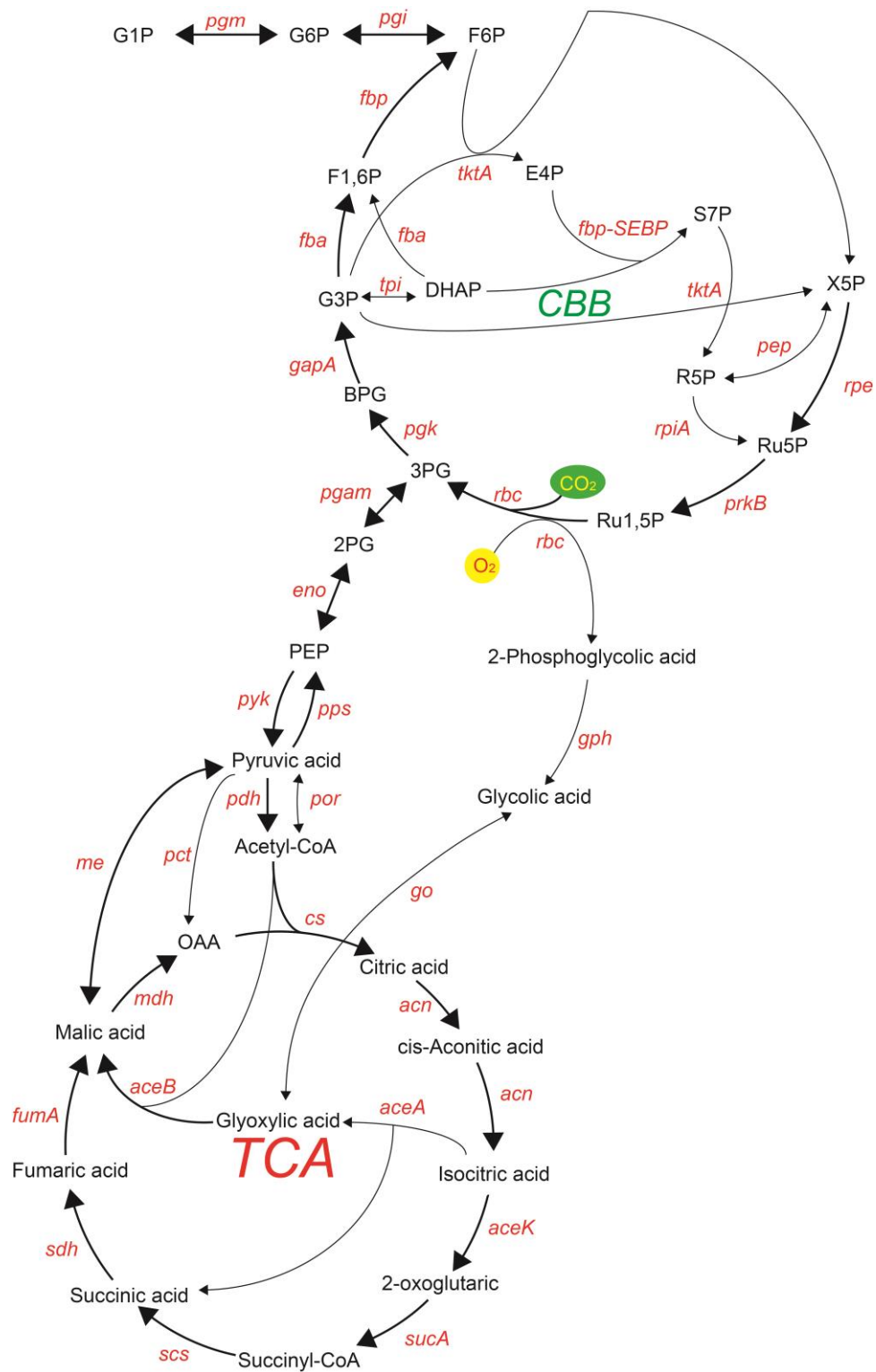


Figure 4-44. Proposed central metabolic pathway of butyrate metabolism in *H. thermoluteolus* TH-1 under autotrophic, heterotrophic or mixotrophic condition with butyrate.

Strain TH-1 was isolated from a soil around hot-spring, a harsh ecology since it has to compete hydrogen gas with other hydrogen-oxidizing bacteria.

Furthermore, strain TH-1 is a unique thermophilic aerobic bacterium that carries CBB cycle at 50°C - 55°C under oxygen atmosphere 10%. RubisCO, the key enzyme of CBB cycle, can utilize both carbon dioxide ( $\text{O}=\text{C}=\text{O}$ ) and oxygen ( $\text{O}=\text{O}$ ) because of the similarity of structure. In addition, under high temperature condition, the evaporation rate of  $\text{CO}_2$  from medium increases. So under autotrophic culture, with gas component of  $\text{H}_2:\text{O}_2:\text{CO}_2$  (75%: 10%: 15%), photorespiration will be enhanced. As a result, the toxic compound such as glycolate may accumulate at high concentration [62]. This compound inhibits the growth of strain TH-1. Glycolate inhibits RubisCO, which results in reduced incorporation of  $\text{CO}_2$  into the intermediates of CBB cycle [62, 63].

However, it is very interesting that under autotrophic growth condition strain TH-1 showed the highest specific growth rate,  $0.68\text{ h}^{-1}$ . Thus, for dealing with trouble about toxic compound from photorespiration, the operation of glyoxylate cycles is a good strategy for this bacterium in metabolizing the toxic compounds from photorespiration. In this point, glyoxylate cycle is functioning as the detoxification system under autotrophic or mixotrophic condition.

When strain TH-1 grows autotrophically, heterotrophically or mixotrophically, many metabolites were found in metabolomics analysis profile. Especially many derivatives of amino acid or organic acids were detected, such as 2-methylserine, 2-aminobutyric acid, homocysteic acid, isoglutamic acid or benzoic acid, hexanoic acid, octanoic acids (figure 4-43). In this point of view, it has high potential for intermediates producer.

## Chapter 5. The production of poly-3-hydroxybutyrate in *Hydrogenophilus thermoluteolus* TH-1 under autotrophic and heterotrophic conditions

### 5.1. Introduction

The trend of the material science of last century was to invent and develop new synthetic plastic such as nylon, rubber, plastic, and fiberglass for daily demand and convenience [64]. However, they are non-biodegradable and the garbage continues to accumulate. Increasing consumption together with the increasing human population is making a serious problem about the environmental pollution [65]. Nowadays, to face with this situation, one of the most important concerns of scientist is to develop a new synthetic material which can be degraded biologically. Poly- $\beta$ -hydroxybutyrate (PHB) is one of those types of biocompatible and biodegradable plastic belonging to the group of endocellular poly-hydroxyalkanoates (PHAs). PHB has high potential for application in agriculture, industry, medicine, and other fields [66-68]. In medical application, PHB was used for making surgical meshes, screws, plates for bone fixation, and wound dressing, etc. (Fig.5-1).

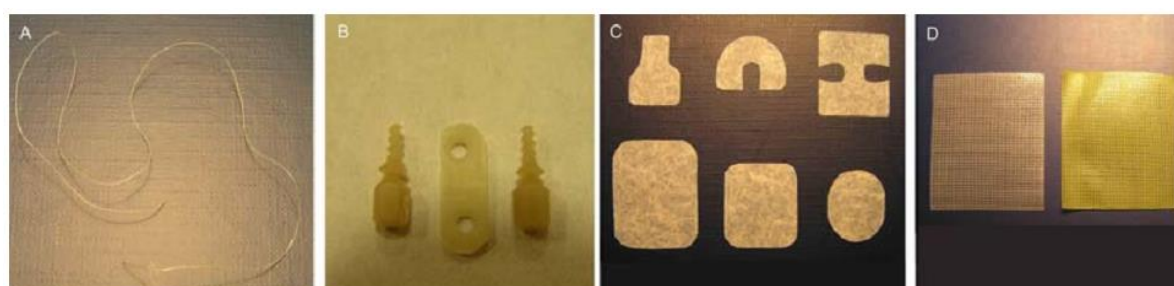


Figure 5-1. Medical devices based on of PHB. (A) bioresorbable surgical suture; (B) biodegradable screws and plate for cartilage and bone fixation; (C) biodegradable membranes for periodontal treatment; (D) surgical meshes with PHB coating for hernioplastic surgery (left) and loaded with antiplatelet drug, dipyridamole (right) [68].

Medical application is a new and promising approach. Especially, the more promising trend in application of PHB is to develop the therapeutic system of sustained drug

delivery such as microsphere and microcapsule from PHB. If this perspective comes true, it introduces a cheap medical treatment for patients. Moreover, this solution also supplies an abundant biopolymer source; those qualities can be controlled by manipulation of culture condition of microorganisms. Literature reported that up to 60 different monomer compounds could be incorporated to PHA, leading to the new materials with new characteristics [68].

PHA is classified into three types. The first type of PHA is the short chain length PHAs (scl-PHA that contains up to C<sub>5</sub> monomers). This kind of PHA is estimated to have high value for application since its structure is very close to the conventional plastic. The second type of PHA is the medium chain length (mcl-PHA) with monomer containing from C<sub>6</sub>–C<sub>14</sub>, and the last type of PHA is the long chain length (lcl-PHA) PHAs with the monomer containing more than C<sub>14</sub>. Moreover, PHA synthase, the key enzyme of PHA production process, is also divided into four classes: I, II, III, and IV based on their *in vivo* substrate specificities and the structure of PHB that is produced by them [10, 69]. Class I and class II are the PHA synthases with only one polypeptide chain, whereas class III and class IV synthases have two subunits. Class I PHA synthase, from *Burkholderia* sp., *Cupriavidus necator*, and *Ralstonia eutropha* produce scl-PHA [70]. Most PHA synthases of genus *Pseudomonas* such as *Pseudomonas aeruginosa*, *Pseudomonas putida*, *Pseudomonas fluorescens* are found to belong to class II. Although class II has one chain polypeptide, the major product of class II is mcl-PHA. Class III of PHA synthase is composed of two subunits. It also produces scl-PHA similar to class I. Sometimes, class III PHA synthase produces mcl-PHA [10]. Class III is represented by PHA synthase of *Xanthomonas* sp. such as *Xanthomonas campestris* and *Xanthomonas oryzae*. Recently, class IV was discovered and their product is the short chain length type (R)-3-hydroxyacyl-CoA [69].

PHB is a carbon storage material which is produced by various microorganisms. Since PHB was first detected in *Bacillus megaterium* and reported by Lemoigne in 1926, the number of microorganisms which can produce PHB is increasing. Now, more than 90 genera of Archaea and Bacteria (gram + and gram -) have been reported to have the ability to produce PHB [64]. PHB is produced by many microorganisms as they enter

stationary phase of growth under nitrogen, phosphate limitation, or pH stress and excess carbon source. Until now, most reports about PHB production were conducted under heterotrophic condition because PHB productions from autotrophs are rather rare due to many features associated with autotrophic cultures for example biomass accumulations, are quite slow [5].

*H. thermoluteolus* TH-1<sup>T</sup> (=IFO14978T) is a chemolithoautotrophic, gram-negative, non spore-forming, thermophilic hydrogen-oxidizing microorganism. It was isolated from a hot spring in Izu district, Japan. The optimum temperature and pH for growth are 50°C and 7.0, respectively [71]. The maximum specific growth rate ( $\mu_{\max}$ ) of strain TH-1 under optimal condition was determined as  $0.68\ h^{-1}$ , which is the highest among autotrophs. High specific growth rate is a desirable feature for using in biotechnological applications [72]. Under autotrophic continuous culture condition, cell productivity of strain TH-1 was  $3.0\ g\ l^{-1}h^{-1}$ , but in case of *Ralstonia eutropha*, a famous PHB production bacteria, was only  $0.4\ g\ l^{-1}h^{-1}$  under similar condition [5]. TH-1 showed the ability to fix CO<sub>2</sub> under high temperature with good growth rate. It also utilizes many kinds of carbon substrates. Therefore, it could become an advantageous platform for biotechnological application [3]. Furthermore, the PHB accumulation from moderate thermophiles has not been studied in detail. Hence, investigation of PHB accumulation in thermophilic microorganism is an interesting approach.

By genome analysis, I have found that three copies of PHA synthase genes, the key enzyme of PHB biosynthesis, existed in strain TH-1 genome (Fig.5-2). Hence, TH-1 can become a new and effective platform for PHB production.



Figure 5-2. Locus *phbC<sub>1</sub>B<sub>1</sub>B<sub>2</sub>P<sub>1</sub>A<sub>1</sub>C<sub>2</sub>P<sub>2</sub>C<sub>3</sub>A<sub>2</sub>A<sub>3</sub>A<sub>4</sub>* with three copies of *phbC* genes (*C<sub>1</sub>*, *C<sub>2</sub>*, and *C<sub>3</sub>*), two copies of *phbB* gene, and four copies of *phbA* gene (*A<sub>1</sub>*, *A<sub>2</sub>*, *A<sub>3</sub>*, *A<sub>4</sub>*) in *H. thermoluteolus* TH-1.

The biosynthesis of PHB is simple. This process involves three enzymes *phbA* gene encodes acetyl-CoA acetyltransferase, the first enzyme for condensation of two

acetyl-CoA molecules to form acetoacetyl-CoA. The reduction of acetoacetyl-CoA to R-3-hydroxybutyryl-CoA is carried-out by an NADPH-dependent acetoacetyl- CoA reductase (*phbB*). Lastly, the polymerization of R-3-hydroxybutyryl-CoA monomer is catalyzed by PHA synthase which is encoded by the *phbC* gene [73].

*H. thermoluteolus* TH-1 contains three genes that involve PHB production pathway: *phbA*, *phbB* and *phbC*. Those genes are not organized in an operon: four copies of gene acetyl-CoA acetyltransferase (*contig00015\_orf00048*, *contig00019\_orf00056*), two copies of acetoacetyl-CoA reductase gene (*contig00001\_orf00065*, *contig00001\_orf00066*), and three copies of poly-3-hydroxybutyrate synthase (*contig00001\_orf00064*, *contig00005\_orf00043*, *contig00008\_orf00031*). The location of two copies of *phbB* gene (*contig00001\_orf00065*, *contig00001\_orf00066*) is adjacent to one *phaC* gene (*contig00001\_orf00064*) implying that these genes are regulated together.

The phasin protein family is an important factor that is used for the formation of PHA granules. They play a role as structural proteins by non-covalently attached to the polyester core of the granules. Strain TH-1 genome contains 2 copies of phasin (*contig00001\_orf00137*, *contig00005\_orf00112*) which support PHB assemble. The literature emphasized that the number of copy of phasin gene effect PHA granules size [10].

So, I investigated the localization of PHB granules in strain TH-1 at the early step of induction by TEM analysis. In this chapter, two phase of culture was investigated under autotrophic and heterotrophic conditions to produce PHB (Fig. 5-3).

## **5.2. Materials and methods**

### **5.2.1. Bacterial strains and growth condition**

*H. thermoluteolus*, gram-negative, non spore-forming, thermophilic hydrogen-oxidizing microorganism, was isolated from a hot spring in Izu district, Japan.

#### **5.2.1.1. Autotrophic cultivation**

The medium employed for *H. thermoluteolus* growth consisted of  $(\text{NH}_4)_2\text{SO}_4$  3.0 gL<sup>-1</sup>,  $\text{KH}_2\text{PO}_4$  1.0 gL<sup>-1</sup>,  $\text{K}_2\text{HPO}_4$  2.0 gL<sup>-1</sup>, NaCl 0.25 gL<sup>-1</sup>,  $\text{FeSO}_4 \cdot 7\text{H}_2\text{O}$  0.0014 gL<sup>-1</sup>, and trace element solution (pH 7.0). In the vial (100 ml), 10 ml of the mineral salts

medium was inoculated and incubated with the cell at 50°C under H<sub>2</sub>-O<sub>2</sub>-CO<sub>2</sub> mixture (75:10:15).

#### 5.2.1.2. Heterotrophic cultivation

Growth experiment under heterotrophic condition was performed in air atmosphere using the medium similar to the autotrophic condition with the addition of only one organic acid as a substrate. The organic acid was malate (C<sub>4</sub>). The carbon concentration was 60 mM. Strain TH-1 was inoculated and shaken on a reciprocating shaker at 50°C under the air atmosphere.

Growth experiments for strain TH-1 were carried-out under autotrophic or heterotrophic conditions; the initial optical density at wavelength 540 nm was 0.04-0.06.

#### 5.2.2. Induction of PHB formation

After 9 hours of pre-culture grown autotrophically, it was transferred (1%) to fresh mineral salts medium without malate for autotrophic culture and with malate (15 mM) for heterotrophic culture and was shaken at 50°C. The initial pH was controlled at pH 7.0. The vial was incubated until the bacterium entered a stationary phase. After 12 hours of autotrophic growth or 9 hours of heterotrophic growth (OD<sub>540</sub> ~ 2.0), the bacteria were harvested by centrifugation at 40,000 xg for 2 minutes at 4°C, and subsequently the cells were transferred to an induction culture. The induction condition contained the components similar to autotrophic medium or malate medium but without (NH<sub>4</sub>)<sub>2</sub>SO<sub>4</sub>.

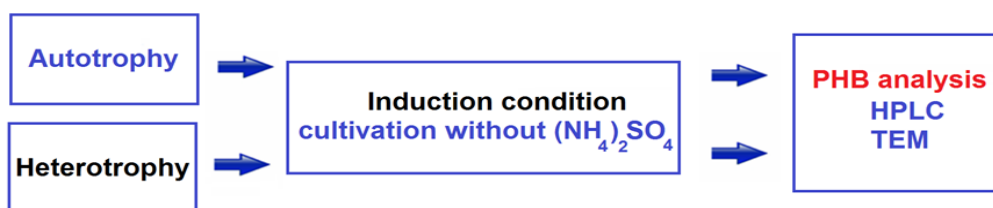


Figure 5-3. Two phase PHB accumulation systems. For the experiment to clarify whether accumulated PHB can be re-consumed in proper condition, the bacteria that cultured in induction medium for 180 minutes was harvested, subsequently transferred to a normal medium that lacks carbon source.

The cells were harvested, and PHB was analyzed by using Transmission Electron Microscope and High Performance Liquid Chromatography. The preferred method for PHB quantification was based on HPLC. PHB was hydrolyzed to crotonic acid monomers by acid treatment. The absorbance at 210 nm was used for the detection.

#### 5.2.3. High Performance Liquid Chromatography (HPLC) analysis

The PHB content of the biomass was determined by acid hydrolysis of PHB to crotonic acid. Culture sample of *H. thermoluteolus* TH-1 was centrifuged for 5 minutes at 10,000 x g. The pellet was re-suspended in 1 mL of distilled water and transferred to pre-weighed Eppendorf tubes. The sample was centrifuged for 5 minutes at 12,000 x g, dried over night at 100°C, and weighed again for the determination of total biomass. Dried pellet was digested with 1 mL of 96% H<sub>2</sub>SO<sub>4</sub> at 100°C for 60 minutes to form crotonic acid. After the reaction mixture was cooled to room temperature, the sample was 10-fold diluted with distilled water, and crotonic acid was analyzed by HPLC system from Waters Company, model Waters 2695 Separation. The solvent used was 0.75 mM H<sub>2</sub>SO<sub>4</sub>, at a flow rate of 0.6 mL/minute. The elution peaks were monitored at 210 nm. Crotonic acid content was calculated from a calibration curve for standards of commercial PHB [74].

#### 5.2.4. Fluorescence microscope

The presence of cytoplasmic PHB granules was monitored by using fluorescence dye Nile red staining and by observing the cells under the fluorescent microscope type Zeiss. Cells were harvested by centrifugation at 4000 x g for 2 minutes and treated with 200 nM Nile-Red, incubated at room temperature for 10 minutes. The observation was made by using a Zeiss Axio Imager M1 wide-field with fluorescence microscope fitted with a x100/1.4 NA oil-immersion Plan-Apochromat objective lens, fluorescence intensity at Ex/Em = 546/590 nm [75]. Images were processed by AxioVision software.

#### 5.2.5. Transmission Electron Microscope (TEM)

Sample was taken, cooled down on ice, and centrifuged at 4,000 x g for 2 minutes. The pellet was re-suspended in phosphate buffer saline (PSB, pH 7.0, NaCl 0.01%) and then chemically fixed overnight at 4°C in PSB containing 0.2% (wt/vol)

formaldehyde, and 0.3% (vol/vol) glutaraldehyde. Samples were washed and embedded in Lowicry K4M resin. Resin section in about 80 nm in thickness was trimmed and cut with a diamond knife. The sections were double stained with 4 % Uranyl acetate for 30 minutes, and washed by distilled water. The sections were stained with lead citrate for 3 minutes, washed by distilled water, and dried. Samples were observed with a JEM-2000X transmission electron microscopic (JEOL, Tokyo, Japan), and the images were analyzed by ImageJ v.1.48 software (National Institute of Health, Bethesda [<http://imagej.nih.gov/ij/>]).

#### 5.2.6. Phylogenetic analysis

Three PHA synthase genes of strain TH-1 were aligned with 141 sequences of PHA synthase from NCBI (<http://www.ncbi.nlm.nih.gov/>). Alignment was conducted by clustalW Multiple Sequence Alignment program. Phylogenetic tree was constructed and drawn by using Neighbour Joining method and MEGA 6 program (<http://www.megasoftware.net/mega.php>).

### 5.3. Results and discussions

#### 5.3.1. Phylogenetic analysis

In an effort to analyze the relationship between TH-1 PHA synthases and the PHA synthases from other microorganisms, the multiple alignments of PHA synthases are performed. As described before, PHA synthases are divided into four classes: I, II, III, and IV. The candidate sequences which represent each class of PHA synthase were chosen for alignment and a phylogenetic tree was drawn.

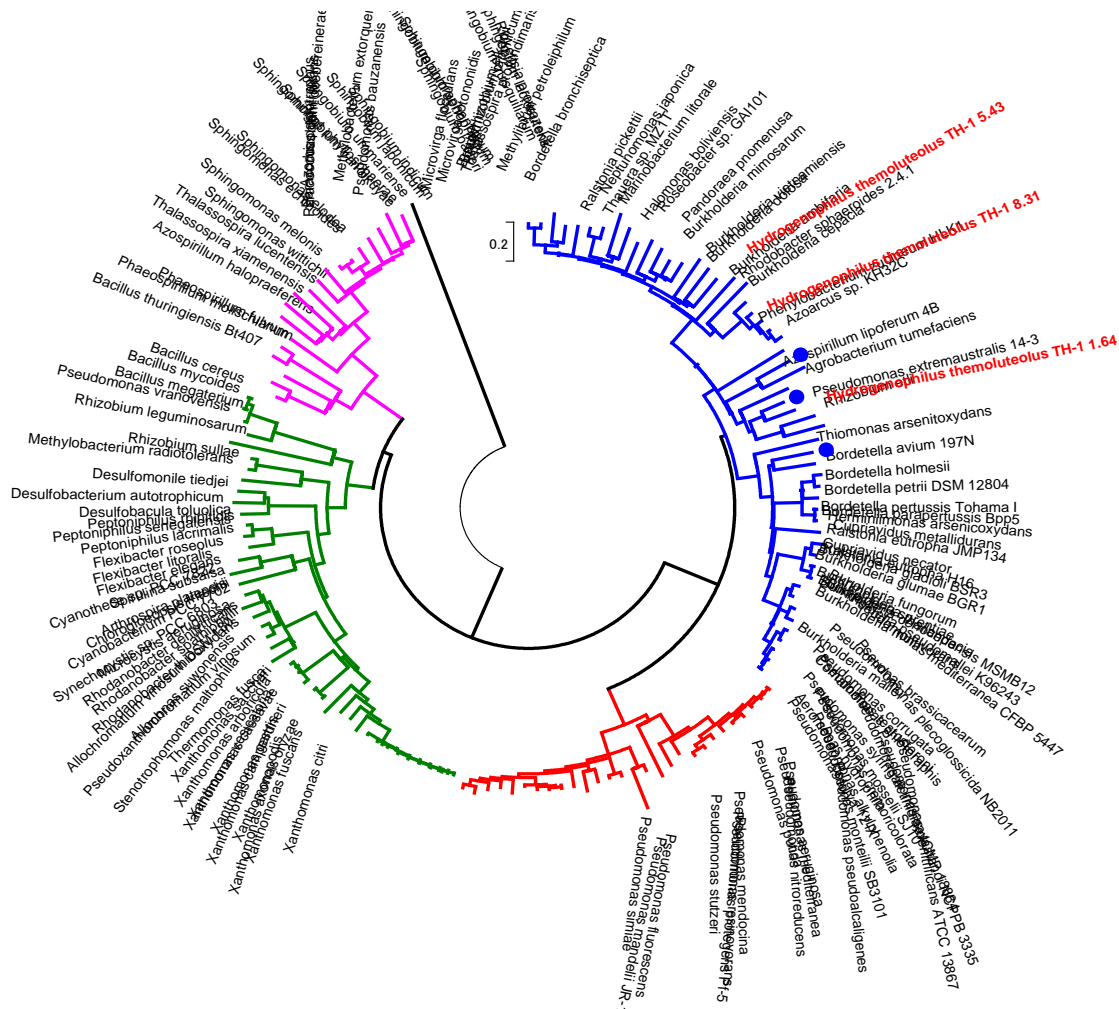


Figure 5-4. Phylogenetic tree of PHA synthase sequences of genes *H. thermoluteolus* and their related sequences from NCBI. Sequences were separated into four classes for tree construction. Class I (Blue branch), Class II (Red branch), class III (Green branch), class IV (Pink branch). The scale bar represents 2 amino acid differences per 10 amino acids.

Via alignment with 141 PHA synthases, three strain TH-1 PHA synthases were found to belong to class I PHA synthase. Class I PHA synthase is the class that preferably makes slc-PHB. Three copies of strain TH-1 PHA synthases located in class I, together with other famous PHB-producing bacteria as *Rastonia eutropha*, *Rhodobacter sphaeroides*.

To understand more about the structure of three strain TH-1 *phbC* genes, I conducted the multiple alignments of the partial deduced amino sequences of three copies of *phbC* gene from *H. thermoluteolus* TH-1 with corresponding *phbC* sequence from *Rhodobacter sphaeroides* 2.4.1, *Ralstonia eutropha*, and *Cupriavidus necator*. The results are shown in figure 5-5. Following literature reports, 5 amino acid residues are involved in enzymatic activity [69]. Beside 3 essential a.a residues cysteins 319, aspartate 480 and histidine 508, no PHA synthase activity were observed if PHA synthase sequence lacks serine 260 and serine 546 [69, 76]. These amino acids are conserved in all class I PHA synthase, in which the C319 is involved in catalysis with covalent bound formation. These amino acid residues in strain TH-1 PHA synthases are conserved (Fig.5-6).



Figure 5-5. Multiple alignment of the partial deduced amino acid sequences of three copies of *phbC* gene from *H. thermoluteolus* TH-1 (contig00001\_orf00064, contig00005\_orf00043 contig00008\_orf00031) with corresponding *phbC* sequence from *Rhodobacter sphaeroides* 2.4.1 (Genbank accession no. YP\_353458.1), *Ralstonia*

*eutropha* (Genbank accession no.P23608.1), *Cupriavidus necator* (Genbank accession no.WP\_011615085.1).

All gene information supported the idea that strain TH-1 could be a new platform for PHB production.

In chapter 2, part 2.3.1, I mentioned strain TH-1 gave a maximum specific growth rate  $0.60\ h^{-1}$  under autotrophic condition at  $50^{\circ}\text{C}$ . Under heterotrophic conditions, growth was observed on acetate, pyruvate, butyrate, and malate (Fig. 2-7). The highest growth rate  $0.73\ h^{-1}$  was recorded when the bacterium grew on malate. Therefore, malate was chosen as a substrate for the PHB accumulation experiment under heterotrophic condition.

#### 5.3.2. PHB production by two-step batch cultivation

To investigate the ability of PHB accumulation and the role of carbon source effect to the PHB formation, the cells were cultured in two stages of incubation (Fig.5-3).At the first stage, strain TH-1 was grown under autotrophic condition with gas component of  $\text{H}_2\text{-O}_2\text{-CO}_2$  (75:10:15) or under heterotrophic condition with malate until the optical density of culture medium reaches 1.8 - 2. In the first stage, PHB was not accumulated within the cells. Then, the cells were transferred into an induction medium which was depleted with nitrogen. The cells were incubated at  $50^{\circ}\text{C}$  at pH 7.0 to induce PHB production. As a negative control, the cells were incubated under sufficient nutrition condition.

By using Nile-Red for staining PHB, the PHB was observed under excitation wavelength for Nile-Red. When Nile-Red was attached to PHB, Nile-Red will produce a strong orange fluorescence with an excitation wavelength of 543 nm [75]. Nile-Red staining could be used as a fast and semi-qualitative method for evaluation of the PHB amount with in strain TH-1. Figure 5-6 shows the PHB appearing in orange color under excitation 546-590 nm.

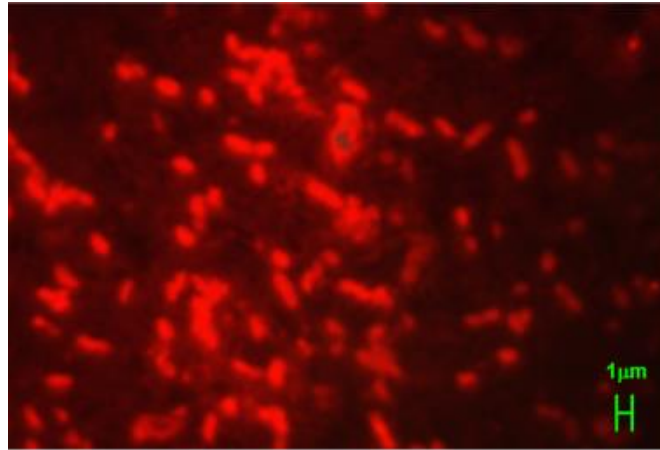


Figure 5-6. TH-1 after 6-h heterotrophic induction stained with Nile Red under excitation 546-590 nm (x1000).

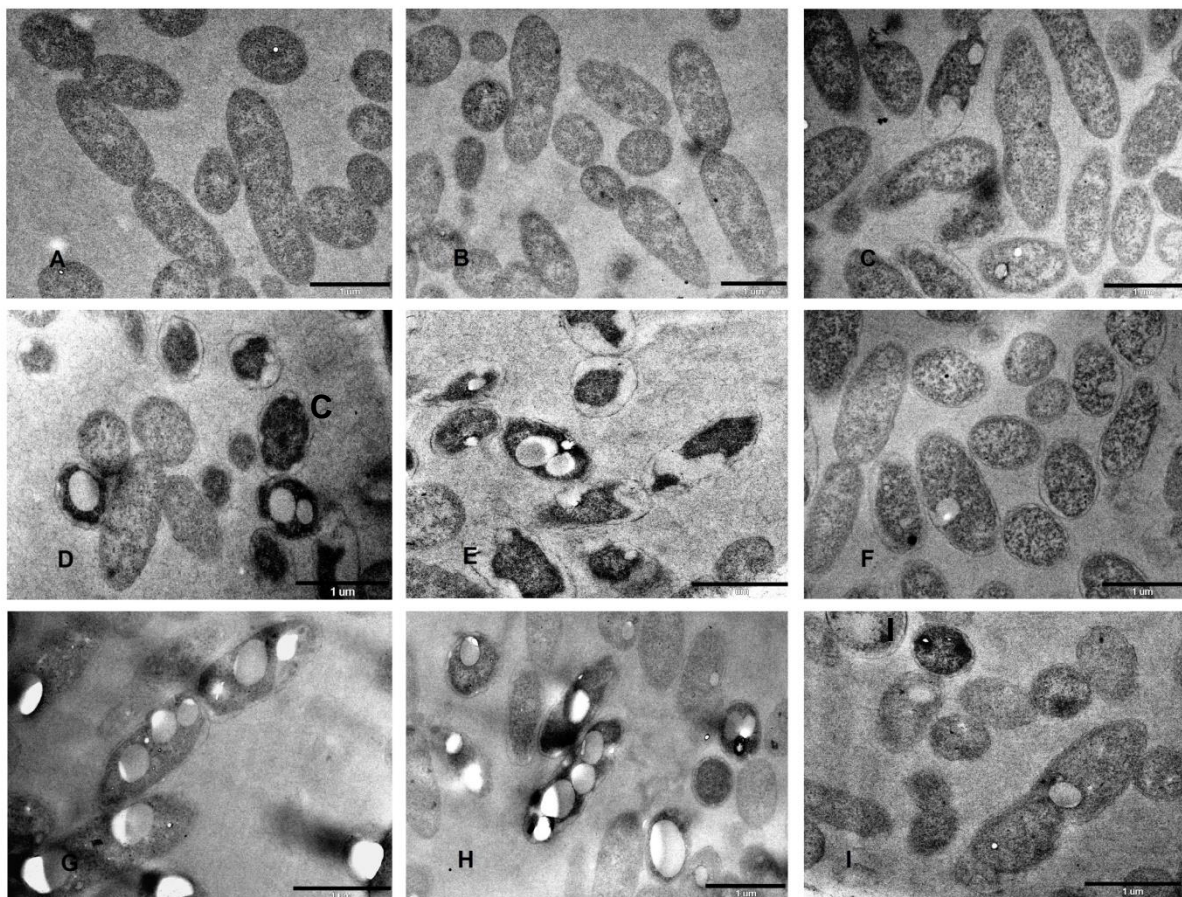


Figure 5-7. Time course of PHB granule formation in strain TH-1 cells. A. Negative control. Incubation times in autotrophic condition for 15 minutes (B), 180 min (C), 360 minutes (D), 540 minutes (E). Incubation times under heterotrophic condition

with malate for 15 minutes (F), 180 minutes (G), 360 minutes (H), 540 minutes (I). The white areas within the bacteria are the PHB inclusions. Scale bars represents for 1  $\mu\text{m}$ .

Notably, PHB granules appeared in a globular shape under autotrophic induction condition after 180 minutes of induction. Under heterotrophic condition, the accumulation process started even earlier, a lot of PHB granules were observed within only 15 minutes of induction.

Following the literature, two models are suggested for the formation of PHA granules: the micelle and the budding model [10]. In micelle model, the PHA granules are randomly formed. On the contrary, the budding model explains the reason why PHA granules are formed near or in contact to cell membrane. The TEM analysis of PHB granules in strain TH-1 in the early stage shows a remarkable difference from the formation and localization of granules under autotrophic and heterotrophic condition. The granules were frequently found to close or in contact to the cytoplasmic membrane under autotrophic condition while under heterotrophic condition, the PHB granules were randomly distributed in the cytosol.

Hence, the formation of PHB granules in strain TH-1 could be explained by both models: the micelle and the budding model.

PHB amount under autotrophic condition increased during the incubation time. The amount after 360 minutes of induction was  $270.1 \pm 14.6 \text{ mgL}^{-1}$ ,  $38.61 \pm 4.06\%$  for PHB concentration and PHB content within cells, respectively. The amount under the heterotrophic condition after 180 minutes induction was  $430.4 \pm 14.3 \text{ mgL}^{-1}$ ,  $53.82 \pm 2.11\%$ . These results suggested that under abundant carbon source and nitrogen depletion condition, PHB can be accumulated drastically.

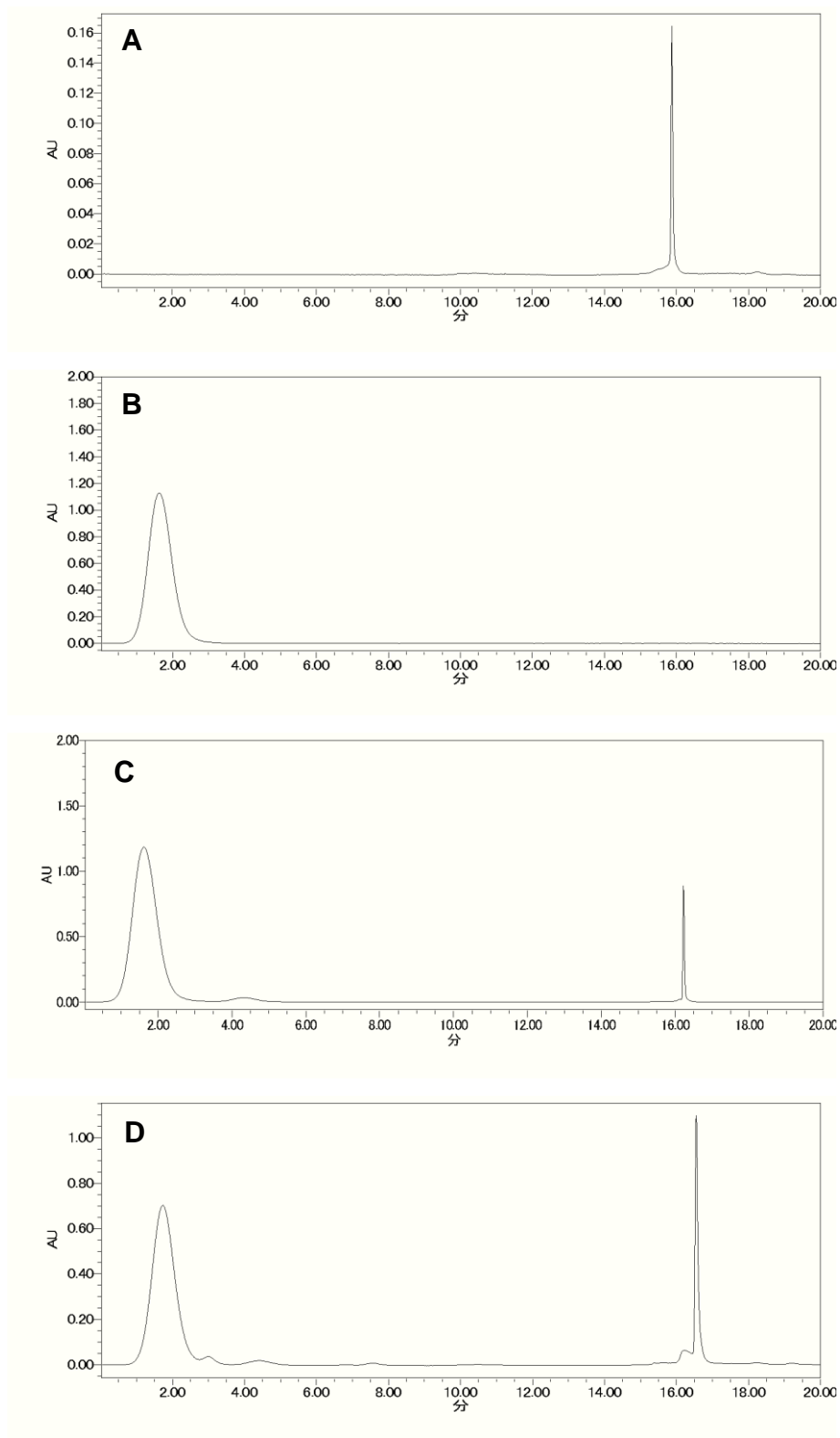


Figure 5-8. HPLC analysis of crotonic acid generated from PHB digested by  $\text{H}_2\text{SO}_4$  96%. The solvent used was 0.75 mM  $\text{H}_2\text{SO}_4$  at a flow rate of 0.6 mL/min. The elution peaks were monitored at 210 nm. Negative control (A); Standard crotonic acid (8

mM) (B); Standard PHB (0.8 mg/mL) was digested by H<sub>2</sub>SO<sub>4</sub> (C); PHB accumulated in strain TH-1 after 540 minutes induction under autotrophic condition (D).

The PHB accumulation in bacterial cells was quantificated by HPLC based on the standard curve which was constructed by using the commercial PHB.

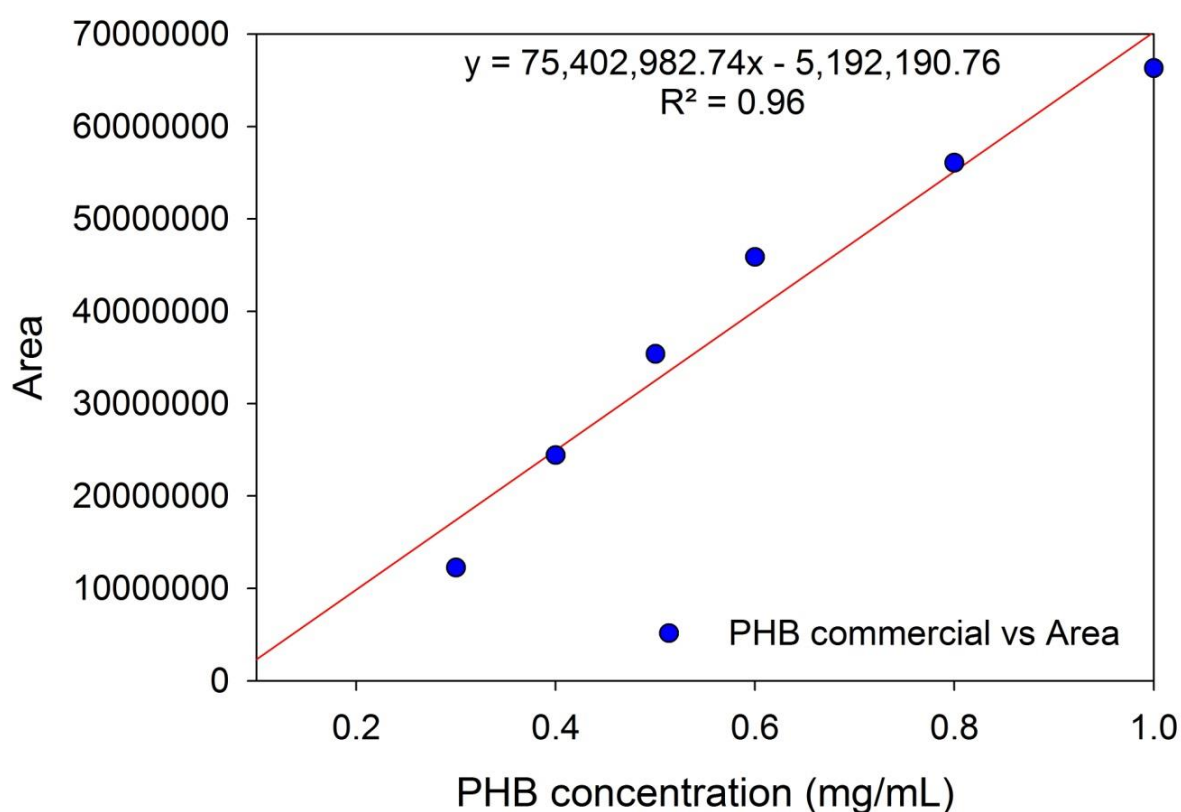


Figure 5-9. Standard curve of commercial PHB

The regress equation:  $y = 75,402,982.74x - 5,192,190.76$  was used for calculation PHB in the sample.

Table 5-2. Result of two-phase culture for PHB production under autotrophic or heterotrophic condition

	Induced phase			
	Post-induced (minute)	Dry cell weight (mg.L <sup>-1</sup> )	PHB cont.(mg.L <sup>-1</sup> )	PHB content in cell (%)
Autotrophic H <sub>2</sub> :O <sub>2</sub> :CO <sub>2</sub> (75: 10: 15)	15	667.8±36.7	ND	ND
	180	671.1±25.5	107.3±4.0	16.01±1.27
	360	702.2±38.6	270.1±14.6	38.61±4.06
	540	771.1±56.7	167.4±9.2	21.85±2.82
Heterotrophic (Malate)	15	828.9±32.0	36.9±3.5	4.45±0.34
	180	801.1±56.0	430.4±14.3	53.82±2.11
	360	745.6±61.6	372.7±16.6	50.15±3.53
	540	833.3±43.3	160.6±11.4	19.26±0.37

ND: not detected

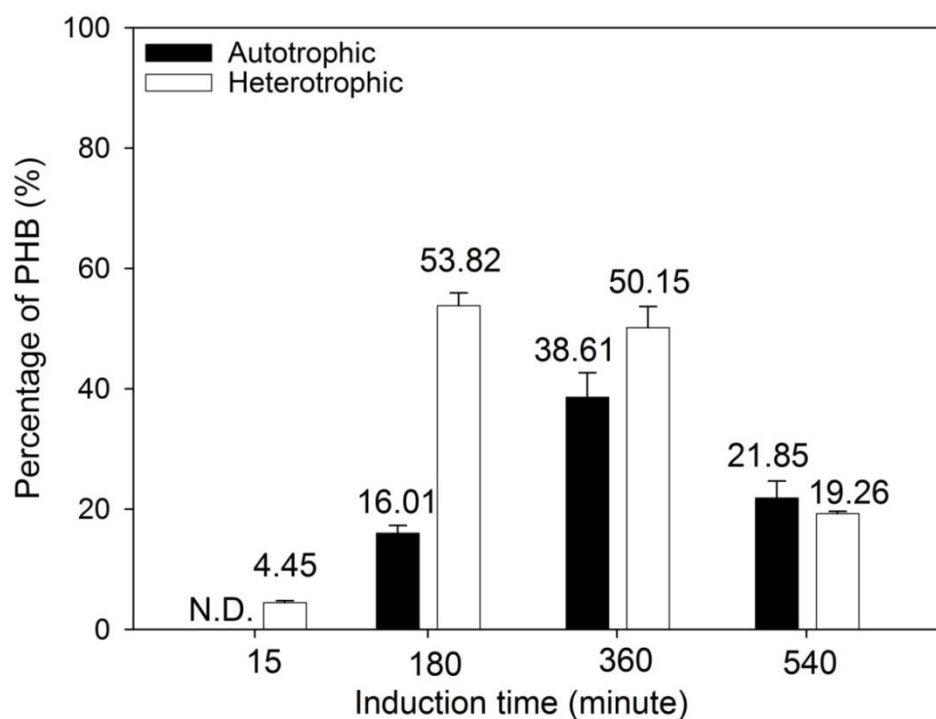


Figure 5-10. Time course of PHB accumulation and degradation by strain TH-1 under autotrophic or heterotrophic condition. ND: not detected.

Interestingly, PHB amount dramatically decreased after it reached the peak. The PHB content after 540 minutes of induction was  $21.85\pm2.82\%$  and  $19.26\pm0.37\%$  under autotrophic or heterotrophic condition, respectively.

Table 5-3. The diameters of PHB granules and the number of PHB granules.

Sample	Autotrophic H <sub>2</sub> :O <sub>2</sub> :CO <sub>2</sub> (75%: 10%: 15%)		Heterotrophic (Malate)	
	180 minutes	360 minutes	180 minutes	360 minutes
Ø (µm)	$0.299\pm0.068$	$0.340\pm0.073$	$0.478\pm0.059$	$0.500\pm0.087$
Granules	$1.9\pm0.8$	$2.4\pm1.2$	$2.4\pm1.0$	$2.3\pm1.2$

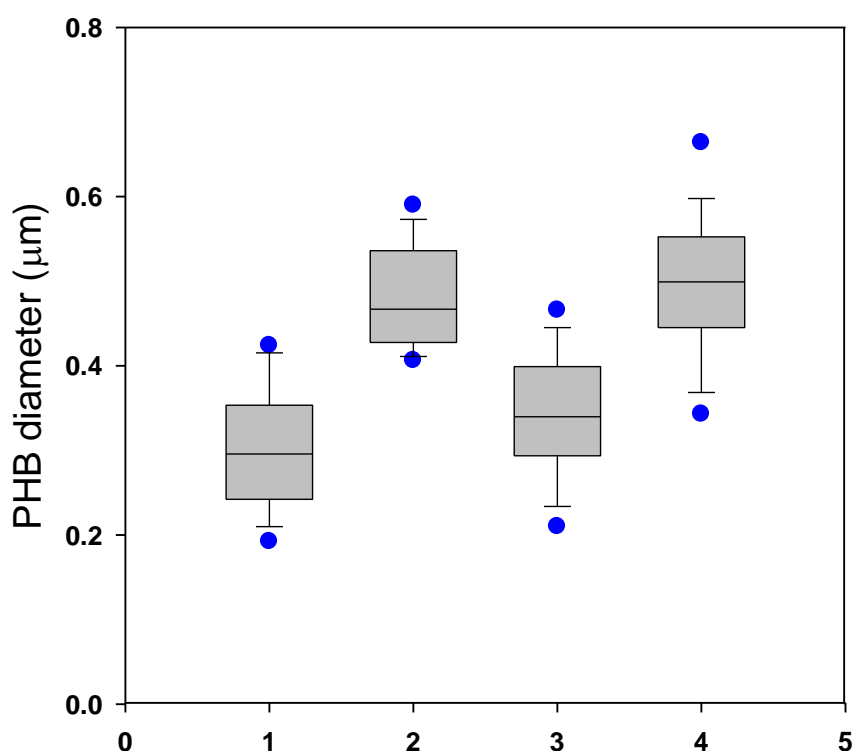


Figure 5-11. The diameter of PHB granules under different conditions, which are presented in the box plot chart. The top, bottom, and the middle lines correspond to 75<sup>th</sup> percentile, 25<sup>th</sup> percentile, and median, respectively; numbers represent mean values. Bars represent the limits of upper and lower quartile (n=30). The dots

represent the outlier of 5<sup>th</sup>/95<sup>th</sup> percentile. Incubation times in autotrophic (1), (3) and heterotrophic condition (2), (4) for 180 minutes and 360 minutes, respectively.

Table 5-3 shows the PHB granule diameter after each period time of induction. PHB granules accumulate in a globular form. The result was calculated from average 30 granules. Figure 5-13 shows that the PHB diameter was  $0.340\pm0.073$   $\mu\text{m}$  and  $0.500\pm0.087$   $\mu\text{m}$  under autotrophic condition and heterotrophic condition after 360 minutes, respectively.

Through the result of strain TH-1 genome annotation, TH-1 genome does not contain any PHB depolymerases. The question comes whether PHB accumulated in the cell will be re-consumed in proper condition without PHB depolymerase or not. To address this question, the PHB production was induced through 180 minutes under heterotrophic condition, and the cells were re-transferred to a new condition without carbon source for 180 minutes of incubation. Although PHB granules were seen, the density of PHB granules was thinner. Even more, the PHB diameter under this condition was smaller. Cells in dividing state was observed, implying that bacteria can re-consume the stored PHB, even though it does not contain PHB depolymerase.

In summary, the highest percentages of PHB accumulation under autotrophic and heterotrophic conditions were 38.6% after 360 minutes and 53.8% after 180 minutes, respectively.

## 5.4. Conclusions

Although *H. thermoluteolus* TH-1 was reported to have the highest growth rate among autotrophs, there has been no report about the application of strain TH-1. By this study, it was shown that PHB could be rapidly produced under autotrophic inducing condition. PHB granules were observed after 180 minutes of induction. Under heterotrophic condition, only 15 minutes was enough for the cells to start producing PHB. This observation can be explained by the flexibility of the metabolic system. At first, the metabolic system in strain TH-1 quickly switches from growth stage to PHB production stage. The second is the role of three copies of PHA synthase genes in strain TH-1 genome. PHA synthase is the key enzyme that is required for PHB monomers assembly [76]. In genome of *Rasltonia eutropha*, there is only one PHA gene [8]. In contrast, there are three copies of PHA gene in strain TH-1 genome.

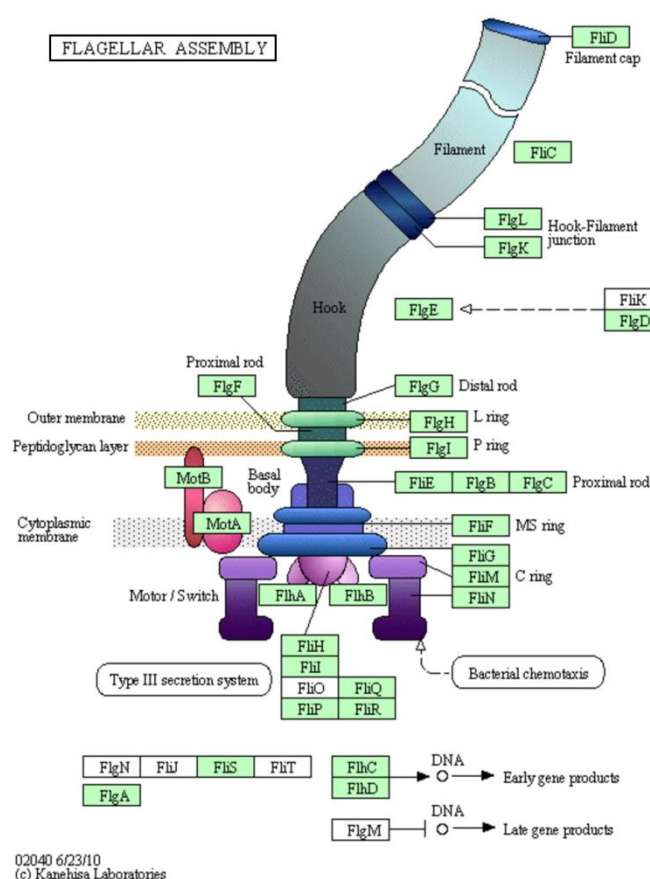


Figure 5-12. Genes coding for flagella structure in strain TH-1. Green boxes indicate the genes that exist in strain TH-1 genome. This figure is from alignment strain TH-1 genome with KEEG pathway database (<http://www.genome.jp/kegg/pathway.html>).

Therefore, all these genes can function for PHB accumulation. An unexpected result is that PHB granules were drastically degraded after 6 and 9 hour of induction under heterotrophic and autotrophic conditions, respectively. Other authors who investigated the accumulation of PHB also found the similar phenomenon [77, 78]. In previous report, TH-1 was classified as *Pseudomonas hydrogenothermophila*, which means strain TH-1 is a motile bacteria with flagellar structure [2].

In addition, strain TH-1 genome analysis revealed that TH-1 possesses all necessary genes required for making flagellar. Flagellar is a hair like structure that acts primarily as an organelle of locomotion. These genes are organized in clustal of contig 12 of TH-1 genome such as: flagellin (*contig00012\_orf00011*, *contig00012\_orf00013*, *contig00012\_orf00016*), flagellar hook-associated (*contig00012\_orf00015*), flagellar hook-basal body complex (*contig00012\_orf00024*), flagellar M-ring (*contig00012\_orf00029*), flagellar motor switch (*contig00012\_orf00030*, *contig00012\_orf00044*, *contig00012\_orf00045*), flagellar assembly (*contig00012\_orf00032*), flagellar hook-length control protein (*contig00012\_orf00038*), etc.

Drastic decrease of PHB amount can be explained by stress condition with nitrogen starvation, the motility of bacterium increased in an effort to look for nitrogen source. Naturally, in order to increase the bacterial motility, high amount of ATP is required. When the bacterial cells were in PHB-storaging stage, there is no ATP sink support for such activity. Hence, for ATP acquisition duty, PHB was re-converted into 3-HBCoA and to acetyl CoA. Finally, acetyl-CoA enters into TCA cycle for total oxidation. The product of this process is NADH, which will generate ATP by a process so-call respiration.

From the results mentioned above, due to ATP demand for locomotion, PHB was drastically degraded. However, no PHA depolymerase was found in the genome of TH-1. Hence, a question arose how PHB could be degraded. To prove that PHB will be converted into acetyl CoA and utilized under proper condition, an experiment was designed. In this experiment, strain TH-1 was cultured and induced under heterotrophic condition with malate after 180 minutes. At this stage, PHB

accumulation was seen. The bacteria cells were collected and re-transferred to a new medium that only contains mineral elements plus nitrogen, phosphorus, but without carbon source. As I expected, PHB granules which accumulated under heterotrophic condition were degraded and the cells were proved to be able to utilize PHB in reverse direction. Optical density of cultural medium also increased because the cell condition switched to growth mode. PHB granules diameter was significantly reduced from  $0.48 \pm 0.06 \mu\text{m}$  under heterotrophic induction to  $0.31 \pm 0.07 \mu\text{m}$  under new condition without carbon source after 180 minutes (Appendix, Table 5-5). Moreover, the physiology of the cells was significantly changed; the cell containing PHB under induction condition changed the shape. The cells changed from inactive state to active state for growth.

Recently, the presence of thiolysis activity was proposed for PHA synthase. By itself, PHA synthase could perform a reverse reaction of PHB synthesis. PHB could be degraded via a novel pathway that is thiolysis with CoASH [79, 80]. Therefore, in case of strain TH-1, PHA synthase could function in both ways.

In conclusion, the accumulation ability of PHB under autotrophic or heterotrophic condition was characterized. Under autotrophic condition, PHB granules were formed after 180 minutes of induction. *H. thermoluteolus* TH-1 was found to produce up to  $430.4 \pm 14.3 \text{ mgL}^{-1}$  of PHB after 180 minutes of induction under heterotrophic or  $270.1 \pm 14.6 \text{ mgL}^{-1}$  of PHB after 360 minutes of induction under autotrophic condition. The highest percentages of PHB accumulation under autotrophic and heterotrophic conditions were 38.6% after 360 minutes and 53.8% after 180 minutes, respectively. Also, the results clearly showed PHB accumulation degradation process in strain TH-1.

# Conclusions and prospects

The object of this study was to elucidate the energy metabolism and carbon metabolism of *H. thermoluteolus* TH-1. I would like to clarify such metabolism in terms of trophic system of this strain. This study clarifies the molecular basis for autotrophy, heterotrophy or mixotrophy and leads us to some value-added products by using *H. thermoluteolus* in future. In order to elucidate the energy metabolism and carbon metabolism of strain TH-1, the growth profile and the expression of key enzymes of autotrophic metabolism during heterotrophic or mixotrophic growth needed to be investigated. Through this study, I suggested the scheme for strain TH-1 growth under autotrophic, heterotrophic, or mixotrophic condition as figure 6-1.

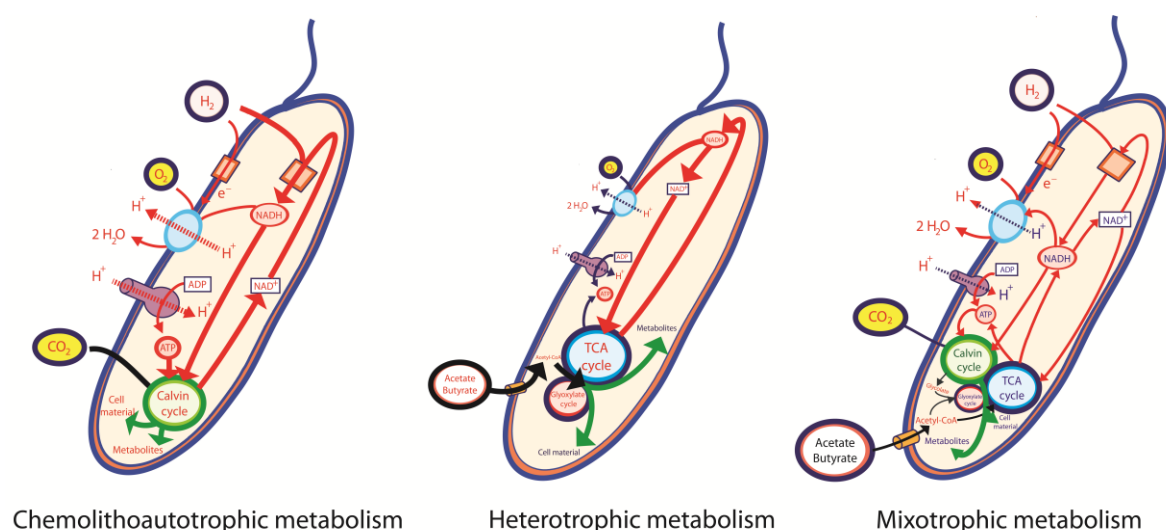


Figure 6-1. The scheme suggested for the growth of *H. thermoluteolus* TH-1 under autotrophic, heterotrophic, or mixotrophic condition.

## The conclusion of my studies:

In Chapter 1: the capacity to utilize various substrates under different mode of growth was investigated under autotrophic, heterotrophic, or mixotrophic conditions. The result in chapter 1 shows that strain TH-1 is a flexible bacterium. The maximum specific growth rate determined under autotrophic condition was  $0.6\ h^{-1}$ . Strain TH-1 showed the ability to grow favorably with malate under heterotrophic or mixotrophic condition with corresponding maximum growth rate of  $0.73\ h^{-1}$  and  $1.0\ h^{-1}$ , respectively.

Under mixotrophic condition with acetate or butyrate, a long lag phase was seen. The growth was delayed for a long time before robust growth started, implying that the cells come to have solution for the problem.

The RubisCO activity was highest under autotrophic condition compared with that under mixotrophic condition, suggesting that CBB cycle under autotrophic condition operates at high level for carbon dioxide fixation.

In Chapter 2: In strain TH-1 grown under heterotrophic condition with acetate or butyrate, carbon metabolism was conducted through glyoxylate cycle, whereas energy metabolism was conducted through TCA cycle. It was suggested that under heterotrophic condition with malate or pyruvate, the enzymatic activities of glyoxylate cycle were depressed, except for malate synthase, suggesting that malate synthase may take part in the glyoxylate detoxification process in the cells

In Chapter 3: The hypothesis about the inhibition of the growth of cells TH-1 under mixotrophic condition when CO<sub>2</sub> and acetate or butyrate co-existed was investigated. The result of this chapter also suggested the function of glyoxylate cycle under mixotrophic condition in detoxification of the harmful compound, possibly glycolate.

In Chapter 4: Based on the analyses of the microarray profile of *H. thermoluteolus* TH-1 under autotrophic, heterotrophic and mixotrophic conditions, I elucidated the central metabolic pathway of strain TH-1. It also revealed the putative role of each metabolic pathway via analyses of the expression levels of genes that belong to them. I uncovered the function of CBB cycle in carbon fixation under autotrophic and mixotrophic growth. Via observation of the constitutive expression of all genes belonging to respiratory machinery, I revealed the important role of TCA cycle and respiratory chain responsible for ATP production in energy metabolism. The evidence from the expression levels of genes belonging to glycolysis/gluconeogenesis pathway as well as the evidences from metabolome profile suggested the role of glycolysis/gluconeogenesis under each specific condition of growth.

Moreover, the high expression level of *cpx* gene coding for cytochrom *c* peroxidase under mixotrophic condition, suggested that cytochrom *c* peroxidase was assumed to be a detoxification system for H<sub>2</sub>O<sub>2</sub>.

In Chapter 5: The accumulation ability of PHB under autotrophic or heterotrophic condition was examined. Under autotrophic condition, PHB granules were formed after 180 minutes of induction. *H. thermoluteolus* TH-1 was found to produce up to  $430.4 \pm 14.3 \text{ mgL}^{-1}$  of PHB after 180 minutes of induction under heterotrophic or  $270.1 \pm 14.6 \text{ mgL}^{-1}$  of PHB after 360 minutes of induction under autotrophic condition. The highest percentages of PHB accumulation under autotrophic and heterotrophic conditions were 38.6% after 360 minutes and 53.8% after 180 minutes, respectively. Also, the results clearly showed PHB accumulation degradation process in strain TH-1.

#### **The future prospects:**

The glyoxylate cycle in strain TH-1 plays a critical role in the growth of this strain under heterotrophic condition with acetate or butyrate as a substrate. Moreover, the functions of glyoxylate cycle combined with glycolate oxidase that works as the detoxification system is also an interesting feature. This strategy enables strain TH-1 to operate CBB cycle at high temperature under high pressure of oxygen. Therefore, the detailed research about the characteristic of glyoxylate cycle in TH-1 is necessary. Especially kinetic investigation of two key enzymes of glyoxylate cycle: isocitrate lyase and malate synthase is required.

Autotrophic growth rate of strain TH-1 is the highest among autotrophs indicating that strain TH-1 has high potential for industrial application. Strain TH-1 shows ability to produce PHB within a short time of incubation, and it has an advantage for being used strain TH-1 as a new platform for PHB production. Especially, the more promising trend in application PHB is the development of the therapeutic system of sustained drug delivery such as microsphere and microcapsule using PHB. If this perspective comes true, it introduces a cheap medical treatment for patients.

The trend of current biotechnology is to make new value-added, environmentally friendly products. So, *H. thermoluteolus* TH-1 is a great candidate for such target. By employing genetic engineering, we could modify the metabolism of PHB pathway. Intermediate substrate acetyl-CoA could be useful for the production of other value-added products such as acetone, iso-propyl alcohol, etc.

## References

1. Bar-Even, A., E. Noor, and R. Milo, *A survey of carbon fixation pathways through a quantitative lens*. Journal of Experimental Botany, 2012. **63**(6): p. 2325-2342.
2. Goto, E., T. Kodama, and Y. Minoda, *Studies on Hydrogen Utilizing Microorganisms .5. Isolation and Culture Conditions of Thermophilic Hydrogen Bacteria*. Agricultural and Biological Chemistry, 1977. **41**(4): p. 685-690.
3. Hayashi, N.R., et al., *Hydrogenophilus thermoluteolus* gen. nov., sp. nov., a thermophilic, facultatively chemolithoautotrophic, hydrogen-oxidizing bacterium. International Journal of Systematic Bacteriology, 1999. **49**: p. 783-786.
4. Stohr, R., et al., *Hydrogenophilus hirschii* sp nov., a novel thermophilic hydrogen-oxidizing beta-proteobacterium isolated from Yellowstone National Park. International Journal of Systematic and Evolutionary Microbiology, 2001. **51**: p. 481-488.
5. Ishizaki, A., K. Tanaka, and N. Taga, *Microbial production of poly-D-3-hydroxybutyrate from CO(2)*. Applied Microbiology and Biotechnology, 2001. **57**(1-2): p. 6-12.
6. Friedrich, B. and E. Schwartz, *Molecular-Biology of Hydrogen Utilization in Aerobic Chemolithotrophs*. Annual Review of Microbiology, 1993. **47**: p. 351-383.
7. Goto, E., T. Kodama, and Y. Minoda, *Studies on Hydrogen-Utilizing Microorganisms .6. Growth and Taxonomy of Thermophilic Hydrogen Bacteria*. Agricultural and Biological Chemistry, 1978. **42**(7): p. 1305-1308.
8. Cho, M., et al., *Purification of Polyhydroxybutyrate Synthase from Its Native Organism, Ralstonia eutropha: Implications for the Initiation and Elongation of Polymer Formation in Vivo*. Biochemistry, 2012. **51**(11): p. 2276-2288.
9. Eggers, J. and A. Steinbuchel, *Poly(3-Hydroxybutyrate) Degradation in Ralstonia eutropha H16 Is Mediated Stereoselectively to (S)-3-Hydroxybutyryl Coenzyme A (CoA) via Crotonyl-CoA*. Journal of Bacteriology, 2013. **195**(14): p. 3213-3223.
10. Rehm, B.H.A., *Genetics and biochemistry of polyhydroxyalkanoate granule self-assembly: The key role of polyester synthases*. Biotechnology Letters, 2006. **28**(4): p. 207-213.
11. Ishizaki, A. and K. Tanaka, *Batch Culture of Alcaligenes-Eutrophus Atcc 17697t Using Recycled Gas Closed-Circuit Culture System*. Journal of Fermentation and Bioengineering, 1990. **69**(3): p. 170-174.
12. Stukus, P.E. and B.T. Decicco, *Autotrophic and Heterotrophic Metabolism of Hydrogenomonas . Regulation of Autotrophic Growth by Organic Substrates*. Journal of Bacteriology, 1970. **101**(2): p. 339-&.
13. Fuchs, G., *Alternative Pathways of Carbon Dioxide Fixation: Insights into the Early Evolution of Life?* Annual Review of Microbiology, Vol 65, 2011. **65**: p. 631-+.
14. Kim, B.H. and G.M. Gadd, *Bacterial physiology and metabolism*. 2008, Cambridge New York: Cambridge University Press. xxii, 529 p.
15. Raines, C.A., J.C. Lloyd, and T.A. Dyer, *New insights into the structure and function of sedoheptulose-1,7-bisphosphatase; an important but neglected Calvin cycle enzyme (Review article) (vol 50, pg 1, 1999)*. Journal of Experimental Botany, 1999. **50**(335): p. 881-881.
16. Jensen, R.G. and J.T. Bahr, *Ribulose 1,5-Bisphosphate Carboxylase-Oxygenase*. Annual Review of Plant Physiology and Plant Molecular Biology, 1977. **28**: p. 379-400.

17. Terazono, K., N.R. Hayashi, and Y. Igarashi, *CbbR, a LysR-type transcriptional regulator from Hydrogenophilus thermoluteolus, binds two cbb promoter regions*. Fems Microbiology Letters, 2001. **198**(2): p. 151-157.
18. Berg, I.A., *Ecological Aspects of the Distribution of Different Autotrophic CO<sub>2</sub> Fixation Pathways*. Applied and Environmental Microbiology, 2011. **77**(6): p. 1925-1936.
19. Ogren, W.L. and G. Bowes, *Ribulose Diphosphate Carboxylase Regulates Soybean Photorespiration*. Nature-New Biology, 1971. **230**(13): p. 159-&.
20. Vignais, P.M. and B. Billoud, *Occurrence, classification, and biological function of hydrogenases: An overview*. Chemical Reviews, 2007. **107**(10): p. 4206-4272.
21. Burgdorf, T., et al., *[NiFe]-hydrogenases of Ralstonia eutropha H16: Modular enzymes for oxygen-tolerant biological hydrogen oxidation*. Journal of Molecular Microbiology and Biotechnology, 2005. **10**(2-4): p. 181-196.
22. Talaro, K.P. and A. Talaro, *Foundations in microbiology : basic principles*. 4th ed. 2002, Dubuque, Iowa: McGraw-Hill. xxix, 534, 42 p.
23. Murooka, Y. and T. Imanaka, *Recombinant microbes for industrial and agricultural applications*. Bioprocess technology. 1994, New York: Dekker. xiv, 877 p.
24. Kalipatnapu, S. and A. Chattopadhyay, *Membrane protein solubilization: Recent advances and challenges in solubilization of serotonin(1A) receptors*. Iubmb Life, 2005. **57**(7): p. 505-512.
25. Sharkey, T.D., L.V. Savitch, and N.D. Butz, *Photometric-Method for Routine Determination of Kcat and Carbamylation of Rubisco*. Photosynthesis Research, 1991. **28**(1): p. 41-48.
26. Yoshida, N., et al., *A novel NAD-dependent dehydrogenase, highly specific for 1,5-anhydro-D-glucitol, from Trichoderma longibrachiatum strain 11-3*. Applied and Environmental Microbiology, 2003. **69**(5): p. 2603-2607.
27. Sawers, R.G. and D.H. Boxer, *Purification and Properties of Membrane-Bound Hydrogenase Isoenzyme-1 from Anaerobically Grown Escherichia-Coli-K12*. European Journal of Biochemistry, 1986. **156**(2): p. 265-275.
28. Yu, L. and M.J. Wolin, *Hydrogenase Measurement with Photochemically Reduced Methyl Viologen*. Journal of Bacteriology, 1969. **98**(1): p. 51-&.
29. Crane, K.W. and J.P. Grover, *Coexistence of mixotrophs, autotrophs, and heterotrophs in planktonic microbial communities*. Journal of Theoretical Biology, 2010. **262**(3): p. 517-527.
30. Alber, B.E., *Biotechnological potential of the ethylmalonyl-CoA pathway*. Appl Microbiol Biotechnol, 2011. **89**(1): p. 17-25.
31. Tang, K.H., Y.J. Tang, and R.E. Blankenship, *Carbon metabolic pathways in phototrophic bacteria and their broader evolutionary implications*. Front Microbiol, 2011. **2**: p. 165.
32. Yoon, K.S., et al., *Purification and characterization of pyruvate:ferredoxin oxidoreductase from Hydrogenobacter thermophilus TK-6*. Archives of Microbiology, 1997. **167**(5): p. 275-279.
33. Schneider, K., et al., *The Ethylmalonyl-CoA Pathway Is Used in Place of the Glyoxylate Cycle by Methylobacterium extorquens AM1 during Growth on Acetate*. Journal of Biological Chemistry, 2012. **287**(1): p. 757-766.
34. Shimizu, K., *Bacterial cellular metabolic systems : metabolic regulation of a cell system with 13c-metabolic flux analysis*. Woodhead publishing series in biomedicine. 2012, Philadelphia, PA: Woodhead Pub.

35. Serrano, J.A., M. Camacho, and M.J. Bonete, *Operation of glyoxylate cycle in halophilic archaea: presence of malate synthase and isocitrate lyase in Haloferax volcanii*. Febs Letters, 1998. **434**(1-2): p. 13-16.
36. Dunn, M.F., J.A. Ramirez-Trujillo, and I. Hernandez-Lucas, *Major roles of isocitrate lyase and malate synthase in bacterial and fungal pathogenesis*. Microbiology-Sgm, 2009. **155**: p. 3166-3175.
37. Wang, Z.X., C.O. Bramer, and A. Steinbuchel, *The glyoxylate bypass of Ralstonia eutropha*. FEMS Microbiol Lett, 2003. **228**(1): p. 63-71.
38. Bentrup, K.H.Z., et al., *Characterization of activity and expression of isocitrate lyase in Mycobacterium avium and Mycobacterium tuberculosis*. Journal of Bacteriology, 1999. **181**(23): p. 7161-7167.
39. Brown, J.P. and R.N. Perham, *Selective inactivation of the transacylase components of the 2-oxo acid dehydrogenase multienzyme complexes of Escherichia coli*. Biochem J, 1976. **155**(2): p. 419-27.
40. Dorner, E. and M. Boll, *Properties of 2-oxoglutarate : ferredoxin oxidoreductase from Thauera aromatica and its role in enzymatic reduction of the aromatic ring*. Journal of Bacteriology, 2002. **184**(14): p. 3975-3983.
41. Karr, D.B., et al., *Enzymes of the Poly-Beta-Hydroxybutyrate and Citric-Acid Cycles of Rhizobium-Japonicum Bacteroids*. Plant Physiology, 1984. **75**(4): p. 1158-1162.
42. Dixon, G.H. and H.L. Kornberg, *Assay Methods for Key Enzymes of the Glyoxylate Cycle*. Biochemical Journal, 1959. **72**: p. P3-P3.
43. Geer, B.W., et al., *Comparative-Study of the Nadp-Malic Enzymes from Drosophila and Chick Liver*. Comparative Biochemistry and Physiology B-Biochemistry & Molecular Biology, 1980. **65**(1): p. 25-34.
44. Kornberg, H.L., *The role and control of the glyoxylate cycle in Escherichia coli*. Biochem J, 1966. **99**(1): p. 1-11.
45. Salido, E., et al., *Primary hyperoxalurias: Disorders of glyoxylate detoxification*. Biochimica Et Biophysica Acta-Molecular Basis of Disease, 2012. **1822**(9): p. 1453-1464.
46. Gourdon, P., et al., *Cloning of the malic enzyme gene from Corynebacterium glutamicum and role of the enzyme in lactate metabolism*. Appl Environ Microbiol, 2000. **66**(7): p. 2981-7.
47. Shih, P.M., et al., *Introduction of a synthetic CO(2)-fixing photorespiratory bypass into a cyanobacterium*. J Biol Chem, 2014. **289**(14): p. 9493-500.
48. Tolbert, N.E., C.O. Clagett, and R.H. Burris, *Products of the oxidation of glycolic acid and L-lactic acid by enzymes from tobacco leaves*. J Biol Chem, 1949. **181**(2): p. 905-14.
49. Zelitch, I. and S. Ochoa, *Oxidation and reduction of glycolic and glyoxylic acids in plants. I. Glycolic and oxidase*. J Biol Chem, 1953. **201**(2): p. 707-18.
50. Zelitch, I., *Oxidation and reduction of glycolic and glyoxylic acids in plants. II. Glyoxylic acid reductase*. J Biol Chem, 1953. **201**(2): p. 719-26.
51. Richardson, K. and N.E. Tolbert, *Oxidation of Glyoxylic Acid to Oxalic Acid by Glycolic Acid Oxidase*. Journal of Biological Chemistry, 1961. **236**(5): p. 1280-&.
52. Stekel, D., *Microarray bioinformatics*. 2003, Cambridge ; New York: Cambridge University Press. xiv, 263 p., 8 p. of plates.
53. Whitworth, G.B., *An Introduction to Microarray Data Analysis and Visualization*. Methods in Enzymology, Vol 470: Guide to Yeast Genetics:, 2010. **470**: p. 19-50.
54. Selzer, P.M., R.J. Marhöfer, and A. Rohwer, *Applied bioinformatics : an introduction*. 2008, Berlin: Springer. xiv, 287 p.

55. Grant, R.P., *Computational genomics : theory and application*. 2004, Wymondham: Horizon Bioscience. ix, 305 p.
56. Schuchmann, K. and V. Muller, *A bacterial electron-bifurcating hydrogenase*. J Biol Chem, 2012. **287**(37): p. 31165-71.
57. Koolman, J. and K.-H. Röhm, *Color atlas of biochemistry*. 2nd ed. Flexibooks. 2005, Stuttgart ; New York: Thieme. x, 467 p.
58. Eprinte, A.T., et al., *Regulation of carbon flows in the tricarboxylic acid cycle-glyoxylate bypass system in Rhodospirillum rubrum under different growth conditions*. Microbiology, 2008. **77**(2): p. 132-136.
59. Maurino, V.G. and C. Peterhansel, *Photorespiration: current status and approaches for metabolic engineering*. Current Opinion in Plant Biology, 2010. **13**(3): p. 249-256.
60. Mallmann, J., et al., *The role of photorespiration during the evolution of C-4 photosynthesis in the genus Flaveria*. Elife, 2014. **3**.
61. Wakai, S., et al., *Oxidative phosphorylation in a thermophilic, facultative chemoautotroph, Hydrogenophilus thermoluteolus, living prevalently in geothermal niches*. Environmental Microbiology Reports, 2013. **5**(2): p. 235-242.
62. Gonzalez-Moro, M.B., et al., *Effect of photorespiratory C-2 acids on CO<sub>2</sub> assimilation, PSII photochemistry and the xanthophyll cycle in maize*. Photosynthesis Research, 2003. **78**(2): p. 161-173.
63. Glacoleva, T.A., O.V. Zalensky, and A.T. Mokronosov, *Oxygen Effects on Photosynthesis and C-14 Metabolism in Desert Plants*. Plant Physiology, 1978. **62**(2): p. 204-209.
64. Zinn, M., B. Witholt, and T. Egli, *Occurrence, synthesis and medical application of bacterial polyhydroxyalkanoate*. Advanced Drug Delivery Reviews, 2001. **53**(1): p. 5-21.
65. Marshall, C.W., E.V. LaBelle, and H.D. May, *Production of fuels and chemicals from waste by microbiomes*. Curr Opin Biotechnol, 2013. **24**(3): p. 391-7.
66. Steinbuchel, A., *Perspectives for biotechnological production and utilization of biopolymers: Metabolic engineering of polyhydroxyalkanoate biosynthesis pathways as a successful example*. Macromolecular Bioscience, 2001. **1**(1): p. 1-24.
67. Ibrahim, M.H.A. and A. Steinbuchel, *Poly(3-Hydroxybutyrate) Production from Glycerol by Zooglea denitrificans MW1 via High-Cell-Density Fed-Batch Fermentation and Simplified Solvent Extraction*. Applied and Environmental Microbiology, 2009. **75**(19): p. 6222-6231.
68. Bonartsev, A., et al., *Biosynthesis, biodegradation, and application of poly (3-hydroxybutyrate) and its copolymers-natural polyesters produced by diazotrophic bacteria*. Communicating Current Research and Educational Topics and Trends in Applied Microbiology, 2007. **1**: p. 295-307.
69. Lau, N.S. and K. Sudesh, *Revelation of the ability of Burkholderia sp. USM (JCM 15050) PHA synthase to polymerize 4-hydroxybutyrate monomer*. AMB Express, 2012. **2**(1): p. 41.
70. Li, R., H. Zhang, and Q. Qi, *The production of polyhydroxyalkanoates in recombinant Escherichia coli*. Bioresour Technol, 2007. **98**(12): p. 2313-20.
71. Goto, E., et al., *Studies on Hydrogen-Utilizing Microorganisms .4. Improvement of Initial and Exponential-Growth of Hydrogen Bacteria, Strain 9-5*. Agricultural and Biological Chemistry, 1977. **41**(3): p. 521-525.
72. Kodama, T., Y. Igarashi, and Y. Minoda, *Studies on Hydrogen-Utilizing Microorganisms .1. Isolation and Culture Conditions of a Bacterium Grown on*

- Hydrogen and Carbon-Dioxide*. Agricultural and Biological Chemistry, 1975. **39**(1): p. 77-82.
73. Suriyamongkol, P., et al., *Biotechnological approaches for the production of polyhydroxyalkanoates in microorganisms and plants - a review*. Biotechnol Adv, 2007. **25**(2): p. 148-75.
  74. Karr, D.B., J.K. Waters, and D.W. Emerich, *Analysis of Poly-Beta-Hydroxybutyrate in Rhizobium-Japonicum Bacteroids by Ion-Exclusion High-Pressure Liquid-Chromatography and Uv Detection*. Applied and Environmental Microbiology, 1983. **46**(6): p. 1339-1344.
  75. Spiekermann, P., et al., *A sensitive, viable-colony staining method using Nile red for direct screening of bacteria that accumulate polyhydroxyalkanoic acids and other lipid storage compounds*. Archives of Microbiology, 1999. **171**(2): p. 73-80.
  76. Jia, Y., et al., *Mechanistic studies on class I polyhydroxybutyrate (PHB) synthase from Ralstonia eutropha: Class I and III synthases share a similar catalytic mechanism*. Biochemistry, 2001. **40**(4): p. 1011-1019.
  77. Doi, Y., et al., *Cyclic Nature of Poly(3-Hydroxyalkanoate) Metabolism in Alcaligenes-Eutrophus*. Fems Microbiology Letters, 1990. **67**(1-2): p. 165-169.
  78. Taidi, B., D.A. Mansfield, and A.J. Anderson, *Turnover of Poly(3-Hydroxybutyrate) (Phb) and Its Influence on the Molecular-Mass of the Polymer Accumulated by Alcaligenes-Eutrophus during Batch Culture*. Fems Microbiology Letters, 1995. **129**(2-3): p. 201-205.
  79. Uchino, K., et al., *Isolated poly(3-hydroxybutyrate) (PHB) granules are complex bacterial organelles catalyzing formation of PHB from acetyl coenzyme A (CoA) and degradation of PHB to acetyl-CoA*. Journal of Bacteriology, 2007. **189**(22): p. 8250-8256.
  80. Uchino, K. and T. Saito, *Thiolysis of poly(3-hydroxybutyrate) with polyhydroxyalkanoate synthase from Ralstonia eutropha*. Journal of Biochemistry, 2006. **139**(3): p. 615-621.

## Appendix

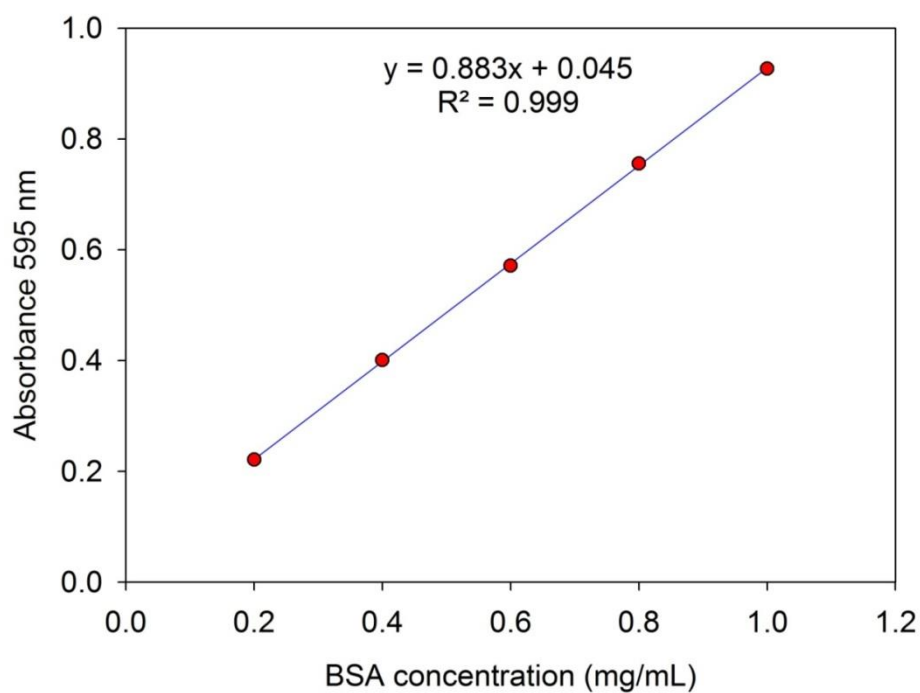


Figure 1-20. The protein standard curve (BSA) was constructed by using bovine serum albumin at wavelength 595 nm in Bradford method.

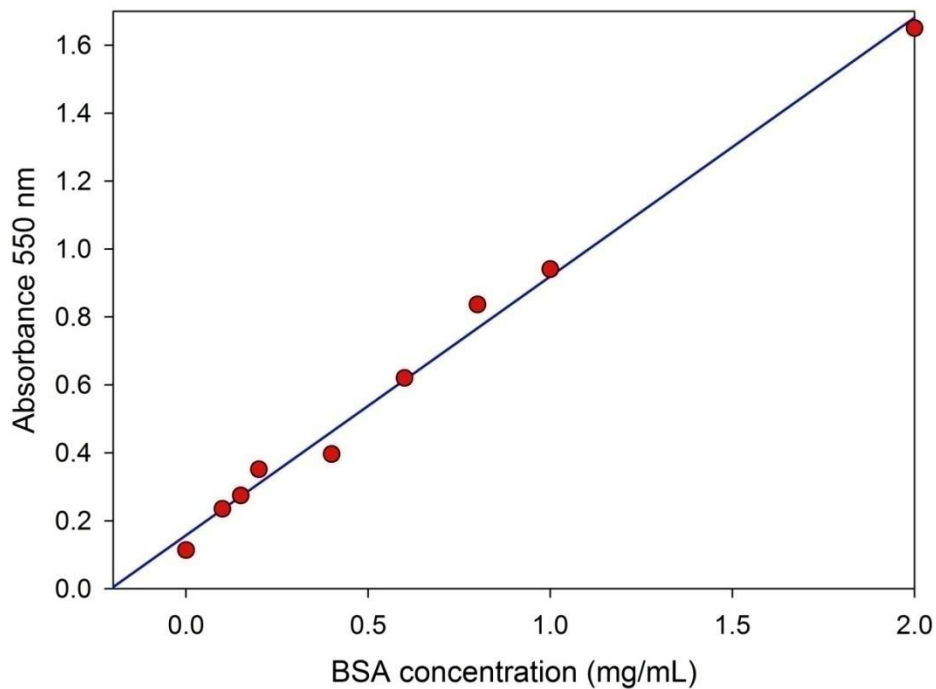


Figure 1-21. The protein standard curve (BSA) was constructed by using bovine serum albumin at wavelength 550 nm in BCA method.

Table 1-9. RubisCO activity in cell-free extract of cells grown under autotrophic or mixotrophic condition with acetate, butyrate, malate or pyruvate.

Condition	Activity (Unit/mg protein)
Autotrophic	0.188±0.005
Mixotrophic Acetate	0.102±0.004
Mixotrophic Butyrate	0.049±0.003
Mixotrophic Malate	0.015±0.006
Mixotrophic Pyruvate	0.023±0.003

Table 1-10. Hydrogenase activity (MBH and SH) in cells TH-1 grown under autotrophic condition.

Hydrogenase	Activity (Unit/ g cell)
Soluble hydrogenase	0.16 ±0.01
Membrane-bound hydrogenase	0.40±0.01

Table 4-29. metabolome profile show 178 differential metabolites concentration under autotrophic, mixotrophic or heterotrophic condition with butyrate.

No	Compound name	KEEG ID	AL	AS	HL	HS	ML	MS
1	GABA	C00334	N.D.	0.0002	N.D.	N.D.	N.D.	0.0005
2	<i>myo</i> -Inositol 2-phosphate	No ID	0.0002	0.0010	N.D.	N.D.	N.D.	0.0012
3	Lauric acid	C02679	0.0006	0.0026	0.0011	0.0014	0.0002	0.0038
4	2-Amino-2-(hydroxymethyl)-1,3-propanediol	C07182	0.0000	0.0001	0.0000	0.0000	0.0002	0.0021
5	XA0027	No ID	0.0001	0.0003	0.0001	0.0001	N.D.	0.0004
6	His	C00135	0.0016	0.0048	0.0025	0.0005	0.0001	0.0030
7	Triethanolamine	C06771	0.0001	0.0003	0.0001	0.0000	0.0001	0.0001
8	Decanoic acid	C01571	0.0004	0.0010	0.0004	0.0004	0.0001	0.0011
9	Ser	C00065	0.0029	0.0069	0.0011	0.0005	0.0009	0.0021
10	Nicotinamide	C00153	0.0004	0.0010	0.0007	0.0021	0.0001	0.0023
11	Urocanic acid	C00785	0.0002	0.0005	0.0001	0.0001	0.0001	0.0004
12	3-Phosphoglyceric acid	C00197	0.0002	0.0005	0.0010	0.0001	N.D.	0.0006
13	Asn	C00152	0.0042	0.0095	0.0027	0.0001	0.0001	0.0019
14	Undecanoic acid	No ID	0.0001	0.0002	0.0001	0.0001	0.0000	0.0002
15	dTTP	C00459	0.0005	0.0010	0.0003	N.D.	N.D.	0.0006
16	Urea	C00086	0.0028	0.0059	0.0017	0.0015	0.0016	0.0047
17	2-Phosphoglyceric acid	C00631	0.0001	0.0002	0.0002	0.0000	N.D.	0.0002
18	Octanoic acid	C06423	0.0002	0.0005	0.0002	0.0002	0.0001	0.0005
19	Lactic acid	C00186	0.0032	0.0062	0.0021	0.0017	0.0016	0.0065
20	Phosphoenolpyruvic acid	C00074	0.0006	0.0011	0.0008	0.0001	0.0000	0.0006
21	5-Oxoproline	C01879	0.0004	0.0008	0.0002	0.0002	0.0002	0.0005
22	Homocysteic acid	C16511	0.0027	0.0050	0.0002	0.0000	N.D.	0.0000

23	5-Aminoindole	No ID	0.0001	0.0002	0.0001	0.0001	0.0001	0.0003
24	dTMP	C00364	0.0002	0.0003	0.0007	0.0009	0.0001	0.0044
25	Diethanolamine	C06772	0.0005	0.0008	0.0003	0.0002	0.0007	0.0007
26	Pelargonic acid	C01601	0.0009	0.0016	0.0006	0.0007	0.0001	0.0017
27	<i>p</i> -Toluic acid <i>m</i> -Toluic acid <i>o</i> -Toluic acid	C01454 C07211 C07215	0.0106	0.0185	0.0053	0.0046	0.0023	0.0093
28	5-Oxohexanoic acid	C02129	0.0008	0.0014	0.0004	0.0004	0.0002	0.0010
29	Glucose 1-phosphate	C00103	0.0009	0.0015	0.0001	N.D.	N.D.	0.0015
30	Glycerol	C00116	0.2214	0.3694	0.1530	0.1409	0.1061	0.3684
31	2-Hydroxyvaleric acid	No ID	0.0004	0.0007	0.0002	0.0002	0.0001	0.0006
32	4-Methyl-2-oxovaleric acid 3-Methyl-2-oxovaleric acid	C00233	0.0009	0.0014	0.0004	0.0004	0.0002	0.0010
33	ADP-ribose	C00301	0.0000	0.0000	0.0000	0.0001	N.D.	0.0001
34	Phe	C00079	0.0028	0.0045	0.0009	0.0006	0.0002	0.0030
35	Thiamine diphosphate	C00068	0.0001	0.0002	0.0003	0.0001	0.0000	0.0007
36	Choline	C00114	0.0001	0.0002	0.0001	0.0000	0.0001	0.0002
37	Pterin	C00715	0.0036	0.0058	0.0012	0.0001	0.0001	0.0014
38	S-Methylglutathione	C11347	0.0001	0.0002	0.0002	N.D.	N.D.	0.0000
39	3-Phenylpropionic acid	C05629	0.0003	0.0005	0.0002	0.0002	0.0001	0.0005
40	XC0137	No ID	0.0031	0.0049	0.0034	N.D.	0.0000	0.0011
41	Isobutyryl CoA_divalent	C00630	0.0001	0.0002	0.0005	0.0000	0.0000	0.0011
42	XA0003	No ID	0.0003	0.0005	0.0003	0.0002	0.0002	0.0006
43	Cystathionine	C00542	0.0009	0.0013	0.0003	N.D.	N.D.	0.0005
44	Agmatine	C00179	0.0000	0.0000	0.0001	0.0001	N.D.	0.0000
45	Benzoic acid	C00180	0.0008	0.0013	0.0005	0.0004	0.0003	0.0009
46	Pyridoxamine 5'-phosphate	C00647	0.0008	0.0012	0.0007	0.0001	0.0000	0.0015
47	Propionic acid	C00163	0.0004	0.0005	0.0002	0.0002	N.D.	0.0005
48	4-Oxovaleric acid	No ID	0.0001	0.0002	0.0001	0.0001	0.0000	0.0002
49	CTP	C00063	0.0044	0.0064	0.0010	N.D.	0.0001	0.0017
50	Tiglic acid	C08279	0.0002	0.0002	0.0001	0.0001	0.0000	0.0002
51	Dihydroxyacetone phosphate	C00111	0.0001	0.0001	0.0002	0.0000	N.D.	0.0006
52	3-Hydroxybutyric acid	C01089	0.0001	0.0001	0.0000	N.D.	N.D.	N.D.
53	Ala-Ala	C00993	0.0181	0.0248	0.0023	0.0001	0.0003	0.0222
54	Sedoheptulose 7-phosphate	C05382	0.0005	0.0006	0.0003	0.0001	0.0000	0.0014
55	Hexanoic acid	C01585	0.0009	0.0012	0.0004	0.0004	0.0001	0.0010
56	dGTP	C00286	0.0581	0.0736	0.0147	0.0006	0.0014	0.0428
57	ATP	C00002	0.0584	0.0736	0.0147	0.0006	0.0014	0.0428
58	CoA_divalent	C00010	0.0008	0.0010	0.0001	N.D.	0.0001	0.0001
59	UDP-glucose UDP-galactose	C00029 C00052	0.0028	0.0035	0.0018	0.0001	0.0001	0.0017

60	Xanthopterin	No ID	0.0002	0.0003	0.0001	0.0001	N.D.	0.0016
61	<i>N</i> -Acetylputrescine	C02714	0.0001	0.0002	0.0008	0.0000	N.D.	0.0038
62	dTDP	C00363	0.0002	0.0003	0.0002	0.0001	N.D.	0.0006
63	Trehalose 6-phosphate	C00689	0.0001	0.0001	0.0002	N.D.	0.0000	0.0001
64	<i>S</i> -Adenosylhomocysteine	C00021	0.0000	0.0001	0.0000	0.0000	0.0000	0.0001
65	NADP <sup>+</sup>	C00006	0.0065	0.0074	0.0032	0.0017	0.0001	0.0100
66	5'-Deoxy-5'-methylthioadenosine	C00170	0.0014	0.0016	0.0009	0.0001	0.0000	0.0009
67	GTP	C00044	0.0085	0.0096	0.0020	0.0001	0.0002	0.0039
68	3-Methylguanine	C02230	0.0003	0.0004	0.0001	0.0000	0.0000	0.0001
69	$\gamma$ -Glu-2-aminobutyric acid	No ID	0.0007	0.0008	0.0004	0.0000	N.D.	0.0003
70	FMN	C00061	0.0010	0.0011	0.0006	0.0005	0.0001	0.0013
71	Butyric acid	C00246	0.0009	0.0009	0.0003	0.0003	0.0001	0.0009
72	<i>N</i> <sup>6</sup> , <i>N</i> <sup>6</sup> , <i>N</i> <sup>6</sup> -Trimethyllysine	C03793	0.0004	0.0005	0.0004	0.0002	0.0000	0.0006
73	Gly	C00037	0.0027	0.0030	0.0012	0.0004	0.0005	0.0016
74	UDP-glucuronic acid	C00167	0.0025	0.0027	0.0013	0.0003	0.0001	0.0014
75	dATP	C00131	0.0007	0.0008	0.0003	N.D.	0.0000	0.0007
76	3',5'-ADP	C00054	0.0001	0.0001	0.0002	0.0001	0.0000	0.0002
77	CDP	C00112	0.0017	0.0018	0.0006	0.0000	0.0000	0.0018
78	Malic acid	C00149	0.0002	0.0003	0.0001	N.D.	0.0001	0.0003
79	XC0040	No ID	0.0001	0.0001	0.0001	0.0001	N.D.	N.D.
80	Ornithine	C00077	0.0015	0.0015	0.0002	0.0001	0.0004	0.0013
81	4-Guanidinobutyric acid	C01035	0.0000	0.0000	0.0002	0.0001	0.0000	0.0001
82	Ile	C00407	0.0011	0.0011	0.0003	0.0004	0.0003	0.0014
83	Citric acid	C00158	0.0014	0.0014	0.0002	0.0001	0.0001	0.0004
84	Pro	C00148	0.0025	0.0023	0.0011	0.0004	0.0003	0.0009
85	Citrulline	C00327	0.0002	0.0002	0.0001	0.0000	0.0001	0.0001
86	Glyceric acid	C00258	0.0001	0.0001	0.0004	0.0001	N.D.	0.0004
87	Leu	C00123	0.0023	0.0021	0.0005	0.0012	0.0006	0.0033
88	XA0002	No ID	0.0008	0.0007	0.0002	0.0001	N.D.	N.D.
89	Asp	C00049	0.0025	0.0022	0.0010	0.0002	0.0003	0.0009
90	Creatinine	C00791	0.0001	0.0001	0.0001	0.0000	N.D.	0.0002
91	ADP	C00008	0.0211	0.0182	0.0131	0.0024	0.0004	0.0359
92	2'-Deoxyguanosine	C00330	0.0002	0.0002	0.0001	0.0000	0.0000	0.0002
93	Adenine	C00147	0.0030	0.0026	0.0031	0.0010	0.0001	0.0028
94	Adenosine	C00212	0.0002	0.0001	0.0001	0.0002	0.0000	0.0003
95	<i>S</i> -Adenosylmethionine	C00019	0.0141	0.0118	0.0059	0.0003	0.0004	0.0055
96	GDP-glucose GDP-mannose GDP-galactose	C00394 C00096 C02280	0.0270	0.0223	0.0040	0.0002	0.0005	0.0148
97	dCTP	C00458	0.0002	0.0002	0.0001	N.D.	N.D.	0.0001
98	Isovaleric acid	C08262	0.0011	0.0009	0.0003	0.0004	0.0001	0.0009
99	FAD <sub>divalent</sub>	C00016	0.0010	0.0008	0.0008	0.0006	0.0001	0.0010
100	Guanine	C00242	0.0021	0.0016	0.0017	0.0007	0.0000	0.0014

101	N <sup>8</sup> -Acetylspermidine	C01029	0.0001	0.0001	0.0001	0.0000	N.D.	0.0002
102	GDP	C00035	0.0036	0.0028	0.0026	0.0007	0.0001	0.0052
103	Val	C00183	0.0045	0.0034	0.0021	0.0011	0.0008	0.0030
104	N-Acetylglucosamine 6-phosphate	C00357	0.0004	0.0003	0.0001	0.0000	0.0000	0.0001
105	UTP	C00075	0.0135	0.0100	0.0016	N.D.	0.0002	0.0025
106	Spermidine	C00315	0.0009	0.0006	0.0023	0.0003	0.0000	0.0025
107	dADP	C00206	0.0003	0.0002	0.0003	0.0000	0.0000	0.0006
108	ADP-glucose GDP-fucose	C00498 C00325	0.0028	0.0020	0.0018	0.0006	0.0002	0.0026
109	CMP-N-acetylneuraminate	C00128	0.0008	0.0006	0.0003	N.D.	0.0000	0.0001
110	Isoglutamic acid	C05574	0.0088	0.0062	0.0078	0.0001	N.D.	0.0000
111	Ribose 5-phosphate	C00117	0.0001	0.0001	0.0002	0.0000	0.0000	0.0007
112	Glycerol 3-phosphate	C00093	0.0006	0.0004	0.0001	0.0000	0.0000	0.0002
113	Lys	C00047	0.0996	0.0680	0.0708	0.0222	0.0037	0.1296
114	Erythrose 4-phosphate	C00279	0.0001	0.0001	0.0000	0.0000	0.0000	0.0001
115	NAD <sup>+</sup>	C00003	0.0219	0.0143	0.0127	0.0096	0.0010	0.0153
116	P <sup>1</sup> , P <sup>4</sup> -Di(adenosine-5') tetraphosphate_divalent	C01260	0.0002	0.0001	0.0001	0.0000	0.0000	0.0002
117	Cadaverine	C01672	0.0030	0.0019	0.0014	0.0010	0.0001	0.0035
118	N-Acetyllysine	C12989	0.0005	0.0003	0.0001	N.D.	0.0001	0.0002
119	GMP	C00144	0.0005	0.0003	0.0006	0.0002	N.D.	0.0003
120	Putrescine	C00134	0.0702	0.0431	0.0937	0.0063	0.0048	0.3317
121	5-Hydroxylysine	C16741	0.0001	0.0001	0.0001	0.0000	N.D.	0.0001
122	UDP-N-acetylgalactosamine UDP-N-acetylglucosamine	C00203 C00043	0.0153	0.0092	0.0066	0.0003	0.0006	0.0120
123	Tyr	C00082	0.0042	0.0024	0.0014	0.0002	0.0003	0.0015
124	AMP	C00020	0.0083	0.0047	0.0170	0.0079	0.0004	0.0252
125	Glucose 6-phosphate	C00668	0.0015	0.0008	0.0004	0.0001	0.0001	0.0008
126	Succinic acid	C00042	0.0015	0.0008	0.0002	0.0001	0.0001	0.0004
127	Glutathione (GSSG)_divalent	C00127	0.0900	0.0499	0.0274	0.0000	0.0006	0.0089
128	Propionyl CoA_divalent	C00100	0.0015	0.0008	0.0002	0.0000	0.0000	0.0008
129	Trp	C00078	0.0010	0.0005	0.0005	0.0000	0.0000	0.0004
130	2,6-Diaminopimelic acid	C00666	0.0002	0.0001	0.0001	N.D.	0.0001	0.0001
131	Cytosine	C00380	0.0048	0.0025	0.0045	0.0007	0.0001	0.0061
132	Ribulose 5-phosphate	C00199	0.0003	0.0001	0.0003	0.0001	0.0000	0.0008
133	Ethanolamine	C00189	0.0003	0.0002	0.0001	0.0000	0.0000	N.D.
134	Ala	C00041	0.0124	0.0063	0.0014	0.0004	0.0009	0.0049
135	CMP	C00055	0.0007	0.0004	0.0004	0.0001	0.0000	0.0009
136	N-Acetylglucosamine 1-phosphate	C04256	0.0001	0.0001	0.0006	0.0002	0.0000	0.0010
137	UMP	C00105	0.0012	0.0005	0.0010	0.0004	0.0001	0.0029

138	2-Aminobutyric acid	C02261	0.0028	0.0013	N.D.	N.D.	N.D.	N.D.
139	3-Methylcrotonyl CoA_divalent	C03069	0.0003	0.0001	0.0000	N.D.	0.0000	0.0001
140	Arg	C00062	0.0464	0.0211	0.0473	0.0226	0.0019	0.0317
141	UDP	C00015	0.0049	0.0022	0.0010	0.0000	0.0001	0.0025
142	dAMP	C00360	0.0001	0.0001	0.0002	0.0001	0.0000	0.0002
143	Cysteine glutathione disulfide	C05526	0.0003	0.0001	0.0001	N.D.	0.0000	N.D.
144	Guanosine	C00387	0.0001	0.0000	0.0000	0.0000	N.D.	0.0000
145	2-Aminoadipic acid	C00956	0.0041	0.0017	0.0008	0.0001	0.0001	0.0003
146	Gln	C00064	0.1765	0.0741	0.0083	0.0001	0.0015	0.0026
147	<i>N</i> -Acetylornithine	C00437	0.0002	0.0001	N.D.	N.D.	0.0000	0.0001
148	Glucosamine	C00329	0.0057	0.0021	0.0006	0.0000	0.0000	0.0015
149	Morpholine	C14452	0.0005	0.0002	0.0001	0.0001	0.0001	0.0002
150	Cyclohexylamine	C00571	0.0005	0.0002	0.0001	0.0000	0.0001	0.0001
151	Glu	C00025	0.3219	0.1162	0.0125	0.0007	0.0024	0.0034
152	Acetyl CoA_divalent	C00024	0.0212	0.0070	0.0055	0.0012	0.0009	0.0094
153	Met	C00073	0.0187	0.0059	0.0013	0.0001	0.0001	0.0006
154	Fructose 6-phosphate	C05345	0.0008	0.0003	0.0002	0.0000	0.0000	0.0006
155	Glutathione (GSH)	C00051	0.0014	0.0004	0.0001	N.D.	0.0001	0.0001
156	2-Methylserine	C02115	0.0007	0.0002	0.0001	0.0000	N.D.	N.D.
157	Methionine sulfoxide	C02989	0.0027	0.0006	0.0002	0.0001	0.0000	0.0002
158	<i>N</i> -Acetylglutamic acid	C00624	0.0020	0.0005	0.0000	N.D.	0.0000	N.D.
159	Thr	C00188	0.0280	0.0046	0.0015	0.0002	0.0005	0.0037
160	Homoserine	C00263	0.0061	0.0005	0.0003	N.D.	0.0000	0.0003
161	XC0017	No ID	0.0000	N.D.	0.0001	0.0002	N.D.	0.0002
162	XA0055	No ID	0.0000	N.D.	0.0002	N.D.	N.D.	0.0003
163	Fructose 1,6-diphosphate	C00354	0.0002	N.D.	0.0002	N.D.	N.D.	0.0006
164	IMP	C00130	0.0001	N.D.	0.0001	N.D.	N.D.	N.D.
165	Gly-Asp	No ID	0.0002	N.D.	0.0000	N.D.	N.D.	N.D.
166	Isobutylamine	C02787	0.0007	N.D.	N.D.	N.D.	0.0001	N.D.
167	Hexylamine	C08306	0.0004	N.D.	N.D.	N.D.	0.0000	N.D.
168	2-Oxoglutaric acid	C00026	0.0014	N.D.	N.D.	N.D.	N.D.	N.D.
169	Tyramine	C00483	0.0001	N.D.	N.D.	N.D.	N.D.	N.D.
170	<i>O</i> -Acetylserine	C00979	0.0002	N.D.	N.D.	N.D.	N.D.	N.D.
171	Pyridoxal	C00250	0.0001	N.D.	N.D.	N.D.	N.D.	N.D.
172	$\beta$ -Ala-Lys	C05341	0.0001	N.D.	N.D.	N.D.	N.D.	N.D.
173	<i>N</i> -Acetylmuramic acid	C02713	N.D.	N.D.	0.0000	0.0003	N.D.	N.D.
174	$\beta$ -Ala	C00099	N.D.	N.D.	0.0001	0.0001	N.D.	0.0003
175	Inosine	C00294	N.D.	N.D.	0.0002	0.0001	N.D.	0.0010
176	<i>N</i> <sup>6</sup> -Acetyllysine	C02727	N.D.	N.D.	0.0001	N.D.	N.D.	0.0001
177	<i>N</i> -Acetylserine	No ID	N.D.	N.D.	0.0001	N.D.	N.D.	N.D.
178	Cytidine	C00475	N.D.	N.D.	0.0000	N.D.	N.D.	N.D.

Table 5-4. The standard curve of commercial PHB that uses for calculate the PHB accumulation.

PHB commercial (mg/mL)	Area
0.3	12249842
0.4	24432771
0.5	35373210
0.6	45869384
0.8	56065562.9
1.0	66306823.38

Table 5-5. The diameter of PHB granules of strain TH-1 in different condition

	3HA	3HM	6HA	6HM	6HMA
Mean	0.299	0.478	0.340	0.500	0.305
Bottom	0.25	0.43	0.295	0.455	0.255
2Q Box	0.046	0.037	0.045	0.044	0.043
3Q Box	0.051	0.063	0.056	0.048	0.053
Whisker -	0.068	0.027	0.095	0.122	0.046
Whisker +	0.081	0.067	0.075	0.185	0.144
Offset	1.000	2.000	3.000	4.000	5.000